R. E. Abendroth, F. W. Klaiber, M. W. Shafer

Lateral Load Resistance of Diaphragms in Prestressed Concrete Girder Bridges

December 1991

Sponsored by the
Highway Division of the
Iowa Department of Transportation and the
Highway Research Advisory Board

Iowa DOT Project HR-319
ISU-ERI-Ames-92076

Iowa Department of Transportation

report

College of Engineering
Iowa State University

The opinions, findings, and conclusions expressed in this publication are those of the authors and not necessarily those of the Highway Division of the Iowa Department of Transportation.

R. E. Abendroth, F. W. Klaiber, M. W. Shafer

Lateral Load Resistance of Diaphragms in Prestressed Concrete Girder Bridges

Sponsored by the
Highway Division of the
Iowa Department of Transportation and the
Highway Research Advisory Board

Iowa DOT Project HR-319
ISU-ERI-Ames-92076

engineering research institute
iowa state university

TABLE OF CONTENTS

Page

LIST OF FIGURES vii

LIST OF TABLES xv

ABSTRACT 1

1. INTRODUCTION 3

1.1. General Background 3

1.2. Objective and Scope 7

1.3. Research Program 7

1.4. Literature Review 9

1.5. Review of Current Practice 11

2. DESCRIPTION OF TEST SPECIMENS 17

2.1. Bridge Model 17

2.2. Intermediate Diaphragms 22

2.2.1. Diaphragm Types, Locations, and Designations 22
2.2.2. Reinforced Concrete Intermediate Diaphragms 22
2.2.3. Steel Channel Intermediate Diaphragms 28
2.2.3.1. Deep Channel Diaphragm 28
2.2.3.2. Shallow Channel Diaphragm 28
2.2.4. Steel X-Brace Intermediate Diaphragms 30
2.2.4.1. With Horizontal Strut 30
2.2.4.2. Without Horizontal Strut 35
2.2.5. No Diaphragms 35

3. TESTS AND TEST PROCEDURES 37

3.1. Instrumentation 37

3.2. Loading Mechanisms 42

3.2.1. Vertical Loading 44
3.2.2. Horizontal Loading 47

Page

3.3. Load Tests 51

3.3.1. Vertical Loading 53
3.3.2. Horizontal Loading 54
3.3.3. Horizontal Plus Vertical Loading 55

4. ANALYSIS AND TEST RESULTS 57

4.1. Finite-Element Investigation 57

4.1.1. Finite-Element Model 57
4.1.2. Effect of the End Fixity 65
4.1.3. Load Distribution Analysis 68

4.2. Experimental Investigations 74

4.2.1. Deck Cracking Effects on Bridge Response 74
4.2.2. Reinforced Concrete Diaphragm Connection Effects on Bridge Response 79
4.2.3. Steel Channel Diaphragm Connection Effects on Bridge Response 81
4.2.4. Steel X-Brace Diaphragm Connection Effects on Bridge Response 89
4.2.5. Load Versus Deflection Behavior 89
4.2.6. Load Distribution Study 100
4.2.7. Beam and Deck Strains 106
4.2.8. Diaphragm Strains 113

4.3. Comparison of Analytical and Experimental Results 115

4.3.1. Displacement Distribution Along the Bridge Span 115
4.3.2. Horizontal Load Versus Horizontal Deflection Behavior 124
4.3.2.1. No Intermediate Diaphragms 124
4.3.2.2. Midspan Intermediate Diaphragms 127
4.3.2.3. Third-Point Intermediate Diaphragms 143
4.3.3. Vertical Load Versus Vertical Deflection Behavior 155
4.3.3.1. No Intermediate Diaphragms 155
4.3.3.2. Midspan Intermediate Diaphragms 155
4.3.3.3. Third-Point Intermediate Diaphragms 161

5. SUMMARY AND CONCLUSIONS 163

5.1. Summary 163

5.2. Conclusions 165

Page

6. RECOMMENDED CONTINUED STUDIES 169

7. REFERENCES 171

8. ACKNOWLEDGMENTS 173

APPENDIX A: Design Agency Questionnaire Results 175

APPENDIX B: Bridge Details 187

LIST OF FIGURES

		Page
Fig. 1.1.	Typical diaphragms used in P/C bridges	13
Fig. 2.1.	Photographs of bridge model	18
Fig. 2.2.	Model bridge	20
Fig. 2.3.	Diaphragm layout.	25
Fig. 2.4.	Reinforced concrete intermediate diaphragm (Designations RC.1 and RC.3)	26
Fig. 2.5.	Deep steel channel intermediate diaphragm (Designations C2.1 and C2.3)	29
Fig. 2.6.	Shallow steel channel intermediate diaphragm (Designations C1.1 and C1.3)	31
Fig. 2.7.	Steel X-brace intermediate diaphragm (With horizontal strut, Designation X1.1 and without horizontal strut, Designation X2.1)	33
Fig. 3.1.	Location of strain gages on P/C girders	39
Fig. 3.2.	Location of strain gages on deck.	40
Fig. 3.3.	Location of strain gages on diaphragms.	41
Fig. 3.4.	Location of deflection instrumentation.	43
Fig. 3.5.	Load points	45
Fig. 3.6.	Vertical loading scheme	46
Fig. 3.7.	Horizontal loading scheme	48
Fig. 4.1.	Finite element idealization of bridge and diaphragms	59
Fig. 4.2.	Effect of end restraint and type of centerline diaphragm on vertical load-deflection curves: load at point 4, deflection at point 4	66
Fig. 4.3.	Effect of end restraint and type of centerline diaphragm on horizontal load-deflection curves: load at point 4, deflection at point 4	67

LIST OF FIGURES

Page

Fig. 4.4. Theoretical distribution factors: vertical load at point 4 69

Fig. 4.5. Theoretical distribution factors: vertical load at point 5 70

Fig. 4.6. Theoretical distribution factors: horizontal load at point 4 72

Fig. 4.7. Theoretical distribution factors: horizontal load at point 5 73

Fig. 4.8. Major longitudinal deck cracks 75

Fig. 4.9. Horizontal load versus deflection at point 4 for C1.1 diaphragms 83

Fig. 4.10. Horizontal load versus deflection at point 5 for C1.1 diaphragms 83

Fig. 4.11. Horizontal load versus deflection at point 6 for C1.1 diaphragms 84

Fig. 4.12. Horizontal load versus deflection at point 4 for C2.1 diaphragms 86

Fig. 4.13. Horizontal load versus deflection at point 5 for C2.1 diaphragms 86

Fig. 4.14. Horizontal load versus deflection at point 6 for C2.1 diaphragms 87

Fig. 4.15. Horizontal load versus deflection at point 7 for C2.1 diaphragms 87

Fig. 4.16. Horizontal load versus deflection at point 4 for two positions of C1.1 diaphragms 88

Fig. 4.17. Vertical load-deflection curves: diaphragm at centerline, deflection at point 4, load at point 4 91

Fig. 4.18. Vertical load-deflection curves: diaphragms at third points, deflection at point 4, load at point 4 92

Fig. 4.19. Vertical load-deflection curves: diaphragm at centerline, deflection at point 5, load at point 4 93

Fig. 4.20. Vertical load-deflection curves: diaphragms at third points, deflection at point 5, load at point 4 94

Fig. 4.21. Horizontal load-deflection curves: diaphragm at centerline, deflection and load at point 4 95

Fig. 4.22. Horizontal load-deflection curves: diaphragms at third points, deflection and load at point 4 96

LIST OF FIGURES

Page

Fig. 4.23. Horizontal load-deflection curves: diaphragms at centerline, deflection at point 5, load at point 4 98

Fig. 4.24. Horizontal load-deflection curves: diaphragms at third points, deflection at point 5, load at point 4 98

Fig. 4.25. Horizontal load-deflection curves: diaphragms at third points: load and deflection at point 4; diaphragms at center line: load and deflection at point 7 99

Fig. 4.26. Horizontal load-deflection curves: diaphragms at third points: load and deflection at point 5; diaphragms at center line: load and deflection at point 8 99

Fig. 4.27. Vertical deflection at points 4, 5, and 6, for a 20 kip upwards vertical force at point 4 101

Fig. 4.28. Vertical deflection at points 4, 5, and 6, for a 20 kip upwards vertical force at point 5 101

Fig. 4.29. Vertical deflection at points 4, 5, and 6, for a 20 kip upwards vertical force at point 6 102

Fig. 4.30. Horizontal deflection at points 4, 5, and 6, for a 40 kip horizontal force at point 4 104

Fig. 4.31. Horizontal deflection at points 4, 5, and 6, for a 40 kip horizontal force at point 5 104

Fig. 4.32. Horizontal deflection at points 4, 5, and 6, for a 40 kip horizontal force at point 6 105

Fig. 4.33. Beam horizontal deflections for a 50 kip horizontal force at point 4 and no diaphragms 116

Fig. 4.34. Beam horizontal deflections for a 50 kip horizontal force at point 5 and C1.1 diaphragms 116

Fig. 4.35. Beam horizontal deflections for a 50 kip horizontal force at point 4 and C1.1 diaphragms 117

Fig. 4.36. Beam horizontal deflections for a 50 kip horizontal force at point 5 and RC.1 diaphragms 118

Fig. 4.37. Beam horizontal deflections for a 50 kip horizontal force at point 4 and RC.1 diaphragms 119

LIST OF FIGURES

Page

Fig. 4.38. Beam horizontal deflections for a 50 kip horizontal force at point 4 and C2.1 diaphragms 120

Fig. 4.39. Beam horizontal deflections for a 50 kip horizontal force at point 5 and X1.1 diaphragms 121

Fig. 4.40. Beam horizontal deflections for a 50 kip horizontal force at point 4 and X1.1 diaphragms 121

Fig. 4.41. Beam horizontal deflections for a 50 kip horizontal force at point 4 and X2.1 diaphragms 122

Fig. 4.42. Horizontal load versus deflection curves: load and deflection at point 5, no intermediate diaphragms 125

Fig. 4.43. Horizontal load versus deflection curves: load at point 5, deflection at point 6, no intermediate diaphragms 125

Fig. 4.44. Horizontal load versus deflection curves: load at point 6, deflection at point 5, no intermediate diaphragms 126

Fig. 4.45. Horizontal load versus deflection curves: load and deflection at point 6, no intermediate diaphragms 126

Fig. 4.46. Horizontal load versus deflection curves: load and deflection at point 4, C1.1 diaphragms 128

Fig. 4.47. Horizontal load versus deflection curves: load at point 4, deflection at point 5, C1.1 diaphragms 128

Fig. 4.48. Horizontal load versus deflection curves: load at point 4, deflection at point 6, C1.1 diaphragms 129

Fig. 4.49. Horizontal load versus deflection curves: load and deflection at point 4, C2.1 diaphragms 131

Fig. 4.50. Horizontal load versus deflection curves: load and deflection at point 5, C2.1 diaphragms 131

Fig. 4.51. Horizontal load versus deflection curves: load and deflection at point 6, C2.1 diaphragms 132

Fig. 4.52. Horizontal load versus deflection curves: load at point 4, deflection at point 5, C2.1 diaphragms 133

Fig. 4.53. Horizontal load versus deflection curves: load at point 5, deflection at point 4, C2.1 diaphragms 133

LIST OF FIGURES

Page

Fig. 4.54. Horizontal load versus deflection curves: load at point 4, deflection at point 6, C2.1 diaphragms 134

Fig. 4.55. Horizontal load versus deflection curves: load at point 6, deflection at point 4, C2.1 diaphragms 134

Fig. 4.56. Horizontal load versus deflection curves: load at point 5, deflection at point 6, C2.1 diaphragms 135

Fig. 4.57. Horizontal load versus deflection curves: load at point 6, deflection at point 5, C2.1 diaphragms 135

Fig. 4.58. Horizontal load versus deflection curves: load and deflection at point 4, RC.1 diaphragms 137

Fig. 4.59. Horizontal load versus deflection curves: load at point 4, deflection at point 5, RC.1 diaphragms 137

Fig. 4.60. Horizontal load versus deflection curves: load at point 4, deflection at point 6, RC.1 diaphragms 138

Fig. 4.61. Horizontal load versus deflection curves: load and deflection at point 5, RC.1 diaphragms 138

Fig. 4.62. Horizontal load versus deflection curves: load at point 5, deflection at point 6, RC.1 diaphragms 139

Fig. 4.63. Horizontal load versus deflection curves: load and deflection at point 6, RC.1 diaphragms 139

Fig. 4.64. Horizontal load versus deflection curves: load and deflection at point 5, X1.1 diaphragms 140

Fig. 4.65. Horizontal load versus deflection curves: load at point 5, deflection at point 6, X1.1 diaphragms 140

Fig. 4.66. Horizontal load versus deflection curves: load at point 6, deflection at point 4, X1.1 diaphragms 141

Fig. 4.67. Horizontal load versus deflection curves: load at point 6, deflection at point 5, X1.1 diaphragms 141

Fig. 4.68. Horizontal load versus deflection curves: load and deflection at point 6, X1.1 diaphragms 142

LIST OF FIGURES

Page

Fig. 4.69. Horizontal load versus deflection curves: load and deflection at point 5, X2.1 diaphragms 144

Fig. 4.70. Horizontal load versus deflection curves: load at point 5, deflection at point 6, X2.1 diaphragms 144

Fig. 4.71. Horizontal load versus deflection curves: load at point 6, deflection at point 4, X2.1 diaphragms 145

Fig. 4.72. Horizontal load versus deflection curves: load at point 6, deflection at point 5, X2.1 diaphragms 145

Fig. 4.73. Horizontal load versus deflection curves: load and deflection at point 6, X2.1 diaphragms 146

Fig. 4.74. Horizontal load versus deflection curves, load at point 5, deflection at point 4, C1.3 diaphragms 147

Fig. 4.75. Horizontal load versus deflection curves, load and deflection at point 5, C1.3 diaphragms 147

Fig. 4.76. Horizontal load versus deflection curves, load at point 5, deflection at point 6, C1.3 diaphragms 148

Fig. 4.77. Horizontal load versus deflection curves, load at point 6, deflection at point 4, C2.3 diaphragms 150

Fig. 4.78. Horizontal load versus deflection curves, load at point 6, deflection at point 5, C2.3 diaphragms 150

Fig. 4.79. Horizontal load versus deflection curves, load and deflection at point 6, C2.3 diaphragms 151

Fig. 4.80. Horizontal load versus deflection curves, load and deflection at point 4, RC.3 diaphragms 152

Fig. 4.81. Horizontal load versus deflection curves, load at point 4, deflection at point 5, RC.3 diaphragms 152

Fig. 4.82. Horizontal load versus deflection curves, load at point 4, deflection at point 6, RC.3 diaphragms 153

Fig. 4.83. Horizontal load versus deflection curves, load and deflection at point 5, RC.3 diaphragms 153

LIST OF FIGURES

Page

Fig. 4.84. Horizontal load versus deflection curves, load at point 5, deflection at point 6, RC.3 diaphragms 154

Fig. 4.85. Horizontal load versus deflection curves, load and deflection at point 6, RC.3 diaphragms 154

Fig. 4.86. Vertical load versus deflection curves, load at point 6, deflection at point 5, no intermediate diaphragms 156

Fig. 4.87. Vertical load versus deflection curves, load and deflection at point 6, no intermediate diaphragms 156

Fig. 4.88. Vertical load versus deflection curves, load at point 6, deflection at point 5, C1.1 diaphragms 157

Fig. 4.89. Vertical load versus deflection curves, load and deflection at point 6, C1.1 diaphragms 157

Fig. 4.90. Vertical load versus deflection curves, load and deflection at point 4, RC.1 diaphragms 159

Fig. 4.91. Vertical load versus deflection curves, load and deflection at point 5, RC.1 diaphragms 159

Fig. 4.92. Vertical load versus deflection curves, load and deflection at point 6, RC.1 diaphragms 160

Fig. 4.93. Vertical load versus deflection curves, load at point 6, deflection at point 5, RC.1 diaphragms 160

Fig. 4.94. Vertical load versus deflection curves, load at point 6, deflection at point 5, RC.3 diaphragms 162

Fig. 4.95. Vertical load versus deflection curves, load and deflection at point 6, RC.3 diaphragms 162

Fig. B.1. P/C girder inserts 189

Fig. B.2. P/C girder support details 190

Fig. B.3. Abutment and end diaphragm reinforcement 191

Fig. B.4. Longitudinal reinforcement in top of deck 192

Fig. B.5. Longitudinal reinforcement in bottom of deck 193

Fig. B.6. Transverse deck reinforcement 194

LIST OF TABLES

		Page
Table 2.1.	Concrete strengths	23
Table 2.2.	Intermediate diaphragm designations	24
Table 3.1.	Load tests	52
Table 4.1.	Impact forces on bridge	64
Table 4.2.	Maximum strains due to horizontal loading	107
Table 4.3.	Maximum strains due to vertical loading	109
Table 4.4.	Girder stresses	112
Table A.1.	Impact occurrence and resulting damage	185

ABSTRACT

Each year several prestressed concrete girder bridges in Iowa and other states are struck and damaged by vehicles with loads too high to pass under the bridge. Whether or not intermediate diaphragms play a significant role in reducing the effect of these unusual loading conditions has often been a topic of discussion. A study of the effects of the type and location of intermediate diaphragms in prestressed concrete girder bridges when the bridge girder flanges were subjected to various levels of vertical and horizontal loading was undertaken. The purpose of the research was to determine whether steel diaphragms of any conventional configuration can provide adequate protection to minimize the damage to prestressed concrete girders caused by lateral loads, similar to the protection provided by the reinforced concrete intermediate diaphragms presently being used by the Iowa Department of Transportation.

The research program conducted and described in this report included the following: A comprehensive literature search and survey questionnaire were undertaken to define the state-of-the-art in the use of intermediate diaphragms in prestressed concrete girder bridges. A full scale, simple span, prestressed concrete girder bridge model, containing three beams was constructed and tested with several types of intermediate diaphragms located at the one-third points of the span or at the mid-span. Analytical studies involving a three-dimensional finite element analysis model were used to provide additional information on the behavior of the experimental bridge.

The performance of the bridge with no intermediate diaphragms was quite different than that with intermediate diaphragms in place. All intermediate diaphragms tested had some effect in distributing the loads to the slab and other girders, although some diaphragm types performed better than others. The research conducted has indicated that the replacement of the reinforced concrete intermediate diaphragms currently being used in Iowa with structural steel diaphragms may be possible.

1. INTRODUCTION

1.1. General Background

Each year several prestressed concrete (P/C) girder overpass bridges in Iowa are struck by vehicles with loads too high to pass under the bridge. According to Shanafedt and Horn (10), 201 P/C girder bridges in the United States are damaged in an average year; 162 of these bridges are damaged by overheight vehicles or loads. The actual number of impacts is most likely significantly higher than these numbers since many collisions are not reported because they are minor and go undetected. To minimize the amount of damage a bridge sustains from these accident-induced loadings, the Iowa Department of Transportation (Iowa DOT) requires that one intermediate reinforced concrete diaphragm (located at the midspan) be used in all P/C girder bridges located over traffic. When P/C girder bridges do not have traffic beneath them, the Iowa DOT permits the use of a steel diaphragm at the midspan. In recent years, other states have used various configurations of bolted steel diaphragms in both of these situations. Since steel diaphragms are easier and quicker to install than concrete diaphragms, they are generally preferred by bridge contractors.

The 14th edition of the *Standard Specifications for Highway Bridges, 1989* (1) of the American Association of State Highway and Transportation Official (AASHTO) clearly states the following requirements for using diaphragms in P/C girder bridges:

> 9.10 Diaphragms
>
> 9.10.1 General
>
> Diaphragms shall be provided in accordance with Articles 9.10.2 and 9.10.3 except that diaphragms may be omitted where tests or structural analysis show adequate strength.
>
> 9.10.2 T-Beams
>
> Diaphragms or other means shall be used at span ends to strengthen the free edge of the slab and to transmit lateral forces to the substructure. Intermediate diaphragms shall be placed between the beams at the points of maximum moments for spans over 40 feet.

9.10.3 Box Girders

9.10.3.1 For spread box beams, diaphragms shall be placed...

No change was made in these requirements in the Interim Specifications--Bridges 1991 (2). Although the phraseology was changed in the proposed LRFD Bridge Design Code (7), the requirements are essentially the same. The LRFD Bridge Design Code diaphragm requirement in P/C girder bridges are as follows:

5.13 Specific Members

5.13.2.2 Diaphragms

End diaphragms shall be provided to support the deck at all points of discontinuity. End-type diaphragms may also be required between girders over points of support at piers, abutments and hinges to distribute shear forces to the bearings.

Intermediate diaphragms shall be provided to assist in the distribution of live loads among the girders and to resist torsional forces at the locations specified in Article 5.14.

Diaphragms should generally be designed as deep beams.

5.14 Provisions for Structure Types

5.14.1.1.4

Diaphragms shall be used at the ends of girder spans, unless other means are provided to resist lateral forces, to strengthen the free edge of the slab and to maintain section geometry. Diaphragms may be omitted where tests or structural analysis show adequate strength.

For I-girder and T-girder spans, one intermediate diaphragm shall be placed at the point of maximum positive moment for spans in excess of 40 feet.

For curved box girder bridges having...

Although required by AASHTO specifications, the use of diaphragms in P/C bridges is controversial. Several states do not use intermediate diaphragms of any type in P/C girder bridges whereas other states use either diaphragms at the midspan, one-third points or one-quarter points depending on the span length. As this project involved the use of diaphragms in P/C girder bridges, the authors have chosen to review three of the directly related references in this section.

Sithichaikasem and Gamble (12) and Wong and Gamble (14) reported on the diaphragm research completed at the University of Illinois. Although the goal of this research was to determine

the effectiveness of intermediate diaphragms in load distribution, these authors did convey the following: "One of the practical arguments that has been raised in the past is the feeling that diaphragms help limit damage to an overpass structure which is struck transversely from below by an oversized load. There appears to be conflicting evidence as to whether the diaphragms are damage-limiting or damage-spreading members, and the only comment the authors would make at this time is that the diaphragms currently being used in bridges are probably the wrong shape and size, and are usually in the wrong locations, if one of their valid functions is the reduction of damage to the structure due to horizontal impact on the side of the bridge. The analyses reported here are not relevant to this particular question."

The primary objective of the Illinois investigation was to study the effects of diaphragms on load distribution characteristics in simple and continuous span P/C girder and slab highway bridges. In their theoretical analysis, the parameters studied included the number, stiffness, and location of diaphragms; the relative girder stiffness; the ratio of girder spacing to span; the girder torsional stiffness, the girder spacing; and the location and type of loading.

For simple span bridges (12) the following conclusions were made:

- In structures in which the outer line of wheels can fall directly over the edge girders, diaphragms should not be used as they will increase the controlling moment in the bridge.
- The influence of a single midspan diaphragm and two diaphragms located near midspan were determined to be about the same structurally.
- Location and spacing of diaphragms should not be a function of span length alone. For example, many short bridges could benefit from having diaphragms while many long span bridges with diaphragms either receive no benefit or are harmed by them. Only diaphragms at or very near the section of maximum moment result in measurable changes in the controlling girder moments.

- Diaphragms must be of the correct flexural stiffness to be effective. Diaphragms with stiffnesses greater than an optimum value may increase the moments in the girders.

For continuous span bridges (14) with various diaphragm stiffnesses and bridge properties, the following conclusions were made:

- Diaphragms improved the load distribution characteristics of some bridges that have a large beam spacing to span length ratio.
- The usefulness of diaphragms is minimal and they are harmful in most cases.
- On the basis of cost effectiveness, diaphragms are not recommended for highway bridges.

In 1973, Sengupta and Breen (11) also investigated the role of end and intermediate diaphragms in typical prestressed concrete girder and slab bridges. They tested four 1/5.5 scale microconcrete simple span model bridges to determine the contribution of cast-in-place concrete diaphragms. Experimental variables included span length, skew angle of the bridge, and number, location, and stiffness of the diaphragms. The elastic response of the bridge was studied under static, cyclic, and impact loads--with and without intermediate diaphragms. Overload and ultimate load behavior was also documented from various static load and impact load tests. Experimental results were used to verify a computer program, which in turn was used to generalize some of the results.

Two of the four bridge models were subjected to lateral impact loading at the midspan on the bottom flange of the exterior girders. In both bridges, one exterior girder was impacted while the diaphragms, which were located at the one-third points of the span, were in place; the other exterior girder was impacted after the diaphragms were removed. With identical impacting forces, both models showed considerably more damage in the exterior girders when the diaphragms were in place. After the bridge testing was completed, all four exterior girders were removed and subjected to midspan vertical loading. The ultimate load capacity of the girders which had intermediate diaphragms in place during the impact loading had a slightly higher ultimate load capacity than the exterior girders which had no intermediate diaphragms present. The authors concluded that the

diaphragms made the girders more rigid when subjected to lateral impacts. Therefore, the energy absorption capacity of the girders was reduced, which made the girders more susceptible to lateral impact damage.

On the basis of the other load tests and results from the theoretical analysis, Sengupta and Breen concluded that under no circumstances would significant reductions in design girder moment be expected because of the presence of intermediate diaphragms. In fact, in certain situations the presence of intermediate diaphragms might even increase the design moment. These authors also stated that intermediate diaphragms do not seem necessary for construction purposes. For these reasons, the authors recommended that intermediate diaphragms should not be provided in simply supported P/C girder and composite slab bridges.

1.2. Objective and Scope

Very little research has been completed on the effectiveness of diaphragms in distributing lateral impact forces. Thus, the primary objectives of this project was to investigate the effectiveness of intermediate reinforced concrete and steel diaphragms when used in P/C girder and slab bridges subjected to lateral load and to determine whether steel diaphragms of some conventional configuration are structurally equivalent to cast-in-place reinforced concrete diaphragms presently being used by the Iowa DOT.

The research team pursued its objectives by undertaking a comprehensive literature review, surveying other departments of transportation, performing an analytical study of P/C girder-slab bridges with various types of intermediate diaphragms, and testing a full-scale model P/C girder-slab bridge. Details of these tasks are outlined in the following section.

1.3. Research Program

The research program consisted of the distinct parts outlined above; however, emphasis was placed on the laboratory testing. Initially, a comprehensive literature review was made. In addition

to using the Geodex System - Structural Information Service, two computerized literature searches were made.

To obtain information on the use of intermediate diaphragms in P/C girder bridges in other states, Canadian provinces, and appropriate federal agencies, the researchers developed a survey that was relatively easy to complete and yet thorough enough to obtain the desired data such as diaphragms used, type employed, spacing, limitations, etc.

In the experimental portion of the investigation, a full-scale simple span P/C girder bridge model was designed and constructed in the ISU Structural Engineering Research Laboratory Annex. The model was essentially the same as an existing P/C girder bridge except it only had three girders (reducing both fabrication costs and space requirements) and had a reduced deck thickness (requiring more load to be distributed by the diaphragm(s) than the deck). Since the deck was not one of the variables in the testing program, the deck was reinforced with considerably less reinforcement (see Sec. 2.1) than an actual bridge deck.

The P/C girders used in the model bridge were fabricated by Iowa Prestressed Concrete (Iowa Falls, Iowa). Special inserts were cast in the girders so that various configurations of steel intermediate diaphragms could be tested. In addition to the cast-in-place reinforced concrete diaphragms and steel channels presently being used in Iowa at road and stream crossings, respectively, several other configurations of steel diaphragms were tested. The bridge model was tested with the diaphragms at midspan and at the one-third span locations. The P/C girders, various diagrams, and bridge deck were instrumented with strain gages. During the various load tests, strains as well as deflections were monitored.

The bridge was subjected to a combination of vertical and horizontal loads, which were applied at the same location, to simulate an inclined force that could result from an overheight vehicle. Loading was applied at various locations on the lower flanges of the three girders to reflect the possibility that an overheight vehicle could strike any girder in a given bridge at essentially any

location along its length. Although the purpose of the investigation was to determine the effects of lateral loading, additional tests were undertaken to determine the distribution of vertical loading.

In the analytical portion of the investigation, finite-element bridge models were developed by using the commercial software program ANSYS. Using the program, the researchers could theoretically determine the effects of various diaphragm arrangements (type, and location) on the behavior of the bridge. The program was written so that the supports could be analyzed as fixed ends or pinned ends.

The results from the various parts of the research program are summarized in this report. The literature review and results of the survey are given in Sections 1.4 and 1.5, respectively. Chapters 2 and 3 describe the bridge model tested as well as the instrumentation and test procedures employed. The results from the laboratory testing program and the finite-element analysis are summarized in Chapter 4. The summary and conclusions of the research programs are presented in Chapter 5.

1.4. Literature Review

A literature search was conducted to gather available information on the use of diaphragms in P/C bridges and on lateral loading of P/C girder bridges constructed with reinforced concrete or steel intermediate diaphragms. Several methods of searching were used. The Geodex System - Structural Information Service in the ISU Bridge Engineering Center Library as well as computerized searches using Knowledge Index, available at the university library, and the Highway Research Information Service through the Iowa DOT were checked.

The literature review revealed that very little information has been published on the response of bridges to lateral loading. However, our review of the literature involving bridge diaphragms revealed that there have been numerous investigations on the lateral distribution of vertical loading in multi-girder bridges. A report by Cheung, Jategaonkar, and Jaeger (4) attempted to provide some basis for the inclusion of intermediate diaphragms in beam and slab bridges. They noted that "the

outcome of previous studies is a set of recommendations that are contrary to one another." The various studies disagree on the effectiveness of intermediate diaphragms in the lateral distribution of live load. They also noted that these studies disagree on the most effective positioning of intermediate diaphragms. Some research has concluded that intermediate diaphragms have no effect on the lateral distribution of vertical loading. Research by Kostem and deCastro (6) found that when all traffic lanes were loaded, the diaphragms were ineffective in distributing the loads laterally. These studies have pertained only to the lateral distribution of vertical forces in various types of bridges.

In addition to studying the effectiveness of intermediate diaphragms in P/C girder bridges, Sengupta and Breen (11) also investigated many aspects of diaphragms among which was a limited study of lateral loads applied to the bottom flange of prestressed concrete girders. Scale models were used to document their work experimentally. They suggest that intermediate diaphragms make the prestressed concrete girders more vulnerable to damage from lateral impacts by stiffening the girder near the point of impact and also transferring the damage to the next girder. They also state that the "AASHTO requirements for interior diaphragms are mainly for the purpose of construction (as a beam spacer) and for girder stability (to prevent buckling of the girder webs)," and thus they recommend that intermediate diaphragms be eliminated. Their recommendations, however, have not been universally accepted. As previously documented, current *AASHTO Standard Specification for Highway Bridges* (1,2) still require intermediate diaphragms in P/C girder bridges.

McCathy, White, and Minor (8), estimated that the exclusion of intermediate diaphragms could reduce the cost of the superstructure by 3%-5% in addition to reducing construction time and deck scheduling without modifications to the bridge design. As mentioned earlier, researchers at the University of Illinois (12,14) concluded that using diaphragms in most situations is not beneficial and in some situations harmful. Thus, bridge engineers, with countless years of experience, cannot agree on the inclusion or exclusion of intermediate diaphragms in P/C girder bridges!

1.5. Review of Current Practice

A survey of the fifty U.S. state departments of transportation, the District of Columbia, three U.S. commonwealths, seven Canadian departments of transportation, and three tollway/port authorities was conducted to obtain information on intermediate diaphragms used in P/C girder bridges. The survey addressed seven topics: (1) type of diaphragm employed, (2) diaphragm location and depth, (3) connection details to the P/C girder and slab, (4) limitations on the use of either steel or reinforced concrete diaphragms, (5) design criteria for lateral impact loading, (6) approximate occurrence of high-load traffic collisions, and (7) categorization of the type and extent of bridge damage caused by overheight loads. The questionnaire as well as responses to the questionnaire are given in Appendix A.

Approximately 86% of the 64 design agencies selected to receive the questionnaire returned it. All but two state departments of transportation in the U.S. completed the inquiry. Of those agencies responding, about 93% indicated that in the past they have specified intermediate diaphragms for P/C girder bridges and about 85% are still currently requiring these diaphragms.

The respondents chose from the following types diaphragms: (1) cast-in-place concrete, (2) precast concrete, (3) steel channel, (4) steel I-shape, (5) steel truss, (6) steel cross bracing, and (7) other (respondents were allowed to input other choices). Respondents could specify all diaphragms in the list that were used on P/C girder bridges under their jurisdiction. In the following paragraphs, the percentages are based on the number of those responding. The selection of the material used for the diaphragm is influenced by the type of traffic beneath the bridge.

Ninety-six percent of the respondents use cast-in-place concrete diaphragms when the bridge is located above a highway or navigable waterway, and 23% also specify steel channel. When a bridge spans a railway, cast-in-place concrete is used by 85% of the responding agencies; steel channel by 17%; and steel cross bracing by 10%. Bridges spanning grade separations that have no traffic (highway, navigable waterway, or railway) beneath them most often have cast-in-place concrete

diaphragms, although 25% of the agencies allow steel channel. Cross bracing and I-shape steel are allowed by about 10% agencies. A few agencies indicated that precast concrete intermediate diaphragms have been used in all cases.

Diaphragm location along the span varies with span length as well as with bridge type. Bridges built according to the various editions of the AASHTO Standard Specifications for Highway Bridges have diaphragms placed at different positions along the span. Approximately 50% of the respondents indicated that they specified intermediate diaphragm locations that met AASHTO spacing requirements. Half of the agencies place diaphragms at the mid-span according to current AASHTO requirements. Thirty percent of the design agencies require that diaphragms be positioned at the one-third points along the span, while 10% locate diaphragms at the one-quarter points of the span.

Of those respondents that use cast-in-place intermediate diaphragms, most use those that are nearly the full girder depth, from the underside of the slab to the top of the girder bottom flange. About 20% of the design agencies specify that the cast-in-place diaphragms have depths equal to the depth of only the girder webs.

Of the approximately 40% who specify steel channel intermediate diaphragms (see Fig. 1.1a), the most commonly used shapes are: C15X33.9, C12X20.7, C10X15.3, and MC18X42.7. Some agencies commented that the size of channel is determined on a case by case basis. When bent plates are used, they are usually about 3/8-in. thick with 3 1/2 in. flanges. The few agencies which use steel I-shape diaphragms specify W12X26 sections or W-sections that have a depth equal to the girder web depth.

Approximately 30% of the respondents have specified truss intermediate diaphragms (see Fig. 1.1b and c). The truss usually consists of diagonal members and one or two chords. Most often, the chord is a WT6X15, WT12X26, or L5X3X1/2 shapes. The diagonal member is usually a L3X3X5/16 or a L3 1/2X3 1/2X1/2. Fifteen percent of the respondents specify diagonal brace or cross brace

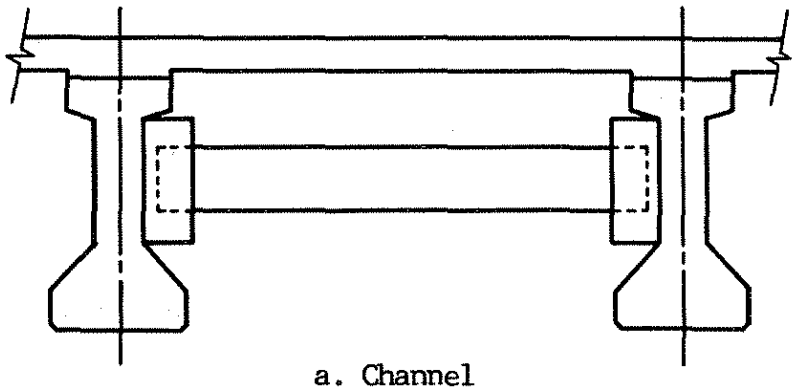

a. Channel

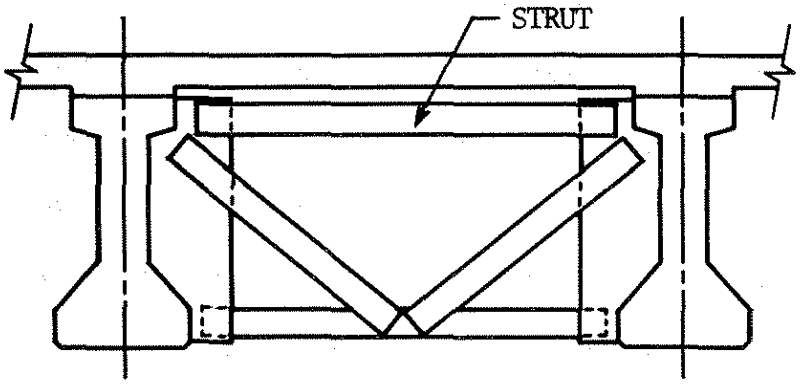

b. K-brace

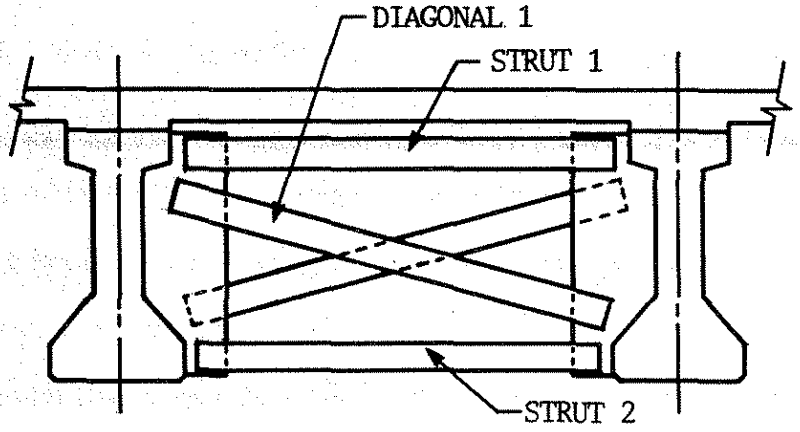

c. X-brace

Fig. 1.1. Typical diaphragms used in P/C bridges.

diaphragms, which are similar to truss diaphragms except that there are no struts. Diagonal brace diaphragms are simply cross brace diaphragms with only one diagonal member (i.e. Fig. 1.1c with strut 1 and diagonal 1 removed). The most used steel shape for these types of diaphragms are: L5X3X1/2, L4X4X3/8, L3X3X5/16, L3 1/2X3 1/2X1/2, and WT6X15.

Less than 50% of those who responded said that intermediate diaphragms are used for the purpose of temporarily supporting the girders during construction. And less than 20% of the respondents claimed that they use intermediate diaphragms to minimize the damage to bridge girders caused by impact forces from overheight traffic beneath the bridge.

Cast-in-place concrete diaphragms that are in contact with the underside of the deck are usually connected to the deck by reinforcing bars that extend from the top of the diaphragm and are later cast into the deck. The connection with the girders usually consists of coil ties or other threaded inserts used with coil rods or bolts. Another type of girder-diaphragm connection noted by respondents is accomplished by passing normal reinforcing bars from the diaphragms through holes cast in the girder web that are later grouted. Steel diaphragms are usually connected to the webs of the girders with bolts that pass through the girder web and a steel bracket or angle(s) to which the diaphragm is attached.

Over 90% of those completing the questionnaire stated that the design of their standard diaphragms and connections are established by a "rule of thumb" approach. The few who apply specific design criterion to intermediate diaphragms consider lateral forces (not necessarily impact) in their analysis. Diaphragm connections are reported to be designed to resist shear. Steel intermediate diaphragms are reportedly designed according to accepted steel design methods.

Many agencies were unable to provide accurate data regarding the number of prestressed concrete girder bridges in their jurisdiction. Only 60% of all respondents reported the number of P/C girder bridges they had. According to data from the National Bridge Inventory, there are

approximately 27,000 P/C girder bridges in the United States; this number is approximately 5.5% of the bridge population.

When a bridge is struck by an overheight vehicle, one or more girders can be damaged. Multiple girder impacts are common and are probably caused by vehicles that are just over the height of the bridge opening. Therefore, these vehicles are able to continue under the bridge once the first impact has occurred and strike an additional girder(s). It is not uncommon to find that the first girder is damaged while the adjacent girder is not damaged. This occurrence is most likely caused by the deflection of the impacting portion of the vehicle as the vehicle continues to move under the bridge. One or more of the remaining girders can be damaged as the impacting portion of the vehicle rebounds after the initial impact. Damage to three or more girders is not uncommon.

Of the reported incidences of impact from overheight vehicles, there was no damage to the girders in 40% of the cases. In 24% of the accidents, there was only minor damage that did not require repair. Damage to the bridge girder(s) that requires minor repair occurs in about 10% of the accidents. Moderate girder damage is caused in approximately 13% of the incidences; one out of every twenty impacts causes major damage that requires girder replacement(s).

On the basis of the total number of repairs to prestressed concrete girder bridges, about 50% of those responding to the questionnaire reported that 75% of the repairs are related to overheight vehicle impacts. Each agency was asked to include copies of their standard details and specifications for all types of intermediate diaphragms used in their jurisdiction. The plans received were reviewed to determine the various diaphragms used by other agencies and to assist in the determination of the types of diaphragms to be used in the experimental portion of the investigation. Several different diaphragms were considered, but due to time and budget constraints and limitations imposed by the girder depth, only those diaphragms most likely to be used as possible replacements for the cast-in-place concrete diaphragms used by the Iowa DOT were tested.

2. DESCRIPTION OF TEST SPECIMENS

This chapter outlines the details of the model bridge used in this investigation. The instrumentation, procedures employed, and the actual tests performed are presented in Chapter 3. Discussion and analysis of the measured responses and descriptions of the behavioral characteristics that were noted during the testing are presented in Chapter 4.

2.1. Bridge Model

A large bridge model, shown in Fig. 2.1, was constructed and tested to establish characteristic behavioral responses to lateral and vertical load combinations applied to the bottom flange of the prestressed concrete (P/C) bridge girders. Shown in Fig. 2.1a are the P/C bridge girders in place as well as the P/C load girder that was used as a reactive member for the horizontal loadings. A photograph of the completed bridge model is shown in Fig. 2.1b. Strains and displacements at selected locations (discussed in Chapter 3) on the superstructure were monitored during load applications to establish how these parameters were influenced by changes in the intermediate diaphragm construction, configurations, and locations. The bridge model was not built to represent a complete full-scale replica of an actual bridge. To keep the size of the experimental model within the space constraints of the structural engineering laboratory and to obtain measurable deformations and strains induced by lateral loads, the researchers minimized the width of the model by using only three P/C girders. A two-girder bridge model was not considered to be appropriate because an interior girder condition would not be represented. The thickness of the reinforced concrete bridge deck was set equal to 4 in. (approximately one-half the thickness of a conventional bridge deck) in order to further reduce the stiffness of the model. The reduced deck thickness increased the response of the superstructure to horizontal loading and increased the sensitivity of the structure for the diaphragms used. Therefore, less load was transferred by the deck and more load was transferred by the diaphragms.

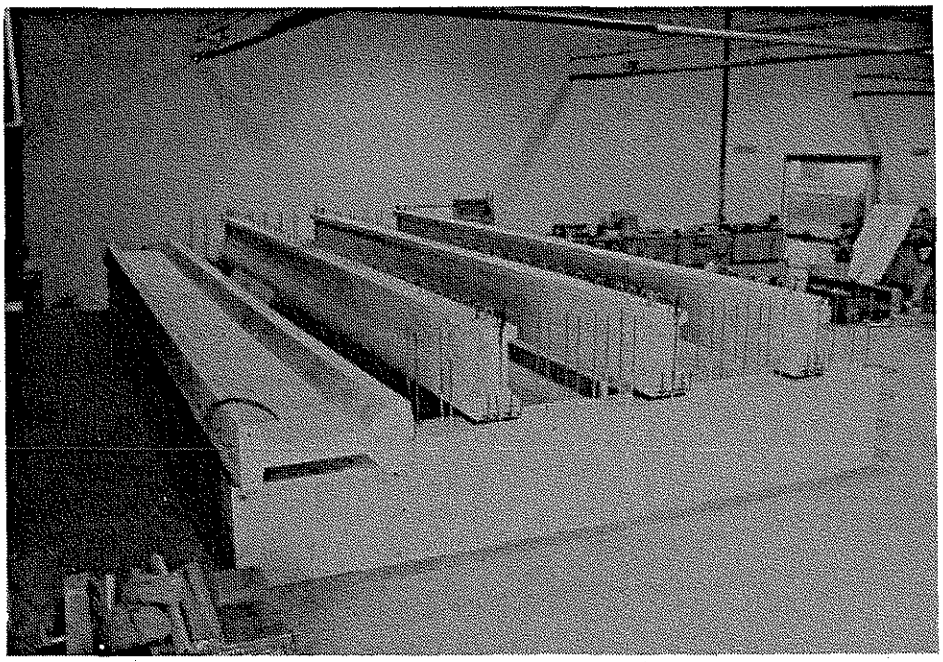

a. P/C Girders in place.

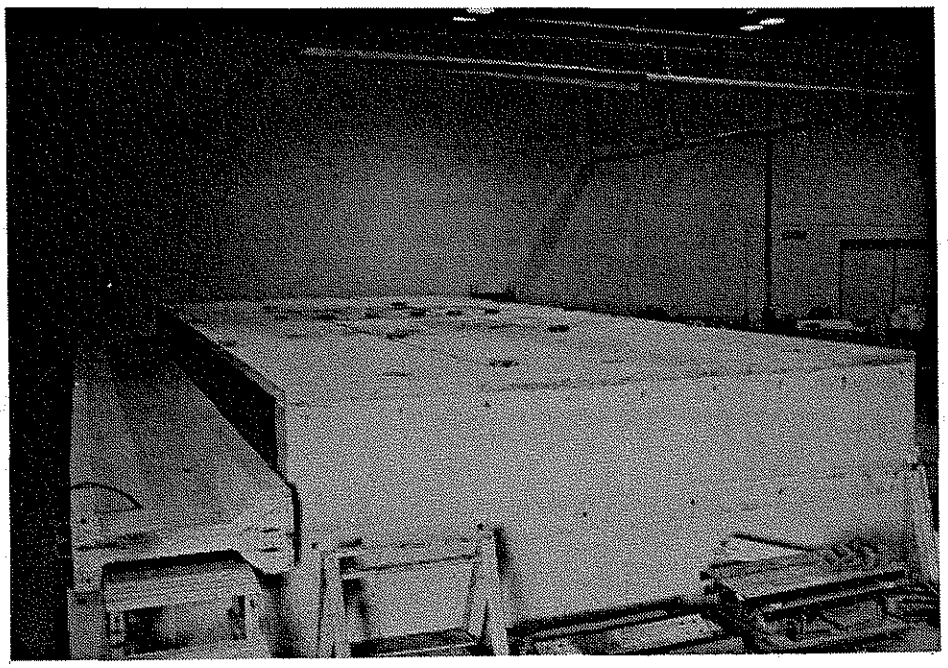

b. Complete bridge model.

Fig. 2.1. Photographs of bridge model.

Figure 2.2 shows the single span bridge model that was 40 ft-4 in. long and 18 ft wide. The P/C girders were spaced at 6 ft on center, which produced a 3-ft slab overhang along both edges of the deck. The three bridge girders, which were the standard Iowa DOT A38 Beams, had additional coil tie inserts and pipe sleeves to accommodate intermediate diaphragm attachments. Figure B.1 (Appendix B) shows the P/C bridge girder cross-sectional dimensions, the locations of the prestressing strands, and the accessory inserts. The A38 bridge beams were supported at their ends on 42-in.-high by 18-in.-wide reinforced concrete abutments. A 17-in.-wide by 12-in.-long by 1-in.-thick elastomeric bridge bearing pad was positioned between the underside of each end of a girder and the concrete abutment as shown in Fig. B.2. The ends of the P/C girders made complete contact over the entire pad surface. Since the bearing pads were the same as those used in bridge construction, the girder support conditions in the bridge model were similar to those present in an actual bridge. The distance between the center lines of the girder supports was 38 ft.-4 in.

As shown in Figs. B.2 and B.3, a full-depth reinforced concrete (R/C) end diaphragm was cast to encase the ends of each P/C concrete girder by 8 in. The full-height No. 5 reinforcing bars, which projected above the concrete abutments and were embedded along each face of the end diaphragms, provided a tie between the end diaphragms and the abutments. To increase the horizontal shear resistance along this construction joint required the top surfaces of the abutments to be roughened, except at the locations where the P/C girders were supported. Additional reinforcement for the end diaphragms consisted of horizontal No. 5 reinforcing bars in each face. As shown in Fig. B.2, the horizontal bars in the outside face of an end diaphragm were continuous and passed by the ends of the P/C girders. The length of the horizontal reinforcement in the inside face of these diaphragms was limited by the clear distance between the P/C girders. Figure B.3a shows that the bottom interior horizontal row of reinforcement was lapped with the 3/4-in.-diameter coil rods, which were threaded into the coil tie inserts cast near the ends of the girders. To produce monolithic construction with the bridge deck (Fig. B.2), No. 5 reinforcing bars were bent and lapped with each

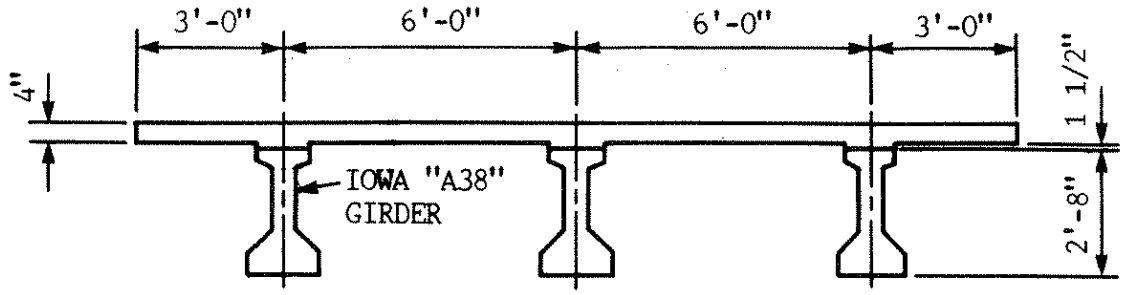

a. Section A-A

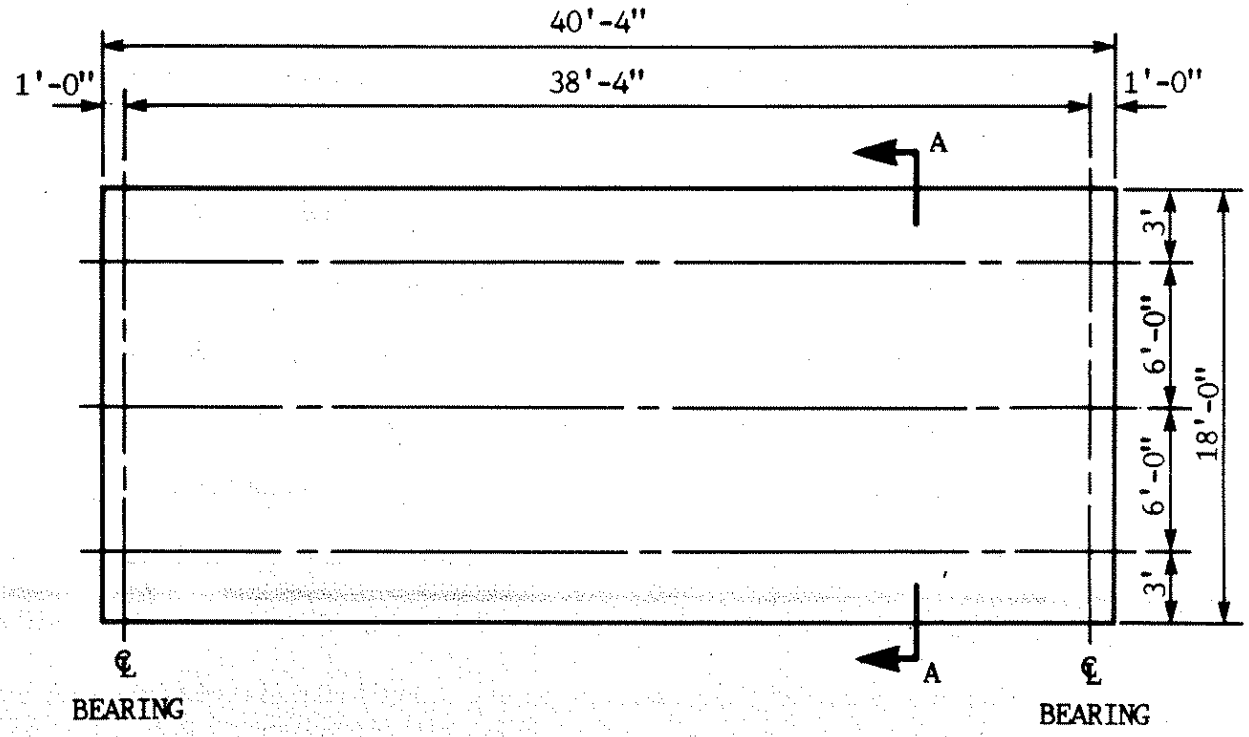

b. Plan view

Fig. 2.2. Model bridge.

vertical bar in an end diaphragm. The horizontal leg of these bent bars were later cast into the concrete deck.

A 1 1/2-in. concrete haunch was formed with the slab over each of the P/C girders in order to facilitate the bridge deck forms. Since only a 4-in.-thick deck was used, the haunch provided additional depth for encasement of the looped tie bars that projected above the top of the P/C girders. The longitudinal slab reinforcement in the bridge deck consisted of two layers of No. 5 reinforcing bars. The spacing for the top longitudinal bars (Fig. B.4) was 9 in. on center near the P/C girders and 12 in. on center between the girders, and the spacing for the bottom longitudinal bars (Fig. B.5) was 12 in. on center, except at the girder location. The transverse slab reinforcement, shown in Fig. B.6, consisted of No. 5 reinforcing bars at 12 in. on center throughout the bridge length, resulting in an 8 in. edge distance for the bars at the end diaphragms. Since the bridge deck was 4 in. thick, the transverse reinforcement was positioned essentially at the mid-thickness of the slab. This location produced minimal flexural resistance to transverse bending moments which were induced in the slab by both horizontal and vertical loading on the bottom flange of the P/C girders.

All steel bar reinforcement was ASTM A615 Grade 40 steel. Since stiffness and not strength or durability performance was the behavioral response being investigated, Grade 60 steel and epoxy-coated reinforcement, which is normally specified for bridge construction, were not used in this experimental investigation. Tension tests of the steel reinforcement were not conducted since the deck flexural strength was not of the variables in this research.

The experimental bridge was built to establish the response characteristics of various types of intermediate diaphragms; therefore, installation and removal of the intermediate diaphragms was necessary. To produce essentially identical initial conditions for all of the intermediate diaphragms, the researchers cast the bridge deck prior to the installation of any of the intermediate diaphragms.

In order to facilitate the casting of the R/C intermediate diaphragms, which occurred after the bridge deck was in place, access holes were provided through the slab by short segments of 6-in.

diameter poly-vinyl-chloride (PVC) plastic pipe. The sleeve inserts were placed between the P/C bridge girders at the third-point locations and at the midspan of the bridge, as shown in Figs. B.4 and B.5. These holes remained open during the testing of the bridge, except when the R/C diaphragms were installed. Reinforcement from the R/C diaphragms was extended into the holes to provide a positive connection between the diaphragms and the deck.

The concrete strength for the abutments, P/C girders, diaphragms, bridge deck, and intermediate concrete diaphragms are listed in Table 2.1.

2.2. Intermediate Diaphragms

2.2.1. Diaphragm Types, Locations, and Designations

Since the same end diaphragms (shown in Figs. B.2 and B.3) were used throughout the experimental testing of the various intermediate diaphragm types, the term diaphragms will be used to refer to intermediate diaphragms throughout this report. The type and location of the diaphragms affects the response of a bridge superstructure. The types of diaphragms that were incorporated into the experimental bridge model were reinforced concrete, two sizes of structural steel channels, and steel cross braces with and without a horizontal strut. Diaphragms at both the midspan and at the third-point locations of the span, as shown in Fig. 2.3, were tested. The diaphragm locations labelled A1, A2, and B1, B2 indicate the positions of the intermediate diaphragms at the third points of the bridge span and at the midspan, respectively. In addition, the response of the bridge model without any intermediate diaphragms was investigated. To identify each diaphragm arrangement, the researchers adopted the designations presented in Table 2.2 for this report.

2.2.2. Reinforced Concrete Intermediate Diaphragms

Except for the 6-in. width, the geometric configuration for the R/C intermediate diaphragm, shown in Fig. 2.4 (detailed in Fig. 2.4a and photographed in Fig. 2.4b), was modeled after the standard Iowa DOT reinforced concrete intermediate diaphragm. The spacing and bar size for the vertical and horizontal reinforcement matched those for the Iowa DOT standard R/C intermediate

Table 2.1. Concrete strengths.

Element	Age (days)	f'_c (psi)	Notes
P/C Girders	2/3 1 7 28	5,090 5,300 6,150 7,270	Mix No. 1 5,000 psi 3 3/4-in. slump Unit Wt = 151 lb/ft^3
North Abutment	28	5,630	Mix No. 2 3,500 psi 1 in. max. aggregate size Air-entrained 3 3/4-in. slump
South Abutment	28	4,660	Mix No. 2 except 3 1/4-in. slump
North End Diaphragm	7 28	3,800[a] 5,430	Mix No. 2 except 3 1/2-in. slump
South End Diaphragm	28	4,810	Mix No. 2 except 3 3/4-in. slump
Southern Three-Fourths of Bridge Deck	28	4,360	Mix No. 2 except 3 1/2-in. slump
Northern Portion of Bridge Deck except for Northwest Corner	28 28	5,550 4,920	Mix No. 2 except 2 1/2-in. slump 3-in. slump after water added
North-West Corner of Bridge Deck	28	6,870	Mix No. 2 except 2 3/4-in. slump
Midspan Diaphragm	8 28	3,000 4,280	Mix No. 3 4,000 psi 1/2-in. Limestone chips Air-entrained 4 to 5-in. slump

Table 2.1. Continued.

Element	Age (days)	f'_c (psi)	Notes
North Third-Point Diaphragm	7 28	3,360 4,720	Mix No. 4 4,000 psi 1/2-in. Limestone chips Air-entrained Superplasticizer 6-in. slump
South Third-Point Diaphragm	4[b] 7 28	4,140 4,470 5,680	Mix No. 4 except 4-in. slump
[a]One cylinder test [b]Forms removed			

Table 2.2. Intermediate diaphragm designations.

Designation	Description
C1.1	MC 8x20.8 structural steel channel diaphragm at the midspan
C1.3	MC 8x20.8 structural steel channel diaphragm at the third-points of the span
C2.1	C 15x33.9 structural steel channel diaphragm at the midspan
C2.3	C 15x33.9 structural steel channel diaphragm at the third-points of the span
RC.1	Reinforced concrete diaphragm at the midspan
RC.3	Reinforced concrete diaphragm at the third-points of the span
X1.1	MC 8x20.8 steel cross-brace with horizontal strut diaphragm at the midspan
X2.1	MC 8x20.8 steel cross-brace diaphragm at the midspan
ND	No intermediate diaphragms

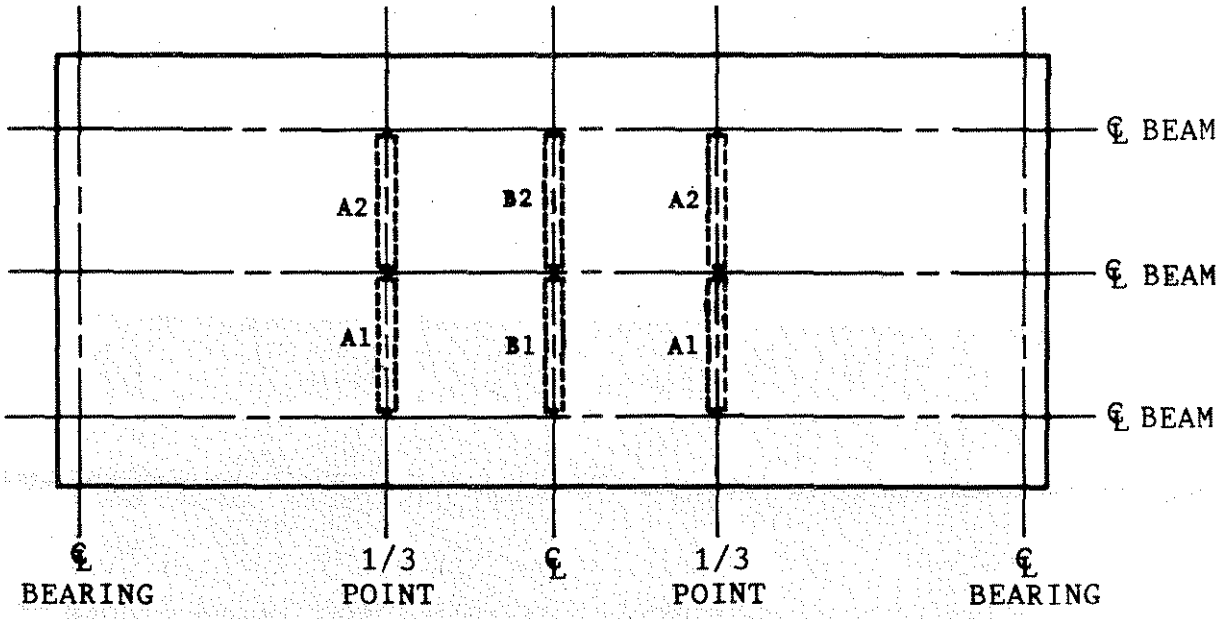

Fig. 2.3. Diaphragm layout.

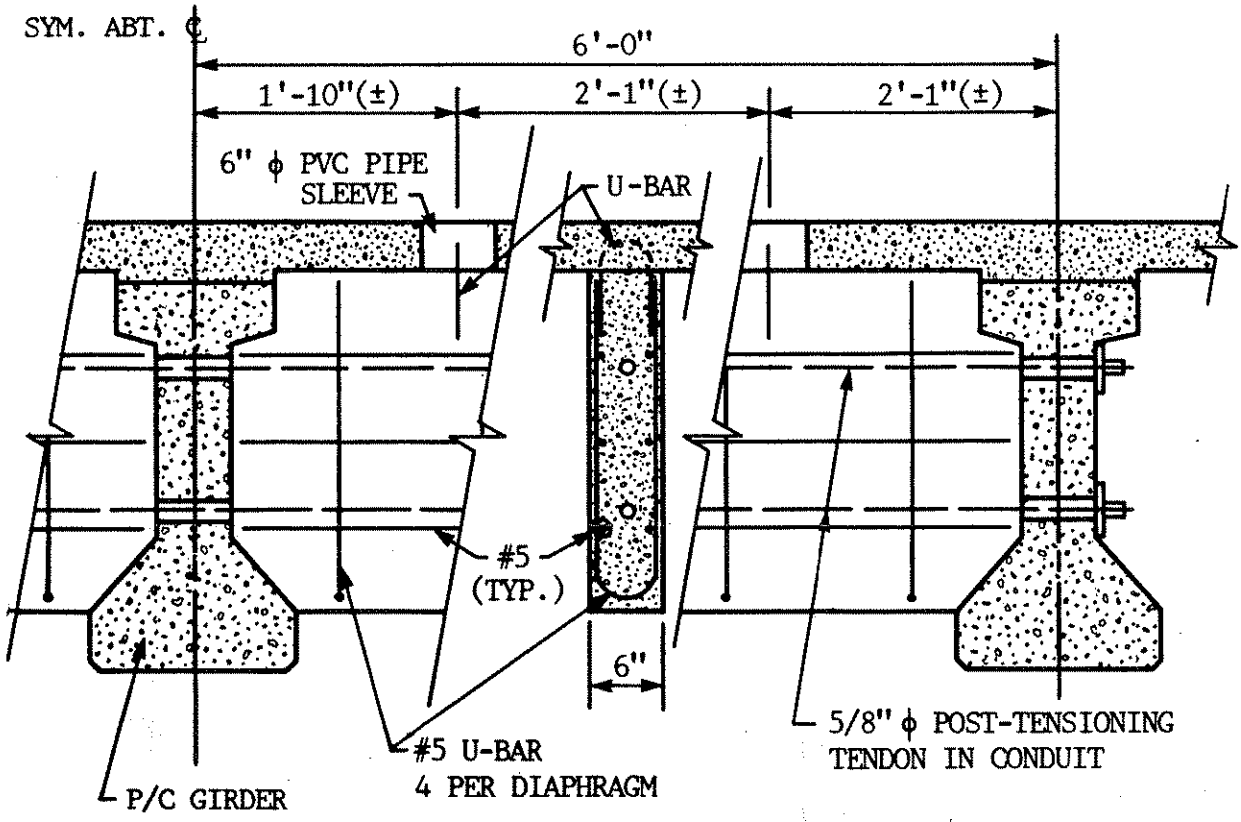

a. Details

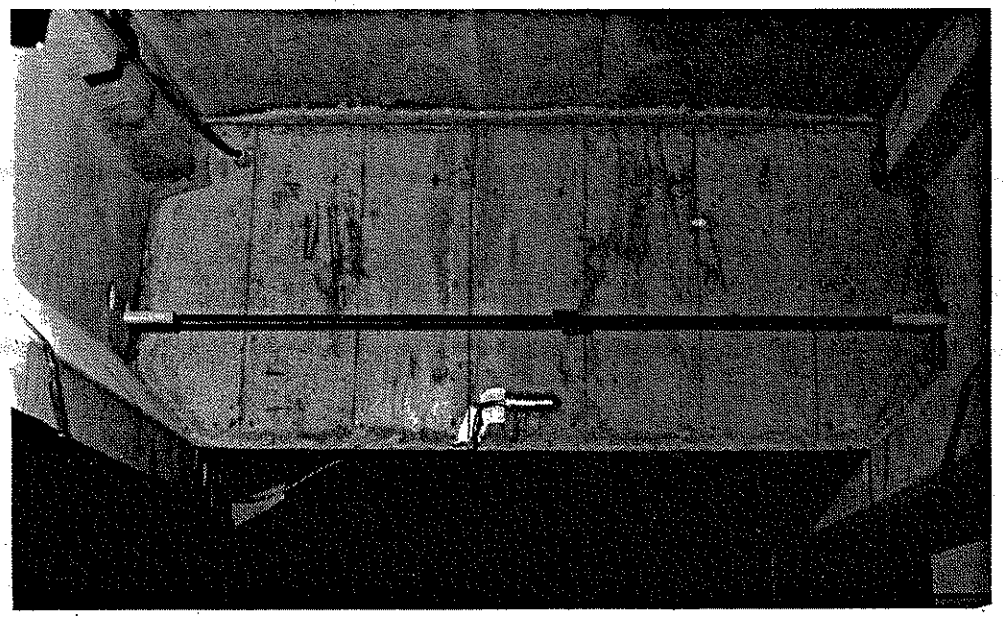

b. Photograph

Fig. 2.4. Reinforced concrete intermediate diaphragm (Designations RC.1 and RC.3).

diaphragm. Since the slab was already in place when these diaphragms were cast, the connection between these diaphragms and the deck was modified from the Iowa DOT standard detail.

To provide a reinforcement tie between the slab and each diaphragm called for a hair-pin-shaped reinforcing bar placed through the access holes in the slab. These bars extended through the construction joint between the slab and a diaphragm. At the midspan, No. 5 reinforcing bars were used for the hooped ties; but at the third-points of the span, No. 3 reinforcing bars were used because bending a No. 5 reinforcing bar in a tight radius was difficult to accomplish.

Since the concrete for the diaphragms was cast through the PVC pipe sleeves in the deck, the higher slump concrete mix as noted in Table 2.1 was used to allow the fresh concrete to flow and fill the forms. For consolidating the concrete within the diaphragms, a concrete vibrator was probed through the access holes and was held against the sides of the forms.

Figure 2.4a reveals that at a depth of about 8 in. and 20 in. below the 4-in.-thick bridge deck, 3/4 in. diameter PVC plastic pipes were cast in the center of the diaphragms. These pipe sleeves, which were in horizontal and vertical alignment with holes cast in the web of the P/C girders, were provided as access conduits for 5/8 in. diameter post-tensioning tendons. The high-strength tendons were continuous through the three P/C girders and two R/C diaphragms. For each tendon, 1/2-in. thick steel bearing plates were positioned against the outside face of the web of each exterior P/C girder. By tightening the nuts on the tendons, the P/C girders and the diaphragms were structurally connected. The tendons were tightened with a wrench after the concrete for the diaphragms had cured for a minimum of 7 days.

After completion of the testing involving the R/C midspan intermediate diaphragms, these diaphragms had to be removed. The tendons were withdrawn from the conduits, and the concrete was broken at selected locations with an air hammer. The concrete within the access holes in the slab was sufficiently removed so that the hair-pinned-shaped dowels could be cut. The midspan

diaphragms were removed so that the bridge could be tested with R/C diaphragms at only the third-points of the span.

2.2.3. Steel Channel Intermediate Diaphragms

2.2.3.1. Deep Channel Diaphragm

Figure 2.5 (details in Fig. 2.5a and photograph in Fig. 2.5b) shows the standard Iowa DOT steel channel diaphragm. The C15 x 33.9 structural steel diaphragm had a depth equal to almost 50% of the P/C girder depth and about 94% of the web depth of the girders. After the bridge deck had cured, the channels were installed by bolting the web of each diaphragm to the outstanding legs of the angles that had been bolted to the webs of the P/C girders as shown in Fig. 2.5a. To facilitate two sizes of channel diaphragms and different vertical positions for the smaller channels requires equal bolt spacing, which is slightly different from the bolt spacing shown in the standard Iowa DOT diaphragm connection detail; however, the hole size in both the channel web and angle leg matched the Iowa DOT Standard. The horizontally slotted hole in the outstanding angle leg allowed for variations in the alignment at the P/C girders as recommended by the Iowa DOT. To increase the frictional resistance induced by the clamping forces generated by tightening the high tensile strength bolts at the diaphragm connection, the researchers used 1-in. diameter rather than 7/8-in. diameter (Iowa DOT Standard) A325 bolts. The connection between the angle bracket and the P/C girder webs was made using 1-in. diameter A307 bolts. The A325 bolts, which fastened the channel webs to the angles, were tightened to the minimum bolt tension by using the turn-of-the nut method during the bolt installation.

2.2.3.2. Shallow Channel Diaphragm

To investigate the effect of the channel size on the load distribution behavior, the researchers replaced the standard Iowa DOT channel diaphragm (C15 x 33.9) by a shallower channel (MC8 x 20). The depth of the MC8 diaphragms was equal to 25% of the 32-in. depth of the P/C girders and

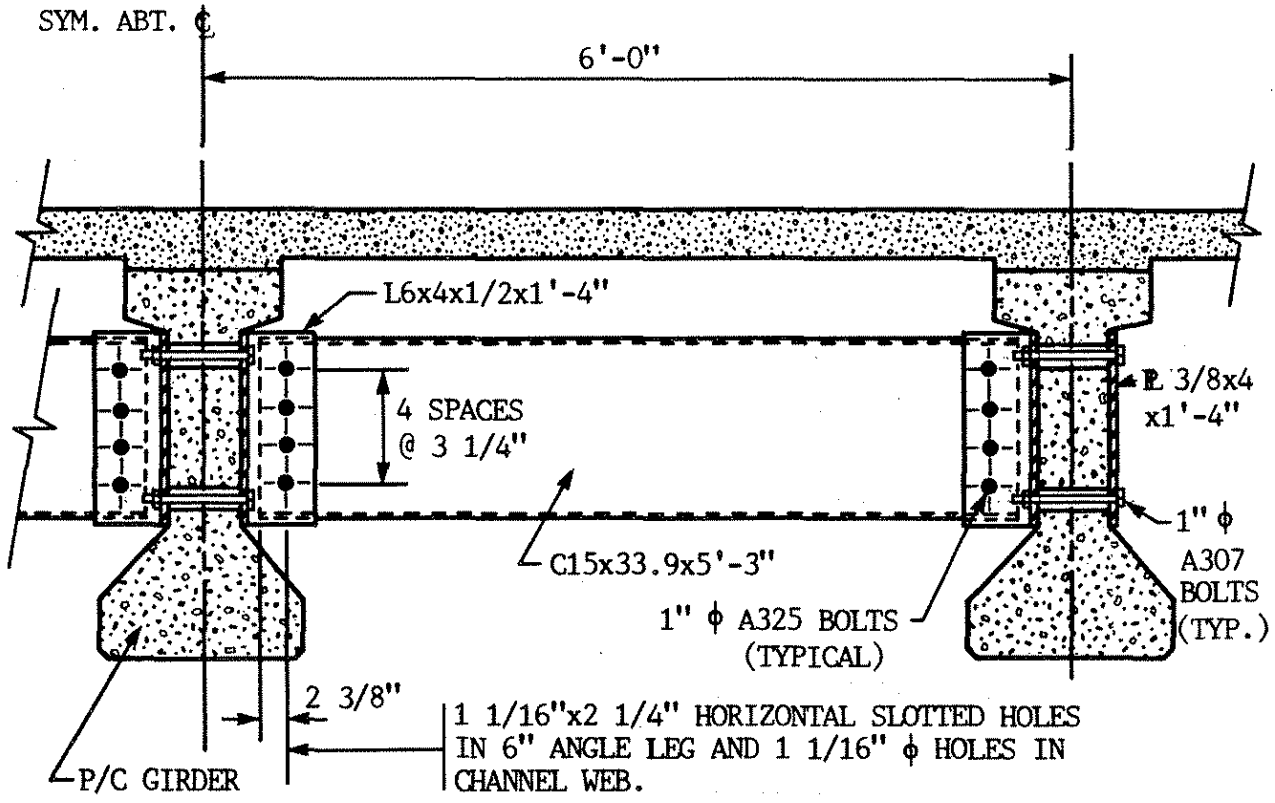

a. Details

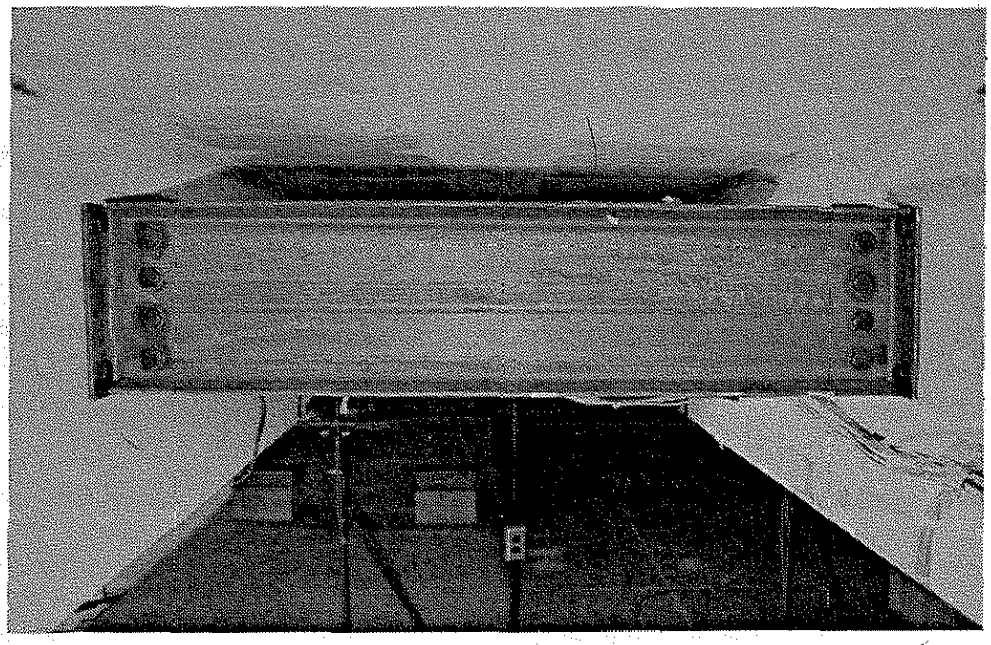

b. Photograph

Fig. 2.5. Deep steel channel intermediate diaphragm (Designations C2.1 and C2.3).

50% of the web depth of the girders. The shallower channel depth more closely represented the geometric configuration of intermediate diaphragms in bridges containing larger P/C girders.

As shown in Fig. 2.6 (details in Fig. 2.6a and photographs in Figs. 2.6b and 2.6c), the 8-in. deep channels were attached to the same angles which had previously supported the 15-in. deep channels. For all tests except one, the vertical position for the mid-depth of the MC8 diaphragms was at the mid-height for the web of the P/C girders as shown in Fig. 2.6b. Therefore, the center two bolt holes in the outstanding leg of the angle bracket were used to bolt the channel diaphragms to the girders. The alternate position for the MC8 diaphragms involved connecting these channels to the angle brackets by using the lower two bolt holes in the outstanding angle legs as shown in Fig. 2.6c. This diaphragm position was used only for the midspan diaphragm tests when loads were applied to the south exterior girder as discussed in Section 3.3.

2.2.4. Steel X-Brace Intermediate Diaphragms

2.2.4.1. With Horizontal Strut

Figure 2.7 (details in Fig. 2.7a and photograph in Fig. 2.7b) shows the steel strut and cross-brace assembly that was developed and modeled after the diaphragms used by some state agencies. This diaphragm provided lateral support to the P/C girder along essentially the entire depth of the girder at the diaphragm location. A wood template was used for a pattern in the fabrication of the actual structural steel diaphragm. The 3/4-in.-thick gusset plate was cut to match the general cross-sectional profile of the girder along one side. Along four of the five fitted edges of the gusset plate, 3/4-in.-thick by 6-in.-wide plates were welded at right angles to the gusset plate. These edge plates were used to fasten the gusset plate to the P/C girders. Holes were drilled in the 3/4-in.-thick edge plates to match the coil inserts that had been installed in the flanges of the P/C girders and to match the holes cast in the girder webs. Bolts were used to secure the steel brackets to the girders.

After the steel brackets were attached to the girders, the MC8 x 20 cross brace and strut members were installed. Four 1-in.-diameter A325 bolts were used to fasten each end of the

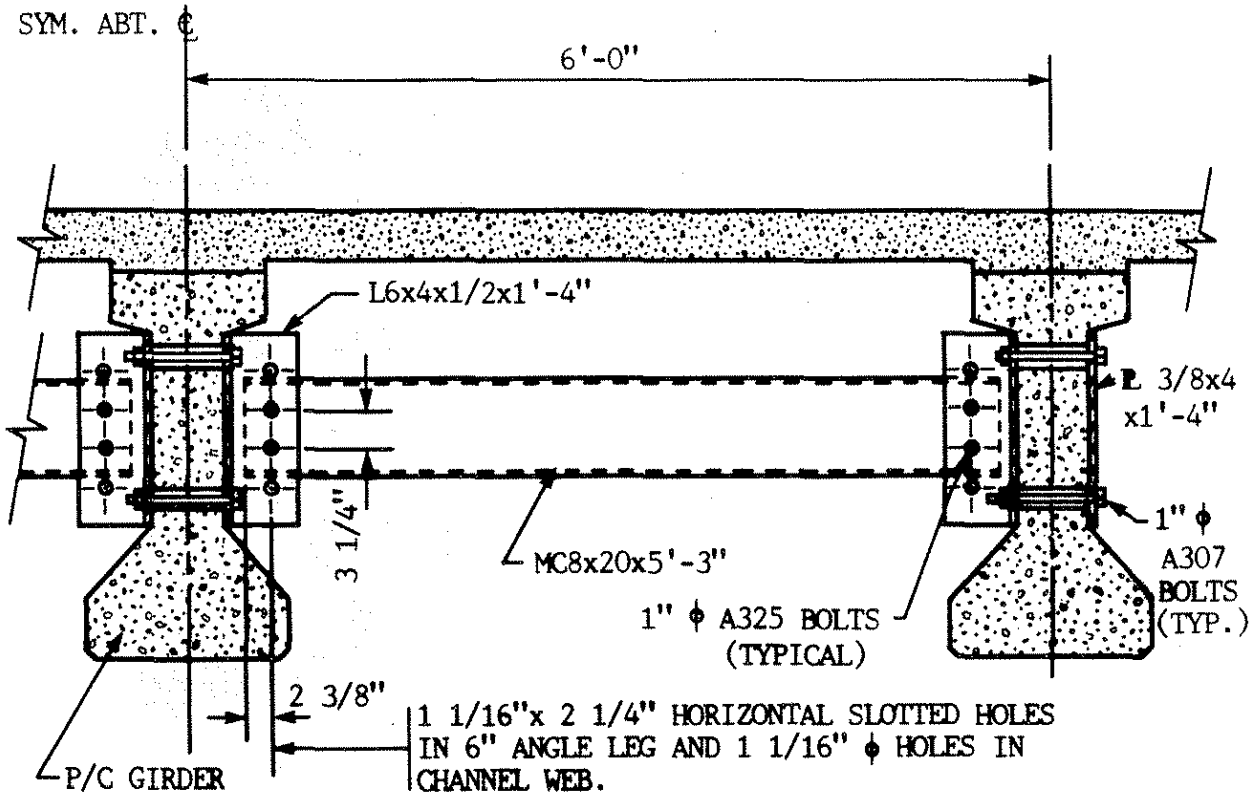

a. Details

Fig. 2.6. Shallow steel channel intermediate diaphragm (Designations C1.1 and C1.3).

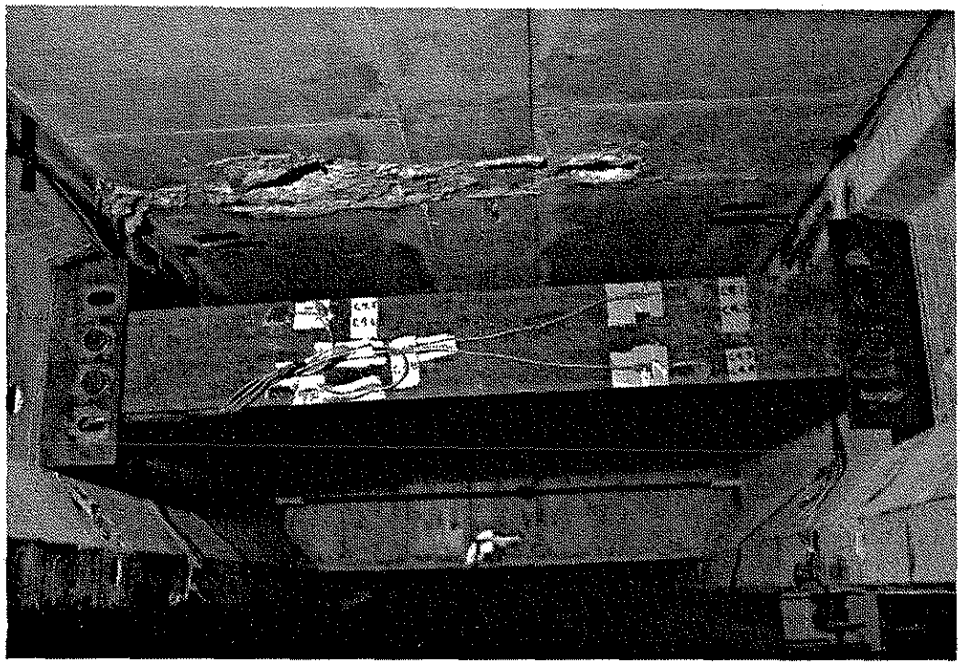

b. Photograph of channel in normal position.

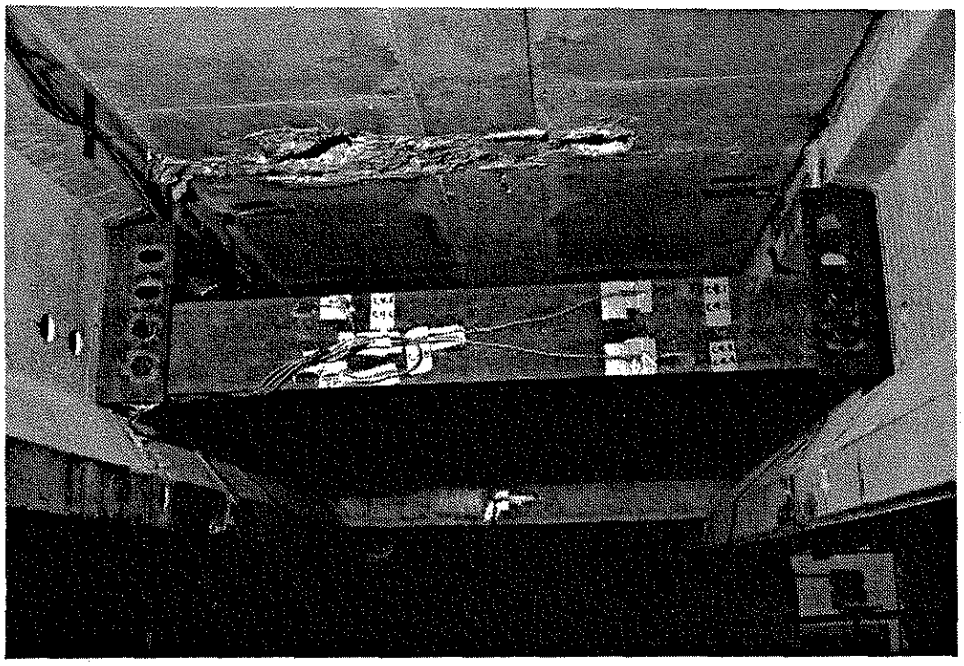

c. Photograph of channel in alternate position.

Fig. 2.6. Continued.

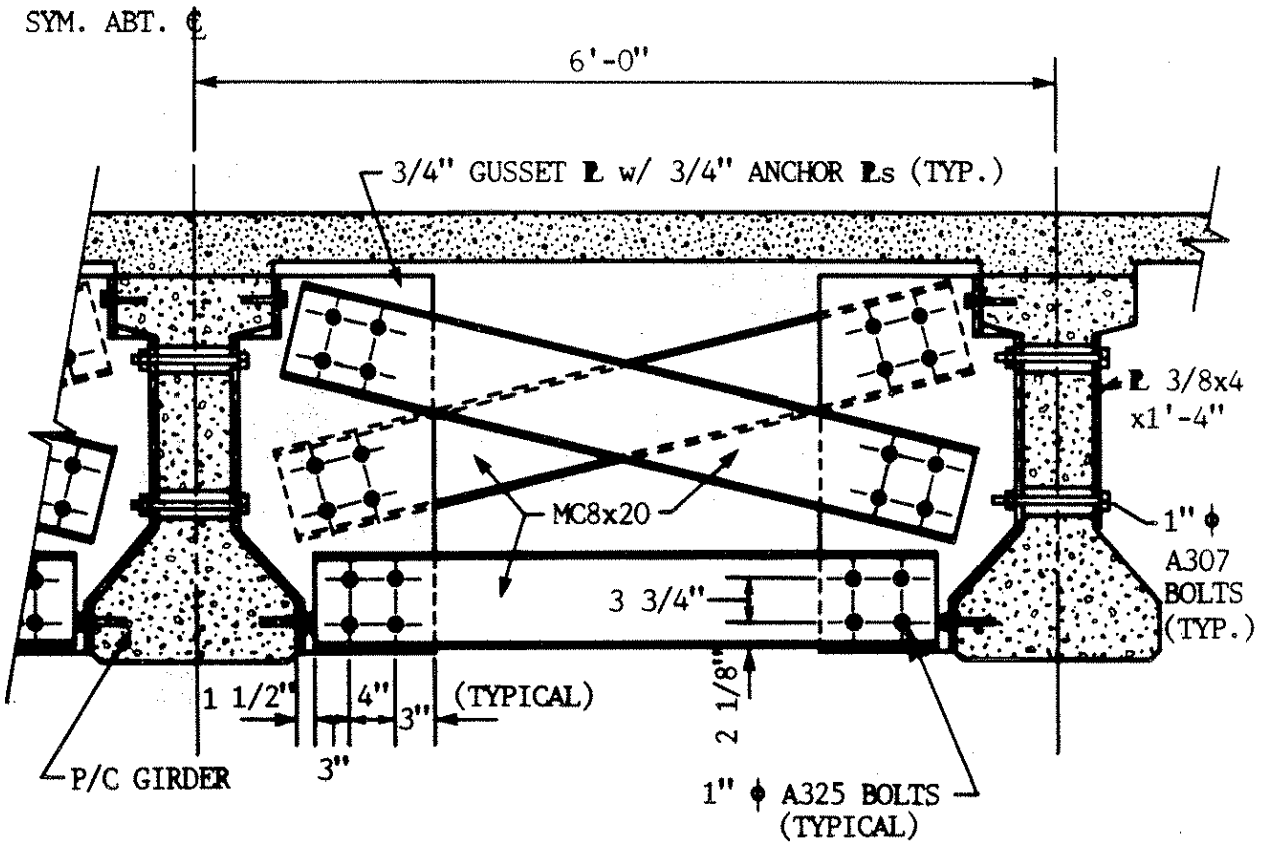

a. Details

Fig. 2.7. Steel X-brace intermediate diaphragm (With horizontal strut, Designation X1.1 and without horizontal strut, Designation X2.1).

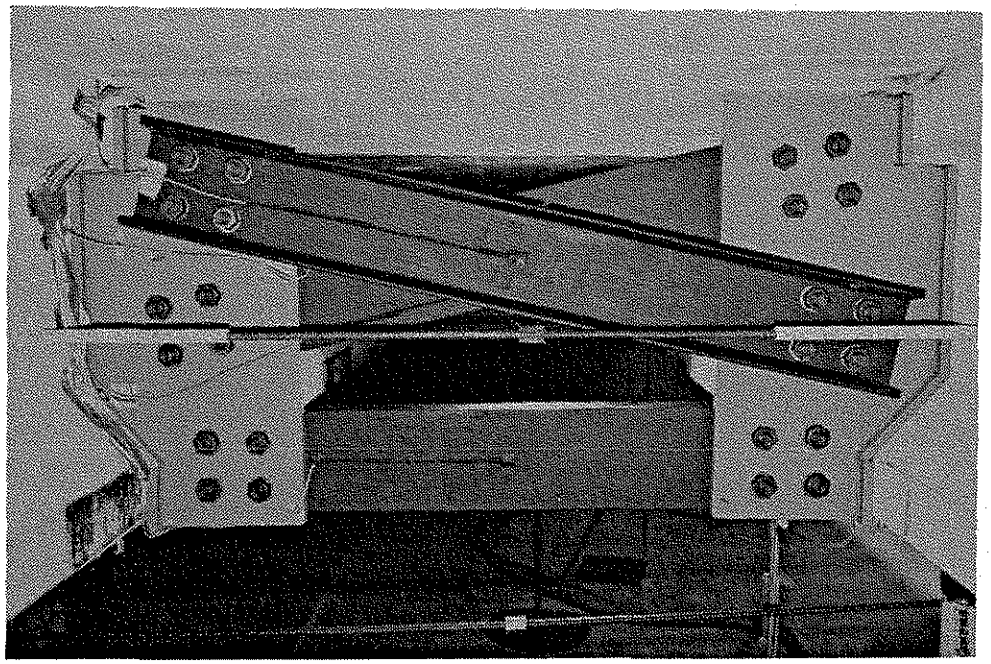

b. Photograph of X-brace diaphragm with horizontal strut.

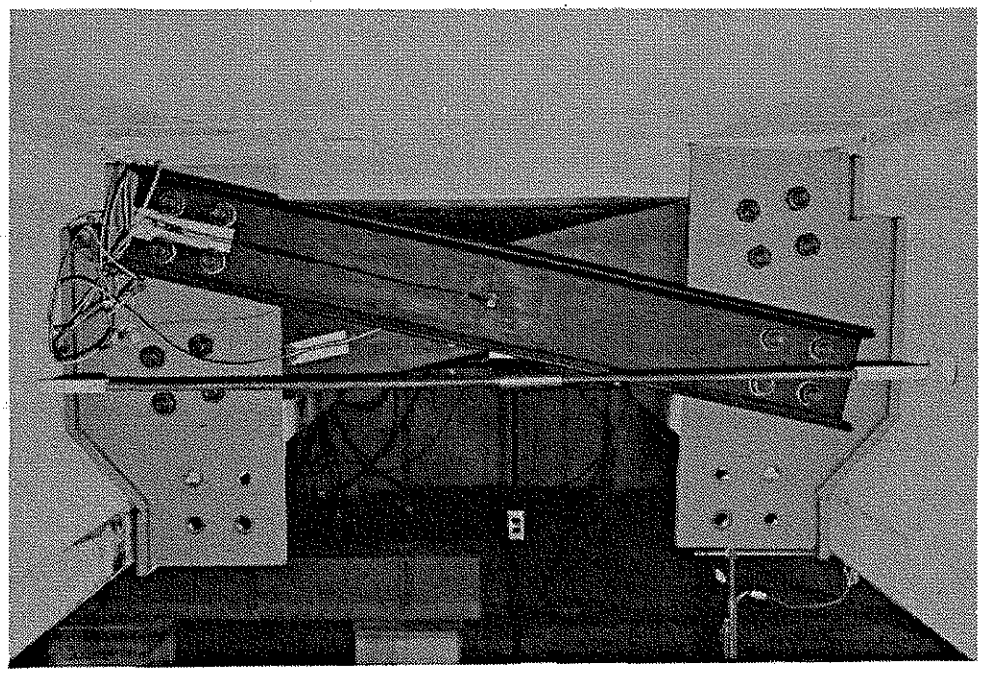

c. Photograph of X-brace without horizontal strut.

Fig. 2.7. Continued.

channel-shaped members to the gusset plates. The turn-of-the nut method was applied to develop the minimum bolt tension for proper installation of these fasteners.

2.2.4.2. Without Horizontal Strut

Another configuration for a steel diaphragm was established by removing the horizontal strut from the intermediate diaphragm described in Section 2.2.4.1. The configuration for the diaphragm was a single cross brace as shown in Fig. 2.7c. To simplify the construction of the assembly, the bottom connections for the MC8 cross-bracing members were not lowered towards the girder bottom flange. The presence of the 3/4-in.-thick gusset plate, which extended to and was attached to the girder bottom flange, provided a significant amount of lateral support to this flange. Greater diaphragm stiffness might have been obtained if the cross braces had been repositioned by lowering the bottom connections of the cross members.

2.2.5. No Diaphragms

The model bridge was also tested without any intermediate diaphragms present. However, as previously discussed, the end diaphragms were present.

3. TESTS AND TEST PROCEDURES

This chapter outlines the details of the specific tests and events that occurred in conducting the laboratory tests. The model bridge with the various configuration of diaphragms (located at either the midspan or at the third points of the span) was subjected to horizontal and vertical loading. In the following sections, test setups, instrumentation and procedures will be presented; discussion and analysis of results obtained, as well as the behavior of the various configurations of diaphragms, will be presented in Chapter 4.

3.1. Instrumentation

The instrumentation for all of the tests consisted of electrical-resistance strain gages (strain gages), direct current displacement transducers (DCDTs) and a limited number of mechanical deflectometers (dial gages). The strain gages used on the concrete were manufactured by Texas Measurements, Inc. (College Station, Texas). Polyester PL-90 gages (gage length = 3.54 in., gage width = .04 in.) and PL-60 gages (gage length = 2.36 in., gage width = .04 in.) were used on the prestressed concrete beams, and on the deck and the cast-in-place diaphragms, respectively.

Strain gages employed on the various steel components were manufactured by Vishay Measurements Group (Raleigh, North Carolina). Polyimide encapsulated gages CEA-06-125UN-120 (gage length = .125, gage width = .10 in.) were used on the post-tensioning tendons of the loading apparatus and on the various steel diaphragm elements. All strain gages (concrete and steel) were appropriately temperature compensated and were attached with recommended surface preparation and adhesives. Three-wire leads were used to minimize the effect of the long lead wires and potential temperature changes. All strain gages were water-proofed with a minimum of two layers of protective coatings. Strain gages and DCDTs on the various elements of the bridge were read and recorded with a computerized data acquisition system (DAS). Dial gage readings were recorded by hand in all tests.

A total of 36 strain gages were mounted on the three P/C beams in the bridge model. Figure 3.1 indicates the location of the strain gages; three sections (1/4 span, midspan, and 3/4 span) of each beam were instrumented. At each section, four strain gages--two on the top flange and two on the bottom flange--were oriented with their axis parallel to the longitudinal axis of the P/C beams. As shown in Fig. 3.1, the strain gages at midspan were actually positioned one foot off center to facilitate installation of the various configurations of diaphragms at that location.

Location of the strain gages on the bridge deck are shown in Fig. 3.2. Note that the instrumented Sections B, C, and D are the same sections on the P/C beams shown in Fig. 3.1. Thus, the longitudinal deck gages and beam gages at these sections are in the same plane. At each location where a longitudinal gage is indicated (gage axis parallel to the P/C beam axis) there is one gage on the top surface of the deck. At locations where transverse gages are indicated (gage axis perpendicular to the P/C beam axis), there are two strain gages--one on the top and bottom surfaces of the deck. There are a total of 22 strain gages on the bridge deck--14 oriented with their axis parallel to the P/C beams and 8 oriented with their axis transverse to the beams.

The location of the strain gages employed on the various configurations of diaphragms tested is shown in Fig. 3.3. Shown in Fig. 3.3a is the position of the strain gages used on the channels (Diaphragms C1 and C2.). Note that the eight strain gages on each channel are positioned with their axis parallel to the longitudinal axis of the channels. Depending on whether the diaphragms were located at midspan (C1.1 and C2.1) or at the third points of the span (C1.3 and C2.3), there were a total of 16 or 32 diaphragm strain gages, respectively. Illustrated in Fig. 3.3b is the location of the strain gages used on the concrete diaphragms. As indicated, each concrete diaphragm was instrumented with two strain gages at the mid-distance between the girders 4 in. up from the bottom of the diaphragm with their axis parallel to the diaphragm axis. With diaphragm configuration RC.1 there were four diaphragm strain gages while with RC.3 there were eight diaphragm strain gages. Figure 3.3c illustrates the position of the strain gages on the X-brace plus strut (X1.1) and X-brace

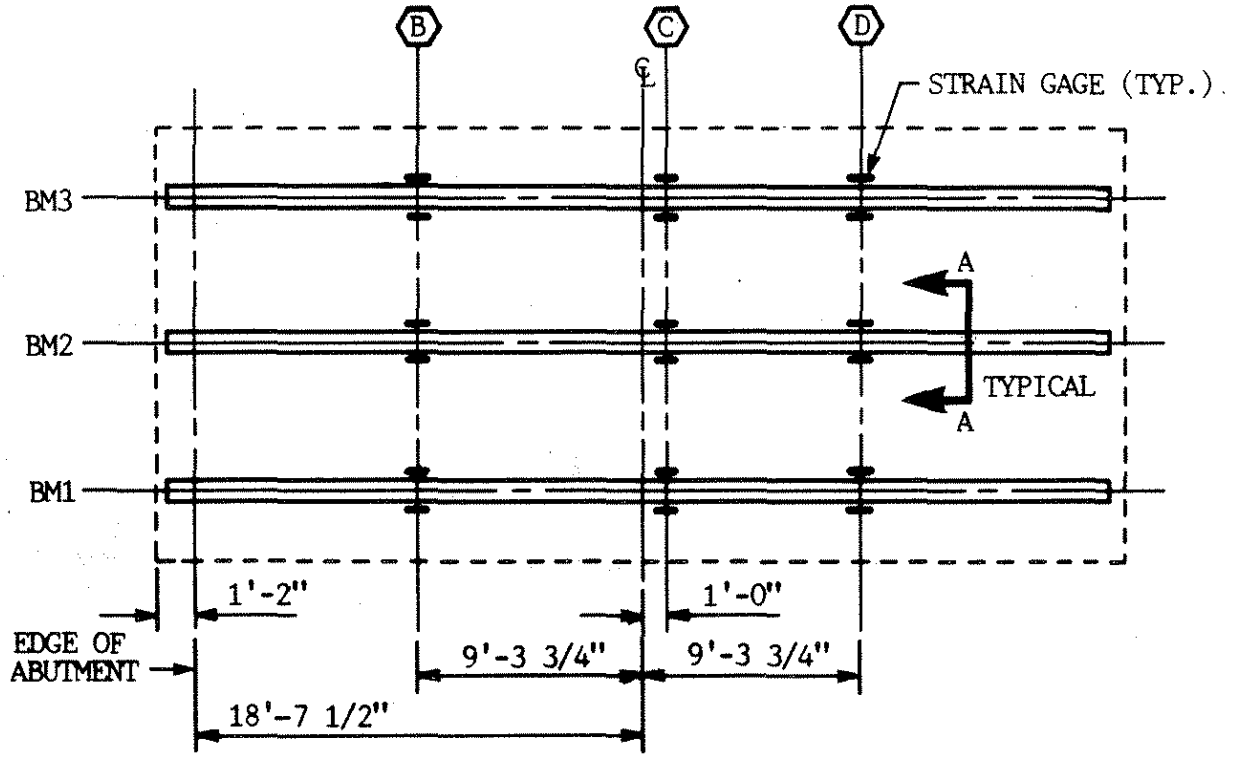

a. Plan view

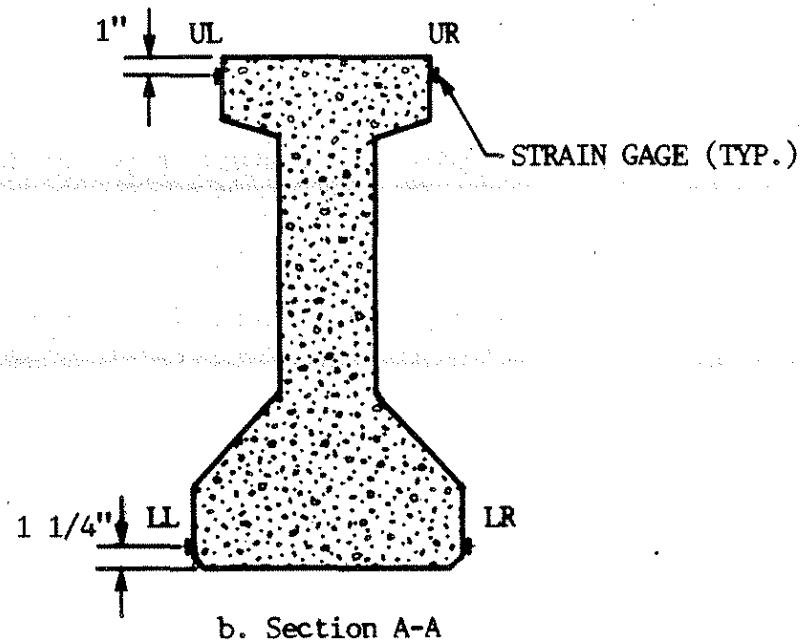

b. Section A-A

Fig. 3.1. Location of strain gages on P/C girders.

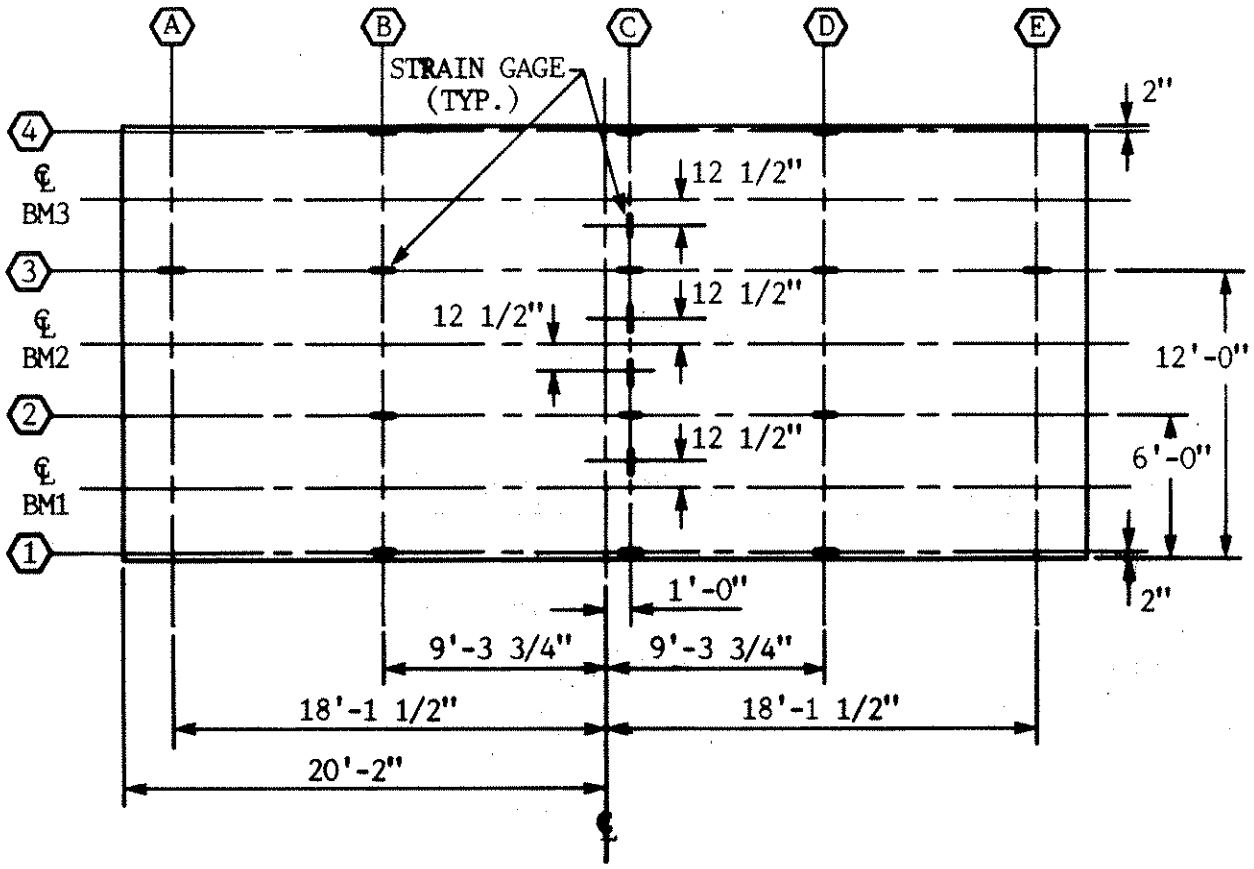

Fig. 3.2. Location of strain gages on deck.

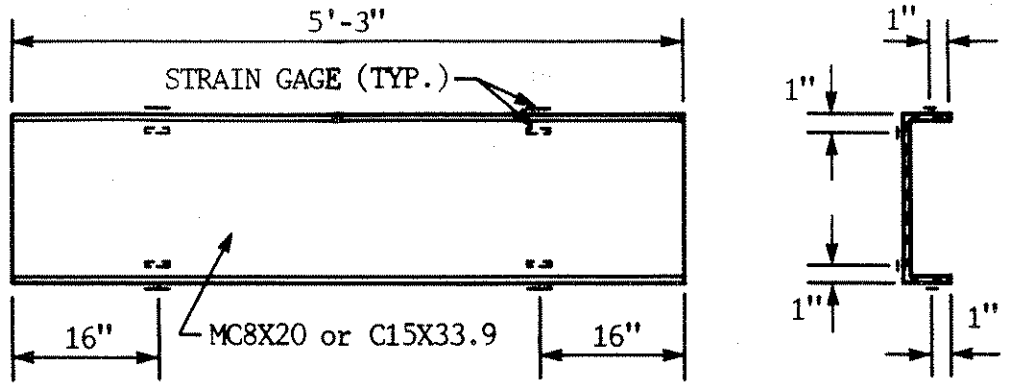

a. C1 and C2 series

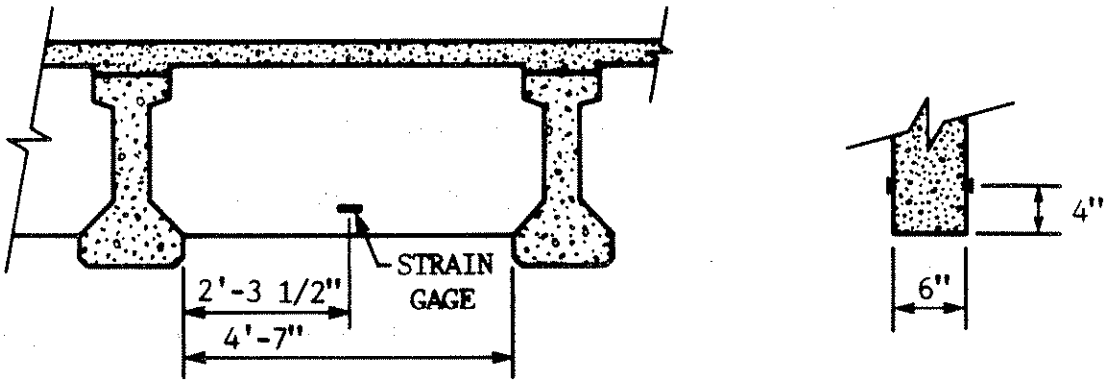

b. RC series

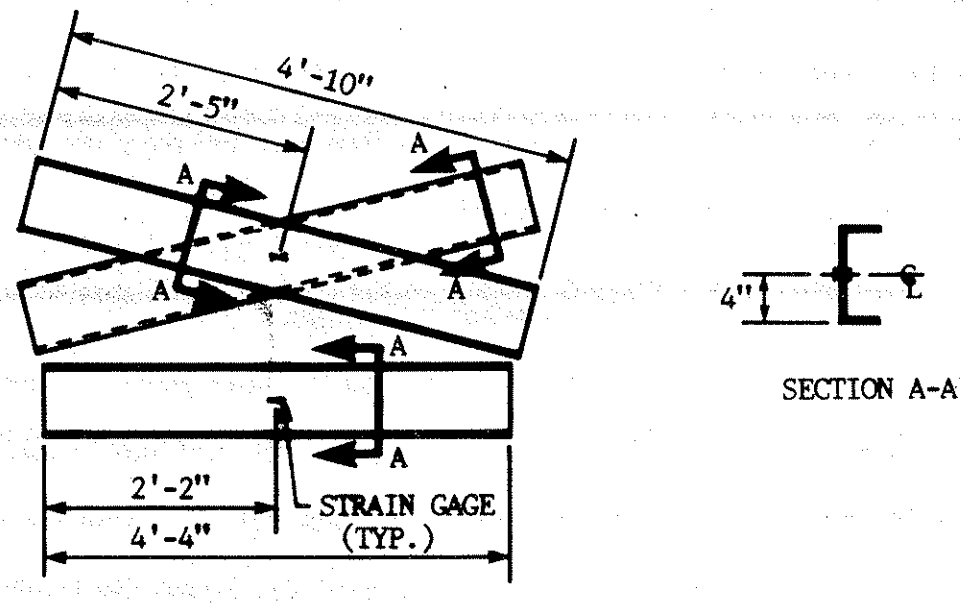

c. X1 and X2 series

Fig. 3.3. Location of strain gages on diaphragms.

(X2.1). All strain gages, two per channel, are positioned with their axis parallel to the axis of each channel member. With the horizontal strut in place (X1.1), there were 12 diaphragm strain gages; while without the struts (X2.1), there were eight diaphragm strain gages.

As the bridge was tested with the various arrangements and configurations of diaphragms, the amount of instrumentation varied. The maximum instrumentation (90 strain gages) occurred with either Diaphragm C1.2 or C2.3 in place, while the minimum amount of instrumentation (62 strain gages) occurred with Diaphragms RC.1 in place.

In addition to the strain gages on the various elements of the bridge, strain gages were also mounted on the post-tensioning tendons employed to apply lateral load to the model (see Section 3.2.2). Two strain gages were mounted on each tendon with their axes parallel with the longitudinal axis of the tendon. The two gages were positioned diametrically opposite each other and thus detected equal and opposite sense bending strains in addition to axial strains. These gages, correctly connected to the DAS, measured the axial force in the tendon as bending strains were cancelled.

As shown in Fig. 3.4, 12 DCDTs were used to measure the vertical and horizontal displacements of the P/C beams. As indicated at the midspan of each beam, both horizontal and vertical displacements were monitored; at the quarterpoints of the span, only horizontal displacements were measured. Also shown in this figure are the three dial gages that were positioned to measure horizontal deck movements.

3.2. Loading Mechanisms

Descriptions of the loading mechanisms used in this investigation are described in the following sections. Due to insufficient available space in the structures laboratory in Town Engineering Building, at the time when this research was initiated, the construction and testing of the bridge was undertaken in the structures laboratory annex (henceforth simply referred to as the annex). The absence of an overhead crane and a structural tie-down floor in the annex required that the loading mechanisms be essentially self-contained. This requirement of self-containment limited

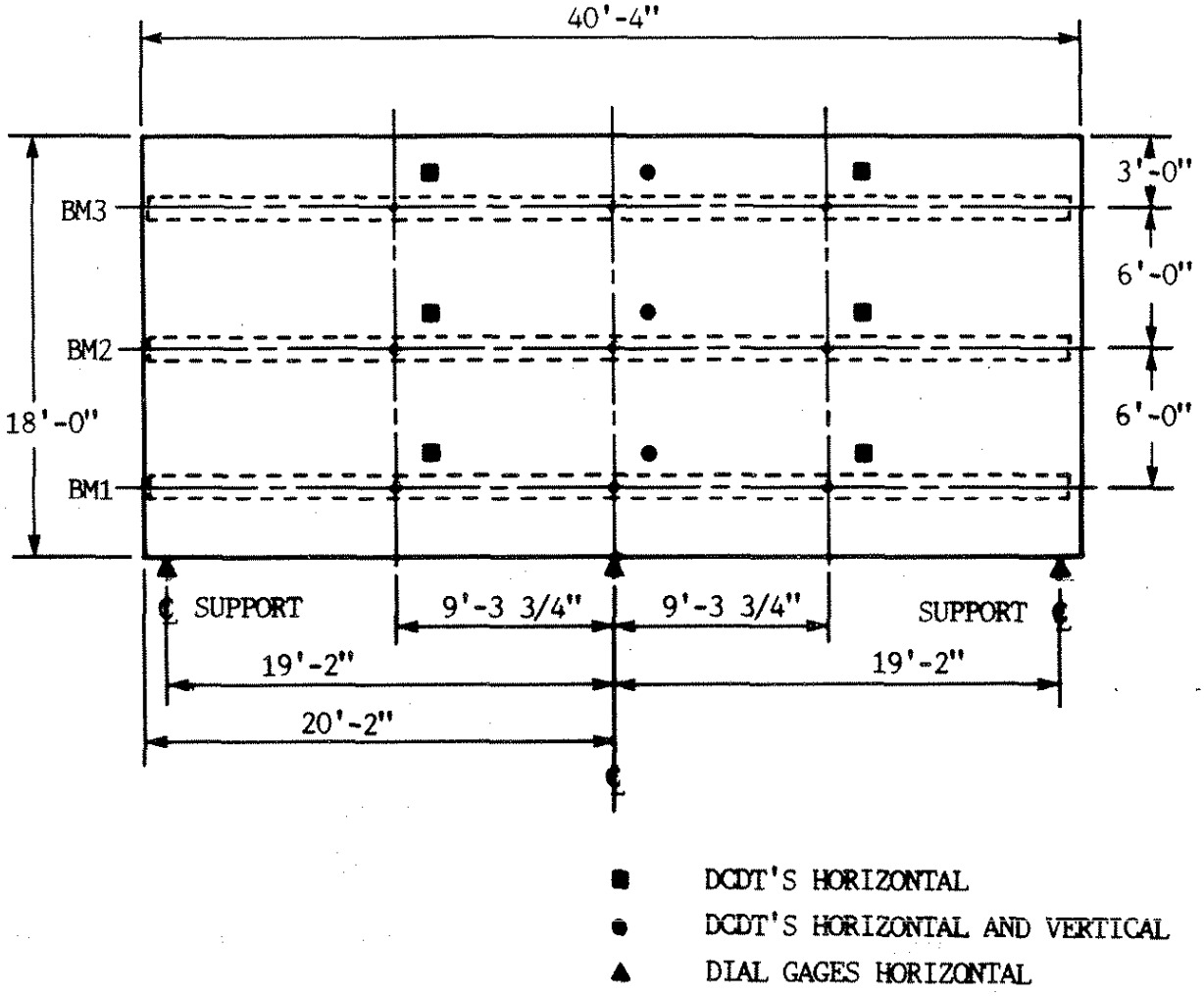

Fig. 3.4. Location of deflection instrumentation.

some of the flexibility in positioning loads and reduced the magnitude of the vertical loads that could be applied. Shown in Fig. 3.5 are the nine loading positions (identified as points 1-9) that were used; a review of this figure and Fig. 2.3 reveals that the load points on the P/C beams are directly in line with the diaphragm locations.

Loading applied to the model bridge simulated loading from overheight vehicles striking a bridge. Overheight vehicles could obviously strike any beam in a bridge and would apply a vertical force as well as horizontal force to the bridge. Thus, the effects of vertical loading, horizontal loading, and vertical plus horizontal loading on the model bridge were investigated. Although the accidental loading previously described could strike the bridge at essentially any location along the beams, the nine locations (see Fig. 3.5) were selected as representative load points.

3.2.1. Vertical Loading

As previously noted, since there was no structural tie-down floor in the annex to resist vertical loads, and since there was no overhead crane to position concrete dead weights on the bridge deck, vertical loading was applied as shown in Fig. 3.6. In Fig. 3.6a, a general schematic of the vertical loading system is illustrated while shown in Fig. 3.6b is a photograph of the vertical loading system as well as the horizontal loading system. Apparent in this figure is that vertical loading (applied with a hydraulic cylinder and measured with a load cell) could only be applied to the three beams of the bridge in an upward direction and that the magnitude of the applied loading was limited by the weight of the bridge (153 kips) and the location of the loading point. Obviously, when vertical loading was applied close to the end of one of the P/C beams, less load could be applied. With this loading system, when loads were to be applied at another location, the entire system had to be moved. Although this system permitted vertical loads to be applied at any location on the three beams, loading was only applied to the nine positions previously noted (see Fig. 3.5).

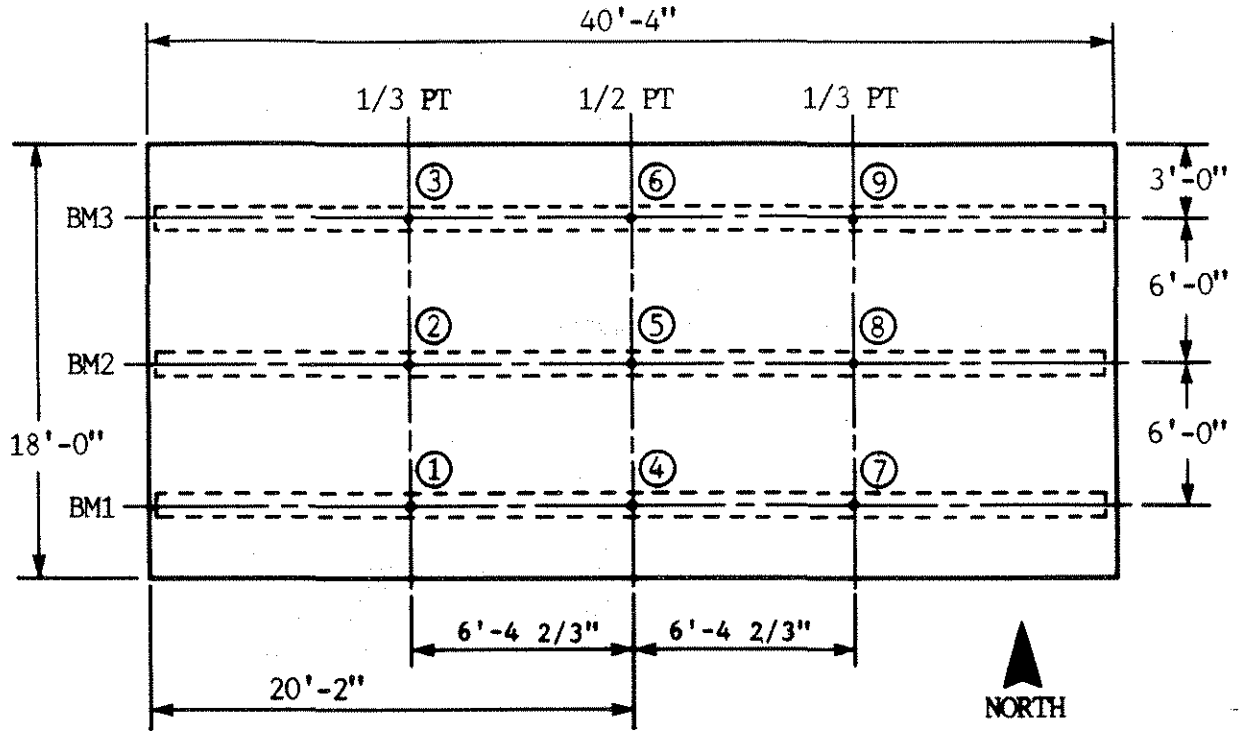

Fig. 3.5. Load points.

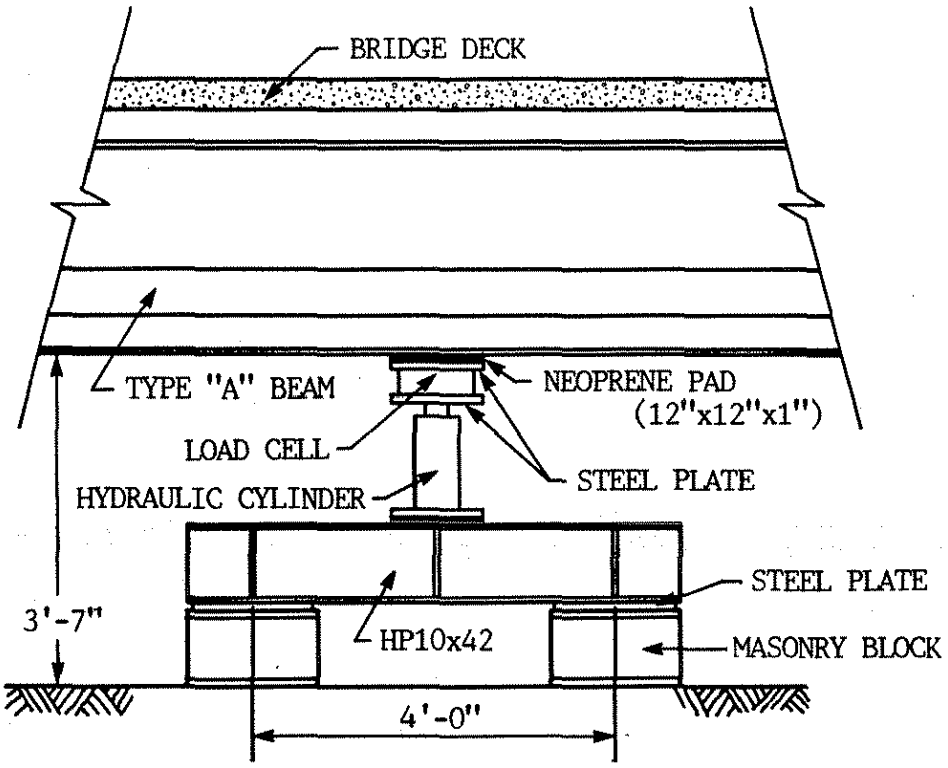

a. Schematic of vertical loading scheme

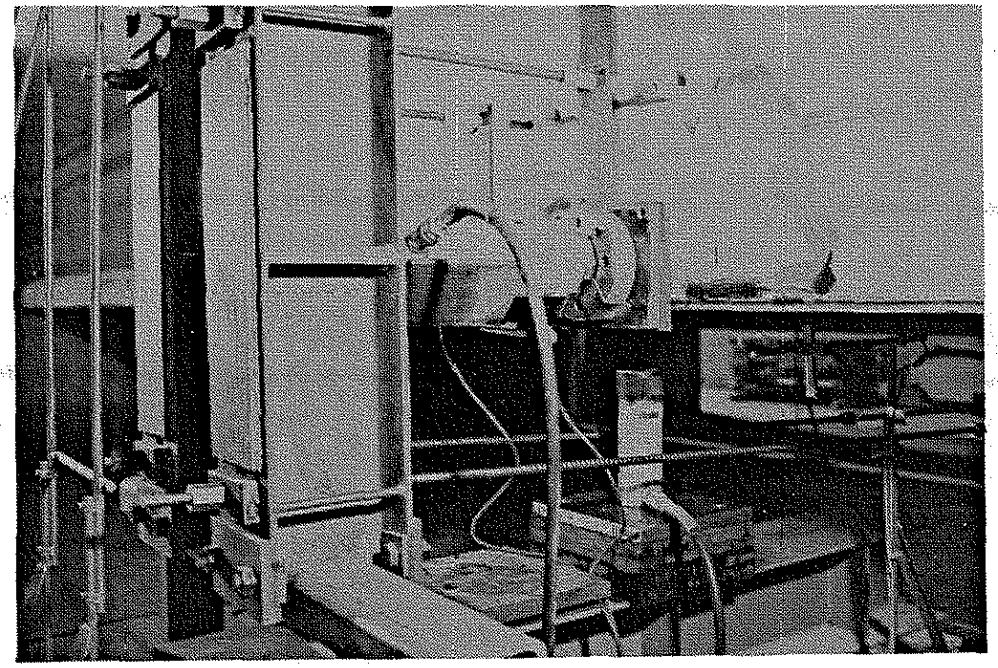

b. Photograph of horizontal and vertical loading schemes.

Fig. 3.6. Vertical loading scheme.

3.2.2. Horizontal Loading

As previously noted, the annex laboratory facilities required loading schemes to be self-contained. Shown in Fig. 3.7 is the loading scheme that was developed for applying horizontal load to the lower flanges of the three bridge beams. As may be seen in Fig. 3.7, horizontal force was applied to the various beams through a system of post-tensioning tendons which induced bending about the major-axis of a Type D P/C girder. This girder was restrained by the aubtment supports and end diaphragms (see Fig. 3.7a). When horizontal loading was applied at the various diaphragm locations, the loading had to be applied as shown in Figs. 3.7d and e rather than at the centerline of the diaphragms in order to avoid interference with the diaphragms. Depending on the type of diaphragm that was in place, horizontal load was applied either at 7 in. or 11 in. on each side of the diaphragm centerline. Force was applied by two 60 ton hydraulic cylinders which were resisted by the system previously described. For an accurate measurement of the horizontal force applied to the P/C beams, a load cell was used with each hydraulic cylinder. Thus, the total horizontal force applied was the sum of the two load cell readings. As a check on the load cell readings, each of the tendons was instrumented with strain gages (see Sec. 3.1) for determining the force in the tendon; applied horizontal force was thus the sum of the forces in the four tendons.

Horizontal force could obviously be applied to the Type D P/C beam at any location along its length. However, the loading scheme used required holes (see Fig. 3.7d) through the web of the P/C bridge beams. Thus, horizontal load could only be applied at the nine points shown in Fig. 3.5 unless additional holes were cored.

Loading different positions on a given beam--for example, points 1, 4, and 7 on P/C beam 1--required moving the four tendons, four load brackets (two at the jacking end [Load brackets 1] and two at the resisting end [Load brackets 2]) as shown in Fig. 3.7b and c, and thus was quite time consuming. Loading at the same section on the three beams--for example, points 4, 5, and 6--only required moving the hydraulic cylinders and Restraining Brackets 1 and tightening the appropriate

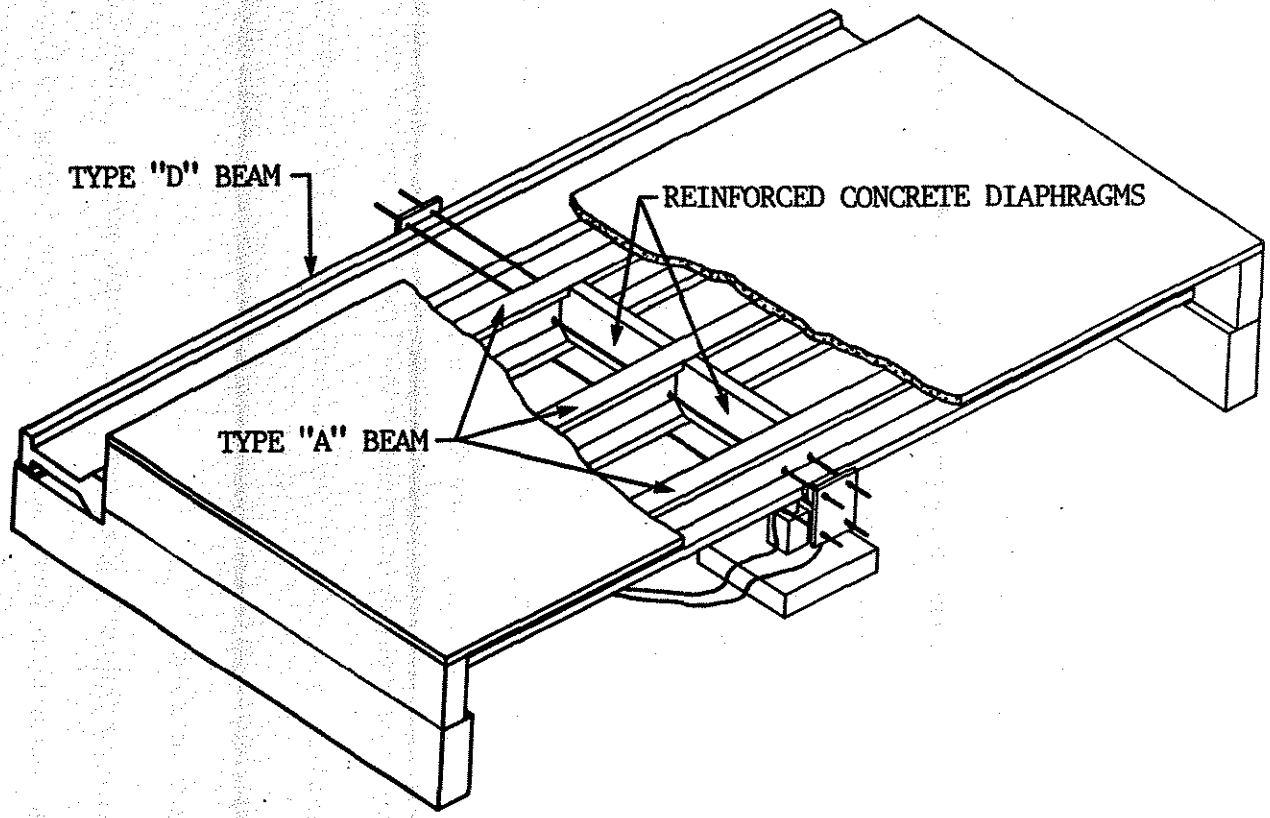

a. Overall view of horizontal loading scheme in position to load point 4.

Fig. 3.7. Horizontal loading scheme.

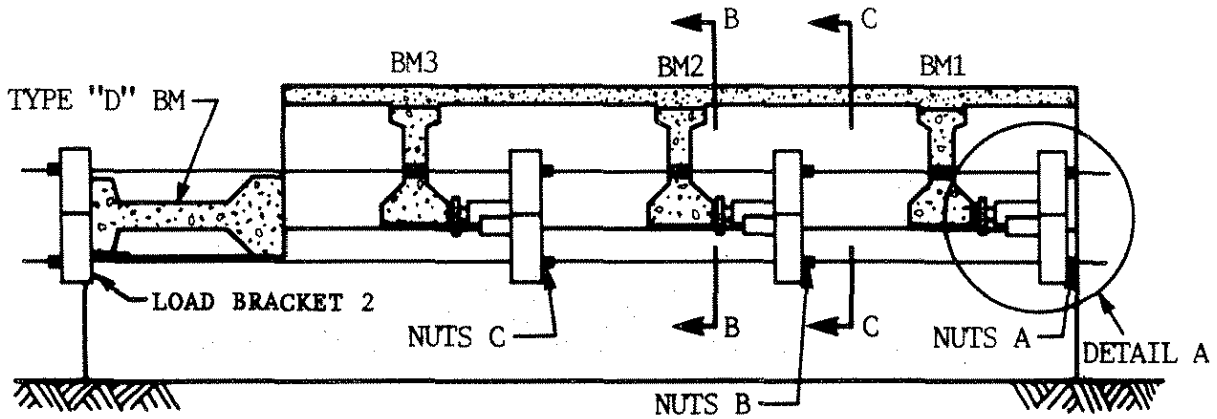

b. Cross-section of horizontal loading scheme

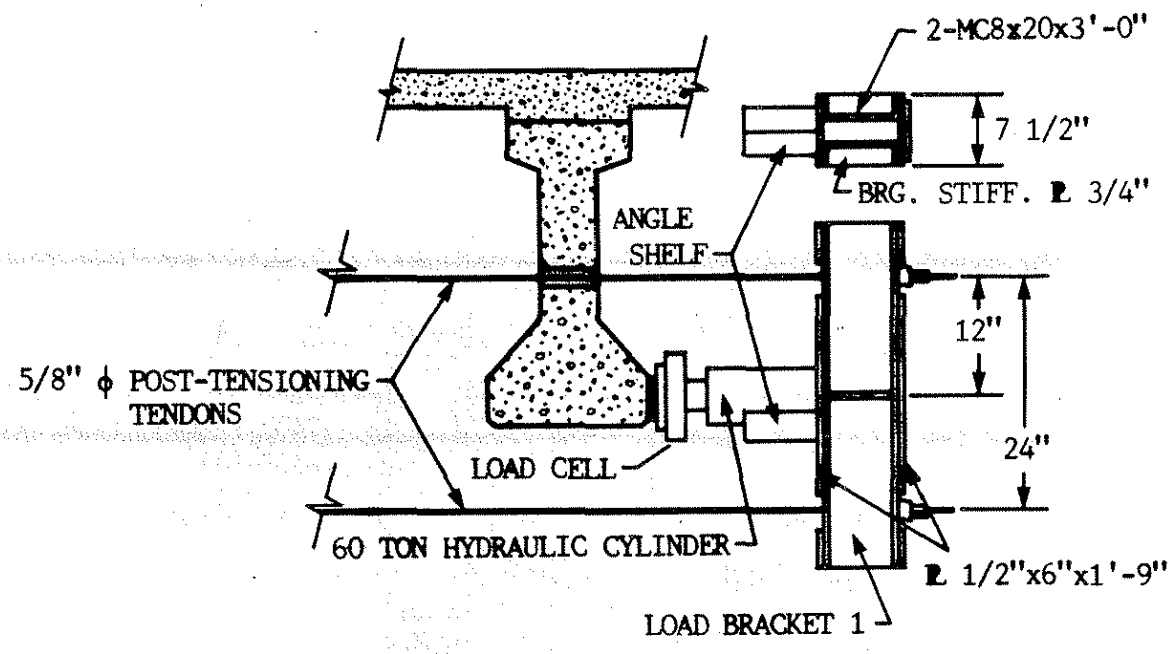

c. Detail A

Fig. 3.7. Continued.

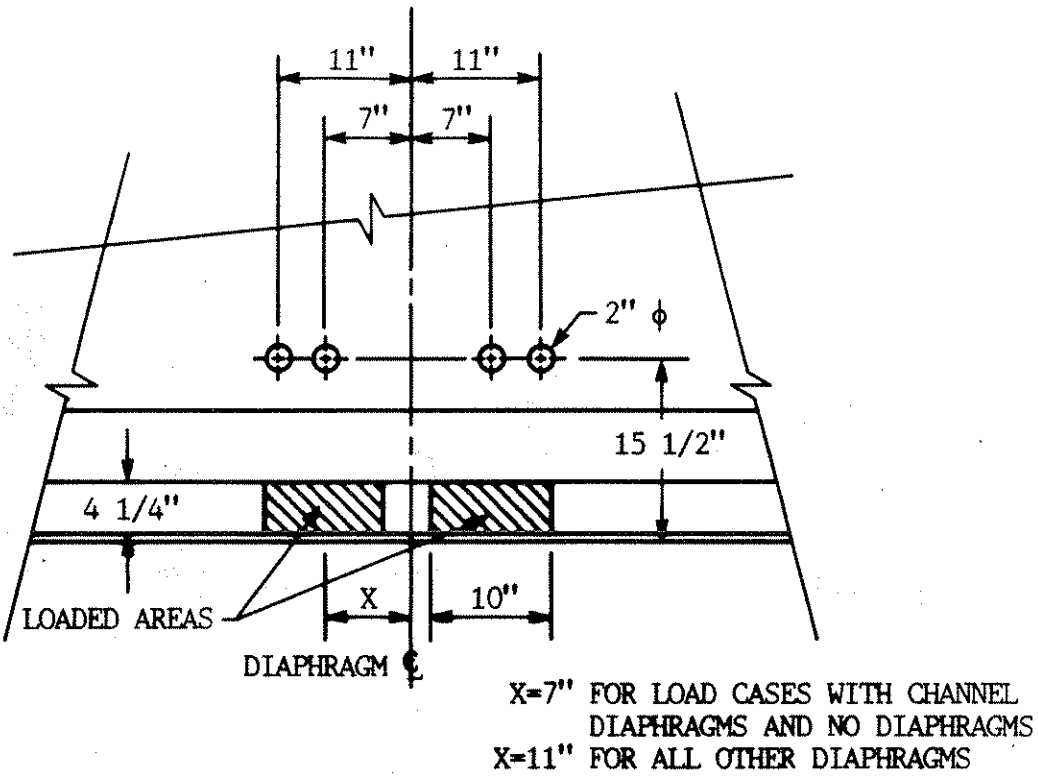

d. Section B-B

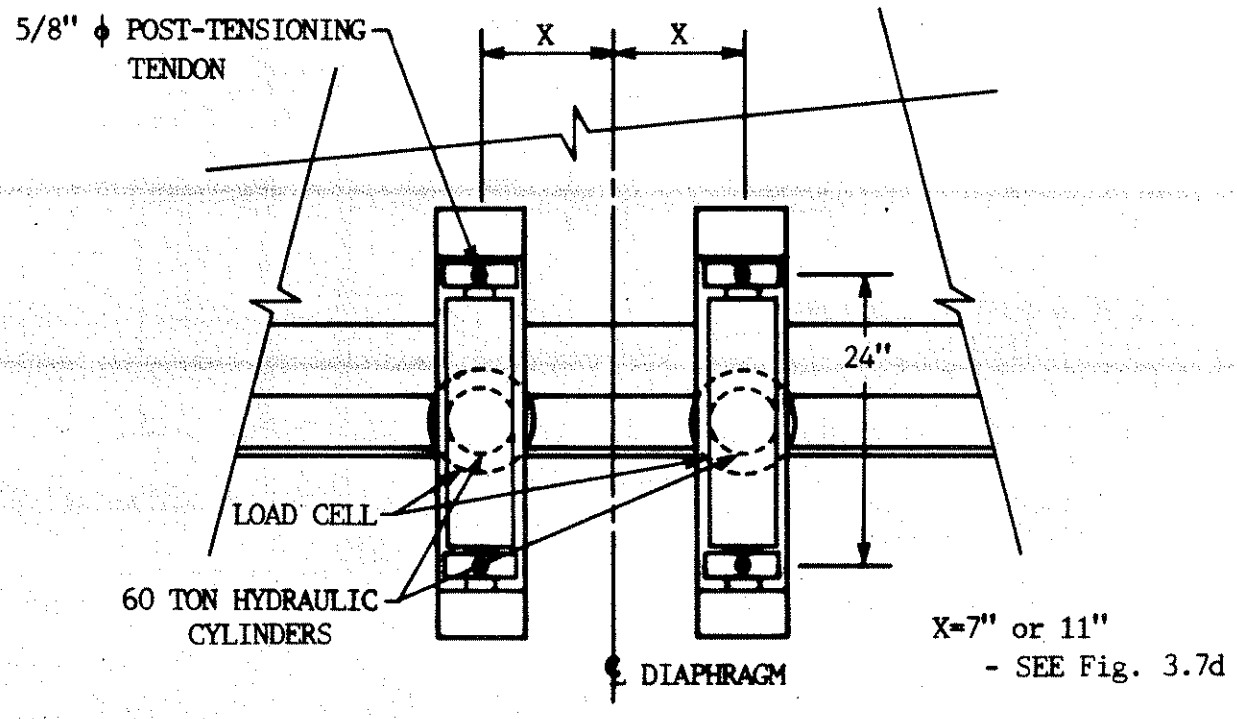

e. Section C-C

Fig. 3.7. Continued.

nuts. For example, if it was desired to apply horizontal load to beam 2, the hydraulic cylinders and Load Brackets 1 were appropriately positioned and Nuts B (see Fig. 3.7b) were tightened. In combination load cases, where vertical and horizontal loading at a given position was applied, a horizontal force of the desired magnitude was initially applied and held constant. Then, the desired magnitude of the vertical force was applied by using the system shown in Fig. 3.6. The two loading systems (vertical and horizontal--shown in Fig. 3.6b) were designed so that there was essentially no interference between them.

3.3. Load Tests

For clarity, the testing program will be described in three separate sections: vertical load tests, horizontal load tests, and vertical plus horizontal load tests. In the various tests, essentially the same procedures were used; the following steps describe the general test procedure:

- Record "zero" strain and "zero" DCDT deflection readings with the DAS. Record "zero" dial gage deflection readings by hand.
- Apply predetermined increment of force at the desired location.
- Record strain gage, DCDT, and dial gage readings as in Step 1. Record any behavioral changes.
- Repeat Steps 2 and 3 until the desired magnitude of force is obtained.
- Remove the applied force in increments taking readings as in Step 1. Take a second "zero" strain and deflection readings as in Step 1 when all force has been removed.
- Repeat Steps 1 and 2 if the loading scheme requires horizontal and vertical loading.

Shown in Table 3.1, is a summary of the 131 tests that were performed on the bridge. As shown, there were 20 separate series of tests; the series designation indicates the type of diaphragm at a specific location with a specified loading. The number of tests in a given series varied from 6 to 9; six was the usual number of tests in a given series, except when a check was made on symmetry--such as in Series 1, 2, 3, 11, 12, 13, and 14. Each series is identified with a two-term designation (e.g.

Table 3.1. Load Tests.

Series		Loading																												
No.	Designation	Vertical Loading Points, i									Horiz. Loading Points, j									Horizontal + Vertical Loading Points, k									
		1	2	3	4	5	6	7	8	9	1	2	3	4	5	6	7	8	9	1	2	3	4	5	6	7	8	9	
1	C2.1-Vi	•	•	•	•	•	•	•	•	•																				
2	C2.1-Hj										•	•	•	•	•	•	•	•	•											
3	C2.1-HVk																			•	•	•	•	•	•	•	•	•		
4	C2.3-Vi				•	•	•	•	•	•																				
5	C2.3-Hj													•	•	•	•	•	•											
6	C1.3-HVk																							•			•			
7	C1.1-Vi				•[a]	•	•	•	•	•																				
8	C1.1-Hj													•[a]	•	•	•	•	•											
9	C1.3-Vi				•	•	•	•	•	•																				
10	C1.3-Hj													•	•	•	•	•	•											
11	RC.1-Vi	•			•	•	•	•	•	•																				
12	RC.1-Hj										•			•	•	•	•	•	•											
13	RC.3-Vi	•			•	•	•	•	•	•																				
14	RC.3-Hj										•			•	•	•	•	•	•											
15	ND-Vi				•	•	•	•	•	•																				
16	ND-Hj													•	•	•	•	•	•											
17	X1.1-Vi				•	•	•	•	•	•																				
18	X1.1-Hj													•	•	•	•	•	•											
19	X2.1-Vi				•	•	•	•	•	•																				
20	X2.1-Hj													•	•	•	•	•	•											

[a] Two diaphragm positions - see Fig. 2.6 for location.

C1.3-Vi for Series 9, X2.1-Hj for Series 20, etc.) The first term of the designation (which was defined in Section 2.2.1) identifies the type and location of diaphragm(s). The second term of the designation identifies the direction (V=vertical, H=horizontal, and HV=horizontal plus vertical) and the location of loading (i, j, or k = 1-9 which are the load points identified in Fig. 3.5). Thus, H7 represents horizontal loading at Point 7, HV3 indicates horizontal plus vertical loading at Point 3, etc.

3.3.1. Vertical Loading

In Table 3.1, the series of tests involving vertical loading are identified (Series 1, 4, 7, 9, 11, 13, 15, 17 and 19). In all these series of tests, the bridge and end diaphragms remained constant--only the type and location of intermediate diaphragms varied. In all the vertical load series of tests, load was applied at a minimum of 6 points. Obviously, the behavior of the various diaphragm combinations can be determined by loading points 4, 7, 5, and 8. However, points 6 and 9 were included to check symmetry. In Series 1 (the first series of tests in the investigation) load points (Points 1, 2, and 3) were also loaded to check symmetry, while in Series 11 and 13, load point 1 was included as a symmetry check. In Series 7, the bridge was tested with the diaphragm in two locations (see Fig. 2.6) when loading was applied at Point 4 to determine if lowering the diaphragm improved its effectiveness.

As was previously described, vertical loading on the bridge was applied upward and thus was limited in magnitude--a function of bridge weight (153 kips). Vertical loading was only applied to the bottom flanges of the three beams at the previously described nine load points (see Fig. 3.5). To avoid stress concentrations, load was applied to the beams by using a combination of a 12"x12"x1" neoprene bearing pad and a 12"x 12" x 1" steel plate (see Fig. 3.6). A review of Fig. 3.5, reveals that the maximum amount of vertical loading that could be applied varies from point to point. To simplify the testing program, the maximum applied vertical loading was limited to 25 kips at each of the nine load points. This magnitude was based on the maximum load that can be applied to load

points 1 and 7 (which obviously have the least resistance of any of the nine load points to vertical load) with an appropriate factor-of-safety against lifting a portion of the bridge.

In all of the series of tests, the vertical load was increased from zero kips to a maximum of 25 kips in 6-kip increments. Data were taken (as described in Sec. 3.3) at each increment of loading. After obtaining data with 25 kips being applied, loading was removed. A final "zero" reading was taken when all vertical loading was removed.

3.3.2. Horizontal Loading

Nine of the series of tests in Table 3.1 involved horizontal loading (Series 2, 5, 8, 10, 12, 14, 16, 18 and 20). The only variables in these series of tests were the type and location of intermediate diaphragms. In all the horizontal load series of tests, the load was applied at a minimum of 6 points. Horizontal loading was applied in the north direction (see Fig. 3.5) in all tests; thus the 6 points loaded are required as the diaphragms will be in compression when Points 4 and 7 are loaded and in tension when Points 6 and 9 are loaded. Symmetrical behavior was checked in Series 2 when three additional points (Points 1, 2, and 3) were loaded and in Series 12 and 14 when Point 1 was loaded.

In Series 8, the bridge was loaded horizontally at Point 4 with the diaphragm in two positions (see Fig. 2.6) to determine the effectiveness of the diaphragm in the lower position.

Horizontal loading was applied to the lower flanges of the beams through neoprene pads (each contact area = 4 1/4"x10") to avoid stress concentrations. As shown in Fig. 3.6, load was applied at two points to avoid interference with the diaphragms.

In all series of tests (except Series 16 where there were no intermediate diaphragms), the horizontal load was limited to a maximum magnitude of 75 kips--large enough to produce measurable strains and deflections, yet small enough to minimize damage to the bridge deck. In Series 16 (no intermediate diaphragms), the horizontal loading was limited to 60 kips to minimize damage to the bridge deck.

The horizontal load in the various tests was increased from zero kips to the desired maximum magnitude in 10-kip increments. At each increment of load, data were recorded as described in Sec. 3.3. After obtaining data for the maximum load applied, the applied load was reduced to 40 kips (30 kips in Series 16)--where data were recorded. After completely removing the horizontal load, the final "zeros" were recorded.

In several of the series (primarily the series involving channels--Series 2, 5, 8 and 10) slippage in the bolted diaphragm connections was noted at certain magnitudes of applied load. After each of the horizontal load tests in these series (e.g., C1.3-H5, C2.1-H7, etc.), the bolts at one end of the channel diaphragms were loosened to allow the beams to return to their original positions. Before the bridge was loaded at another location, the bolts were retightened. This procedure was employed in an attempt to keep the effect of slippage constant in the various tests. This slippage will be discussed and documented in Chapter 4.

3.3.3. Horizontal Plus Vertical Loading

Two of the series of tests in Table 3.1 (Series 3 and 6) involved a combination loading (horizontal and vertical loading). As may be seen in the table, these tests were two of the initial series of tests. Reviewing the data from these series of tests, revealed that superposition was valid. In other words, the results of Series 1 plus Series 2 were the same as the results from Series 3; results from Series 6 were the same as the sum of the results from Series 4 and 5. With the verification of superposition, no additional combination load tests were performed.

In the 11 combination load tests (9 in Series 3 and 2 in Series 6), 50 kips of horizontal load was applied at the desired load point. This force was held constant by continually monitoring load cell outputs and adjusting the force applied by the hydraulic cylinders when necessary. With the horizontal load in place, vertical load was applied at the same location (using the scheme shown in Fig. 3.6) in increments of 5 kips until a maximum vertical load of 25 kips was reached. Data were recorded at each load increment (e.g., H=50 kips, V=5 kips; H=50 kips, V=10 kips; etc.). After

the maximum combined loading (H=50 kips and V=25 kips) was applied and data recorded, loading was removed, vertical first, and final "zeros" recorded.

4. ANALYSIS AND TEST RESULTS

This chapter presents the analytical and experimental results of this research. For clarity, the chapter has been divided into three sections: analytical, experimental, and comparison of analytical and experimental results of the various diaphragms investigated. Diaphragms have been shown to be more effective in reducing the girder moments when point loads are applied directly to the girder (3,11). Thus, the point loading described in Chapter 3 was used to accentuate the behavior of the diaphragms employed. In the field, the vertical loading of a bridge actually involves several point loads (i.e. truck loading), while the lateral loading of the beams due to over-height vehicles would more than likely involve a single-point load. Also, the function of the diaphragms is not significantly different under the action of dynamic loads (in the normal expected frequency range) than under static loads. On average, diaphragms are less effective in terms of load distribution when dynamic loads occur (11).

When static loads (horizontal or vertical) are applied at a particular location on the bridge, the sum of the girder deflections (or moments) at any given transverse section is essentially independent of the presence or absence of diaphragms. Thus, variations in the girder deflections caused by the various types of diaphragms and their location in the span (i.e., midspan or at the third points) can be used as a measure of the effectiveness of the diaphragms.

4.1. Finite-Element Investigation

In this section, the finite-element model is presented as well as a portion of the theoretical results. As previously noted in other portions of this chapter, comparisons between theoretical and experimental results will be presented.

4.1.1. Finite-Element Model

The bridge was analyzed using the ANSYS (5) finite-element program. Solid elements with eight nodes and three degrees of freedom at each node were used in the analysis. The use of this

element in analyzing bridge superstructures has been shown to yield satisfactory results (13) in previous research at ISU. The model consisted of 1,972 nodes and 924 elements (see Fig. 4.1a). The deck was modeled with 420 elements arranged in one layer that contained 15 elements across the width of the bridge (see Fig. 4.1b). Each beam was modeled by using six elements in the cross section; the deck and the beams each contained 28 elements along the length of the bridge (see Fig. 4.1a). The modulus of elasticity of the elements representing the deck was taken as 3,908 ksi, while the modulus of elasticity of the girders was taken as 4,903 ksi. These values correspond to concrete strength of 4,700 psi and 7,400 psi, respectively. Since the end nodes for each girder were prevented from displacing laterally, the end diaphragms were not included in the finite-element model. Various types of intermediate diaphragms were considered in the analysis. Small channel diaphragms were modeled as truss elements that were connected to the concrete beam at their midheight (see Fig. 4.1c). This idealization is consistent with the small bending stiffness of the small channels and the small rotational stiffness between the channels and the concrete girders. This idealization was not used for deep channel diaphragms, however, because of their relatively large bending stiffness. In addition, the connection between the larger channels and the concrete I-girders was deep enough to restrain the torsional rotation of the girders, which developed bending moments in the channels. Therefore, the webs of the channels were idealized as plates connecting the I-girders. The actual height of the channel did not match the distance between the finite-element nodes. To avoid adding more nodes, the dimensions of the plate elements representing a channel web were modified. The height of the channel was assumed to be equal to 16 in., which matched the height of the I-girder webs. The thickness of the web plates was reduced to obtain bending stiffness equal to that of the channels used. Channel flanges were idealized as beam elements connected to the nodes along the longitudinal edges of the web plate (see Fig. 4.1d). Concrete diaphragms were idealized as 6-in.-thick plates (similar to the arrangement shown in Fig. 4.1d). Since the strength of the concrete in the diaphragms was essentially equal to that in the deck, the modulus of elasticity of the concrete

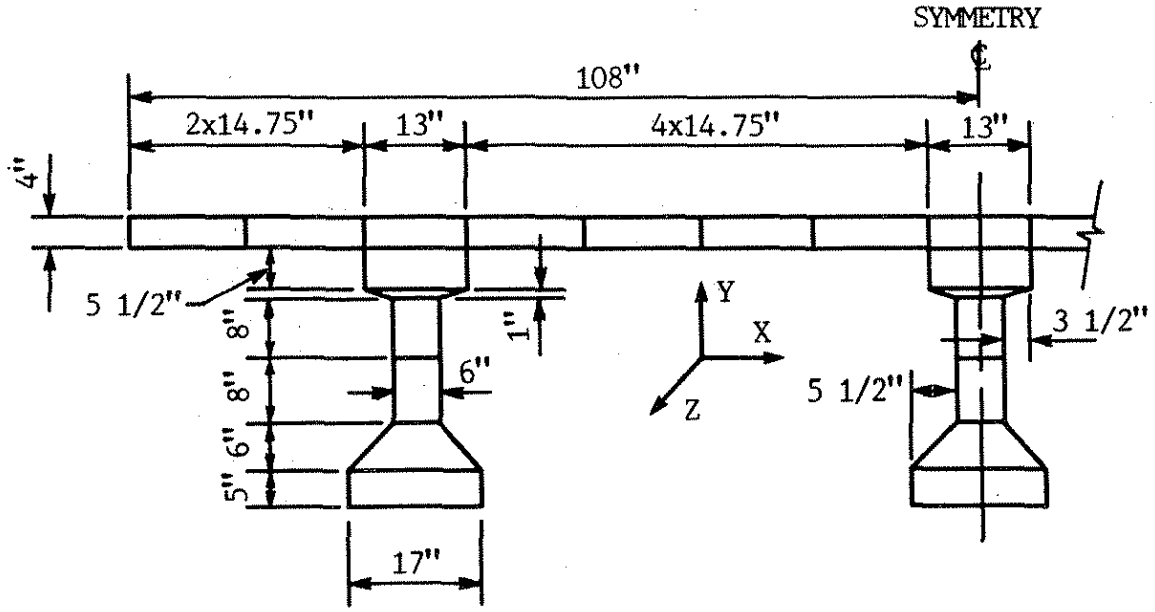

b. Cross section of the finite-element model.

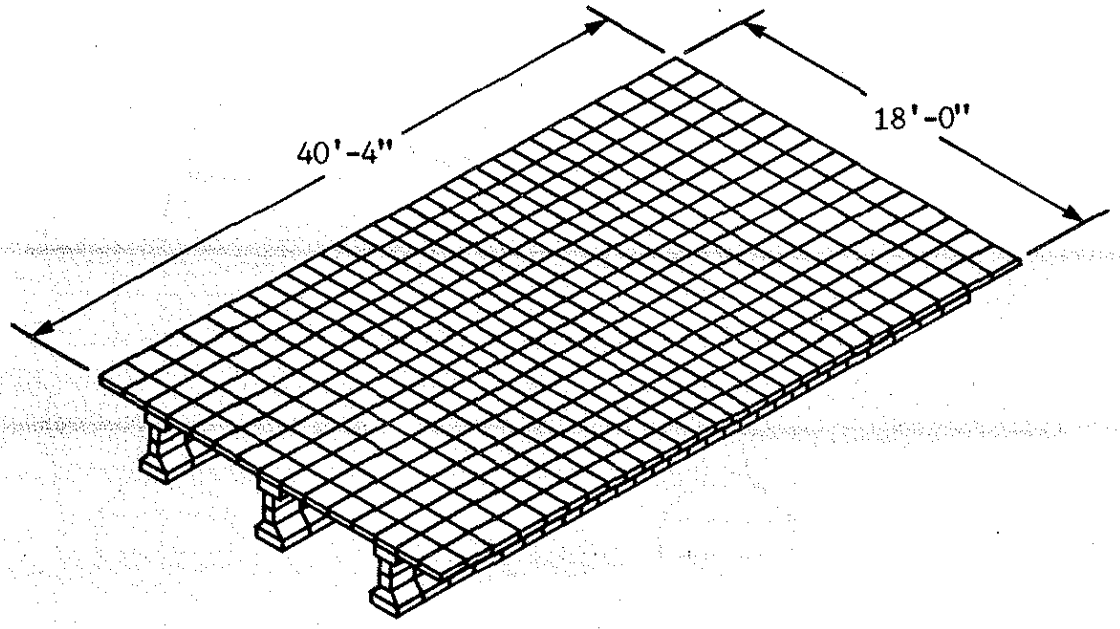

a. Full finite-element model.

Fig. 4.1. Finite-element idealization of bridge and diaphragms.

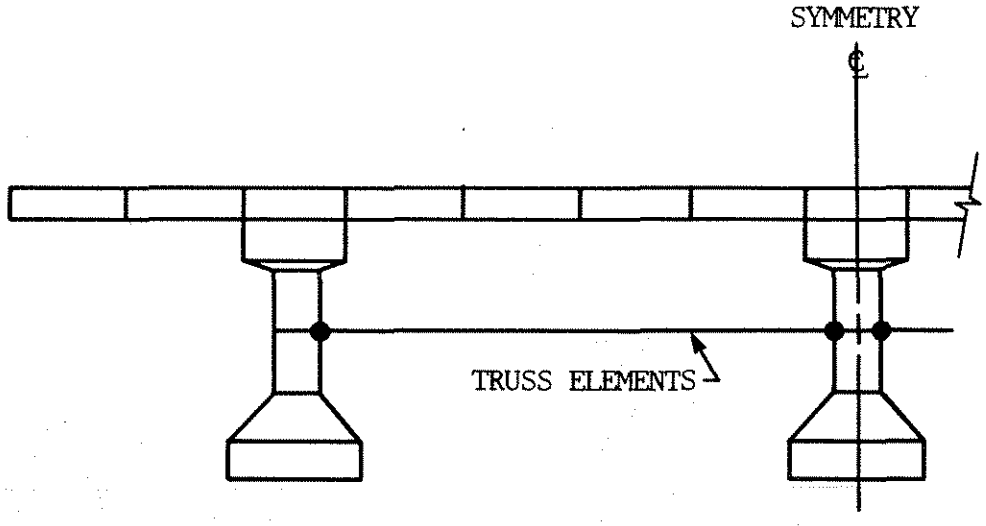

c. Idealization of the small channels.

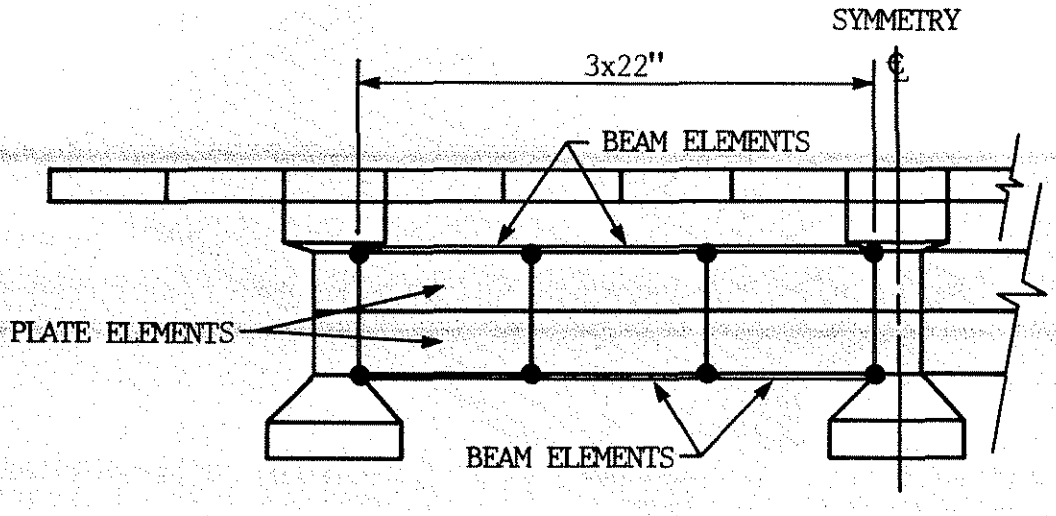

d. Idealization of the deep channels.

Fig. 4.1. Continued.

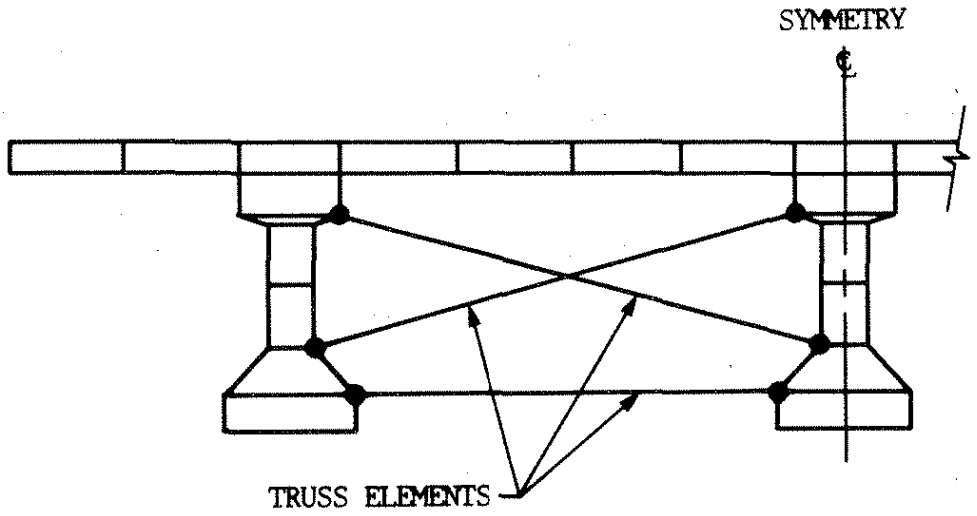

e. Idealization of X-brace plus strut.

Fig. 4.1. Continued.

diaphragm elements was set equal to that of the deck. The X-brace diaphragms were modeled by using truss elements (see Fig. 4.1e). The bridge with these diaphragms in place was analyzed with and without the horizontal truss element at the bottom (see photographs in Fig. 2.7). For each type of diaphragm, the bridge was analyzed with diaphragms at the midpoint of the span and diaphragms at the third points of the span.

Initially, an attempt was made to take advantage of the symmetry of the bridge along its longitudinal and transverse axes. Models of the full, one-half and one-quarter of the bridge were analyzed. Although the last two models required shorter computer time per run than the full bridge model, general cases of loading required the superposition of two runs with different boundary conditions for the one-half model and four runs for the one-quarter model. With the extra load cases, the total running time was not considerably shorter than that required for the full model, and in addition, the required post-processing of the data was a lengthy process. Hence, the model of the full bridge (see Fig. 4.1a) was used throughout the analysis. Iowa State University's Vax 11/780 computer was used in the analysis. Each run of the full model required 21 minutes of CPU time to complete.

Two different end conditions were considered in the analysis. In the first idealization, the movements of the nodes at the two ends of the bridge were restrained in the vertical direction and in the direction parallel to the transverse axis of the bridge (directions x and y in Fig. 4.1b), but these nodes were free to move in the direction of the longitudinal axis of the bridge (direction z in Fig. 4.1b). The analytical model with these end conditions will be referred to as the pinned-end finite-element model. In the second idealization, the three translational movements at the end nodes were restrained. The analytical model with these end conditions will be referred to as the fixed-end finite-element model. These two idealizations bound the actual end conditions in the bridge where a partial restraint is imposed by the connection between the end diaphragms and the abutments.

The finite-element model was analyzed with both horizontal and vertical loads applied to any

one of the three girders at their midspan. Any combination of vertical and horizontal loads could be obtained by the superposition of the results of the respective cases of loading. The midspan load location covered the cases of a load acting at a diaphragm location when applied to the structure with diaphragms at midspan and at a point between the diaphragms when applied to the structure with diaphragms at the third points of the span. The analyses only considered live load; therefore, the strains in the girders due to prestressing and dead load (girder and slab weight) were not considered in the analysis.

Conducting a dynamic analysis of the bridge was not feasible because of the lack of proper time-load curves. Knowing the magnitude of the applied force and its duration are essential in conducting this type of an analysis. The values of these parameters are functions of several variables such as the mass that collides with the bridge and the velocity of this mass at the time of collision. In addition, the damping coefficient of the laboratory bridge was not established. By making several simplifying assumptions, one can calculate a "rough" estimate of the force an overheight vehicle transmits to a bridge. Shown in Table 4.1 is a summary of such forces. By assuming the various vehicle weights, reductions in velocities due to impact, and contact times between the vehicle and the bridge, one can compute the impact forces. As shown in this table, the heavier the vehicle, the larger the decrease in velocity, and the shorter the contact time--the larger the force transmitted from the truck to the bridge. For the assumed values, the impact force varies from 14 to 1,094 kips.

In the idealization of the bridge, the girders were connected to the deck at the common node points between the deck and girders. This modeling assumes a "complete" connection between the girders and the deck at the longitudinal edges of the top flange of the girders. In actuality, the tie between the deck and the girders is through the stirrups that extend from the girders and are cast into the deck. Since the stirrups are near the midwidth of the girders and are spaced on 16-in. centers over 80% of beam's length, the connection between the girders and deck is not as "complete" as assumed in the theoretical model. Therefore, when one of the girders is loaded

Table 4.1. Impact forces on bridge.

	Force on Bridge (kips)								
Reduction in Velocity (MPH)	5			10			15		
Weight of Vehicle (lbs)	Contact Time (sec)								
	.05	.1	.5	.05	.1	.5	.05	.1	.5
30,000	137	68	14	274	137	27	410	205	41
40,000	182	91	18	365	182	36	547	274	55
60,000	274	137	27	547	274	55	821	410	82
80,000	365	182	36	730	365	73	1094	547	109

laterally on the bottom flange, more torsional rotation of the girder is expected to occur than predicted by the finite-element model.

4.1.2. Effect of the End Fixity

Researchers at ISU, as well as at several other universities, have detected and measured rotational end restraint while field testing various types of bridges. Since the end restraint is a function of support and construction details, it varies from bridge to bridge. Although this restraint can be measured with minimal difficulty, the restraint cannot be quantified accurately without actual field test data. With this in mind, the finite-element model was developed so that the bridge model could be analyzed for the two limiting conditions: pinned ends (no rotational restraint) and fixed ends (infinite rotational restraint). The end details of the P/C girders in the model bridge were constructed to be representative of those details existing in actual bridges--elastimetric bridge bearing pad used instead of roller supports, end diaphragm reinforcement bent and cast into deck, end diaphragms connected to P/C girders by means of coil ties in P/C girders, etc. (see details in Appendix B). Thus, the girders in the laboratory bridge model had some end restraint. A review of the construction details in Appendix B, reveals that the degree of girder end restraint is a function of the type of loading applied to the bridge: horizontal loading or vertical loading.

The effect of girder end restraint on the vertical load-deflection response (vertical load at point 4 and vertical deflection at point 4) is illustrated in Fig. 4.2. Although there is a significant difference between the pinned-end condition and fixed-end condition, varying the type of diaphragm essentially has no effect. The load versus deflection curves for the various diaphragms are so close together that in this particular figure they have not been individually identified. The load versus deflection response of the bridge model (as will be shown later) is between these two limiting conditions.

Shown in Fig. 4.3 is the theoretical response of the bridge model to horizontal loading (horizontal loading at point 4 deflection at point 4). In Fig. 4.3a the model is assumed to have

pinned ends. With this type of end restraint, the maximum deflection occurs in the loaded girder when there are no diaphragms present, and the minimum deflection occurs when the reinforced concrete diaphragms (RC.1) are in place. The response of the model bridge with the X-brace plus strut diaphragms (X1.1) is very close to that of the reinforced concrete diaphragms (RC.1).

Although the type of diaphragm had essentially no effect on vertical deflections (see Fig. 4.2), the type of diaphragm does affect horizontal displacements. Shown in Fig. 4.3b are the horizontal load versus horizontal displacement curves for the various diaphragms investigated, assuming either pinned ends or fixed ends. As one would expect, there is considerable overlap of the results. The response to the bridge with the reinforced concrete diaphragms (RC.1) in place is essentially the same as that with the X-brace plus strut (X1.1) in place. A review of Fig. 4.3b, reveals which of the diaphragms investigated in addition to X1.1 results in bridge deflections similar to those that occur when RC.1 diaphragms are used.

4.1.3. Load Distribution Analysis

The theoretical vertical and horizontal load distributions for the diaphragms investigated are presented in this section. In addition to varying the type of diaphragm, the type of end restraint (pinned or fixed) and diaphragm locations (one diaphragm at the midspan; two diaphragms at the third points) are investigated. The distribution factors presented are based on midspan girder deflections.

Shown in Figs. 4.4 and 4.5 are the midspan vertical load distribution percentages. In each of these figures, the percentage of load going to each of the three beams (Parts a-c) is shown. As a result of symmetry, only the response of the bridge to loading at point 4 (Beam 1) and point 5 (Beam 2) will be reviewed. The horizontal axis in these figures identifies the type and location of diaphragms being considered. The vertical axis shows the variation in distribution factors resulting from considering the ends of the girders to be pinned or fixed for each of the diaphragms investigated.

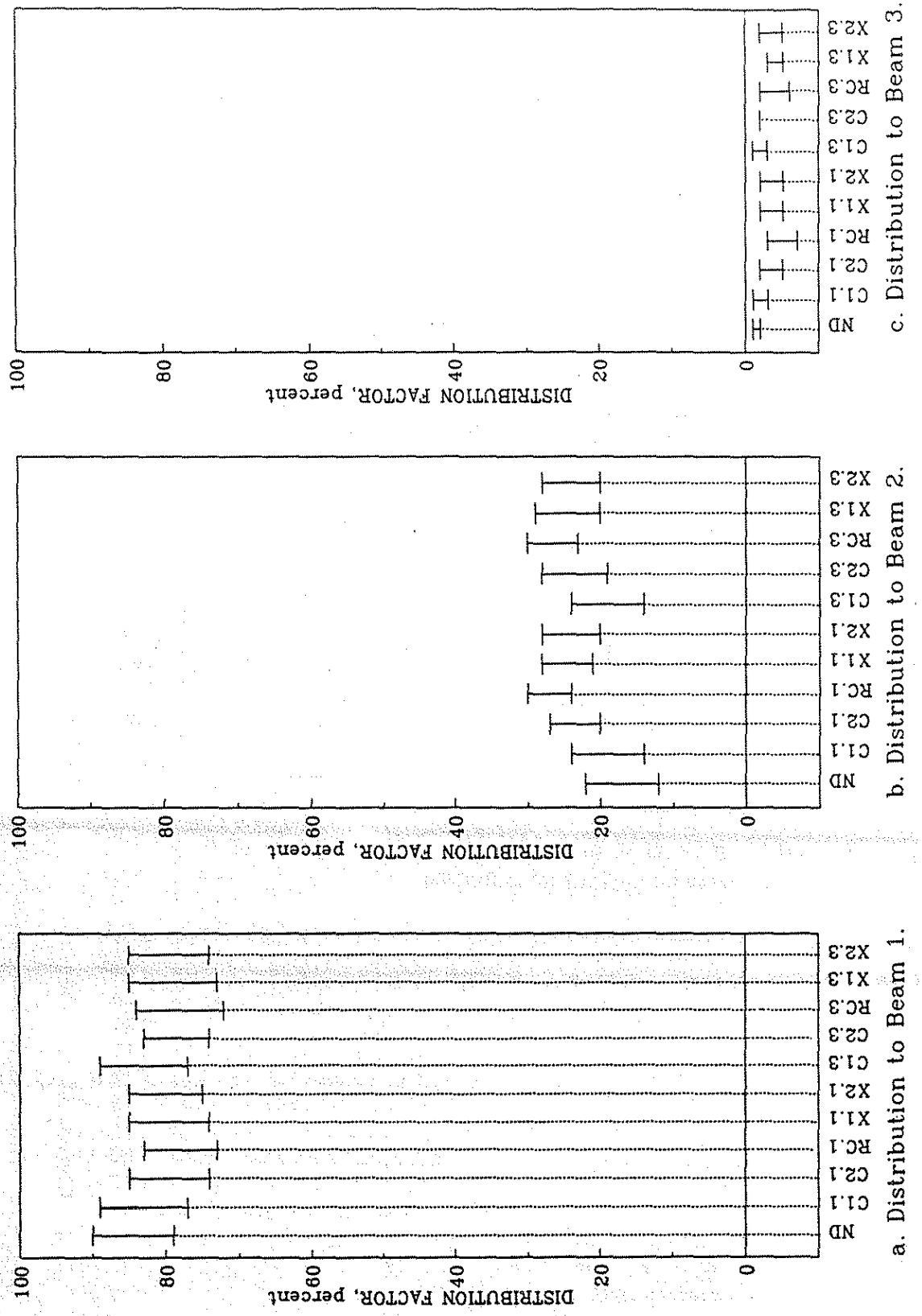

a. Distribution to Beam 1. b. Distribution to Beam 2. c. Distribution to Beam 3.

Fig. 4.4. Theoretical distribution factors: vertical load at point 4.

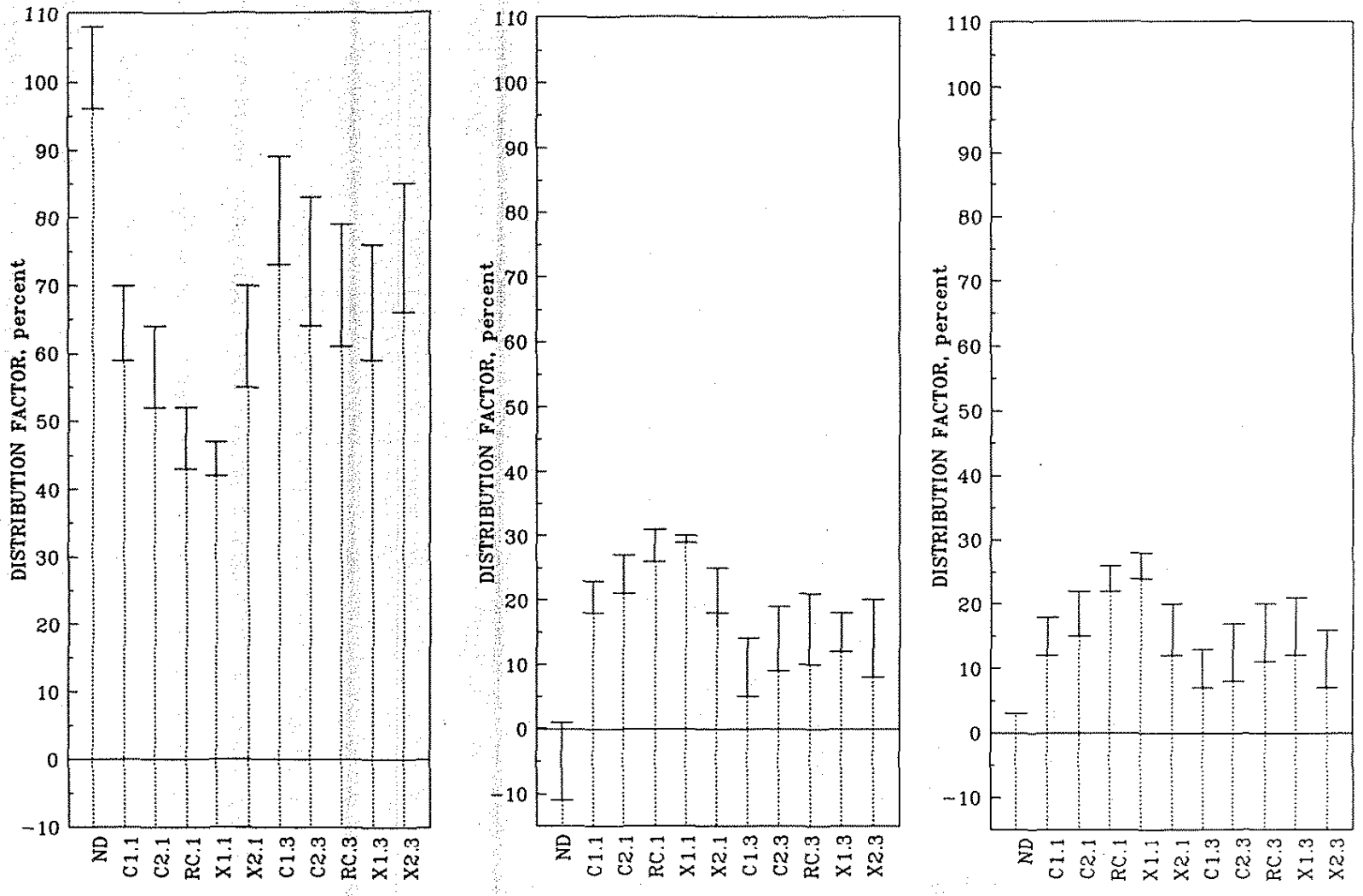

a. Distribution to Beam 1. b. Distribution to Beam 2. c. Distribution to Beam 3.

Fig. 4.6. Theoretical distribution factors: horizontal load at point 4.

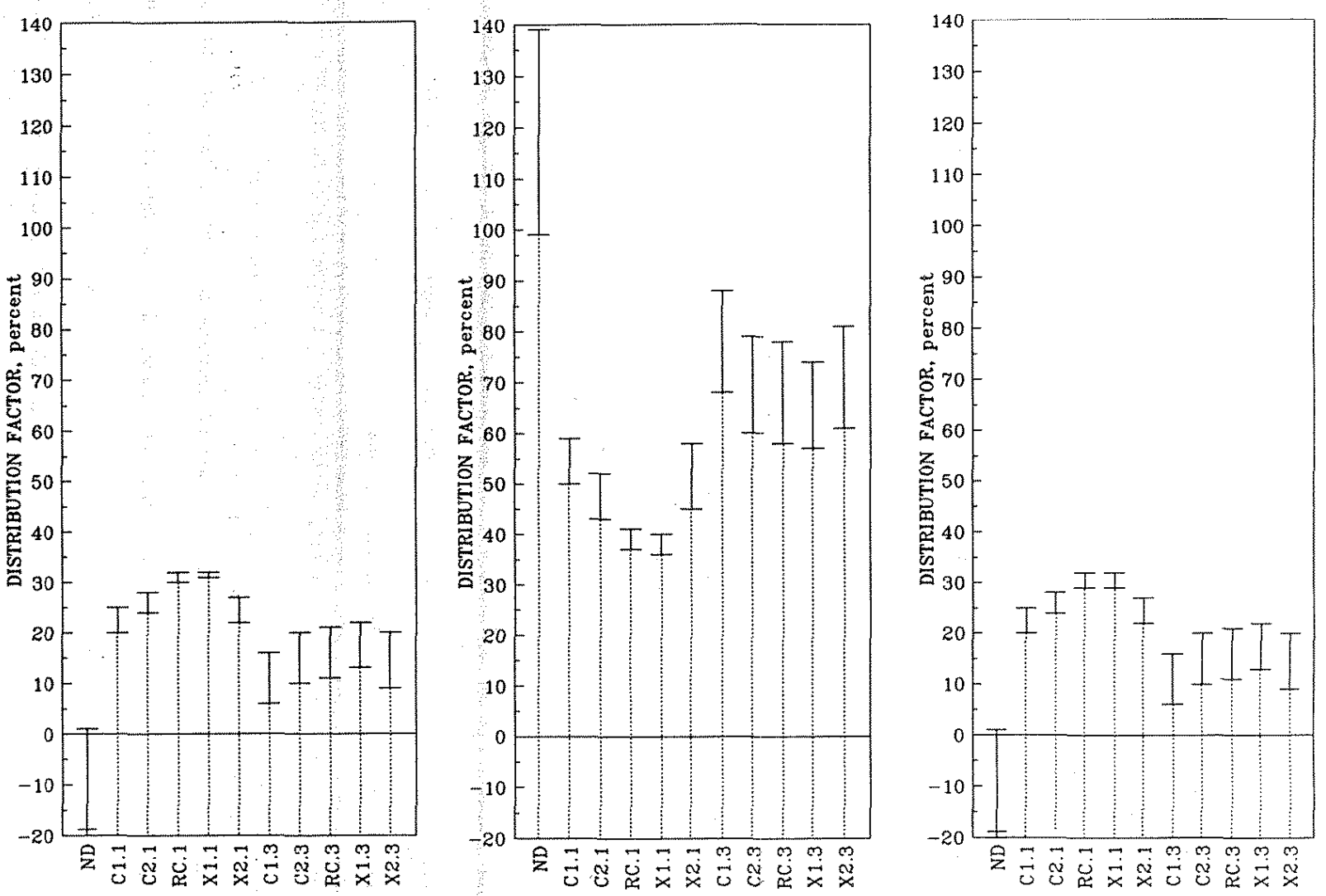

a. Distribution to Beam 1. b. Distribution to Beam 2. c. Distribution to Beam 3.

Fig 4.7. Theoretical distribution factors: horizontal load at point 5.

of the horizontal load to the loaded beam (Beam 1 in Fig. 4.6 and Beam 2 in Fig. 4.7) is greater than 100% and that to the remaining beams is very small or even negative. This effect is caused by the direction of the rotation (and thus the lateral displacement of the bottom girder flanges) that occurs in the various beams.

When intermediate diaphragms are installed at the third points and when midspan horizontal loads are applied, minimal differences occur in the load distributions. When one considers midspan diaphragms, the X-brace plus strut (X1.1) is the least sensitive to changes in the girder end restraint; however, the reinforced concrete diaphragm (RC.1) is also essentially independent of the girder end restraint. For distributing lateral loading, the RC.1 and X1.1 diaphragms are essentially structurally equivalent.

4.2. Experimental Investigations

4.2.1. Deck Cracking Effects on Bridge Response

The response characteristics of a structure are affected by the magnitude of load, which causes elastic or inelastic behavior, the existence of cracks within the concrete members, and the construction details used to connect the various members. The effects of cracks within the concrete deck of the model bridge on the bridge's response will be discussed in this section; the effects of the connection details between the various intermediate diaphragms and the P/C beams on the bridge behavior will be discussed in Sections 4.2.2-4.2.4.

Figure 4.8 shows the four major longitudinal cracks that developed in the concrete deck as a result of horizontal and vertical loads applied to the bottom flanges of the P/C girders. The progression of the formation of these cracks was not documented; however, on the basis of the order and magnitude of the loads applied, the extent and location of these longitudinal cracks can be explained. As discussed in Section 2.1, the thickness of the reinforced concrete deck was set equal to 4 in. With this thickness, the location of the transverse reinforcement (see Fig. B6) was essentially

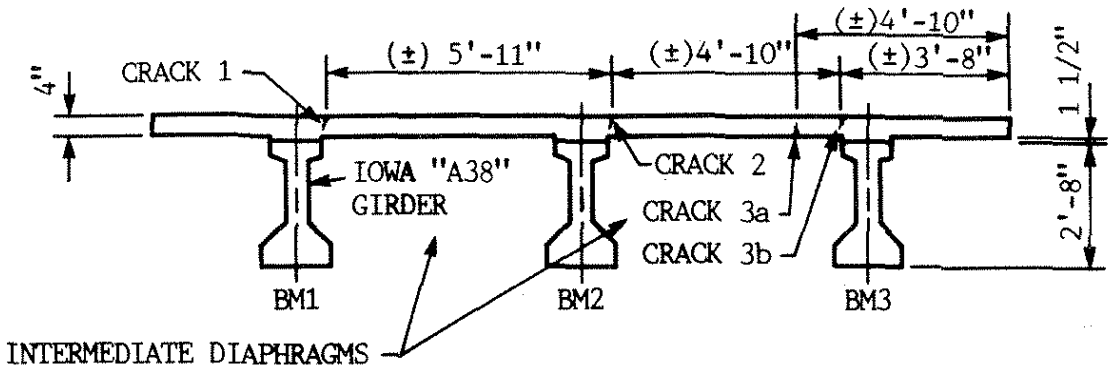

a. Section A-A

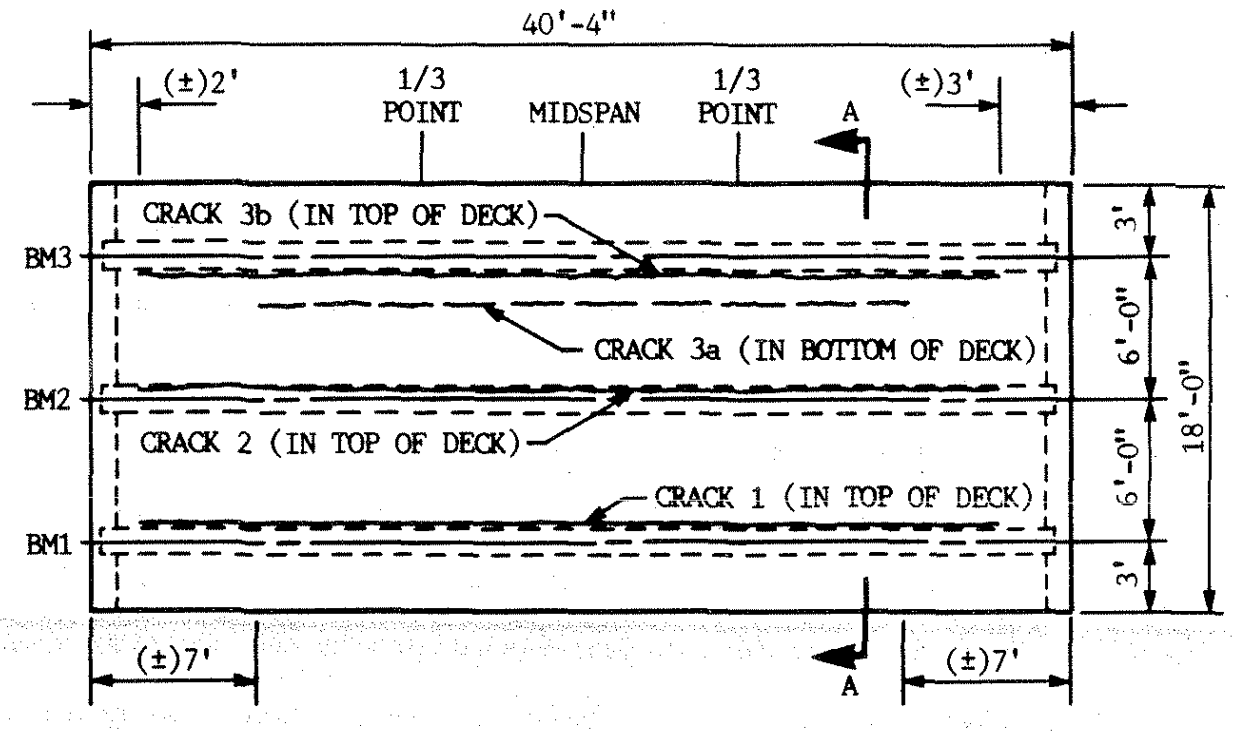

b. Plan view

Fig. 4.8. Major longitudinal deck cracks.

near the midthickness of the deck. Therefore, the flexural strength of the deck in the transverse direction was very small and was essentially the same for positive or negative bending.

The first loads that were applied to the model bridge were horizontal loads at point 4 (BM1 in Fig. 4.8a; see Fig. 3.5) when the steel channel diaphragms C2.1 (see Table 2.2 and Fig. 2.5) were in place at the midspan. The loads, which acted towards the right of this figure, caused the girder to rotate counterclockwise about the longitudinal axis of the composite section. This rotation, induced a counterclockwise rotation of the deck at the joint between the girder and the deck. Since the intermediate channel diaphragms were not connected to the underside of the deck, only the flexural strength of the deck in the transverse direction resisted the rotation of the deck. In addition, the self-weight of the 3-ft. slab overhang produced transverse tensile stresses in the top of the deck above the P/C girder (BM1). The largest flexural stresses would have occurred at the cross section located at the inside face of the top flange of the P/C girder. Crack 1 formed at this location.

After the horizontal load tests at point 4 were completed, horizontal load was applied at point 5 (BM2 in Fig. 4.8a; see Fig. 3.5). The horizontal loads, which induced a counterclockwise rotation of this P/C girder and the slab joint at the top of this girder, produced transverse tensile deck stresses in the top fibers of the slab to the right of BM2 and in the bottom fibers of the slab left of BM2. These stresses were additive to the stresses induced by the self-weight of the concrete deck. The dead load of the slab caused a negative bending moment--tension in the top transverse fibers and compression in the bottom transverse fibers--in the deck at the P/C girder labelled BM2 in Fig. 4.8a. The superposition of the flexural stresses induced by the horizontal loads, therefore, resulted in large transverse tensile stresses at the right face of the top flange of the P/C girder (BM2). As shown in Fig. 4.8a, Crack 2 occurred at this location.

The last horizontal load tests at the midspan location, those involving the intermediate diaphragm C2.1, were conducted at point 6 (see Fig. 3.5). These horizontal loads were applied to the bottom flange of the P/C girder labelled BM3 in Fig. 4.8a. The loads, which were directed

towards the right in the figure, produced a counterclockwise rotation of this girder and the bridge deck at this location. Since the flexural resistance of the deck to rotation is only provided by the continuous portion of the deck, any flexural cracks would have to occur to the left of the loaded P/C girder (BM3) in Fig. 4.8a as the portion of the deck to the right of BM3 is unrestrained. The slab rotation produced transverse tensile stresses in the bottom fibers of the deck to the left of this girder. The self-weight of the 3-ft deck overhang induced transverse compressive stresses in the bottom fibers and transverse tensile stresses in the top fibers of the slab at this exterior girder. The combination of the stresses induced by the horizontal loads and the self-weight of the bridge deck caused a flexural crack (Crack 3a) to occur in the bottom face of the bridge deck approximately 15 in. from the face of the top flange of this exterior P/C girder (see Fig. 4.8a).

After the completion of the horizontal load tests at a particular cross section, a series of vertical load tests were conducted at the same cross section. Considering the cross section involving points 4-6 (see Fig. 3.5) at the midspan of the bridge, upward vertical loads applied at point 4 would tend to reopen Crack 1 and close Crack 2 shown in Fig. 4.8a. Since the presence of Crack 1 at the vertically displaced end of the slab segment between P/C girders BM1 and BM2 reduced the flexural stiffness of this portion of the bridge deck, the induced transverse flexural stresses at the left face (as viewed in Fig. 4.8a) of the top flange of the center P/C girder (BM2) would be smaller than the corresponding stresses associated with an uncracked deck. These reduced transverse tensile stresses occur on the bottom surface of the deck. When the compressive transverse dead load stresses on the bottom fibers of the deck at this same location are added to the stresses caused by the vertical load at BM1, the total stresses will be very small--most likely less than the modulus of rupture stress for the deck concrete. Therefore, a longitudinal crack in the bottom surface of the bridge deck near the center P/C girder should not form. The experimental results agreed with this conclusion.

When upward vertical loads were applied at point 5, Cracks 2 and 3a should have reopened while Crack 1 should have closed. The presence of Cracks 2 and 3a in the deck segment between

P/C girders BM2 and BM3 provides a linkage mechanism for this portion of the bridge deck. Therefore, additional longitudinal cracking in this deck span should not have occurred with the upward vertical movement at BM2. An inspection of the deck revealed no additional cracking. When the deck span between P/C girders BM1 and BM2 is considered, Crack 2 reduced the flexural stiffness of this span. If one follows the same logic that was discussed for transverse stresses induced by an upward movement of BM1, additional longitudinal cracks should not form in the left deck span (as viewed in Fig. 4.8a). The experimental results confirmed this analysis of the behavior.

An upwards vertical load applied at point 6 would have closed Cracks 2 and 3a. The upward vertical movement of the exterior P/C girder (BM3) induced transverse tensile stresses in the top fibers of the bridge deck at this girder. When these stresses were superimposed on the top fiber tensile stresses caused by the self-weight of the 3-ft slab overhang, the total stress exceeded the modulus of rupture to produce the longitudinal crack labelled Crack 3b at the interior face of the top flange of this P/C girder, as shown in Fig. 4.8a. The total transverse tensile stresses in the bottom surface of the bridge deck at the right face (as viewed in Fig. 4.8a) of the top flange of P/C girder BM2 were smaller than the stresses at the location of Crack 3a prior to its formation, because of the self-weight of the bridge deck. Once Crack 3b formed, the transverse stresses in this slab span were relieved. Therefore, with the limited vertical deformations imposed, further cracking of the bridge deck was prevented.

After horizontal and vertical loads were applied at points 1, 2, 3, 7, 8, and 9 during the subsequent load tests, the longitudinal cracks at the four locations shown in Fig. 4.8 propagated along almost the entire length of the bridge. The presence of these cracks in the bridge deck caused load versus displacement relationships to digress from the idealized conditions associated with an elastic and homogenous material. With regards to the bridge's response to horizontally applied loads, the measured horizontal displacements at the bottom flange of the P/C girders were caused by the bridge deck flexural and shear deflection, girder rotation, transverse flexural bending of the girder, axial

deformation of any intermediate diaphragms, and potential movements within the diaphragm connections. When horizontal loads were applied to the bottom flange of the P/C girder labelled BM1, Crack 1 caused additional rotation of this girder beyond the rotation associated with an uncracked bridge deck. Similarly, Cracks 2 and 3a caused additional rotation of the P/C girders labelled BM2 and BM3, respectively. Therefore, the horizontal displacements at the bottom flange of a loaded girder, which were measured during the experimental testing of the model bridge, were larger than those movements that would have resulted with an uncracked bridge deck. This behavior is illustrated in the horizontal load versus displacement relationships shown in Section 4.2.3.

As the longitudinal cracks developed during the initial series of tests and essentially did not change during the investigation, this effect on the response of the bridge to vertical loads can be assumed to be "constant." Recall that the slab thickness was intentionally set equal to about one-half of the thickness of a typical bridge deck and that the transverse slab reinforcement was positioned near the mid-depth of the slab (see discussion in Section 2.1). Therefore, the flexural stiffness of the slab in the direction transverse to the P/C girders was smaller than that found in actual bridges and thus subjected the intermediate diaphragms to more load.

4.2.2. Reinforced Concrete Diaphragm Connection Effects on Bridge Response

The connection details between the intermediate diaphragms and the P/C girders will affect the response of a bridge superstructure to applied horizontal loads. Bridge response to vertical loads applied to the P/C girders was not significantly affected by the diaphragm construction, as discussed in Section 4.1.2. and explained further in Section 4.3.3. Considering horizontal loads applied to the bottom flange of an exterior P/C girder in the experimental bridge, the direction of the load will influence the magnitude of the horizontal displacement of the bottom flange of the loaded girder. The effects of the connection details for the reinforced concrete diaphragms are discussed in this section, and the effect of the steel channel and steel X-brace diaphragm connections are discussed in Sections 4.2.3 and 4.2.4, respectively.

For the intermediate, reinforced concrete diaphragms (RC.1 and RC.3) shown in Fig. 2.4, horizontal loads applied on the outside face of the bottom flange of the exterior girder (BM1 in Fig. 4.8) will induce a bearing condition between the inside flared portion of the girder bottom flange and the diaphragm. Since the diaphragms were cast against the girders, any horizontal loads, which were directed towards the interior girder, produced essentially negligible relative horizontal movement between the girder and the diaphragm. Even though concrete shrinkage may have produced an extremely small gap between these two members, direct load transfer should have occurred, since the connection should have behaved as though the diaphragm were completely connected to the girder along the interface.

When the horizontal load was applied to the inside surface of the bottom flange of the north exterior girder (BM3 in Fig. 4.8), the mechanism of load transfer between the P/C girders and the intermediate diaphragm changes. As discussed in Sec. 2.2.2, the reinforced concrete diaphragms were connected to the P/C girders with two 5/8-in.-diameter post-tensioning tendons, which were placed within conduits. Therefore, with an outward directed horizontal load on the bottom flange of the exterior P/C girder (BM3), the lower tendon was subjected to a tension force. This tension force was resisted by the bearing between the steel plate at the far end of the tendon and the web of the other exterior girder (BM1). Small amounts of relative horizontal movement between the loaded girder (BM3) and the intermediate diaphragm could occur because of the axial lengthening of the lower tendon. This deformation behavior produced greater horizontal displacements of the loaded girder than would have been obtained if relative movements between the girder and the diaphragm were not possible (such as the case in actual construction).

When horizontal loads were applied to the interior P/C girder (BM2 in Fig. 4.8), only the intermediate reinforced concrete diaphragm on the side of the girder opposite to the load point was subjected to a direct compressive force at the sloping face of the girder bottom flange. Additional

discussion on the horizontal displacement response of the bridge with the reinforced concrete diaphragms (RC.1 and RC.3) is presented in a qualitative manner in Section 4.3.2.

4.2.3. Steel Channel Diaphragm Connection Effects on Bridge Response

Similar connection details were used to attach the deep and shallow channel diaphragms to the webs of the P/C girders. Therefore, the response characteristics of the connections for the C15 channels (Fig. 2.5) and MC8 channels (Fig. 2.6) were similar. A tensile force transmitted to the diaphragm by the 1-in. diameter steel bolts passing through the webs of the P/C girders, causes a prying action on the angle leg used to connect the channel diaphragm to the girder web. The flexibility of the connection just described will cause horizontal girder displacements larger than those displacements associated with a more rigid connection. This behavior can occur when the exterior P/C girder (BM3 in Fig. 4.8a) is loaded horizontally in an outward direction and, to a lesser extent, when the interior girder (BM2 in Fig. 4.8a) is loaded horizontally. For the interior girder, the bottom portion of the channel diaphragm, on the side opposite to the applied horizontal load, will be subjected to a compressive force while the bottom portion of the channel diaphragm on the loaded side of the girder will be subjected to a tensile force.

A compressive force transfer to the intermediate channel diaphragms will not cause prying of the connection angle because the heel of the angle will bear directly against the P/C girder web. The load transfer mechanism to distribute an applied horizontal force on the first exterior girder of the model bridge (BM1 in Fig. 4.8a) to the steel channel diaphragm involved a compressive force.

An inherent characteristic of bolted connections is potential slippage between the connected parts. As discussed in Section 2.2.3, high-strength bolts, tightened by the turn-of-the-nut method, connected the steel channels to the outstanding leg of the connection angle as shown in Figs. 2.5a and 2.6a. To allow for tolerances in construction requires horizontally slotted holes placed in the outstanding angle leg. Whenever an applied horizontal load on the bottom flange of a P/C girder induces a diaphragm force that exceeds the slip resistance of the associated connection, slippage will

occur. Slippage was observed during the testing of the channel diaphragms. This relative movement within a diaphragm connection caused the experimentally measured horizontal displacement at the bottom flange of the loaded girder to be larger than the comparable displacements associated with a nonslip connection condition (as assumed in the analytical model).

Figures 4.9-4.11 show the horizontal load versus horizontal deflection relationships for the midspan, shallow channel, intermediate diaphragms (C1.1), at points 4-6, respectively. In each figure, the deflections shown occur at the load point on the bottom flange of the loaded P/C girder. During the application of the horizontal load, the graphs of load versus deflection are essentially bilinear. When horizontal loads were applied independently at points 4-6, the magnitude of the load at which the initial slope of the load versus displacement curve changed occurred at about 42, 22, and 12 kips, respectively. If one defines initial lateral stiffness of the bridge and diaphragm configuration as the initial slope of the load versus displacement response, the greatest lateral stiffness occurred when the horizontal load was applied to the interior P/C girder (BM2 in Fig. 4.8). The least lateral stiffness occurred when the horizontal load was applied in an outward direction to the exterior P/C girder (BM3). When the total horizontal deflection associated with a 70-kip horizontal load at any of the three midspan load points is considered, the least deflection occurred when the load was at point 5, and the largest deflection occurred with the load at point 6. These results are consistent with the previous comments on prying action and connection slip.

Figures 4.9-4.11 also show the unloading displacement behavior for the C1.1 diaphragms. When the horizontal load was slowly removed, connection slippage in the opposite direction was possible. This behavior would occur if slippage had resulted during the loading cycle because the P/C girders were rebounding towards their undisplaced positions. Therefore, the unloading curves of load versus deflection were not linear. Note that after all horizontal load was removed, a horizontal deflection of about 0.02 in. remained for all three load positions. These residual deflections were the results of the slippage that occurred during the loading cycle.

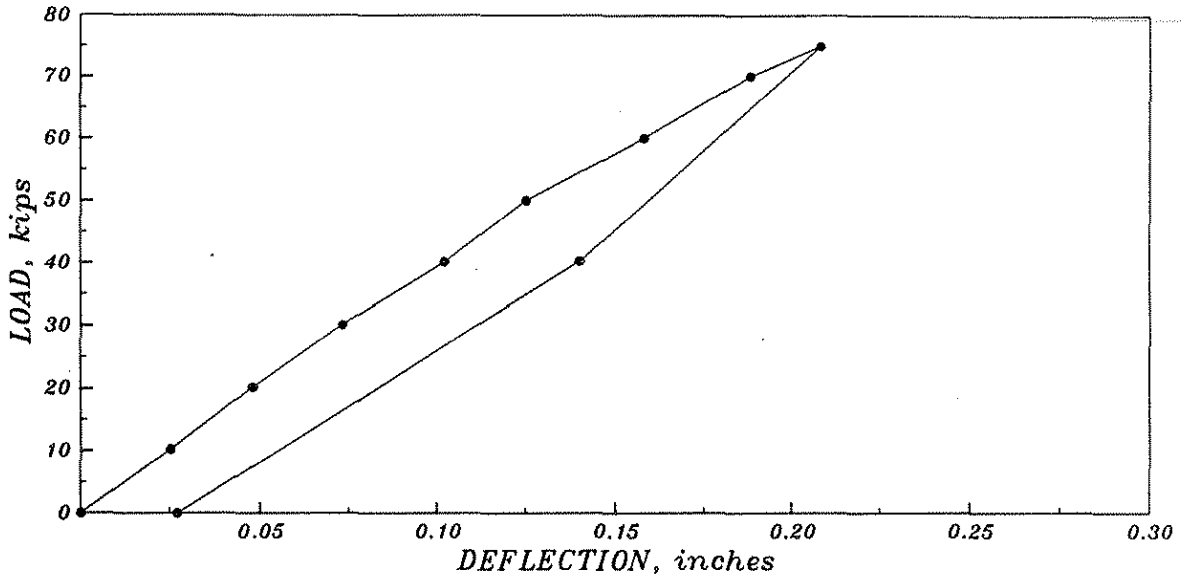

Fig. 4.9. Horizontal load versus deflection at point 4 for C1.1 diaphragms.

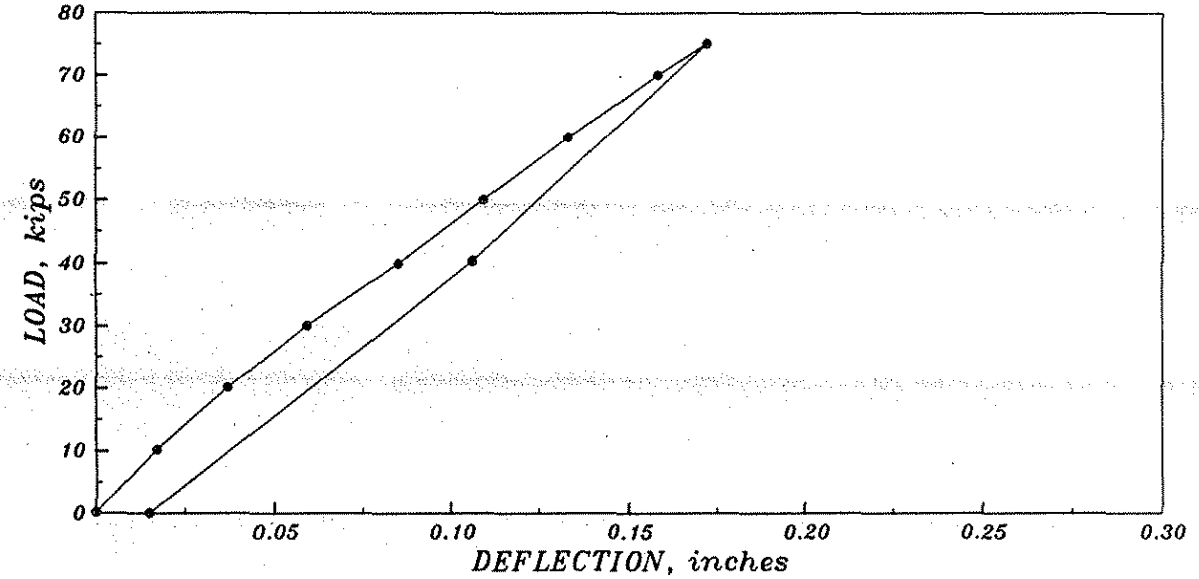

Fig. 4.10. Horizontal load versus deflection at point 5 for C1.1 diaphragms.

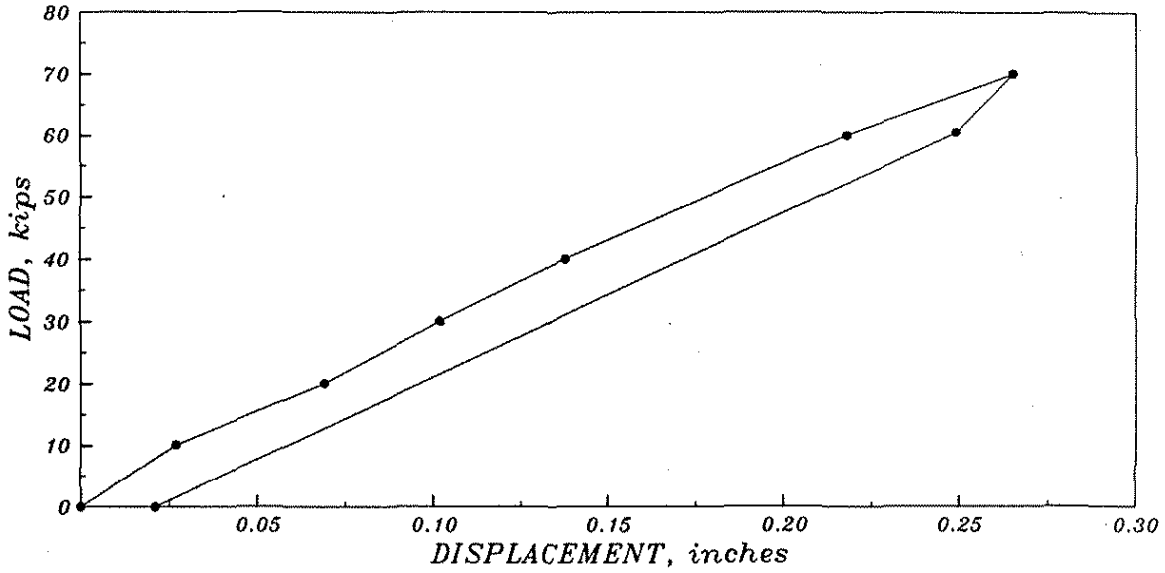

Fig. 4.11. Horizontal load versus deflection at point 6 for C1.1 diaphragms.

Figures 4.12-4.15 show the horizontal load versus horizontal deflection relationships for the midspan, deep channel, intermediate diaphragms (C2.1), at points 4 through 7, respectively. The response shown in these figures was very similar to the behavior associated with the midspan, shallow channel, intermediate diaphragms (Figs. 4.9 through 4.11). However, the initial lateral stiffness for the bridge containing the deep channels was greater than the stiffness associated with the shallow channels when the horizontal load was at points 4 and 6. The initial lateral stiffnesses were essentially equal for the two channel depths (C1.1 and C2.1) when the horizontal load was at point 5. The connection slip resistances for the two diaphragms systems could explain this behavior. The shallow channels had two A325 bolts at each end while the deep channels had four A325 bolts at each end. Apparently, when the load was applied at point 5, the four bolts in the two shallow channels at BM2 provided the same initial lateral stiffness as the eight bolts in the two deep channels at BM2. Note, however, that the load that denoted the bilinear behavior was about 22 kips for the shallow channel diaphragms (Fig. 4.10) and was about 30 kips for the deep channel diaphragms (Fig. 4.13).

Figure 4.15 shows the horizontal load versus horizontal deflection behavior for the C2.1 diaphragms when the load was applied at the third point of the bridge span (point 7). This response, as well as the responses for the other third points, was similar to the responses for the load points previously discussed.

The shallow channel diaphragms were located in two vertical positions at the midspan of the bridge. The normal position, shown in Fig. 2.6a and b, had the channel web bolted through the center two holes in the outstanding angle leg, and the alternate position, shown in Fig. 2.6c, had the channel web bolted through the lower two holes in the same angle leg. By lowering the channel to the alternate position, the distance between the center of the diaphragms and the line of application of the horizontal load was reduced from about 16 1/2 in. to 13 1/4 in. Figure 4.16 shows the horizontal load versus displacement responses of the loaded exterior P/C girder (BM1 in Fig. 4.8)

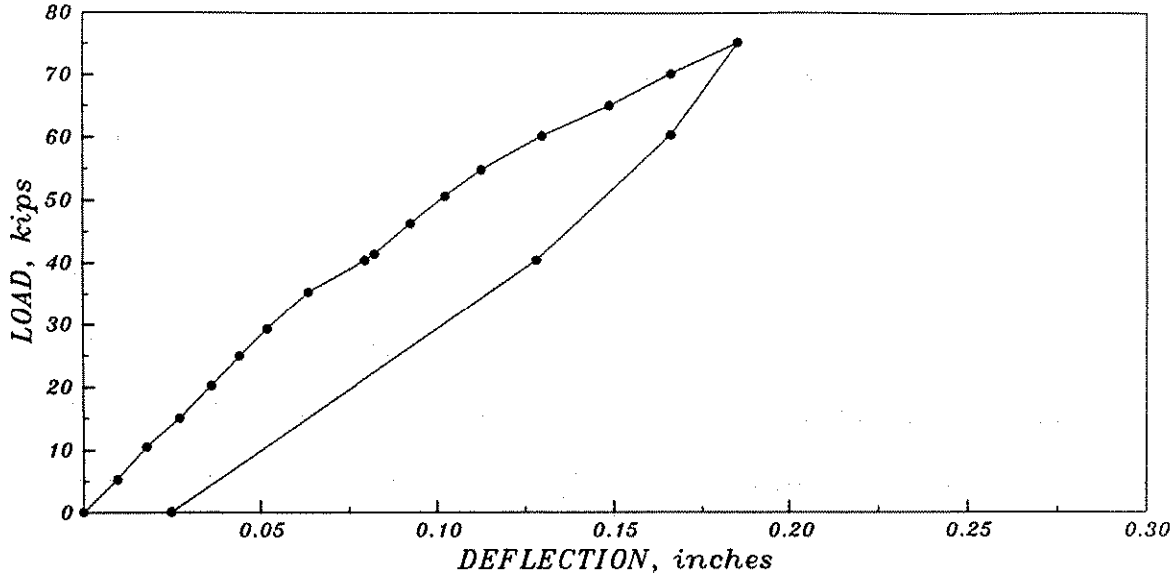

Fig. 4.12. Horizontal load versus deflection at point 4 for C2.1 diaphragms.

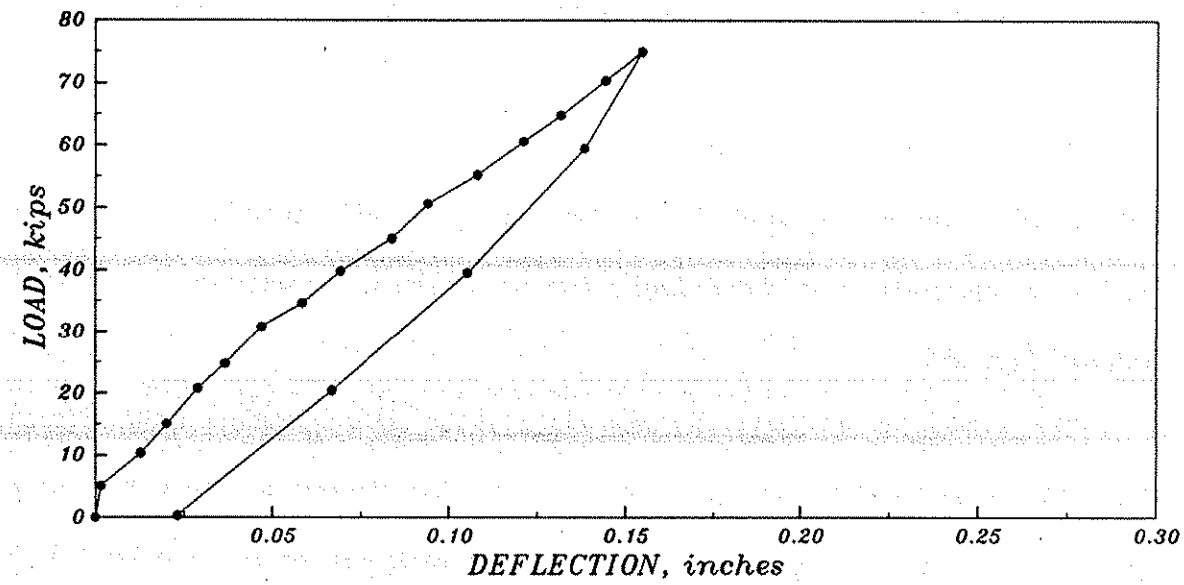

Fig. 4.13. Horizontal load versus deflection at point 5 for C2.1 diaphragms.

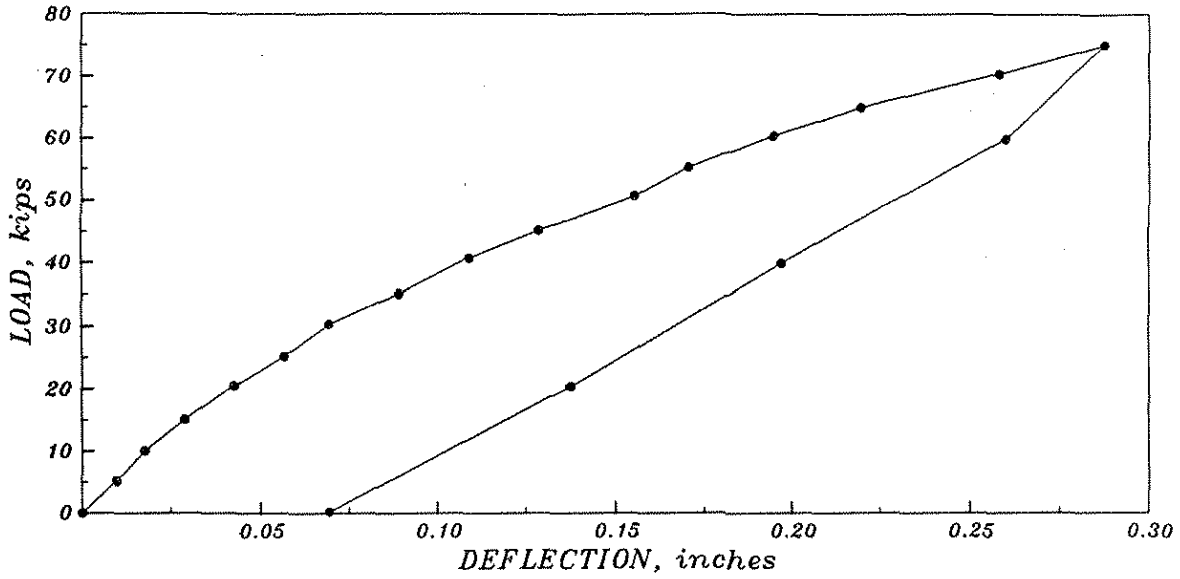

Fig. 4.14. Horizontal load versus deflection at point 6 for C2.1 diaphragms.

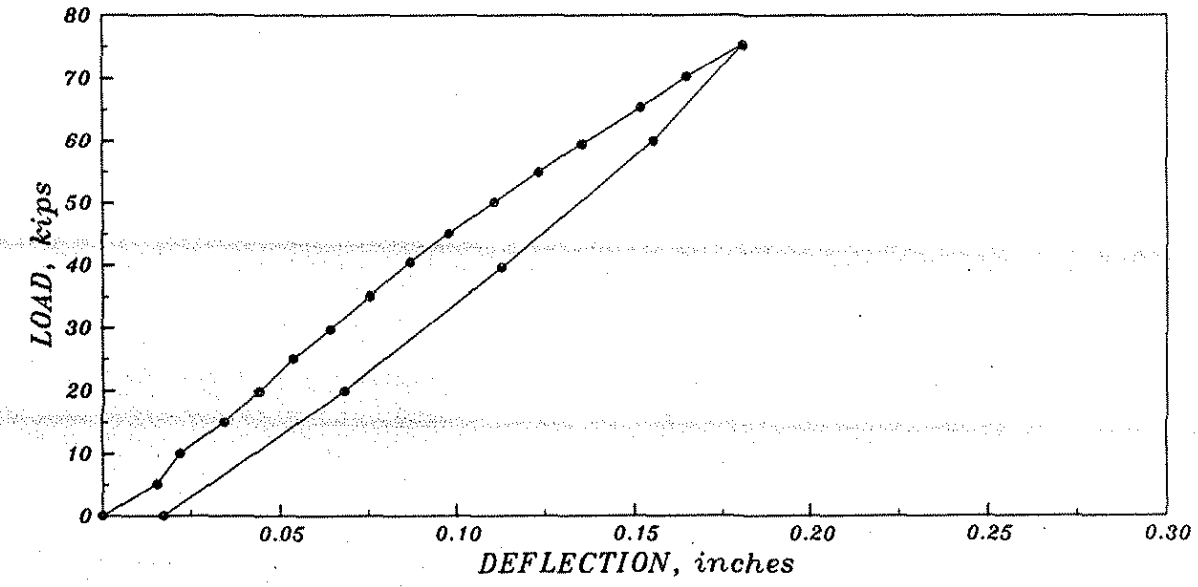

Fig. 4.15. Horizontal load versus deflection at point 7 for C2.1 diaphragms.

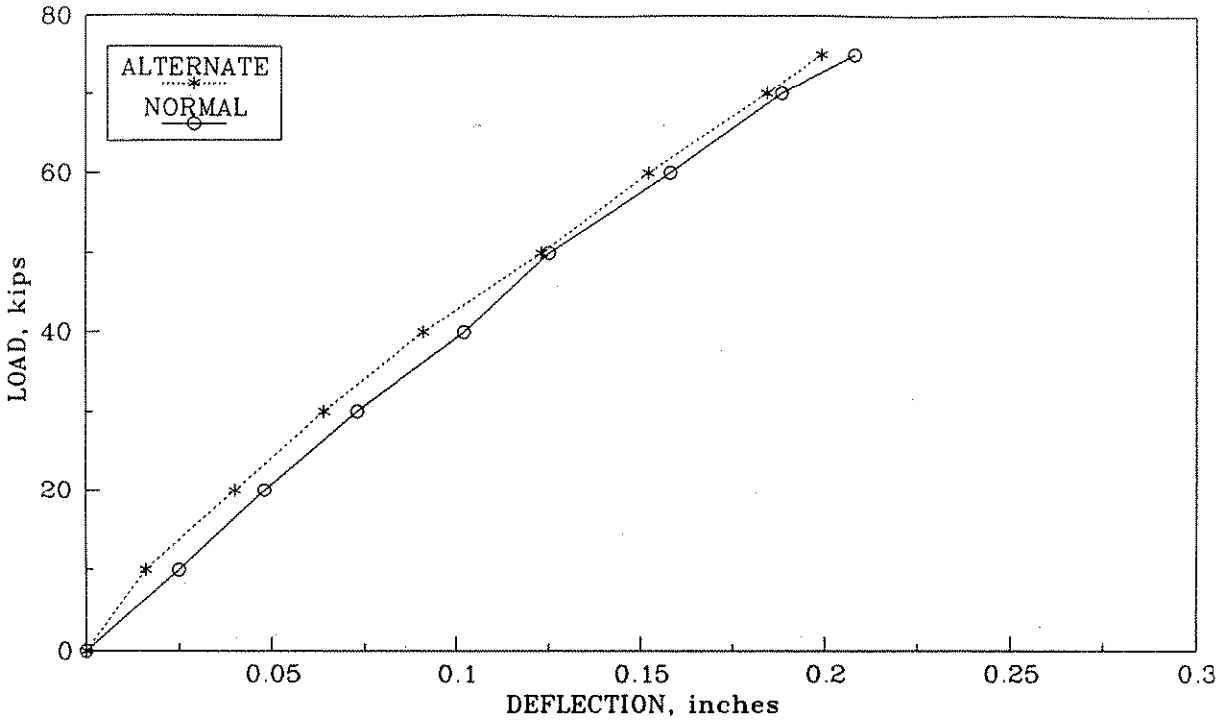

Fig. 4.16. Horizontal load versus deflection at point 4 for two positions of C1.1 diaphragms.

for the normal and alternate positions of the midspan channel diaphragm (C1.1). The experimental behavior for both the loading and unloading phases of the two channel elevations are almost identical. As expected, the alternate channel position produced slightly lower horizontal deflections when compared to the normal channel position. Similar results (not included) were found in the unloaded girders.

Further discussion regarding the effects of connection flexibility and slip on the response of the bridge, is presented qualitatively in Section 4.3.2 for the steel channel diaphragms when horizontal loads are applied to the bottom flanges of the P/C girders.

4.2.4. Steel X-Brace Diaphragm Connection Effects on Bridge Response

The connections for the steel X-brace intermediate diaphragms, with and without the bottom horizontal strut (Fig. 2.7), were substantially more rigid than the connections for the steel channel diaphragms. Prying action caused by a tensile force transfer will not occur in this connection since the steel plates, which are in contact with the girder profile and connected to the P/C girder at four locations (see Fig. 2.7), were welded together along their common edges. Therefore, deformation of these plates will be minimal. Potential bolt slip magnitudes were kept to a minimum by using standard holes (1/16 in. larger in diameter than the bolt diameter) for the high-strength bolts, which attached the MC8 channel members to the large bracket assemblies. These intermediate diaphragms could thus be considered to be rigidly connected to the P/C girders.

4.2.5. Load Versus Deflection Behavior

In this section, the experimental results for both the horizontal and vertical load versus deflection responses of the bridge model with various diaphragms in place, at either the midspan or at the one-third points of the span, will be presented. Comparisons between the experimental results and theoretical results are made in Section 4.3.

As was described in Sections 3.3.1 and 3.3.2, the bridge model was subjected to a maximum vertical load of 25 kips and a maximum horizontal loading of 75 kips (except in the cases with no diaphragms when the horizontal loading was limited to 60 kips) to minimize damage to the deck. This obviously resulted in some strains and deflections of relative small magnitude, especially when deflections and strains were measured at large distances from the point of loading. For some of the experimental curves shown in this section (as well as in some of the experimental curves shown in the following sections) the difficulty in accurately measuring these small deflections and strains is apparent.

Shown in Figs. 4.17 and 4.18 are the vertical load versus vertical deflection curves for the midspan and third-point diaphragms, respectively. As was noted in Section 2.2.1, the bridge model was tested with X1 and X2 diaphragms only at the midspan; therefore, six experimental curves are shown in Fig. 4.17 and four curves are shown in Fig. 4.18. The closeness of the curves in each of these figures indicates that the diaphragms have minimal influence on the vertical load distribution within the bridge. The same conclusion was reached in reviewing the theoretical deflections in Fig. 4.2. The fact that the curves in Figs. 4.17 and 4.18 have essentially the same slope indicates that diaphragms located at midspan or at the third-points of the span provide essentially the same vertical load distribution.

Figures 4.19 and 4.20 present the vertical deflection at the midspan (point 5) of the interior P/C girder (Beam 2) for the midspan and third-point diaphragms, respectively. The same behavior is depicted in these figures as was shown in Figs. 4.17 and 4.18. Lateral distribution of vertical loading is essentially independent of the type and location of the diaphragms.

Figures 4.21 and 4.22 present the horizontal load versus horizontal deflection curves for the midspan and the third-point diaphragms, respectively. The experimental data shown in Fig. 4.21 indicates essentially the same load versus deflection behavior as was shown for the theoretical curves in Fig. 4.3a. The degree of rotational end restraint for the girders in the bridge model may be

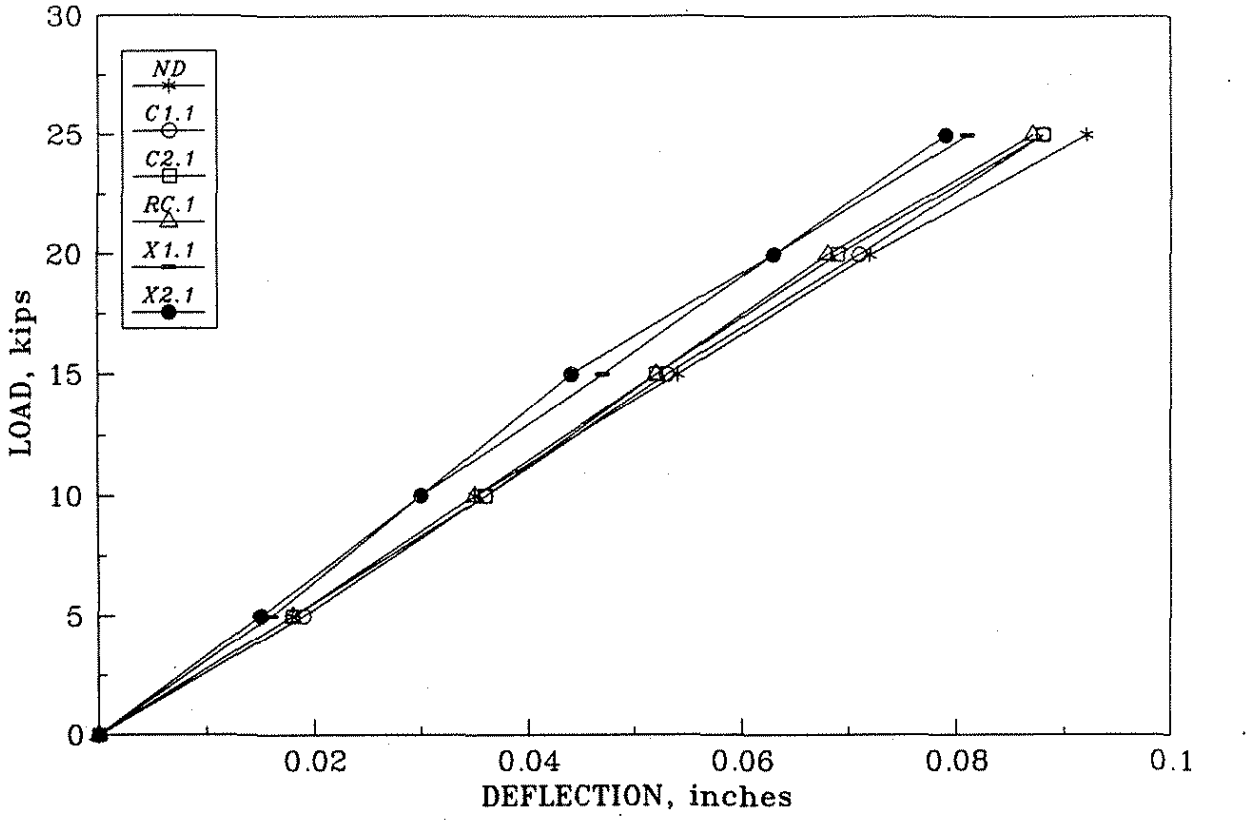

Fig 4.17. Vertical load–deflection curves: diaphragm at centerline, deflection at point 4, load at point 4.

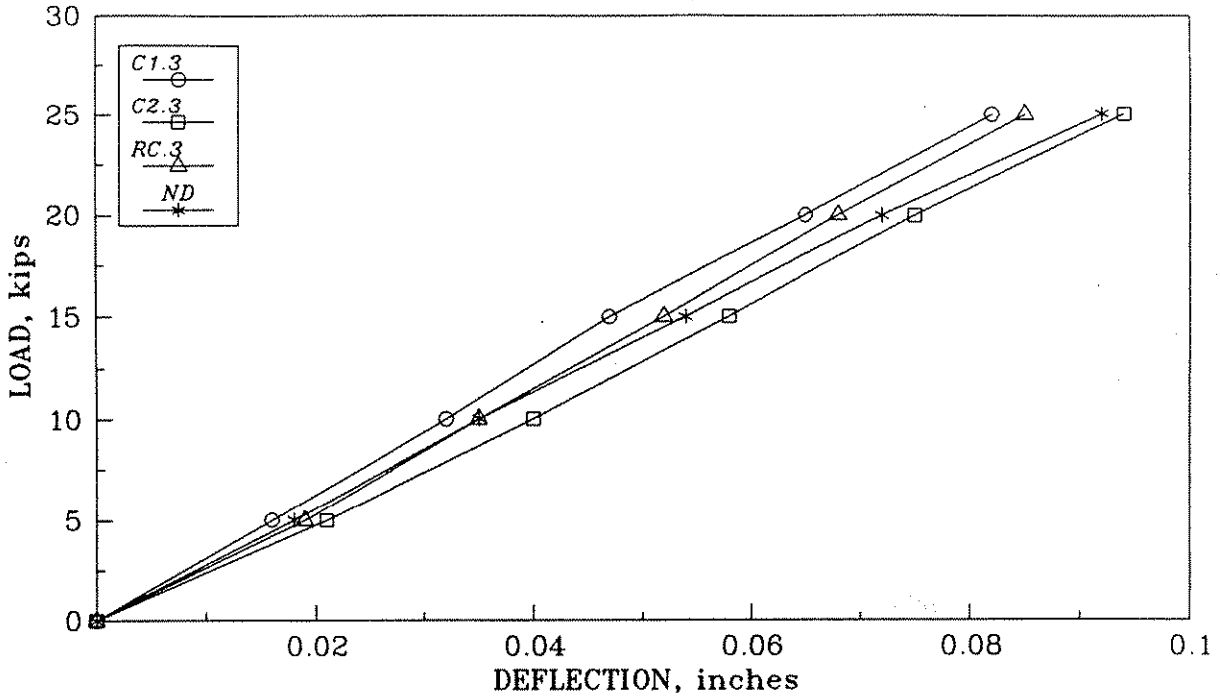

Fig. 4.18. Vertical load–deflection curves: diaphragms at third points, deflection at point 4, load at point 4.

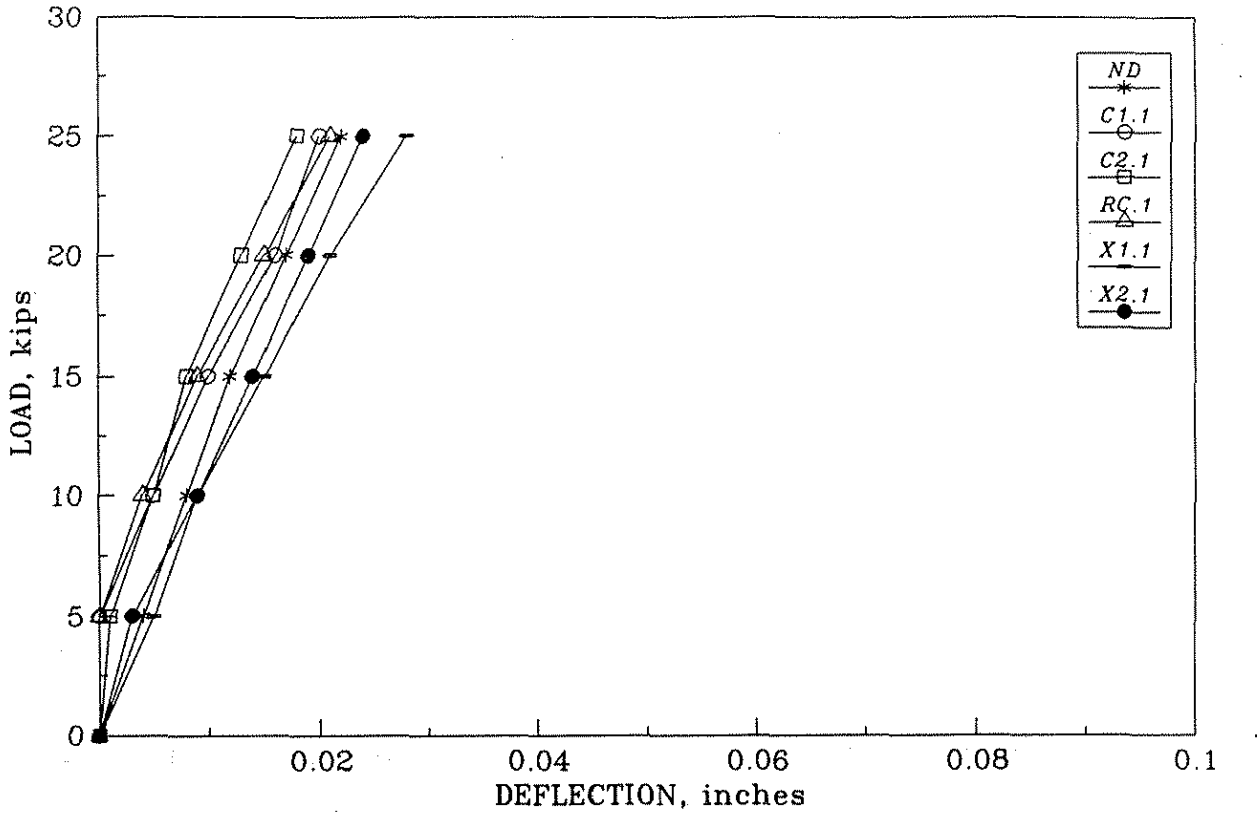

Fig 4.19. Vertical load–deflection curves: diaphragm at centerline, deflection at point 5, load at point 4.

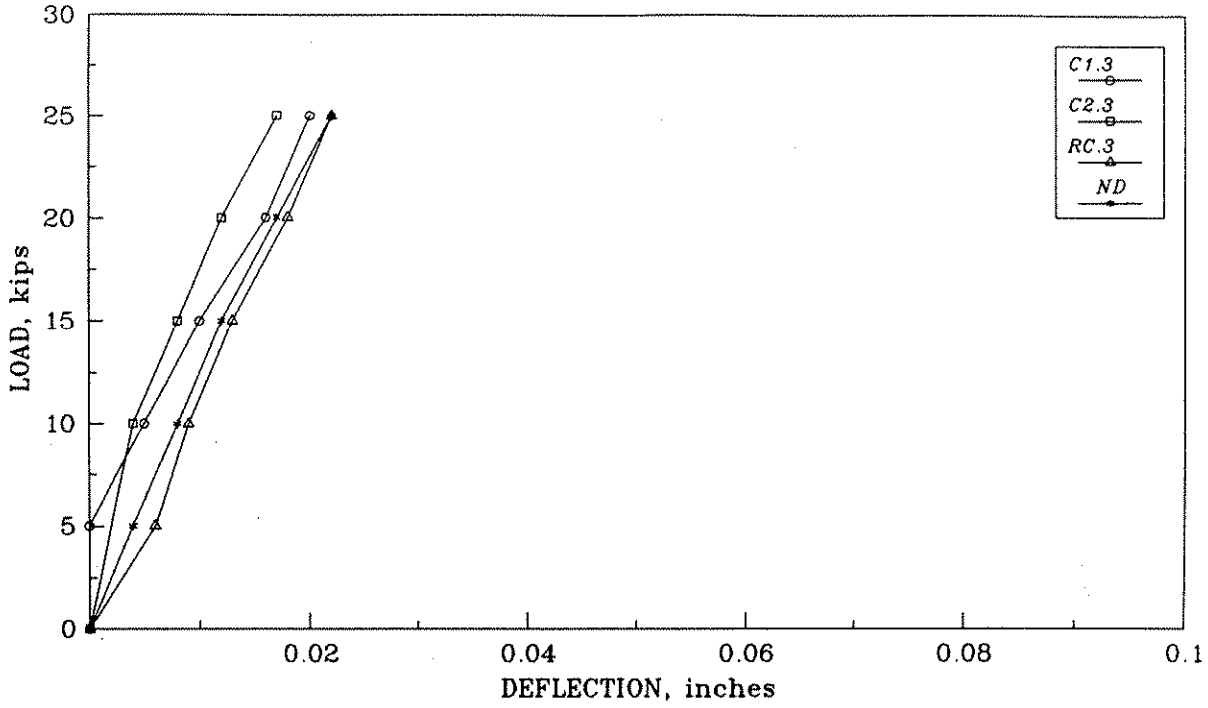

Fig 4.20. Vertical load–deflection curves: diaphragms at third points, deflection at point 5, load at point 4.

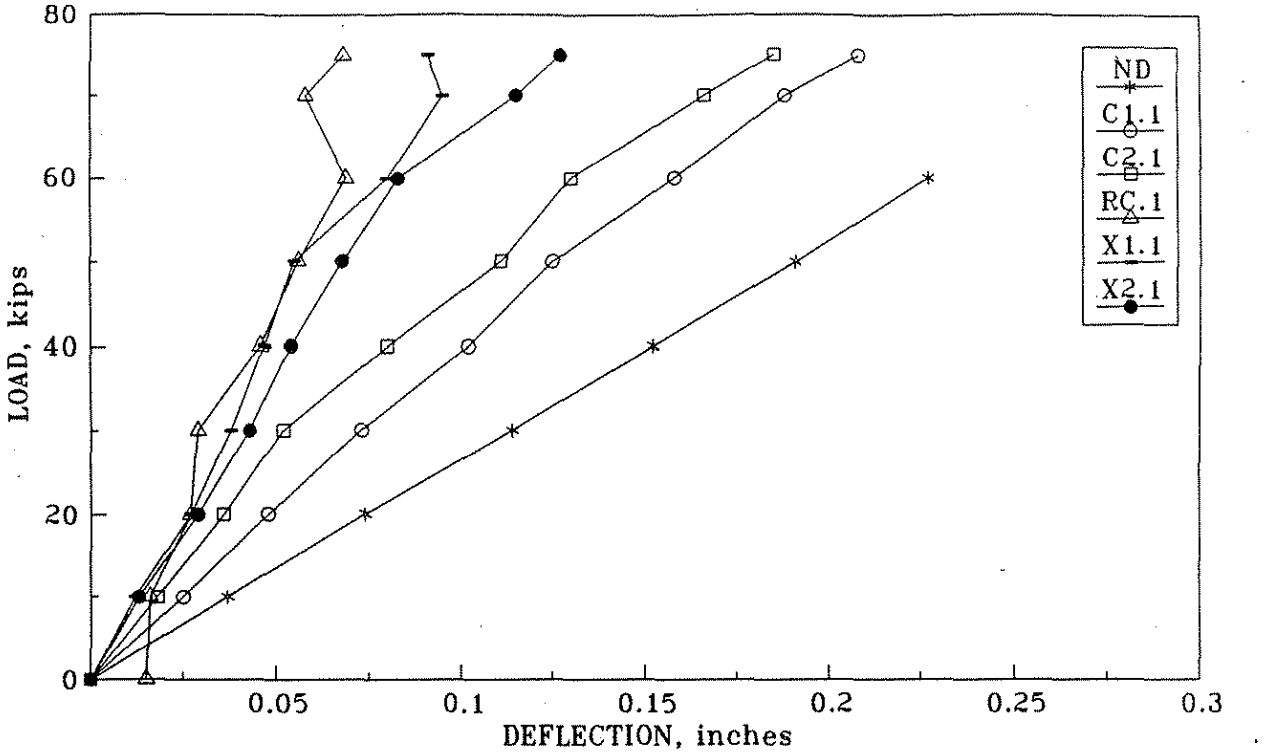

Fig. 4.21. Horizontal load–deflection curves: diaphragm at centerline, deflection and load at point 4.

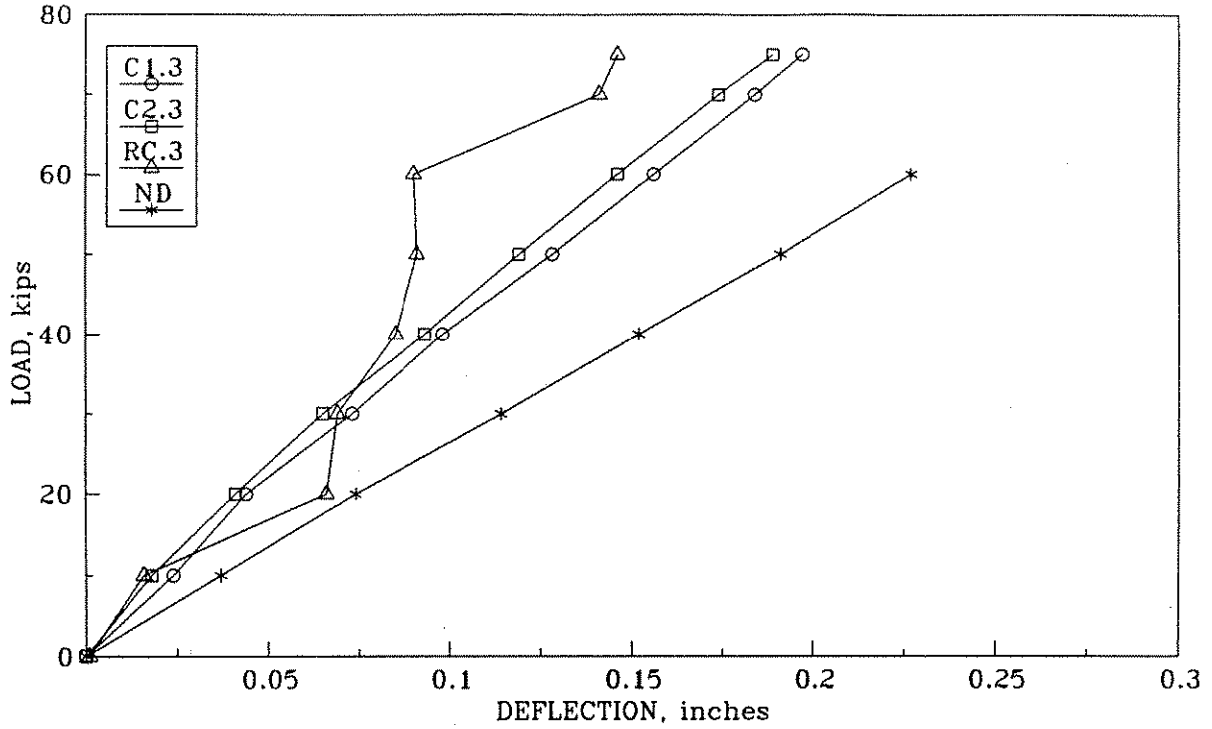

Fig. 4.22. Horizontal load–deflection curves: diaphragms at third points, deflection and load at point 4.

observed by comparing the curves in Fig. 4.21 with like curves (ND experimental versus ND theoretical, etc.) in Fig. 4.3b that shows both fixed-end and pinned-end conditions. The horizontal load versus horizontal deflection curves of the various steel diaphragms investigated fall between the curves for no diaphragms and reinforced concrete diaphragms (RC.1). As was observed in the theoretical curves, the midspan X-brace plus strut diaphragm (X1.1) has essentially the same structural behavior as the midspan reinforced concrete diaphragm (RC.1). A comparison of the horizontal load versus deflection curves for the same type of diaphragms at either the third points or at the midspan as shown in Figs. 4.21 and 4.22 indicates essentially identical results. The curve for RC.3 in Fig. 4.22 was erratic due to instrumentation problems with the DCDT used to measure deflections at this location during this particular test.

Plotted in Figs. 4.23 and 4.24 are the horizontal deflection responses at point 5 when Beam 1 is loaded at point 4 for midspan and one-third point diaphragms, respectively. As has been shown previously, there is less lateral deflection with the reinforced concrete diaphragms (at midspan RC.1 in Fig. 4.23 or at the third points RC.3 in Fig. 4.24) than for any of the other diaphragms. As shown in both curves with no diaphragms in place, the deflection of point 5 on Beam 2 is close to zero.

The horizontal load versus horizontal deflection of the model bridge when subjected to loading between diaphragms is shown in Figs. 4.25 and 4.26. Loading is applied to Beam 1 (points 4 and 7) and Beam 2 (points 5 and 8) in Figs. 4.25 and 4.26, respectively. Problems with the DCDT measuring the horizontal deflection at points in the RC.3 tests previously noted is apparent in Fig. 4.25. Figure 4.25 reveals that with the small channels in place, the horizontal load versus deflection response with the C1.3 diaphragms and the load at point 4 is essentially the same as with the C1.1 diaphragms and the load at point 7. A similar statement can be made for the behavior associated with the reinforced concrete diaphragms (RC.3 and RC.1) as shown in this figure. The horizontal load versus horizontal deflection curves shown in Fig. 4.26 indicate responses similar to those shown

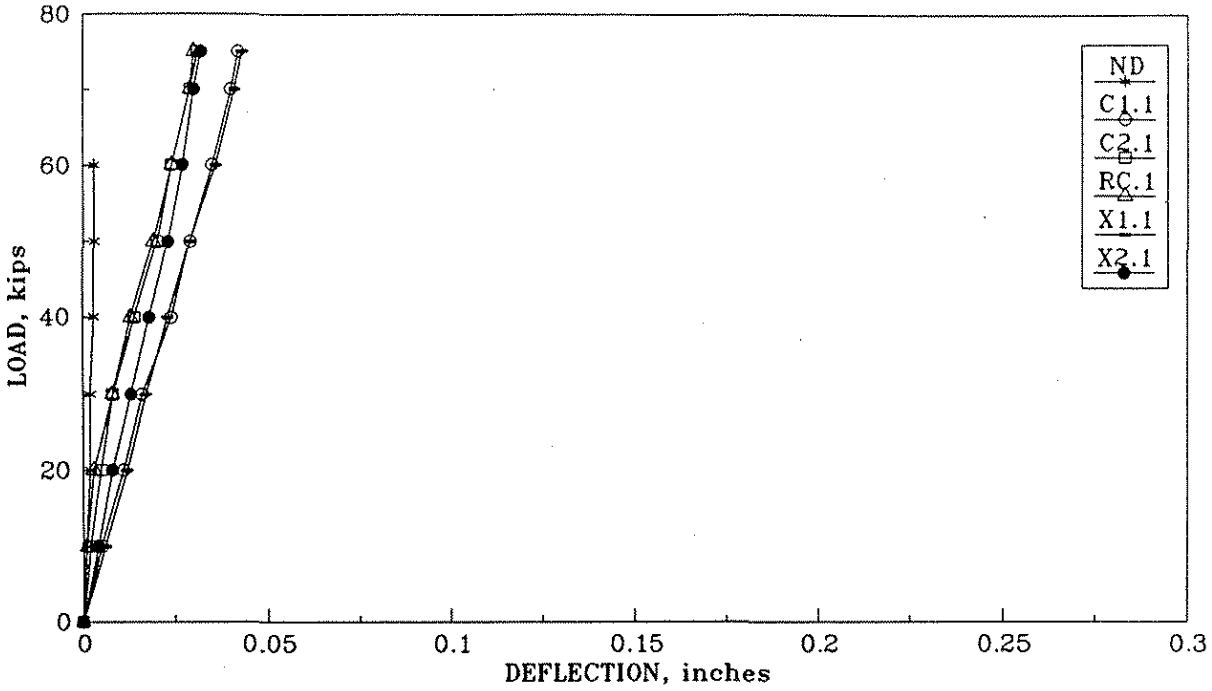

Fig. 4.23. Horizontal load–deflection curves: diaphragms at centerline, deflection at point 5, load at point 4.

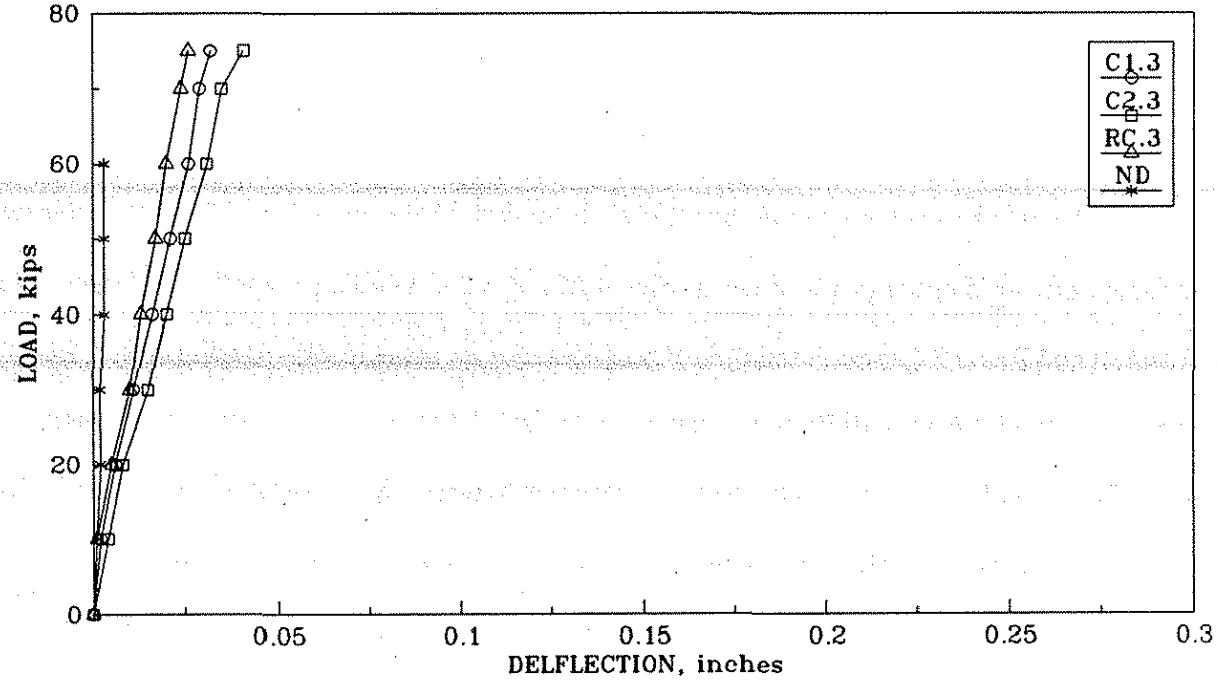

Fig. 4.24. Horizontal load–deflection curves: diaphragms at third points, deflection at point 5, load at point 4.

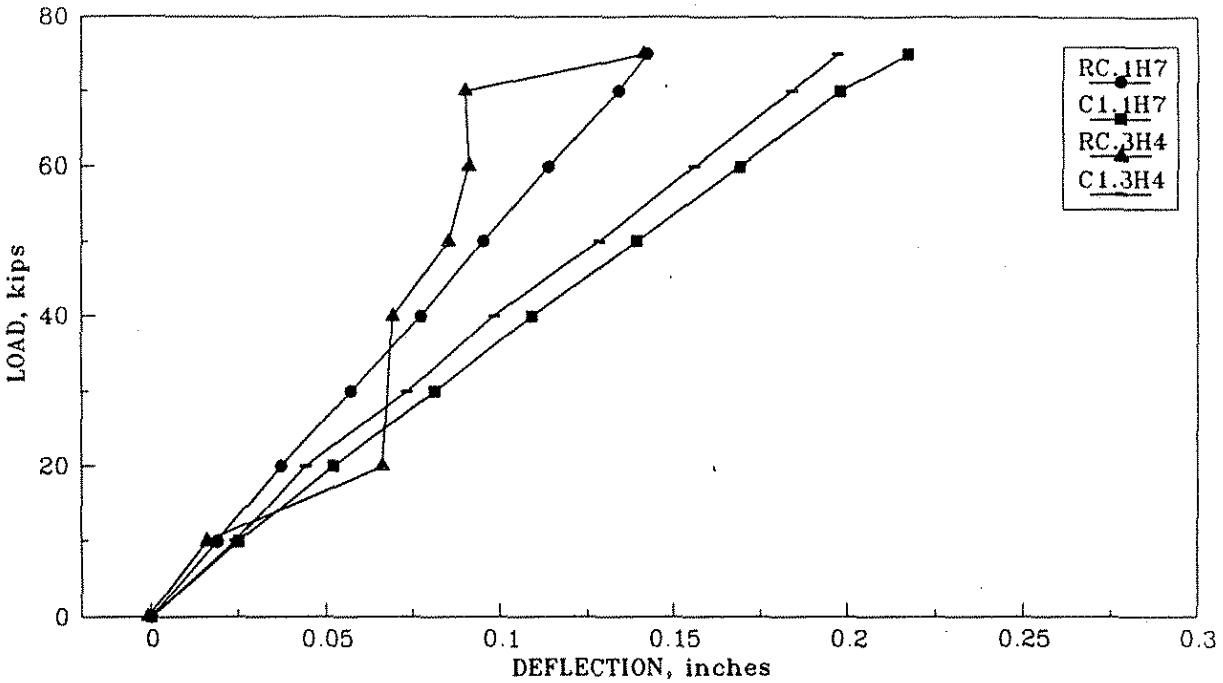

Fig. 4.25. Horizontal load–deflection curves: diaphragms at third points: load and deflection at point 4; diaphragms at center line: load and deflection at point 7.

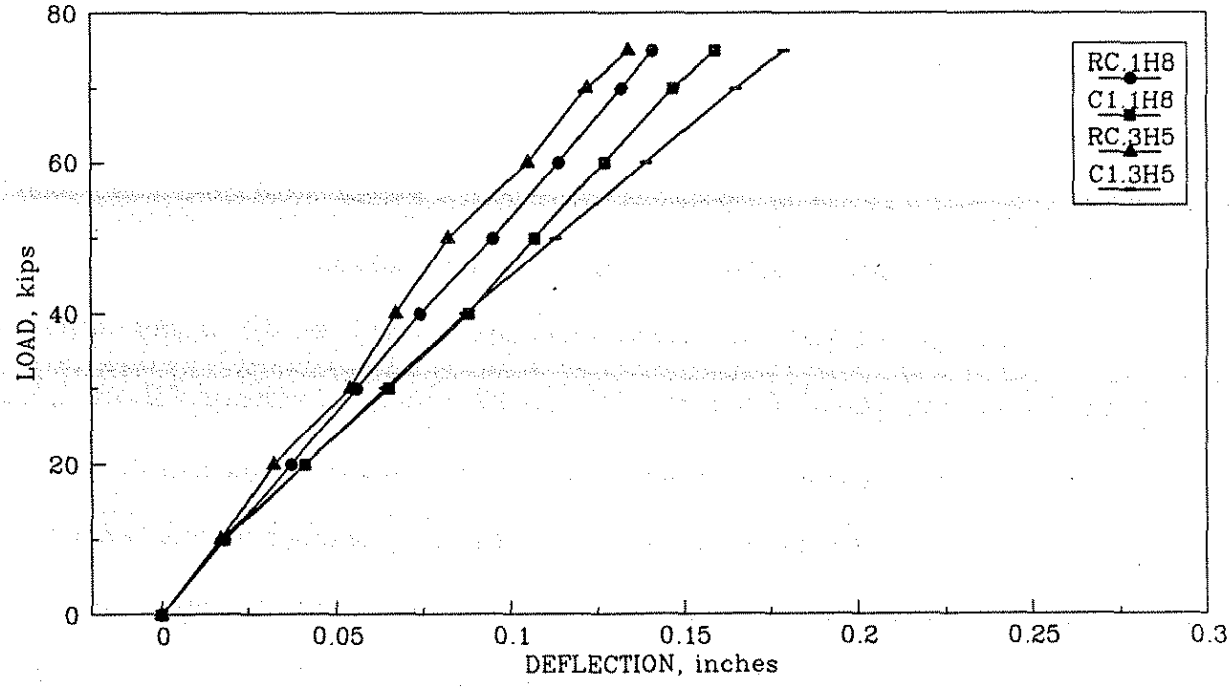

Fig. 4.26. Horizontal load–deflection curves: diaphragms at third points: load and deflection at point 5; diaphragms at center line: load and deflection at point 8.

in Fig. 4.25. A comparison of the data in these two figures reveals there is less horizontal deflection with the reinforced concrete diaphragm and when the interior beam (Beam 2) is loaded. These responses are representative of those that would occur when an overheight vehicle strikes an interior or exterior P/C girder in a given bridge. The horizontal load response of the bridge to loading at points 7 and 8 with the diaphragms at midspan has been shown to be essentially the same for loading at points 4 and 5 with the diaphragms at the third points. However, as previously shown, by loading the beams at the location of the midspan diaphragms (points 4, 5 and 6) the effectiveness of the various diaphragms is more evident. Thus, the majority of the experimental results are presented for midspan diaphragms and midspan loading of the three girders. However, the reader should remember the obvious--overheight vehicles can strike any of the P/C girders of a given bridge at essentially any point along their length.

4.2.6. Load Distribution Study

The bridge model is a three-dimensional complicated structure which is highly indeterminate. One means of obtaining a better understanding of the behavior of the bridge is to investigate its response to the action of a concentrated load moving transverse and parallel to the span. In this section, influence lines are given for the midspan deflections as a concentrated load is applied at the midspan of the three girders. Only midspan diaphragms are reviewed.

Shown in Figs. 4.27-4.29 are vertical deflection "curves" for the various diaphragms investigated for a vertical load of 20 kips that was applied upward at the midspan of Beams 1, 2, and 3, respectively. The three measured deflections have been connected by straight lines for comparison purposes only. The true deflection curves would obviously be higher-order curves. By normalizing these curves, the influence lines for the midspan deflections when vertical loading is applied at the midspan are obtained. As previous theoretical and experimental data obtained by other researchers have verified, the distribution of vertical loading in a P/C bridge is essentially independent of the type of diaphragms used. By comparing Figs. 4.27 and 4.29, the symmetrical behavior of the bridge is

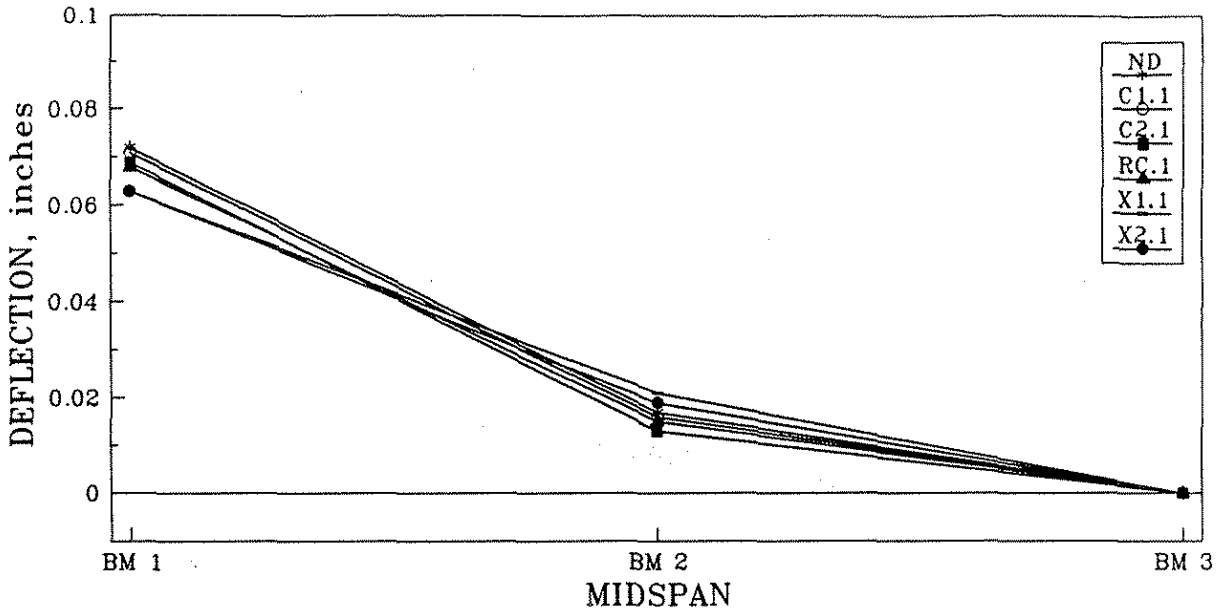

Fig. 4.27. Vertical deflection at points 4, 5, and 6, for a 20 kip upwards vertical force at point 4.

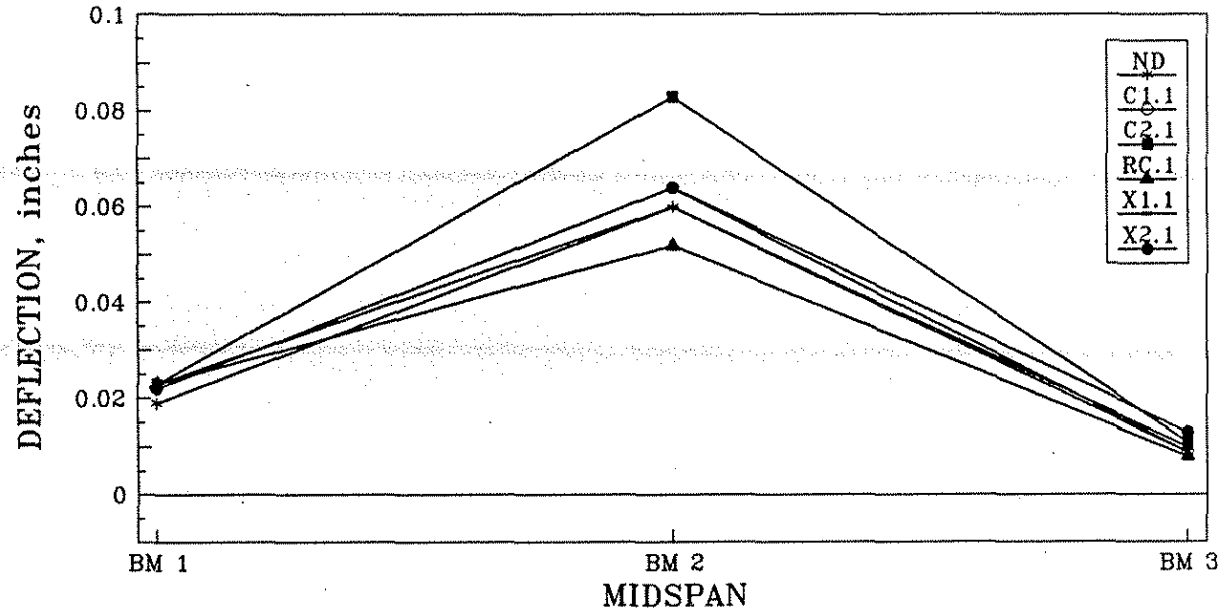

Fig. 4.28. Vertical deflection at points 4, 5, and 6, for a 20 kip upwards vertical force at point 5.

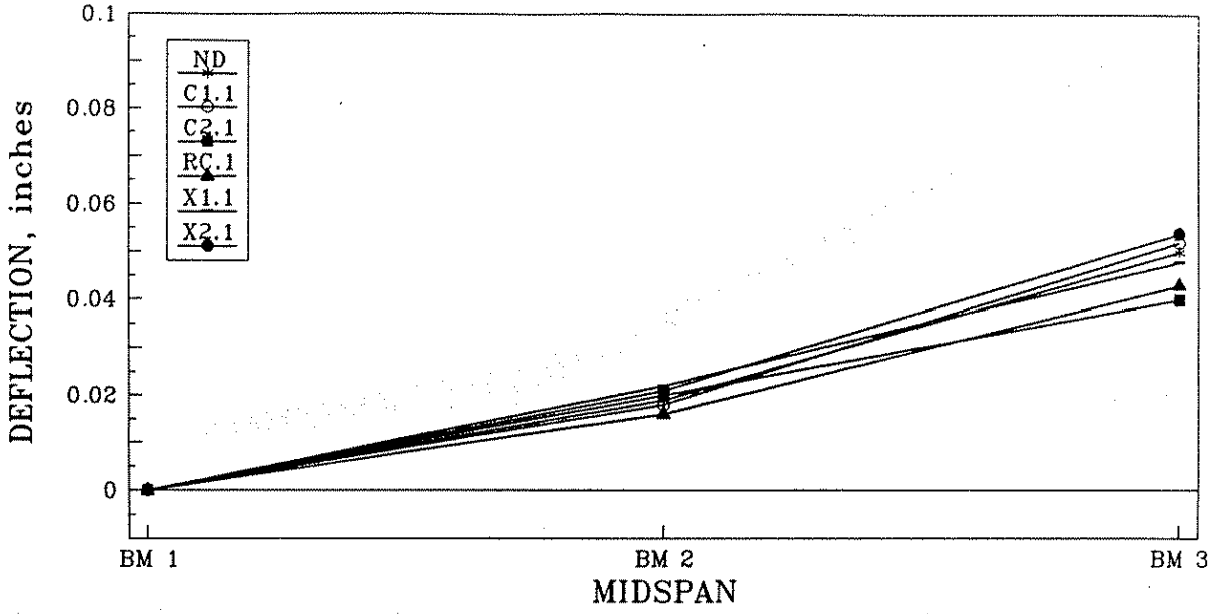

Fig 4.29. Vertical deflection at points 4, 5, and 6 for a 20 kip upwards vertical force at point 6.

confirmed. In Fig. 4.28 there is apparently one bad data point--deflection at Beam 2 with the X2.1 diaphragms in place.

Shown in Figs. 4.30-4.32 are the horizontal deflection "curves" for the various diaphragms investigated for a horizontal load of 50 kips that was applied at the midspan and at the bottom flange of Beams 1-3, respectively. Similar to Figs. 4.27-4.29, the measured deflections have been connected with straight lines for comparison purposes only. The apparent "bad data" in one of these figures have been appropriately identified.

The results shown in these figures are in agreement with the theoretical and experimental results previously presented. By studying these three figures the following observations are evident. Maximum horizontal displacements occur in the loaded beams when there are no diaphragms present. For this configuration, the remaining two beams have close to zero horizontal deflection. The displacement results are essentially symmetrical (Fig. 4.30 compared to Fig. 4.32 and about Beam 2 in Fig. 4.31); however, there are some small differences. As has been previously explained, when Beam 1 is loaded, the diaphragms between Beams 1 and 2 and Beams 2 and 3 are both in compression; when Beam 2 is loaded the diaphragm between Beams 1 and 2 is in tension while the diaphragm between Beams 2 and 3 is in compression; and when Beam 3 is loaded the diaphragms between Beams 1 and 2 and Beams 2 and 3 are both in tension. This behavior plus the connection details, discussed in Sections 4.2.2-4.2.4, produce the small variations from symmetrical behavior. A review of these three figures reveals that the maximum horizontal deflection occurs in the loaded beams for all the diaphragms investigated and that the horizontal deflection in the other two beams is very small. This response indicates that the horizontal deflection of a loaded beam is primarily caused by the rotation of the girder about its longitudinal axis rather than by the deflection of the bridge as a whole.

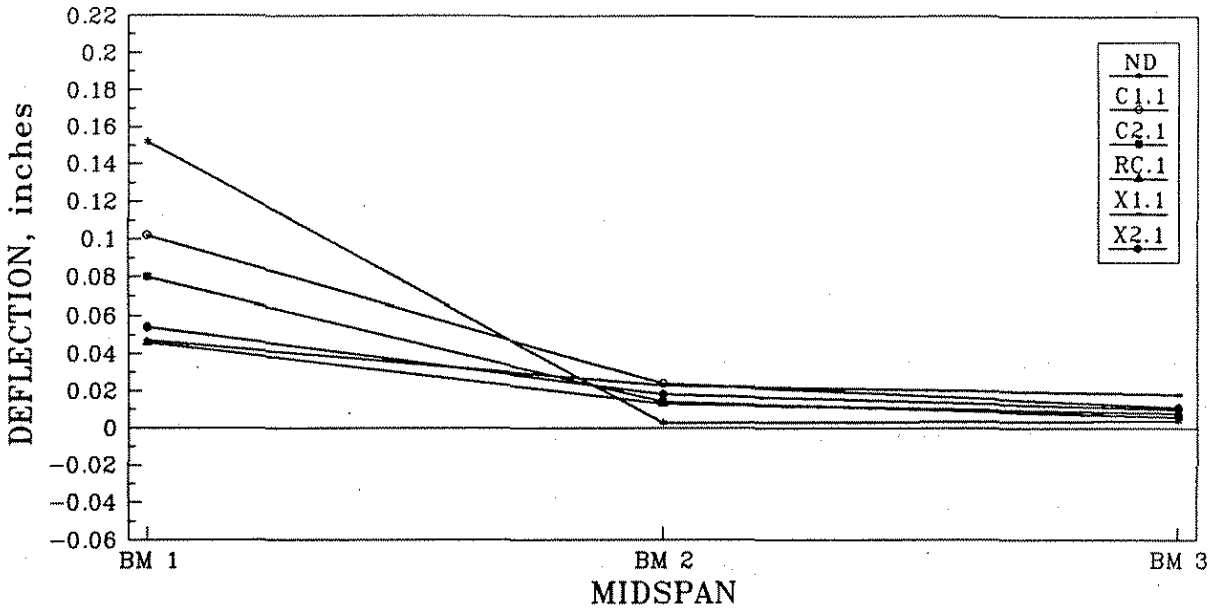

Fig. 4.30. Horizontal deflection at points 4, 5, and 6 for a 40 kip horizontal force at point 4.

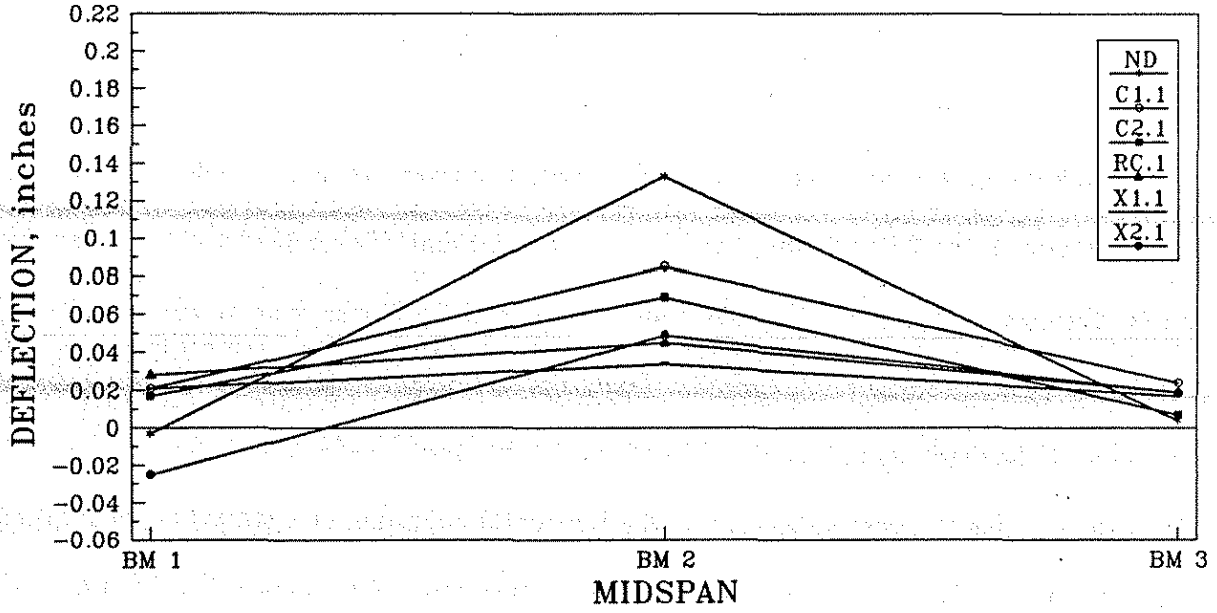

Fig 4.31. Horizontal deflection at points 4, 5, and 6 for a 40 kip horizontal force at point 5.

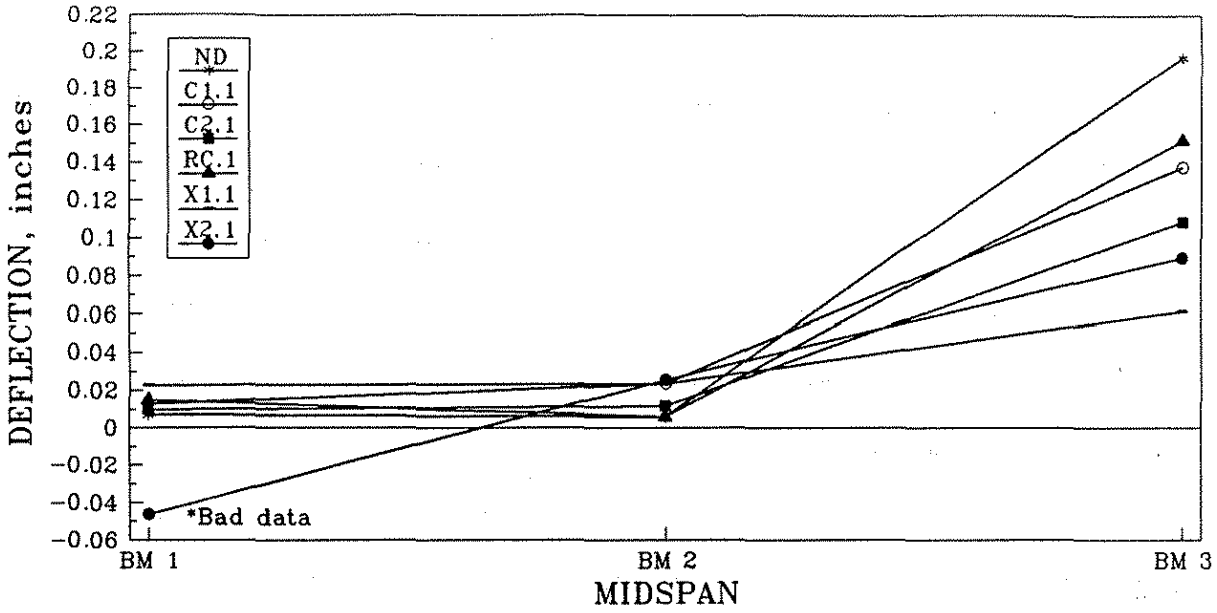

Fig. 4.32. Horizontal deflection at points 4, 5, and 6 for a 40 kip horizontal force at point 6.

4.2.7. Beam and Deck Strains

As previously noted in Section 3.1, strains were measured in the girders and deck. Figures 3.1 and 3.2 show the locations of the gages on the girders and deck, respectively. A summary of the maximum strains (girder, deck and diaphragms) are presented in Tables 4.2 and 4.3. The strains listed in Table 4.2 result from 75 kips of horizontal load, except in the case when no diaphragms were present and when the horizontal load was limited to 60 kips applied at the various load points (see Fig. 3.5). The strains presented in Table 4.3 occurred when a 25-kip upwards vertical load was applied at the various load points.

The left column in each of these tables identifies the type of diaphragm installed and the direction and location of loading. For each diaphragm loading combination, three lines of girder and deck strains are given. In the order listed, these three lines of strains correspond to the measured strains at the 1/4-span, midspan, and 3/4-span locations (Sections B-D in Figs. 3.1 and 3.2). Maximum strains in a particular girder occur when that girder is loaded. Thus, the strains presented are for Beams 1-3 when points 4-6, respectively, were loaded. The girder strains presented were at the sides (1 1/4 in. up from the bottom of the girder) of the bottom flange--LL and LR corresponding to the lower left and lower right sides, respectively. Since the top flange girder strains at UL and UR in Fig. 3.1b were very small, these strains are not presented. As the diaphragm designations indicate (see Table 2.2), the strains given correspond to diaphragms positioned at the midspan of the model. The deck strains presented are along lines 1 and 4 (shown in Fig. 3.2) at Sections B-D (see Fig. 3.2).

The magnitudes of the measured strains presented are relatively small due to the size of the bridge model (full-scale) and the magnitude of the forces applied. As previously explained, the magnitude of force applied to the bridge was controlled to minimize damage to the bridge deck. Although the structure was relatively stiff, a review of the midspan girder strains with the various diaphragms in place verifies that the type of diaphragm has an effect on the strains.

Table 4.2. Maximum strains due to horizontal loading.

Diaphragm Type and Loading Direction and Location	Strain-MII					
	Girder		Deck		Diaphragm	
	LL	LR	Line 1	Line 4	Max +	Max -
C1.1-H4	2 -117 2	BD[a] 147 2	-15 -57 4	-2 3 -1	89 21	-411 -96
C1.1-H5	9 -120 4	-5 81 -13	-21 -52 -4	3 7 BD	229 68	-22 -288
C1.1-H6	2 -176 -9	-3 185 -11	-22 -44 -3	-9 6 BD	86 230	-15 -
C2.1-H4	12 -77 11	2 126 3	-22 -43 -23	15 39 22	121 25	-335 -53
C2.1-H5	23 -120 8	-3 127 4	-35 -40 -27	9 49 17	88 18	-10 -127
C2.1-H6	15 -174 9	-18 161 -18	-25 -35 -24	-1 77 -4	19 58	-3 -4
RC.1-H4	5 -7 3	7 77 10	-25 -65 -3	6 7 12	- -	-107 -18
RC.1-H5	8 -29 7	2 94 7	-30 -42 -7	4 9 6	8 -	- -79
RC.1-H6	-2 -186 -16	-1 182 13	-20 -36 -5	-9 8 -8	1 -	-6 -2

Table 4.2. Continued.

Diaphragm Type and Loading Direction and Location	Strain-MII					
	Girder		Deck		Diaphragm	
	LL	LR	Line 1	Line 4	Max +	Max -
X1.1-H4	2 -42 0	5 96 7	-23 -62 -1	4 6 10	3 20	-178 -63
X1.1-H5	1 -44 -1	0 51 -3	-24 -57 -3	2 6 9	145 42	-54 -90
X1.1-H6	-1 -81 -9	4 61 1	-23 -49 -3	-1 4 10	82 150	-26 -
X2.1-H4	2 -54 3	4 131 7	-22 -60 1	4 6 15	- -	-306 -48
X2.1-H5	7 -52 3	-2 73 -4	-24 -51 -5	1 8 9	94 20	- -191
X2.1-H6	-6 -113 -16	2 86 9	-22 -42 -4	-2 6 11	35 203	- -
ND-H4	6 -175 1	-6 -14 -1	-17 -84 9	4 1 4	NA[b] NA	NA NA
ND-H5	16 -191 9	-7 127 -21	-26 -31 -7	6 3 9	NA NA	NA NA
ND-H6	-1 -228 -13	-8 227 9	-23 -31 -6	-14 7 3	NA NA	NA NA

[a]BD = Bad data.
[b]NA = Not applicable.

Table 4.3. Maximum strains due to vertical loading.

Diaphragm Type and Loading Direction and Location	Strain - MII					
	Girder		Deck		Diaphragm	
	LL	LR	Line 1	Line 4	Max +	Max -
C1.1-V4	-96 -53 -19	-26 -72 -26	82 61 3	-3 -6 BD[a]	27 12	-10 -2
C1.1-V5	-16 -49 -17	-21 -85 -15	10 8 0	-6 1 BD	8 20	-34 -36
C1.1-V6	-28 -66 -24	-15 -49 -15	-9 -13 -1	1 6 BD	14 24	-3 -31
C2.1-V4	-16 -49 -15	-21 -60 -24	21 51 24	-2 -8 -3	24 14	-22 -8
C2.1-V5	-16 -45 -15	3 -54 -14	7 10 9	5 8 7	0 1	-10 -13
C2.1-V6	-17 -56 -21	-17 -56 -14	-3 -8 -4	10 31 14	8 5	-2 -10
RC.1-V4	-19 -45 -22	-21 -78 -24	20 48 3	0 -3 -5	- 2	-3 -
RC.1-V5	-14 -38 -15	5 -46 -13	6 12 3	3 2 -2	1 -	-9 -9
RC.1-V6	-19 -72 -13	-13 -43 -16	-7 -10 0	5 5 5	8 -	- -5

Table 4.3. Continued.

Diaphragm Type and Loading Direction and Location	Strain - MII					
	Girder		Deck		Diaphragm	
	LL	LR	Line 1	Line 4	Max +	Max -
X1.1-V4	-18 -49 -22	-22 -73 -28	23 48 5	0 -3 -2	22 19	-32 -6
X1.1-V5	-13 -39 -15	4 -46 -12	7 13 1	3 1 2	34 29	-49 -32
X1.1-V6	-17 -65 -21	-12 -45 -15	-7 -14 0	4 4 10	24 26	-4 -35
X2.1-V4	-17 -49 -20	-22 -15 -25	24 50 4	0 -2 3	26 10	-26 -
X2.1-V5	-14 -41 -16	5 -50 -13	10 12 2	3 3 3	18 17	-39 -41
X2.1-V6	-19 -73 -26	-12 -48 -17	-7 -11 -1	4 8 12	9 29	- -32
ND-V4	-18 -54 -18	-22 -56 -26	25 45 5	-1 -2 -2	NA[b] NA	NA NA
ND-V5	-16 -53 -18	7 -70 -15	8 6 2	3 0 2	NA NA	NA NA
ND-V6	-21 -67 -23	-13 -67 -17	-9 -11 -3	6 5 9	NA NA	NA NA

[a]BD = Bad data.
[b]NA = Not applicable.

As has previously been documented, cracks in the deck, channel connections, and the reinforced concrete connections to girders influenced the bridge response, especially when loading was applied at point 6 on Beam 3. A review of the strains in Tables 4.2 and 4.3 reveals that the measured strains were considerably larger when Beam 3 (rather than Beams 1 or 2) was loaded. In order to minimize the secondary effects that were induced by the fabrications details in the model bridge, only the results obtained when Beams 1 and 2 were loaded will be discussed. In the following paragraphs, the response of the girders to horizontal and vertical loading will be presented separately. Obviously, comparisons should not be made between the strains listed in the two tables because of the differences in the direction and magnitude of the load applied.

When horizontal loading was applied to the bridge, the largest measured strain (191 MII which corresponds to a stress of approximately 997 psi) occurred in Beam 2. The smallest girders strains occurred when the reinforced concrete diaphragms (RC.1) or X-brace plus strut diaphragms (X1.1) were in place. In order to simplify the comparisons of the effects of the various diaphragm types on the induced girder stresses, the largest strains (LL or LR) in Table 4.2 have been multiplied by the concrete modulus of elasticity. These girder stresses are presented in Table 4.4. As noted in Section 1.2, one of the primary objectives of this investigation was to establish a steel diaphragm configuration that was essentially structurally equivalent to the reinforced concrete diaphragms that are presently used in Iowa. One way of demonstrating the structural equivalency of the diaphragms is to compare the strains or stresses that are induced in the bottom flanges of the beams when loads are applied to the girders with the various diaphragm configurations in place. As may be seen from Table 4.4, the girder stresses are slightly smaller with diaphragms RC.1, X1.1 or X2.1 in place. As previously noted, the model bridge construction details for the RC.1 diaphragms affected the results when horizontal load was applied at point 6. Thus, on the basis of the girder stresses, one can say the response of the bridge to horizontal loading would be essentially the same with one of these three configurations in place. The deck strains measured are very small and are obviously influenced

Table 4.4. Girder stresses.

Diaphragm	Load Point[a]	Stress - psi	
		Horizontal loading[b]	Vertical loading[c]
C1.1	4	767	-326
	5	627	-350
	6	966	-300
C2.1	4	658	-285
	5	663	-258
	6	908	-292
RC.1	4	402	-321
	5	491	-219
	6	971	-300
X1.1	4	501	-318
	5	266	-222
	6	423	-287
X2.1	4	684	-167
	5	381	-238
	6	590	-316
ND	4	914	-287
	5	997	-321
	6	1190	-350

[a]Load points: See Fig. 3.5.
[b]Stress based on largest bottom flange strain tension or compression; absolute value listed.
[c]Stress based on average of bottom flange strains.

by deck cracking. As a result of the direction of the horizontal loading, strains along line 1 are compressive while those along line 4 are tensile.

Since the strains presented in Table 4.2 were induced by upward loading on the girders, the strains measured in the bottom flanges of the beams were compressive. Also shown in Table 4.4 are the maximum midspan girder stresses that result from the various combinations of diaphragms and vertical load. These stresses were obtained by taking an average of the midspan bottom flange strains listed in Table 4.2 and multiplying them by the modulus of elasticity of concrete. The girder stresses presented in Table 4.4 that were induced by the vertical load are essentially equal, indicating that diaphragms have essentially no effect on vertical load distribution. The deck stresses (not presented) which were caused by the vertical loading are extremely small and are basically independent of the type of diaphragms in place. When Beam 2 was loaded vertically, the deck strains along lines 1 and 4 were tensile. When Beam 1 was loaded, the deck strains along line 1 were tensile, while those along line 4 were compressive. Similar deck strains occurred when Beam 3 was loaded--compressive strains along line 1 and tensile strains along line 4.

4.2.8. Diaphragm Strains

As previously noted, the measured diaphragm strains for the various diaphragm configurations and loading cases are also presented in Tables 4.2 and 4.3. The diaphragm location and magnitude of vertical and horizontal loads producing the tabulated strains are noted in Section 4.2.7. Location of the diaphragm gages is shown in Fig. 3.3. The last two columns of these two tables present the maximum and minimum strains recorded in the various series of tests. The measured diaphragm strains from the various series of tests cannot be compared since they occur in the various diaphragm types and at different locations and orientations. For each series of tests, two lines of diaphragm strain data are presented; the first line presents data for the diaphragm between Beams 1 and 2 (Diaphragm B1 in Fig. 2.3) while the second line is for strains in the

diaphragm between Beams 2 and 3 (Diaphragm B2 in Fig. 2.3). In the following paragraphs the effect of horizontal loading and vertical loading will be discussed separately.

With horizontal loading for a given type of diaphragm, the effect of applying load to each of the three beams independently is readily apparent. In the general sense, when load is applied to Beam 1, both Diaphragms B1 and B2 are in compression; when load is applied to Beam 2, Diaphragm B1 is in tension while Diaphragm B2 is in compression; and when load is applied to Beam 3 both diaphragms are in tension. Diaphragm connections and deck cracking obviously influenced the diaphragm strains presented.

For a given diaphragm configuration, a comparison of the measured strains in Diaphragms B1 and B2 reveals the lateral distribution provided by the diaphragm. With the steel channel diaphragms (C1.1 and C2.1) when horizontal load was applied to Beam 1, the measured strains in Diaphragm B2 were approximately 15%-25% of the strains in Diaphragm B1, indicating that about 15%-25% of the horizontal force was distributed to Beam 3. Similar results were obtained in the theoretical investigation (see Fig. 4.6). The X-brace plus strut (X1.1) diaphragm distributed approximately 30% of the horizontal load applied to Beam 1 to Beam 3, while the X-brace without the strut diaphragm (X2.1) distributed approximately 20% of the horizontal load. On the basis of the measured strain data, the reinforced concrete diaphragms (RC.1) distributed approximately 15% of the force to the other exterior beam (Beam 3). The reinforced concrete distribution percentage (15%) should be disregarded since it was influenced by the connections used and was based on very small magnitudes of strain, which obviously are influenced to a greater degree by experimental errors.

A review of the diaphragm measured strains listed in Table 4.3 that were induced by the vertical loading verifies what has been documented by the deflection curves and beam strains. The lateral distribution of the vertical load is essentially independent of the type of diaphragm used. For a given configuration of diaphragms, very little change occurred in the recorded diaphragm strains

as the vertical load was moved from beam to beam. In fact, there was minimal variation between the strain readings occurring in the various diaphragms. The only exception to this statement occurred when reinforced concrete diaphragms were used. Measured strains in the reinforced concrete diaphragm were very small. For additional analysis of the girder, deck, and diaphragm strains the reader is referred to Ref. 9.

4.3. Comparison of Analytical and Experimental Results

In the previous sections, theoretical and experimental results have been presented. In these sections, the effects of the various diaphragms investigated on the horizontal and vertical load distribution have been documented and compared. In this section, the experimental results will be presented in different formats and compared with the theoretical results.

4.3.1. Displacement Distribution Along the Bridge Span

The nine figures (Figs. 4.33-4.41) in this section compare the theoretical and experimental horizontal deflections that occurred when a 50-kip horizontal load was applied to the midspan of Beam 1 (point 4) or the midspan of Beam 2 (point 5). In each of these figures, two theoretical horizontal deflection curves are presented for each beam--one assuming the beams have pinned ends and one assuming the beams have fixed ends. The horizontal displacements, measured at the quarter points of the span and midspan of each of the three beams, is indicated in these figures as black dots. While the data in Figs. 4.30-4.32 were described as being equivalent to influence lines, the data in these figures could be described as being influence surfaces--horizontal deflection for all three beams is given for a particular horizontal load. A quick review of these nine figures reveals that the horizontal deflections are very small. The maximum deflection occurs in the loaded beam.

As would be expected, the absolute maximum deflection occurred when diaphragms were not present. Figure 4.33 presents the horizontal deflections of the three beams when there were no diaphragms present and when the 50-kip horizontal load was applied at the midspan of Beam 1.

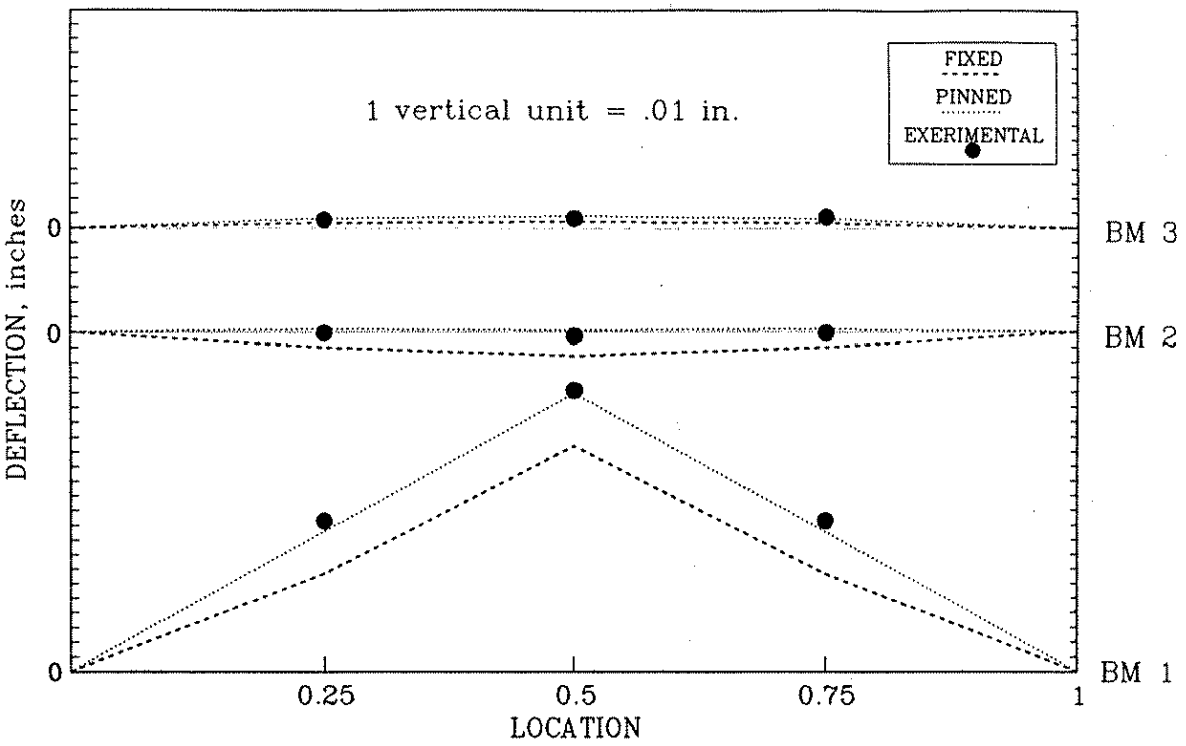

Fig. 4.33. Beam horizontal deflections for a 50 kip horizontal force at point 4 and no diaphragms.

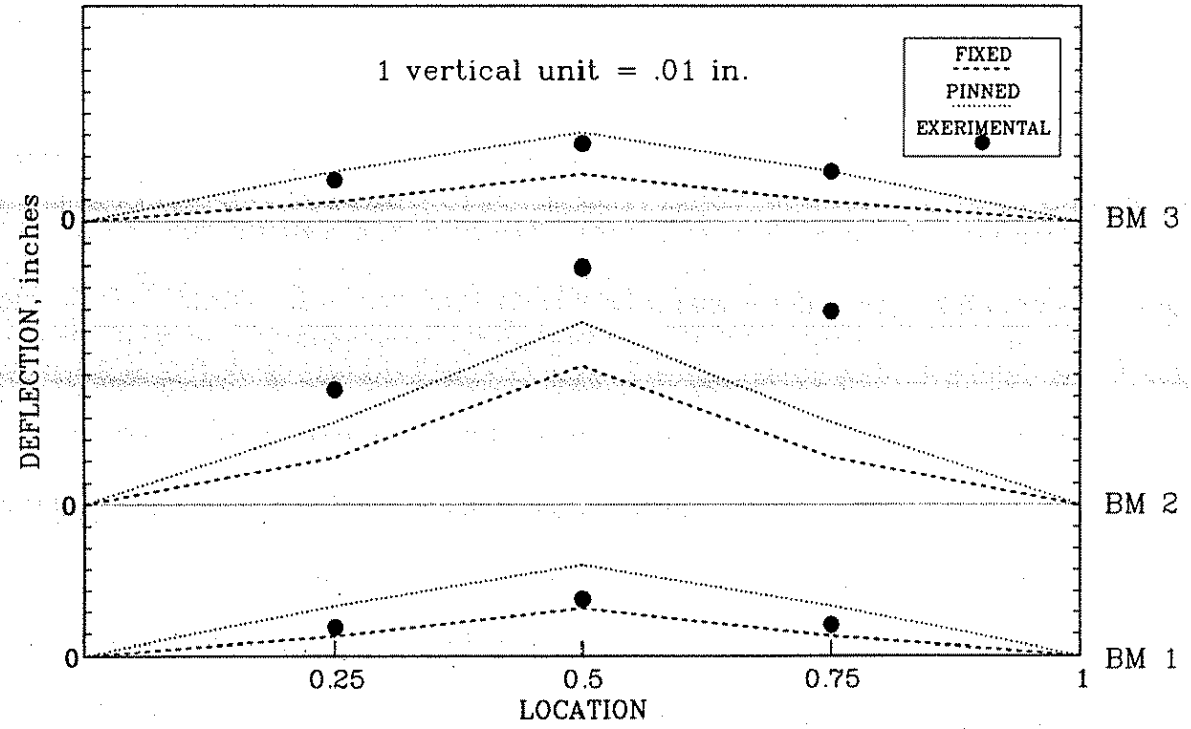

Fig. 4.34. Beam horizontal deflections for a 50 kip horizontal force at point 5 and C1.1 diaphragms.

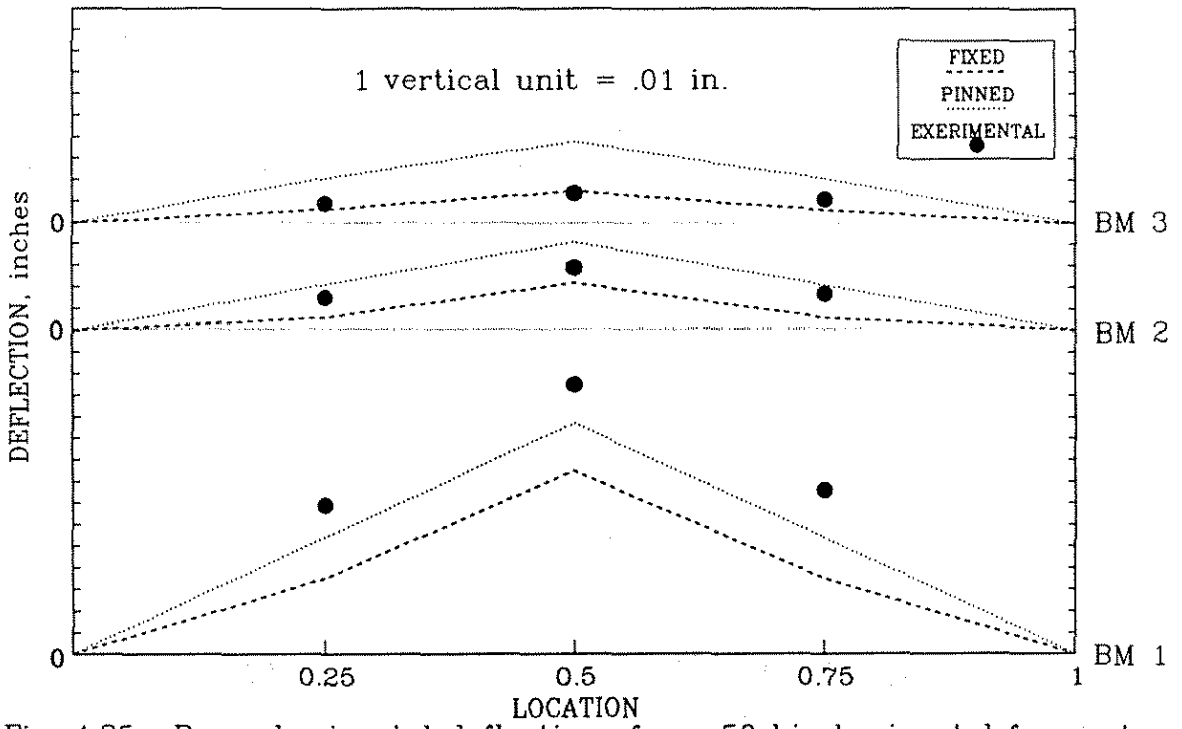

Fig. 4.35. Beam horizontal deflections for a 50 kip horizontal force at point 4 and C1.1 diaphragms.

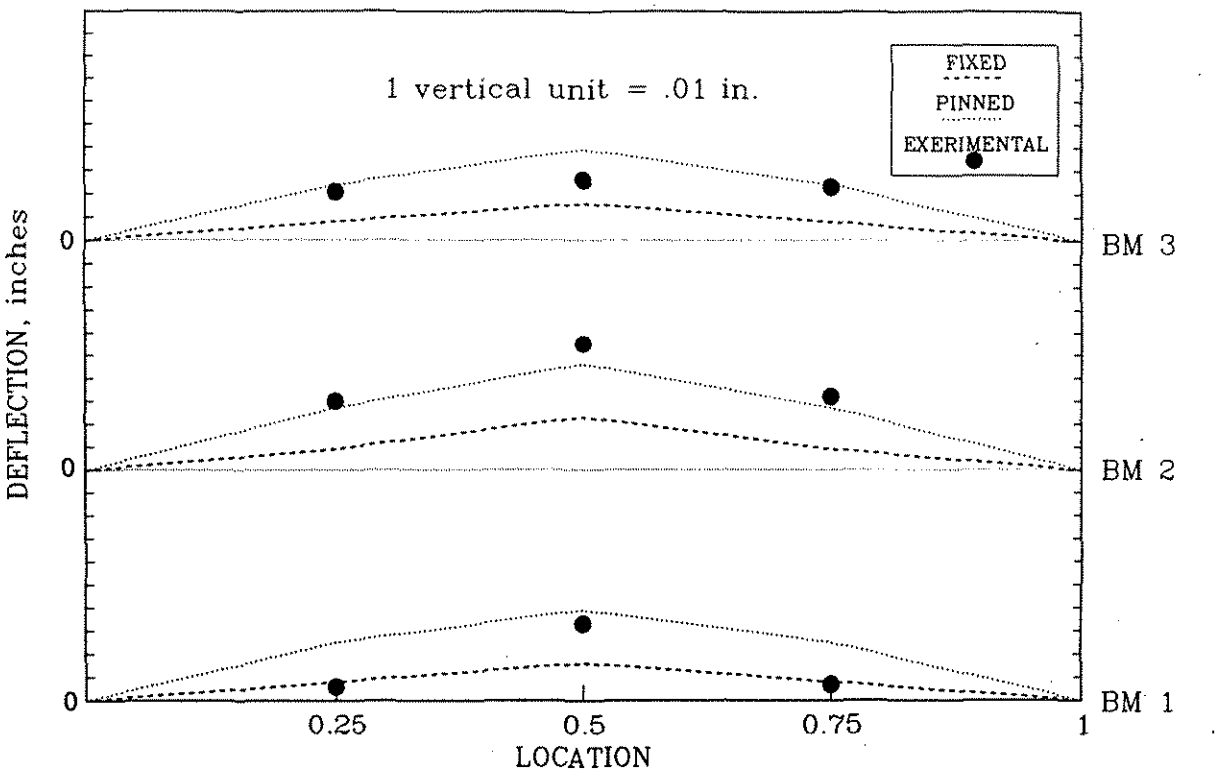

Fig. 4.36. Beam horizontal deflections for a 50 kip horizontal force at point 5 and RC.1 diaphragms.

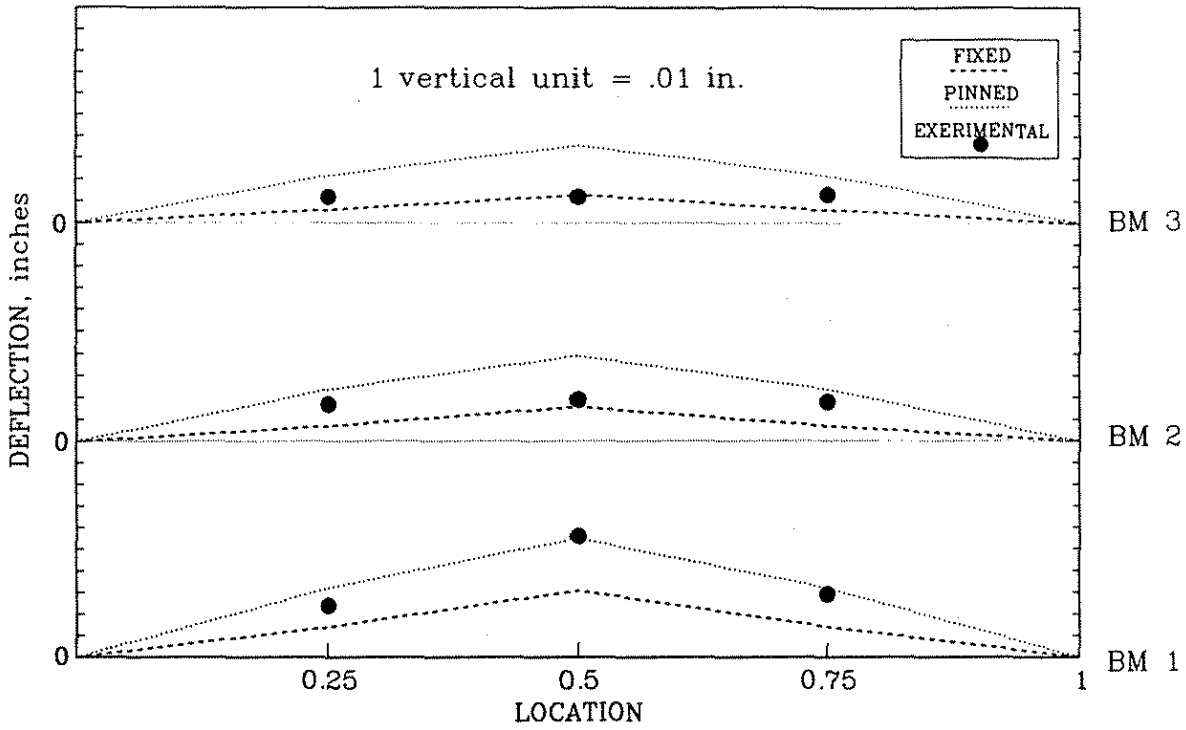

Fig. 4.37. Beam horizontal deflections for a 50 kip horizontal force at point 4 and RC.1 diaphragms.

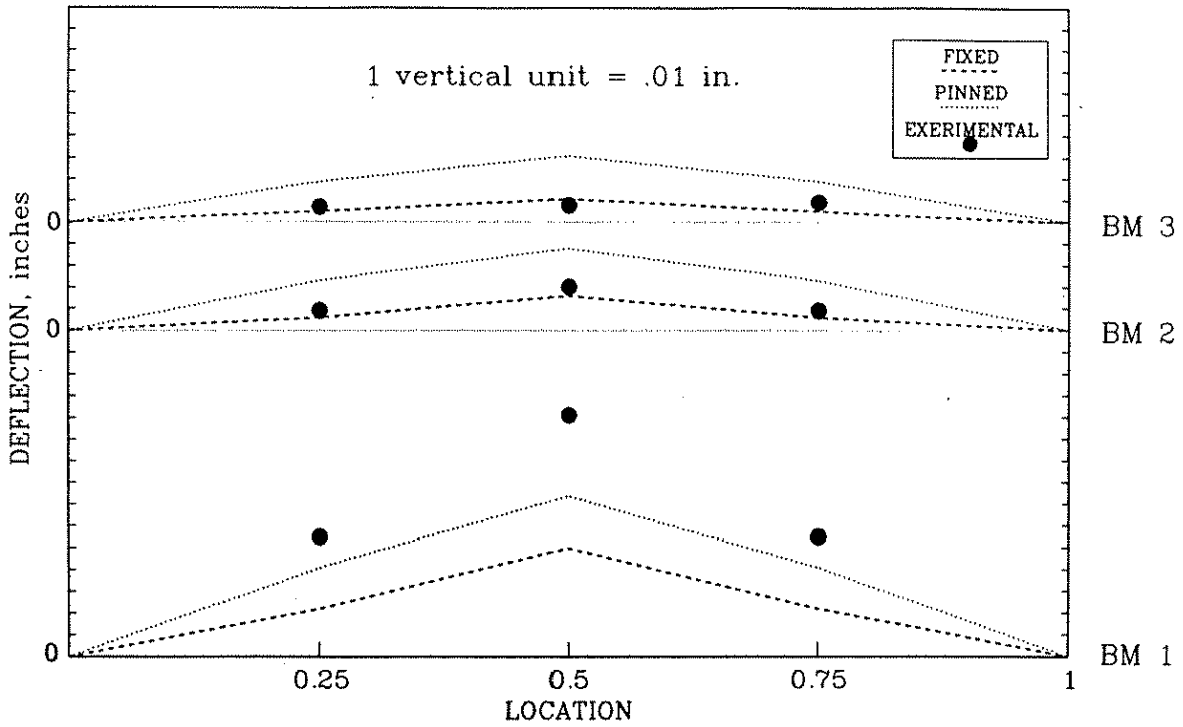

Fig. 4.38. Beam horizontal deflections for a 50 kip horizontal force at point 4 and C2.1 diphragms.

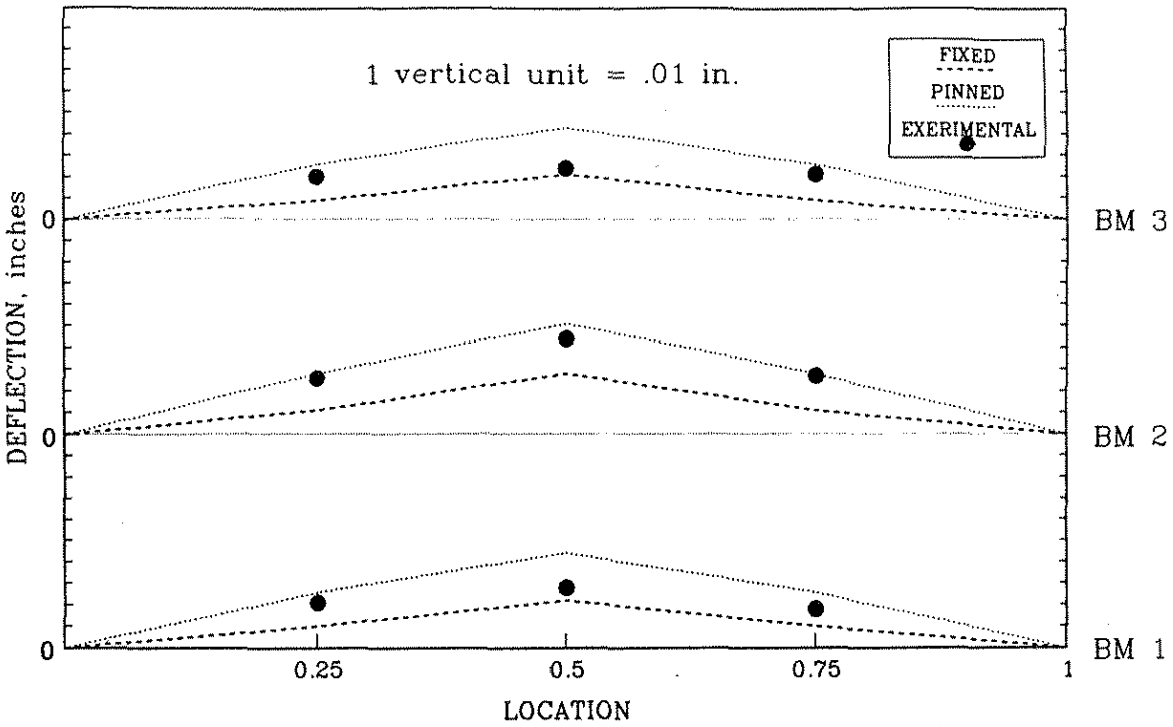

Fig. 4.39. Beam horizontal deflections for a 50 kip horizontal force at point 5 and X1.1 diaphragms.

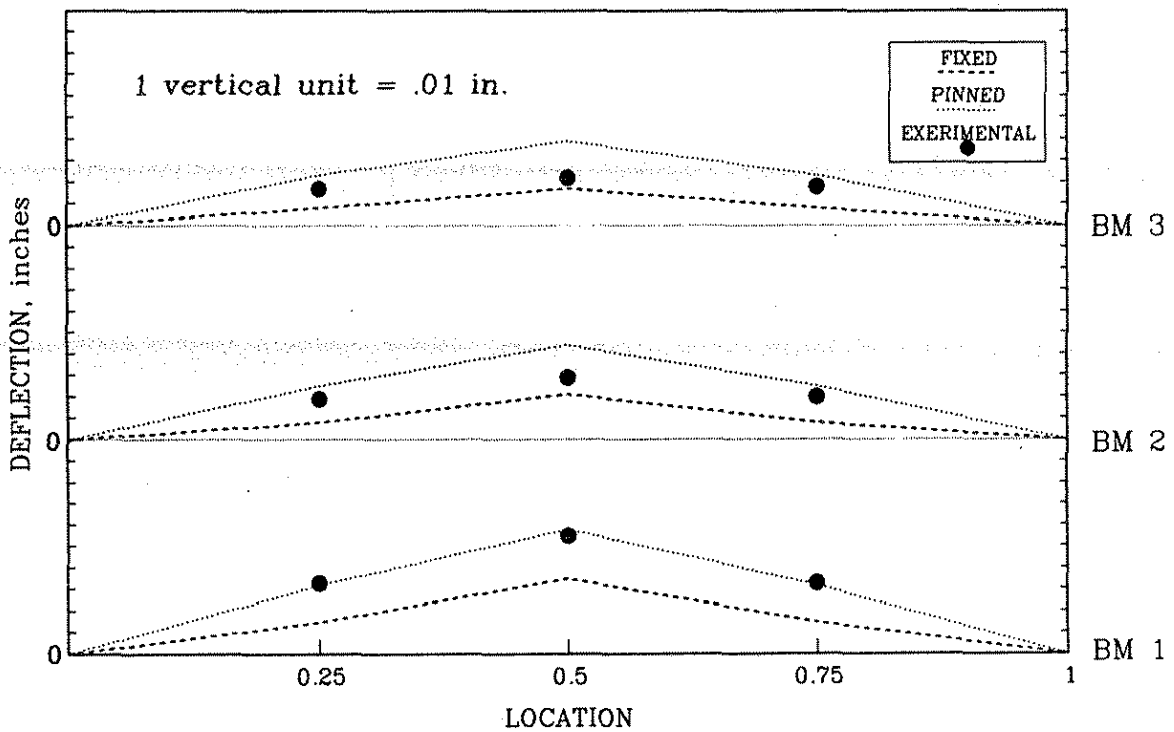

Fig. 4.40. Beam horizontal deflections for a 50 kip horizontal force at point 4 and X1.1 diaphragms.

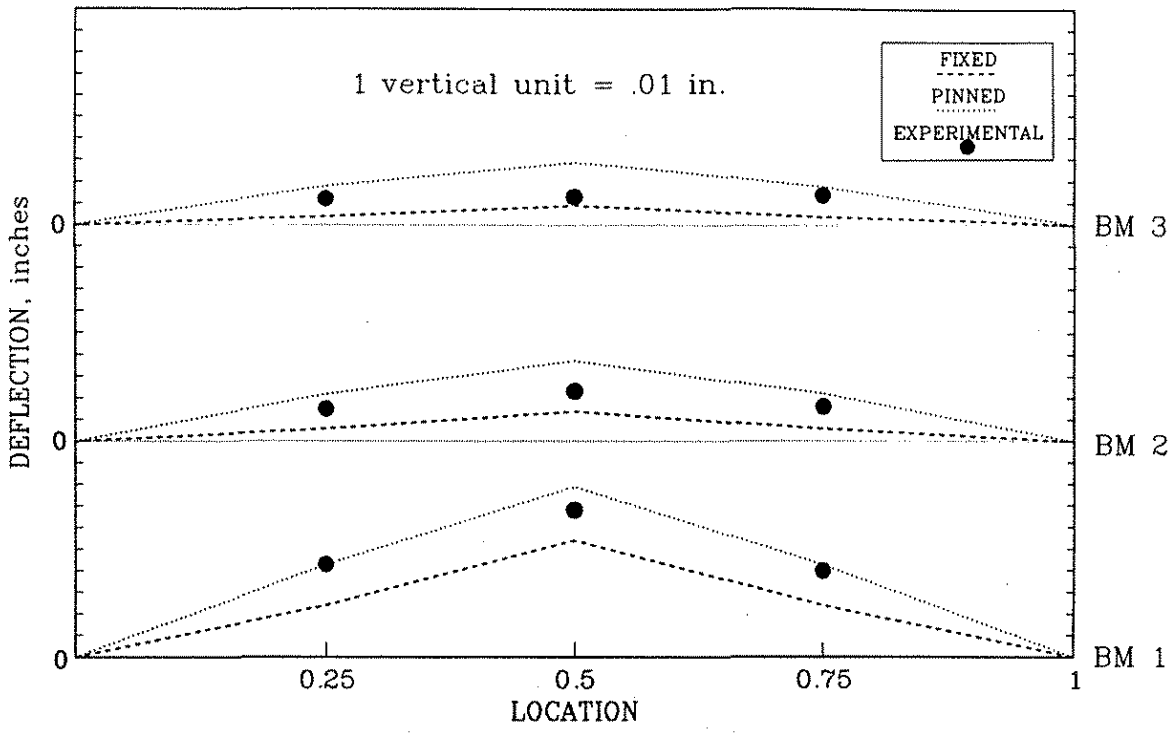

Fig. 4.41. Beam horizontal deflections for a 50 kip horizontal force at point 4 and X2.1 diaphragms.

Cracks in the deck (see Section 4.2.1) and the analytically modeled shear connection between the P/C girders and the bridge deck (see Section 4.1.1) are the primary reasons the measured deflection of the loaded beam exceeds the theoretical deflections (pinned and fixed ends) in these curves. Deflections of the other two unloaded beams are essentially zero. Because of the curvature of the bridge deck, the horizontal deflection at the midspan of Beam 2 was directed towards the loaded beam (Beam 1) by a small amount.

Illustrated in Figs. 4.34 and 4.35 are the horizontal beam deflections that occurred when a 50-kip horizontal force was applied at points 5 and 4, respectively, with diaphragms C1.1 in place. A comparison of the two figures reveals that when Beam 2 was loaded, it deflected slightly less than Beam 1 when it was loaded. Figure 4.34 reveals symmetry of the deflection responses; the horizontal deflections of Beams 1 and 3 are essentially the same. In both of these figures (except for the deflection at the point of loading), there is good agreement between the theoretical and experimental deflections.

The horizontal deflections that occur in the three beams with the RC.1 diaphragms in place and when a 50-kip horizontal force was applied at points 5 and 4 are presented in Figs. 4.36 and 4.37, respectively. Except for the loaded beams, there is excellent agreement between experimental and theoretical results. Since the deflections shown in these figures are small, comparisons of the behavior of the bridge with various diaphragm types is difficult. For such comparisons, the reader is referred to Fig. 4.3 (theoretical results) and Fig. 4.21 (experimental results) that present the deflection of point 4 for all diaphragms.

Comments previously made apply also to the comparisons between theoretical and experimental results shown in Fig. 4.38 for the C2.1 diaphragms, Figs. 4.39 and 4.40 for the X1.1 diaphragms, and Fig. 4.41 for the X2.1 diaphragms.

4.3.2. Horizontal Load Versus Horizontal Deflection Behavior

4.3.2.1. No Intermediate Diaphragms

The horizontal load versus horizontal deflection results for both the experimental and analytical investigations, when no diaphragms were present in the bridge model, are shown in Figs. 4.42-4.45. For all figures in this section, the heavy dotted line and the light dotted line represent the analytical behavior when the ends of the finite model bridge were fixed and pinned, respectively, as discussed in Section 4.1.1. The presence of the longitudinal deck cracks (Section 4.2.1) and the joint detail between the P/C girders and the deck (Section 4.1.1) caused the lateral stiffness of the loaded bridge girders to be more flexible than the stiffness predicted by the pinned-end finite-element model for these members. The deck cracks, which reduced the transverse flexural stiffness of the bridge deck, behaved as internal plastic hinges with small moment strengths. Therefore, the curvature of the deck beyond a crack was small, which caused very small rotations of the unloaded girders. Essentially, the horizontal load induced only horizontal displacements of the unloaded girders. Since the analytical model did not contain any discontinuities in the flexural stiffness of the deck, the curvature of the modeled bridge deck caused the unloaded girders to rotate, which induced additional horizontal displacements at the bottom of the unloaded girders. This effect is shown in Figs. 4.43 and 4.44.

Figures 4.42 through 4.45 show that the horizontal deflection responses were essentially linear up to a horizontal load of 60 kips. As expected, the digression of the experimental results from the analytical predictions were the largest at a loaded girder, as shown in Figs. 4.42 and 4.45. The horizontal deflections for the loaded north exterior girder (BM3 in Fig. 4.8) were greater than for the loaded interior girder (BM2) as shown in Figs. 4.45 and 4.42, respectively, and for the south exterior girder (BM1), figure not included, because of the linkage formed in the bridge deck by Cracks 2 and 3a shown in Fig. 4.8a.

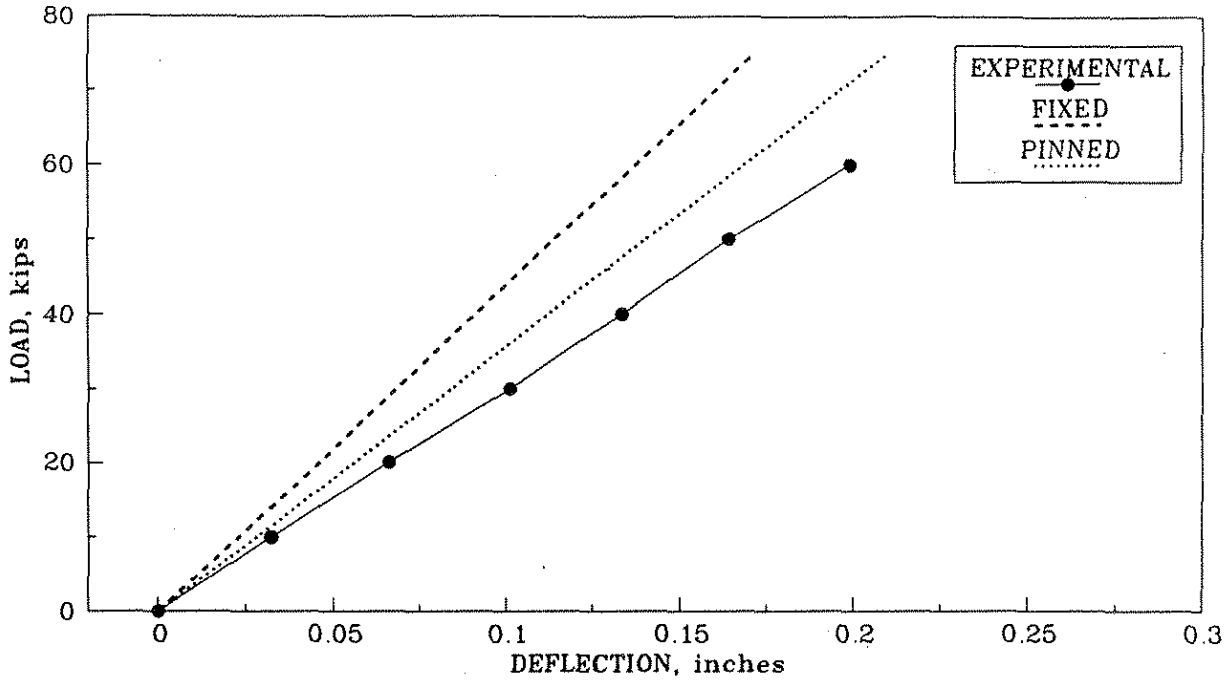

Fig. 4.42. Horizontal load versus deflection curves: load and deflection at point 5, no intermediate diaphragms.

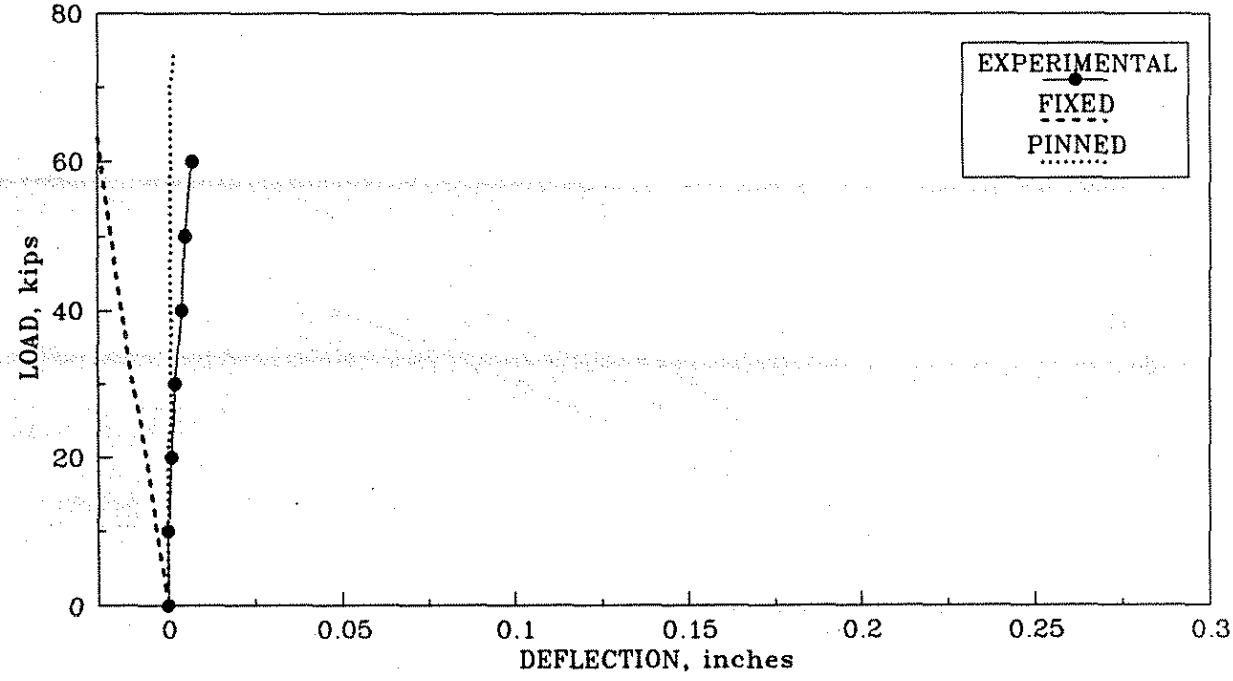

Fig. 4.43. Horizontal load versus deflection curves: load at point 5, deflection at point 6, no intermediate diaphragms.

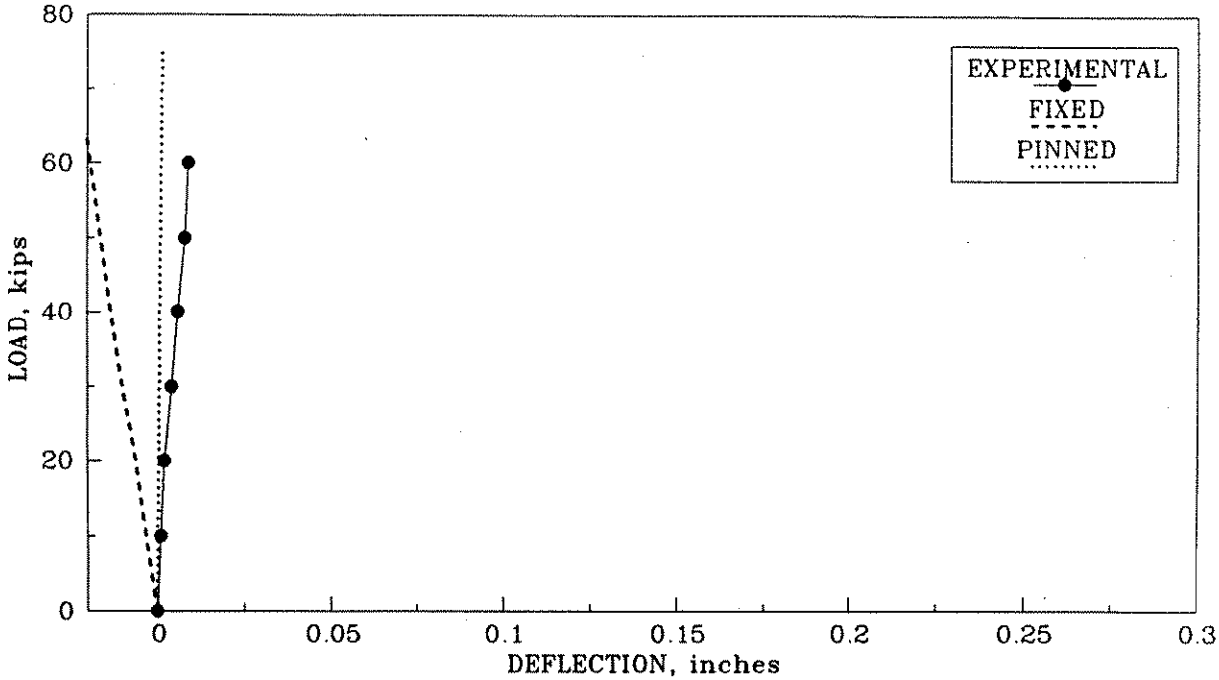

Fig. 4.44. Horizontal load versus deflection curves: load at point 6, deflection at point 5, no intermediate diaphragms.

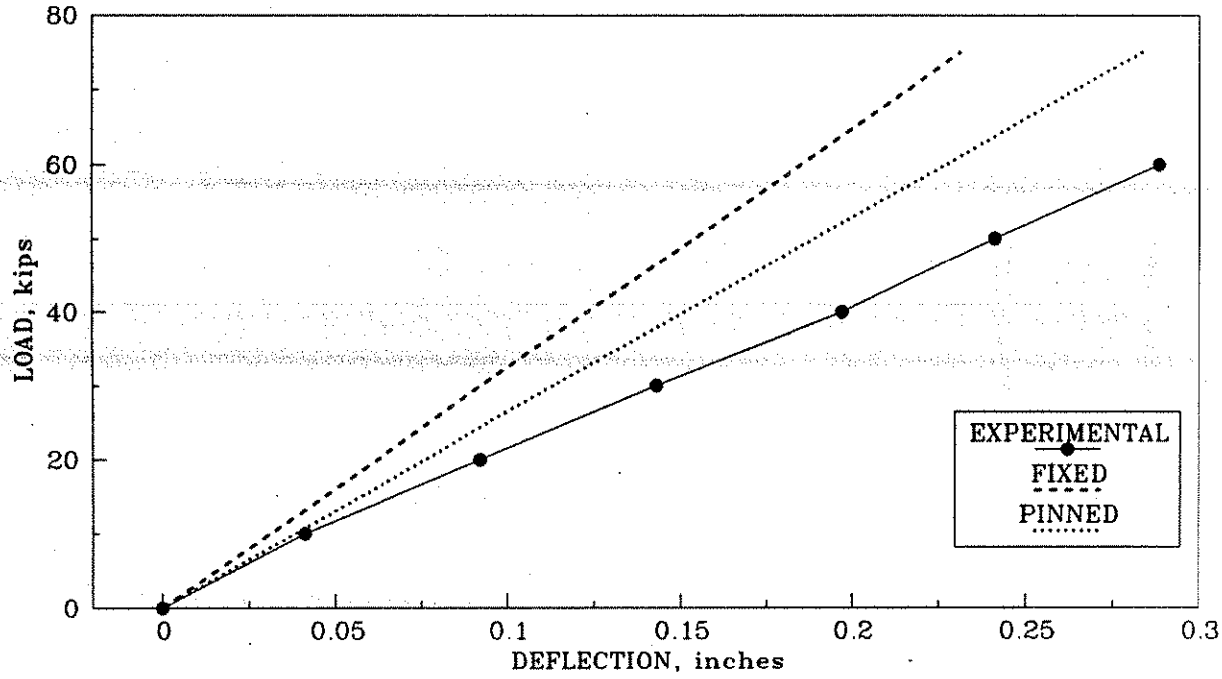

Fig. 4.45. Horizontal load versus deflection curves: load and deflection at point 6, no intermediate diaphragms.

4.3.2.2. Midspan Intermediate Diaphragms

The horizontal load versus horizontal deflection responses of the analytical and experimental bridge models containing the shallow channel intermediate diaphragms at the midspan (C1.1) are shown in Figs. 4.46-4.48. The channel diaphragms were connected to the P/C girders through the center two holes in the angle bracket as shown in Fig. 2.6a. The longitudinal cracks in the bridge deck and the connection detail between the P/C girders and the bridge deck caused a loaded girder to rotate more than the modeled girder in the finite-element analyses. Therefore, the experimental results shown in Fig. 4.46 occurred outside of the range established by the fixed- and pinned-end analytical solutions. Since the lateral stiffness of the experimental bridge was less than that for the analytical model, the experimental horizontal deflection for the loaded girder was greater than the horizontal deflection for the analytical model at each magnitude of horizontal load.

The presence of the intermediate diaphragms cause a direct transfer of horizontal force to each P/C girder and reduced the rotation of each girder about its longitudinal axis compared to the responses when no diaphragms were present. Figure 4.47 shows the horizontal deflection at the bottom flange of the interior P/C girder at point 5 when the horizontal load was applied to the bottom flange of the south exterior girder (BM1 in Fig. 4.8). For this same loading condition, when no intermediate diaphragms were in place, the displacements at point 5 (not shown) were negative for the fixed-end finite element model and were essentially zero for the pinned-end finite-element model and for the experimental bridge. The occurrence of connection slip as discussed in Section 4.2.3 caused a slight increase in the measured horizontal deflections. This behavior can be detected by observing the small digression of the experimental results from initial straight line portion of the measured responses shown in Figs. 4.47 and 4.48.

As shown in Table 3.1, a complete series of load tests were conducted when the deep channel intermediate diaphragms were installed in the experimental bridge (see Fig. 2.5). The tests with the C15 channel diaphragms verified symmetric bridge responses involving load points 1-3 and 7-9, as

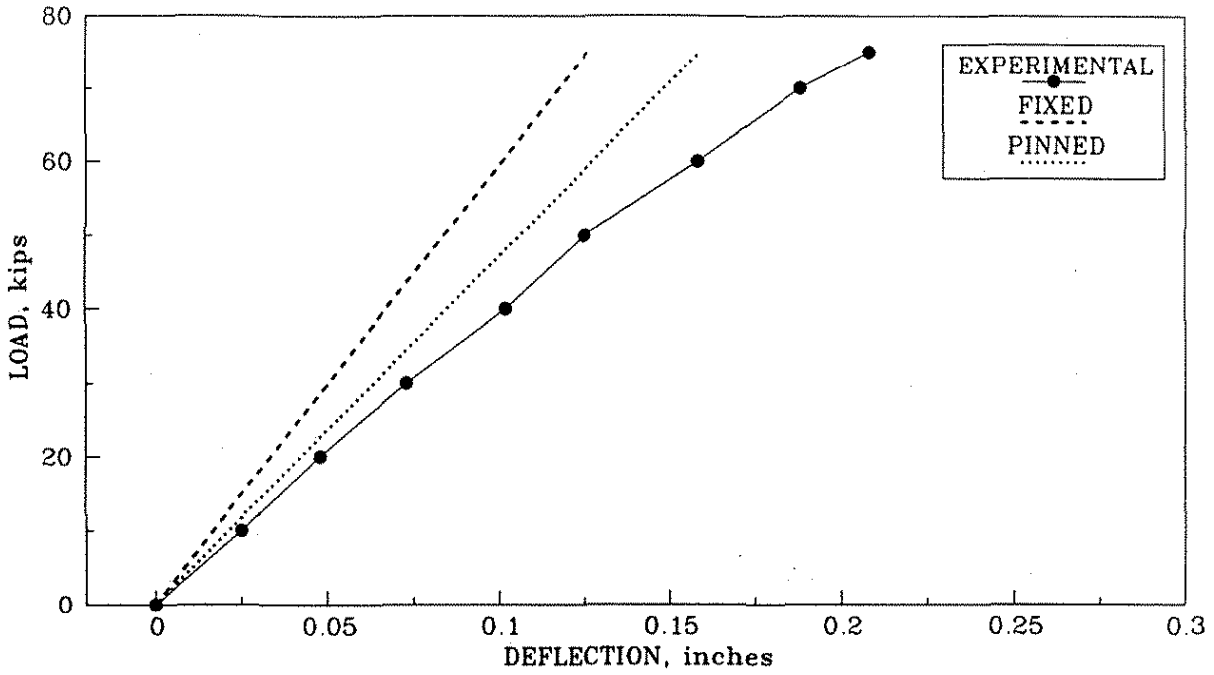

Fig. 4.46. Horizontal load versus deflection curves: load and deflection at point 4, C1.1 diaphragms.

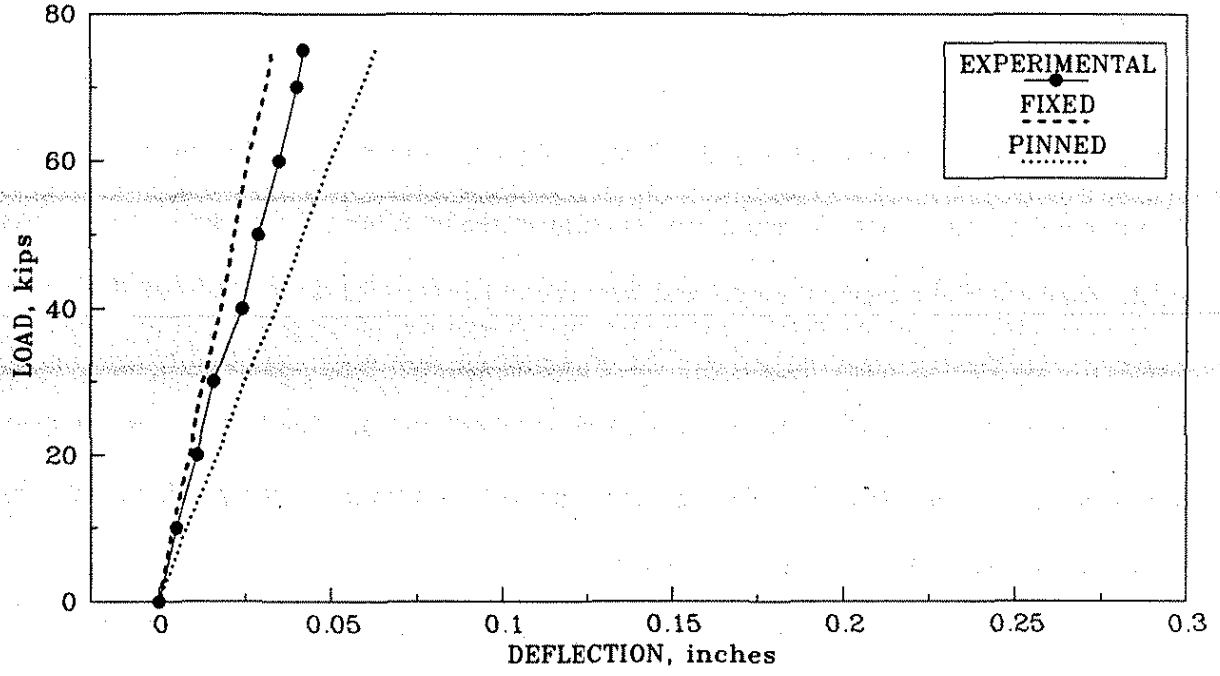

Fig. 4.47. Horizontal load versus deflection curves: load at point 4, deflection at point 5, C1.1 diaphragms.

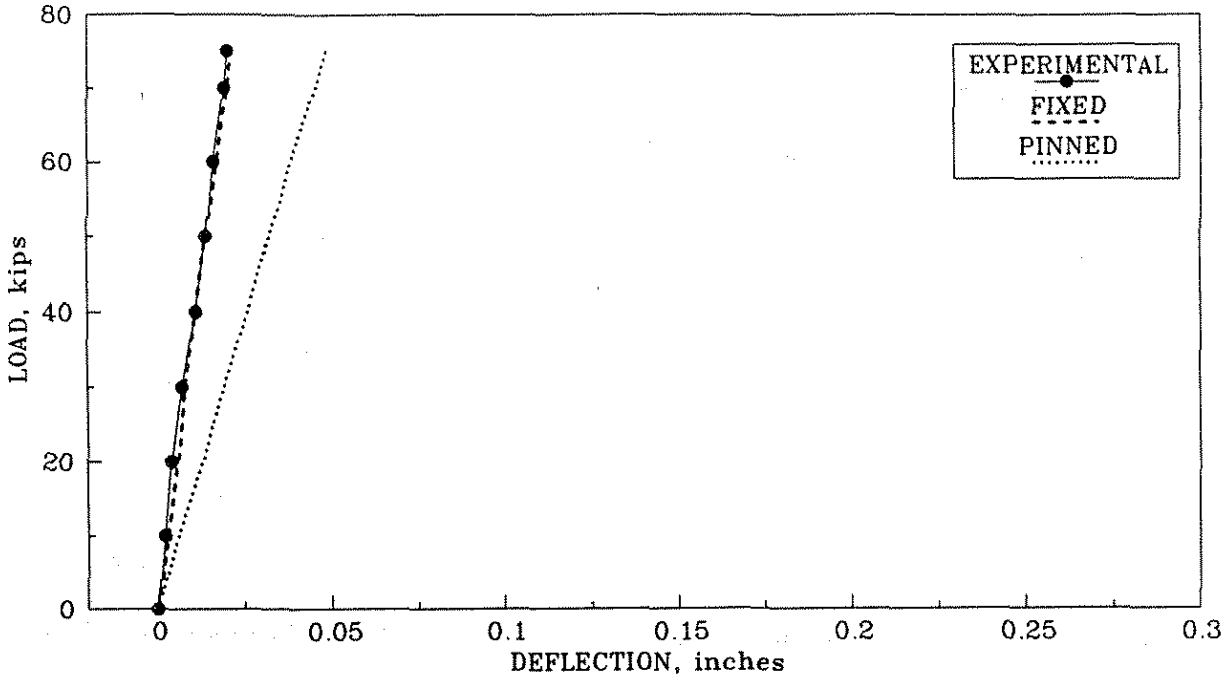

Fig. 4.48. Horizontal load versus deflection curves: load at point 4, deflection at point 6, C1.1 diaphragms.

discussed in Section 3.3. Considering the horizontal load tests with the deep channel midspan diaphragms (C2.1), Figs. 4.49-4.51 show the horizontal deflection response of the bottom flange of the loaded P/C girders, corresponding to points 4-6, respectively. The horizontal deflection responses for the bottom flange of the unloaded P/C girders are shown in Figs. 4.52-4.57.

A comparison of the analytical and experimental displacement results involving the loaded girders (Figs. 4.49-4.51) reveals that the actual response of the model bridge was more flexible than predicted by the analytical models involving either fixed or pinned ends. As previously discussed, the P/C girder rotation associated with the experimental testing caused a significant increase in the horizontal deflection of the loaded flange. As anticipated, the load versus deflection behavior of the interior P/C girder (Fig. 4.50) indicated a stiffer response than for the same behavior associated with the exterior girders (Figs. 4.49 and 4.51) for both the analytical and experimental results. The analytical models showed that symmetric responses occurred when loading points 4 and 6 (Figs. 4.49 and 4.51), while the experimental tests revealed that symmetry did not occur at these two points. The differences in the experimental behavior were attributed to the cracks in the bridge deck, the connection between the P/C girders and the bridge deck, and the connection detail between the diaphragms and the P/C girder webs.

"Exactly" symmetric and essentially symmetric responses for the analytic predictions and experimental results, respectively, occurred for the horizontal load versus horizontal deflection behavior of the unloaded P/C girders. According to the law of reciprocal displacements, the appropriate graphs of load versus deflection behavior should be identical. A comparison of Figs. 4.52 and 4.53, Figs. 4.54 and 4.55, and Figs. 4.56 and 4.57 reveals that this phenomenon was confirmed analytically and was essentially satisfied experimentally. Because of the geometric symmetry of the bridge, additional symmetry for the results can be observed by comparing Figs. 4.52 and 4.57, Figs. 4.53 and 4.56, Figs. 4.52 and 4.56, and Figs. 4.53 and 4.57. The analytically predicted

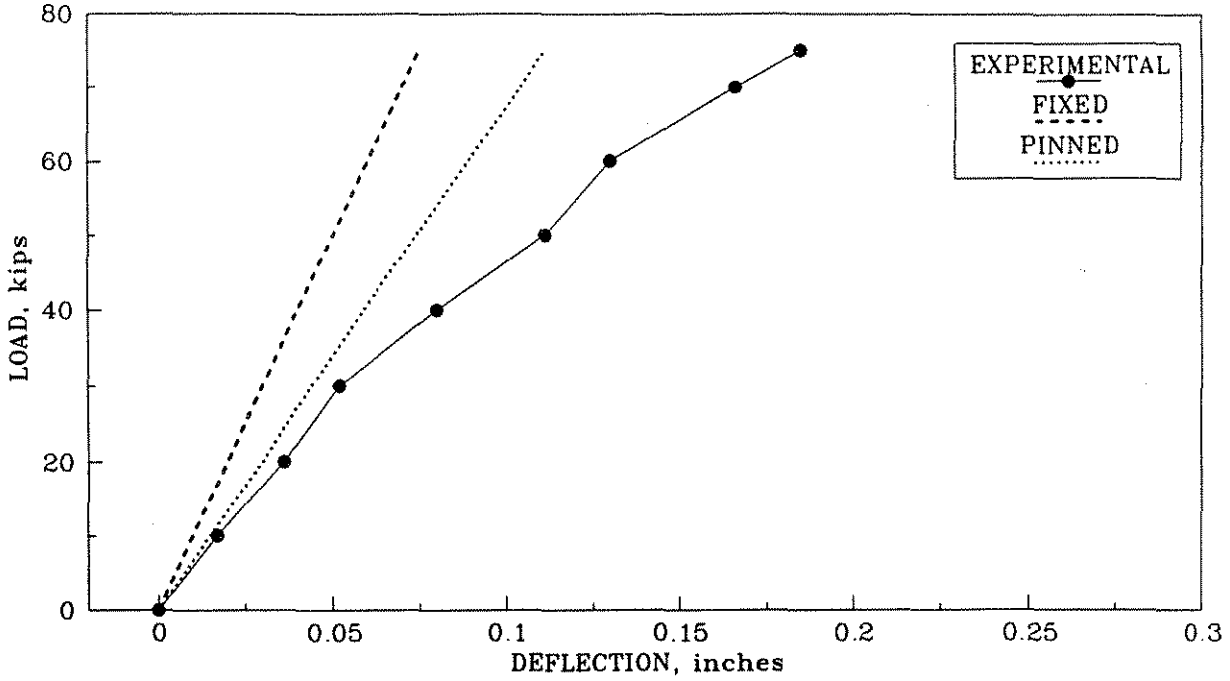

Fig. 4.49. Horizontal load versus deflection curves: load and deflection at point 4, C2.1 diaphragms.

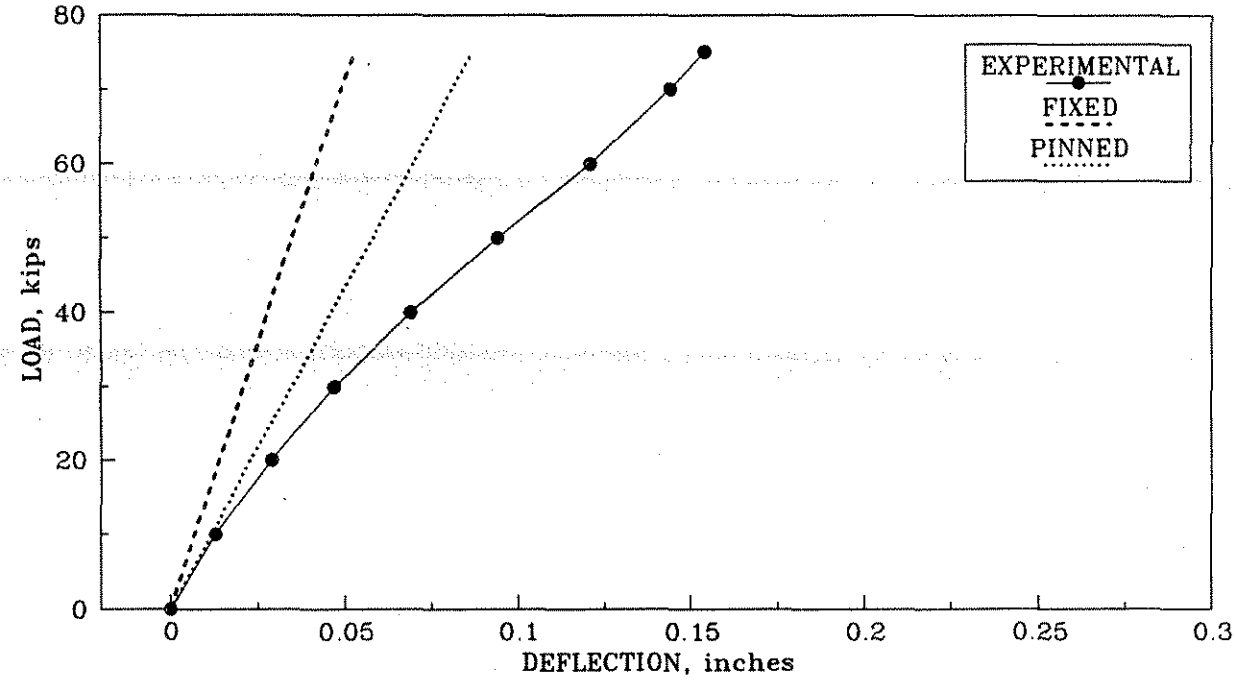

Fig. 4.50. Horizontal load versus deflection curves: load and deflection at point 5, C2.1 diaphragms.

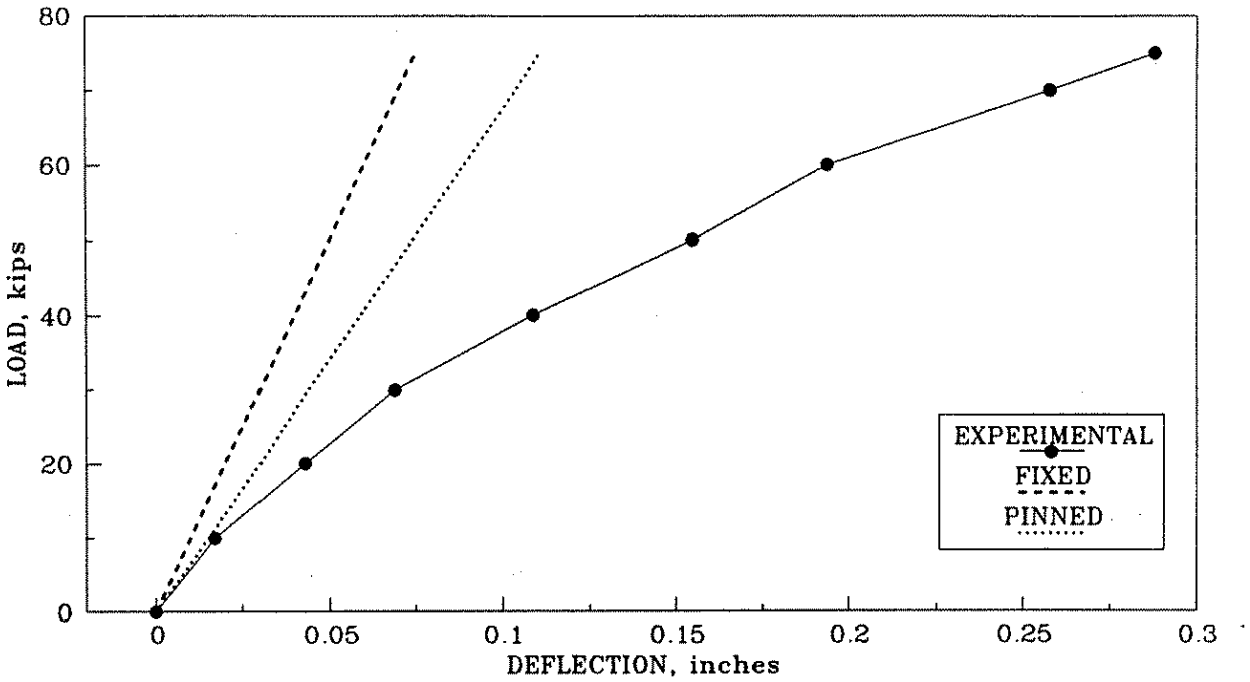

Fig. 4.51. Horizontal load versus deflection curves: load and deflection at point 6, C2.1 diaphragms.

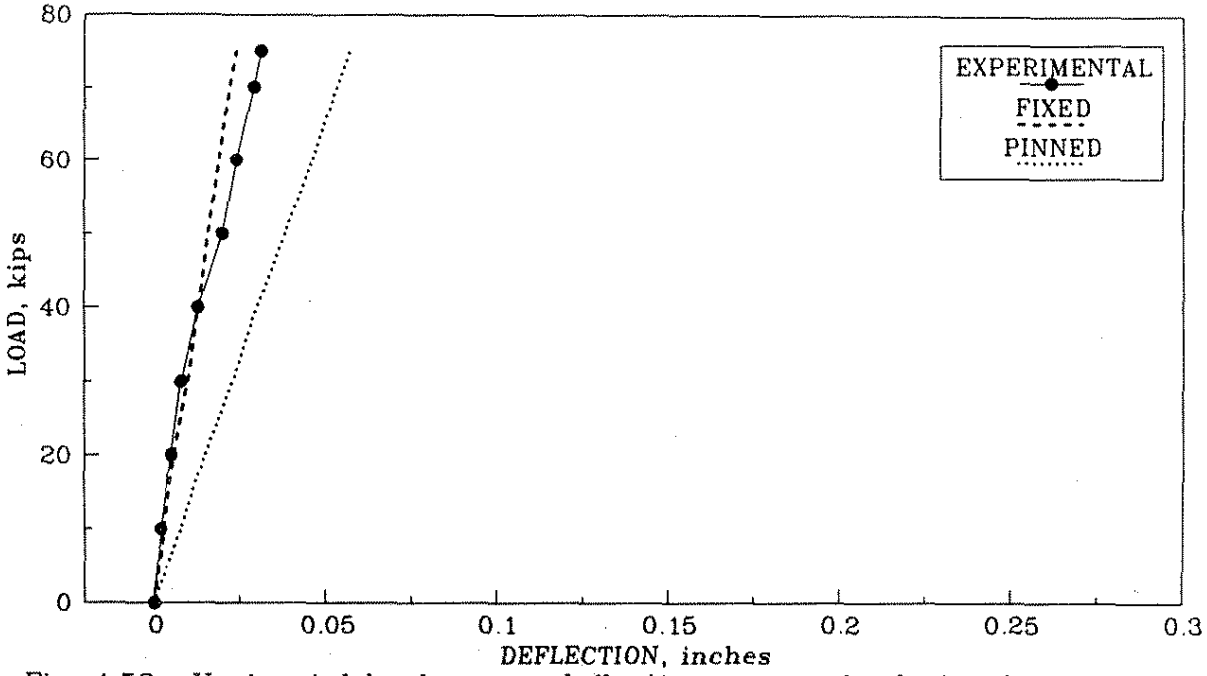

Fig. 4.52. Horizontal load versus deflection curves: load at point 4, deflection at point 5, C2.1 diaphragms.

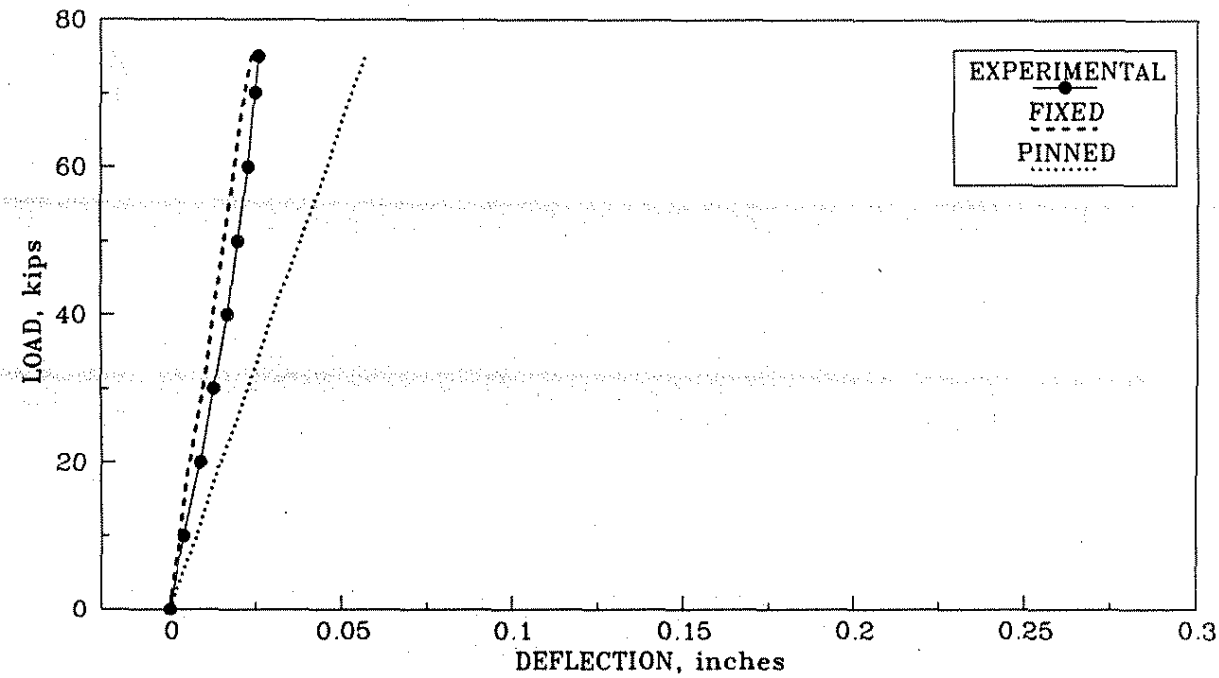

Fig. 4.53. Horizontal load versus deflection curves: load at point 5, deflection at point 4, C2.1 diaphragms.

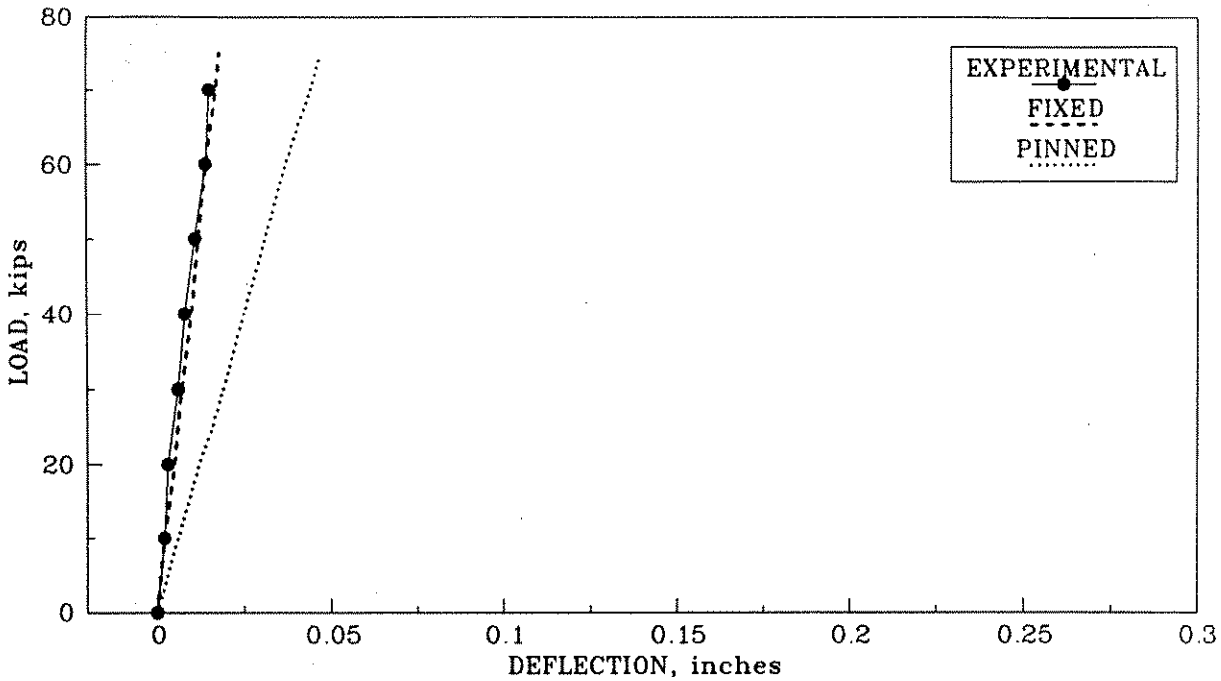

Fig. 4.54. Horizontal load versus deflection curves: load at point 4, deflection at point 6, C2.1 diaphragms.

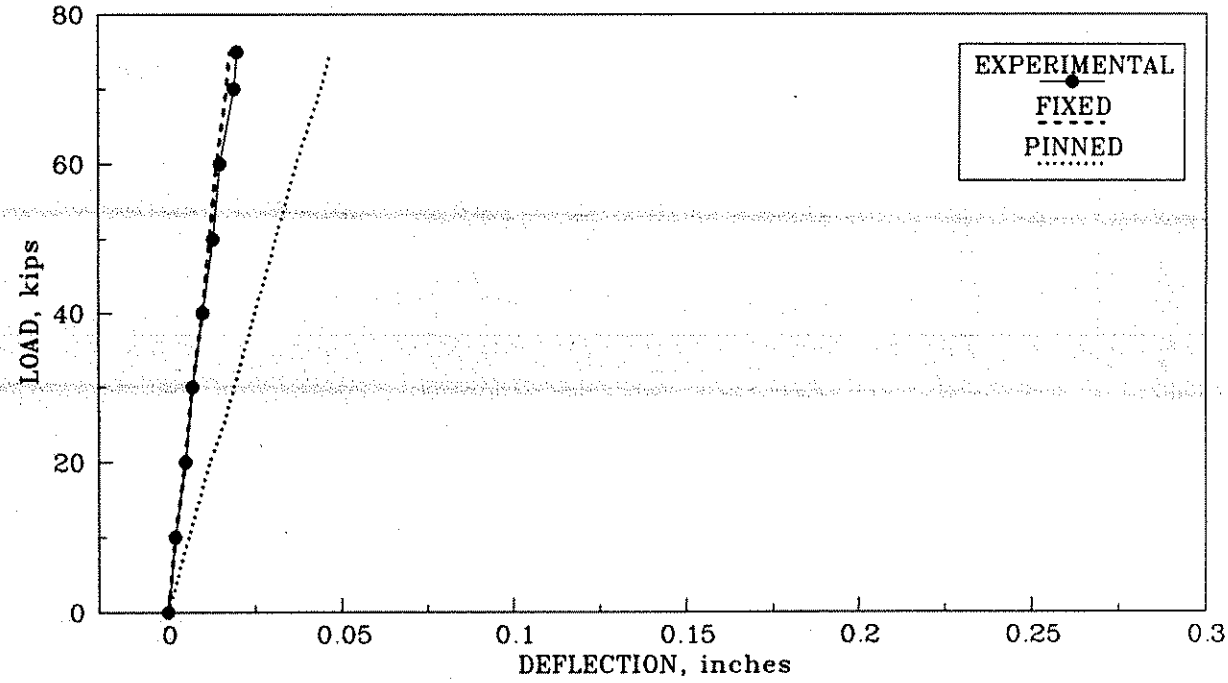

Fig. 4.55. Horizontal load versus deflection curves: load at point 6, deflection at point 4, C2.1 diaphragms.

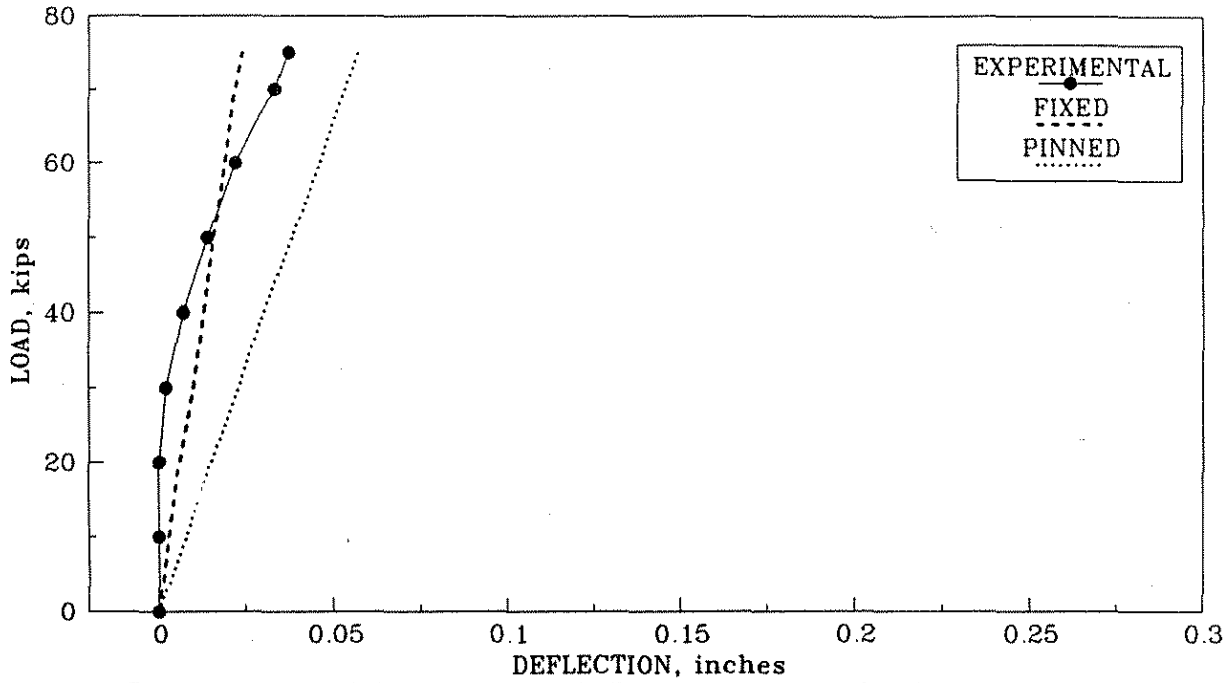

Fig. 4.56. Horizontal load versus deflection curves: load at point 5, deflection at point 6, C2.1 diaphragms.

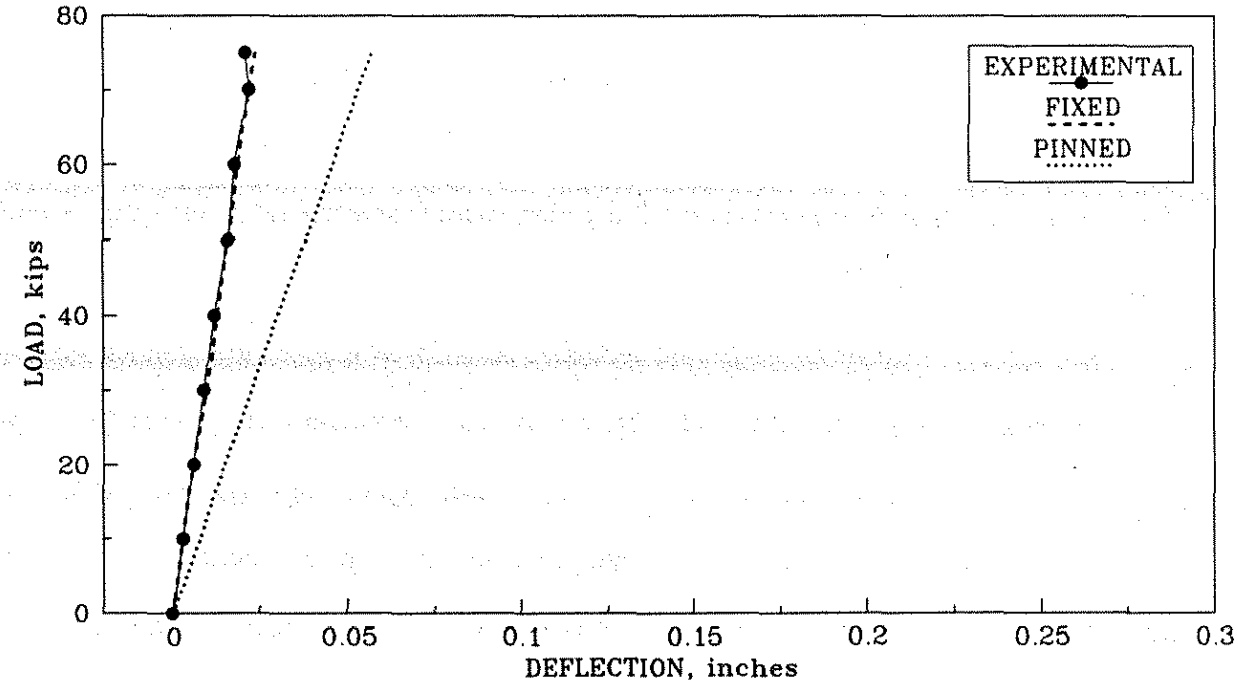

Fig. 4.57. Horizontal load versus deflection curves: load at point 6, deflection at point 5, C2.1 diaphragms.

behavior for both the fixed and pinned-end finite-element models showed "exact" symmetry while the experimentally measured deflections approximate symmetry in these figures.

Figures 4.58-4.63 show the horizontal load versus horizontal deflection behavior at the bottom flange of the P/C girders for six combinations of midspan load and displacement points (points 4-6), when the midspan reinforced concrete diaphragms (RC.1) were used in the bridge (see Fig. 2.4). The differences between the experimentally derived and analytically established responses for the loaded P/C girders (Figs. 4.58, 4.61, and 4.63) can be explained by the differences between the test bridge conditions and the fixed- and pinned-end finite-element models. These differences were discussed in Section 4.1.1 (the connection between the P/C girders and the deck), Section 4.2.1 (the longitudinal cracks in the bridge deck), and Section 4.2.2 (the connection between the intermediate diaphragms and the P/C girders). The experimentally measured responses for the unloaded girder deflections (Fig. 4.59, 4.60, and 4.62) more closely agree with the finite-element predictions, since the effects of the longitudinal cracks, the connections for the P/C girders, and the intermediate reinforced concrete diaphragms were not as dominant as they were for the loaded girder deflections.

Symmetrical load versus deflection responses were noted for the analytic solutions. The construction details involving the high-strength tendons for connection of the intermediate reinforcement diaphragms to the webs of the P/C girders caused some irregularities in experimental symmetry of the bridge response.

The horizontal load versus horizontal deflection behavior at selected midspan locations are presented in Figs. 4.64-4.68, when the steel X-brace plus strut intermediate diaphragms (X1.1) (see Fig. 2.7a and 2.7b) were placed at the midspan of the bridge. Again, the longitudinal deck cracks produced a more flexible response than that associated with an uncracked deck for a loaded P/C girder, such that the experimental results for the interior girder were almost identical with the response predicted by the pinned-end finite-element model, as shown in Fig. 4.64. Considering the north exterior girder (BM3 in Fig. 4.8), the digression of the experimentally measured deflections

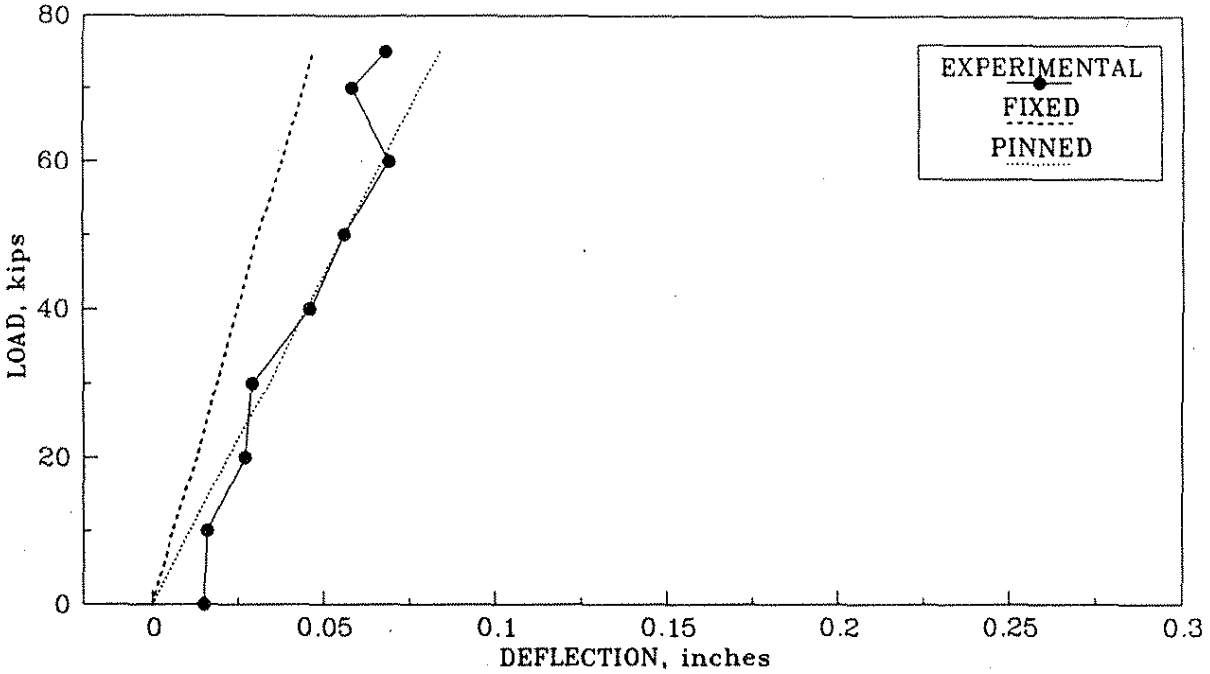

Fig. 4.58. Horizontal load versus deflection curves: load and deflection at point 4, RC.1 diaphragms

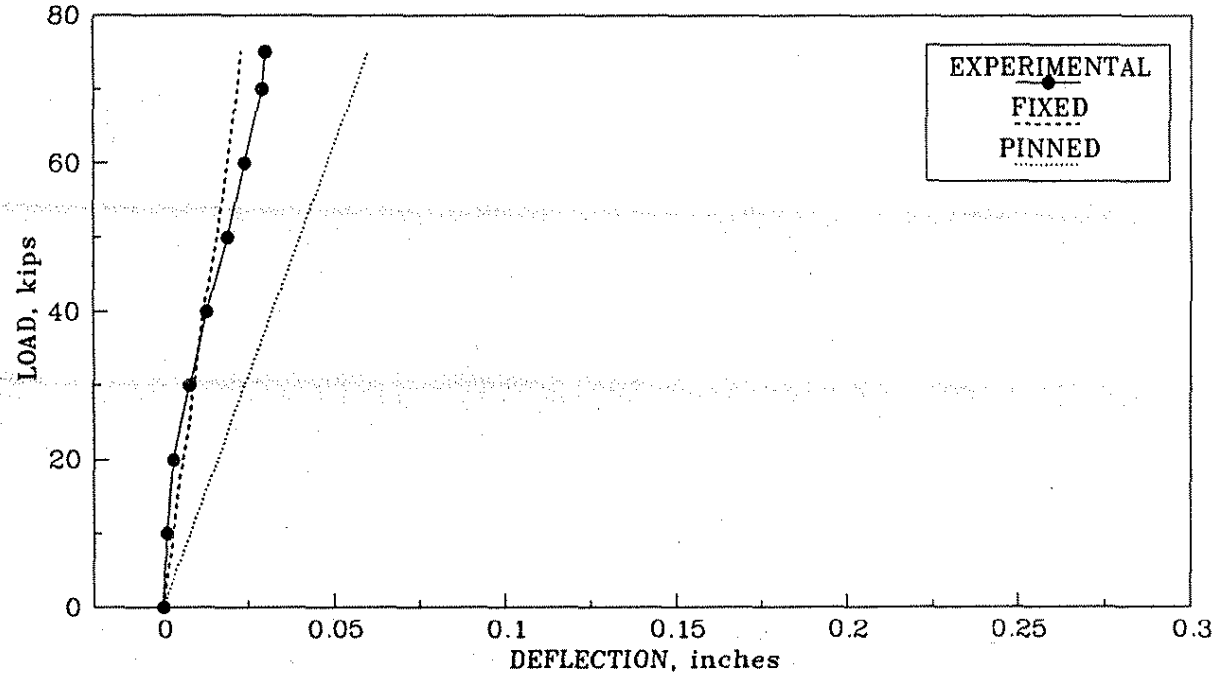

Fig. 4.59. Horizontal load versus deflection curves: load at point 4, deflection at point 5, RC.1 diaphragms.

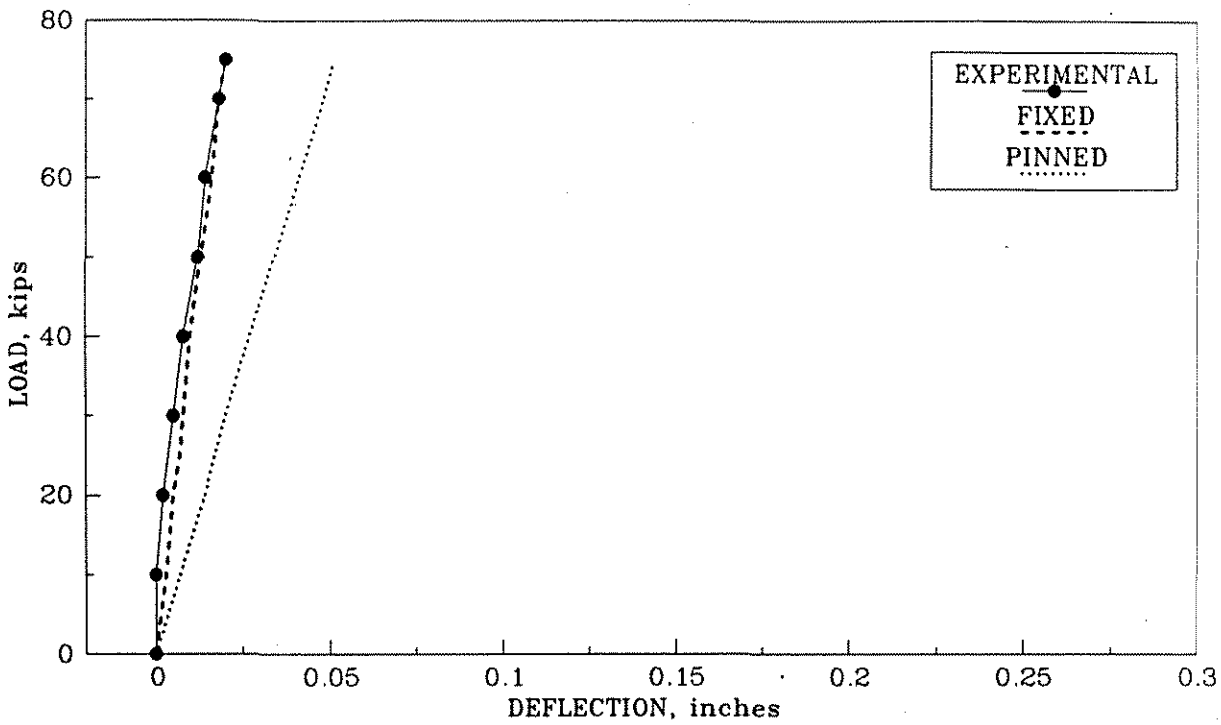

Fig. 4.60. Horizontal load versus deflection curves: load at point 4, deflection at point 6, RC.1 diaphragms.

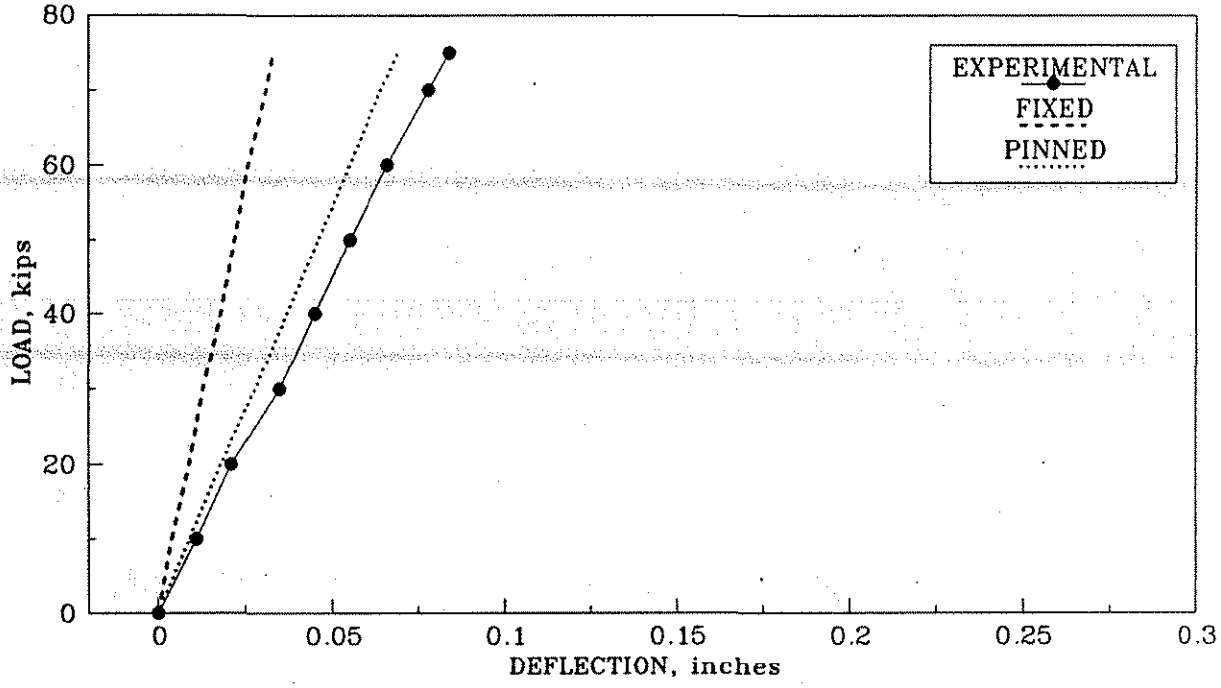

Fig. 4.61. Horizontal load versus deflection curves: load and deflection at point 5, RC.1 diaphragms.

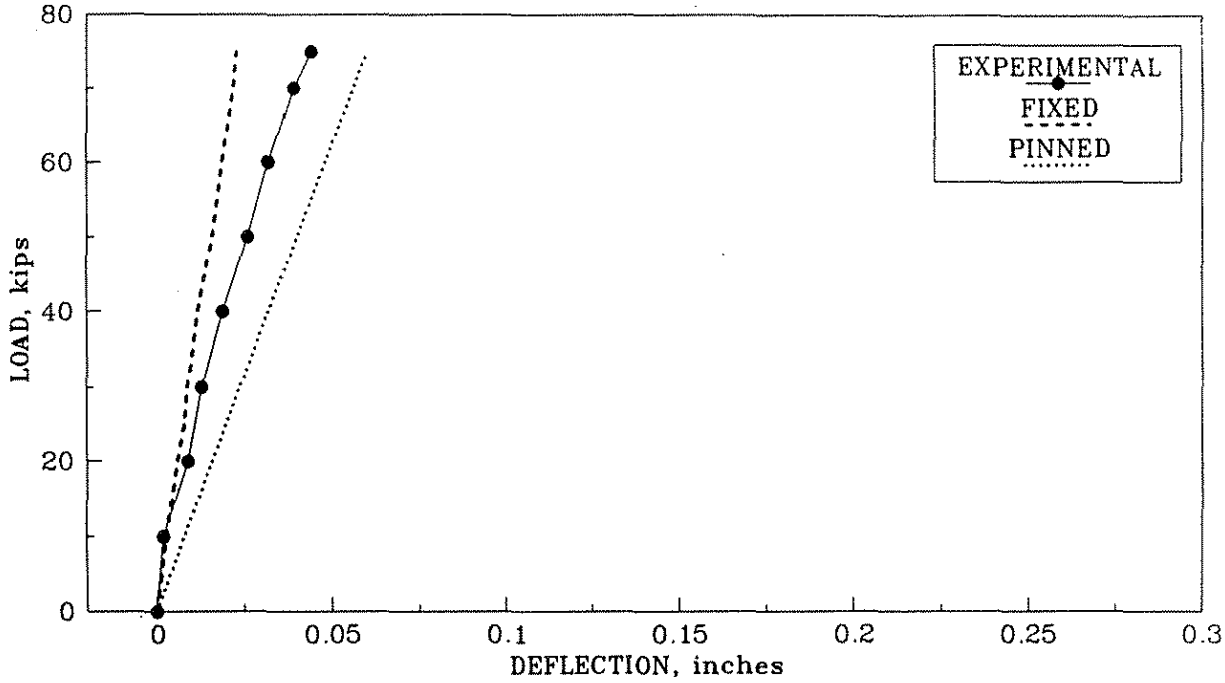

Fig. 4.62. Horizontal load versus deflection curves: load at point 5, deflection at point 6, RC.1 diaphragms.

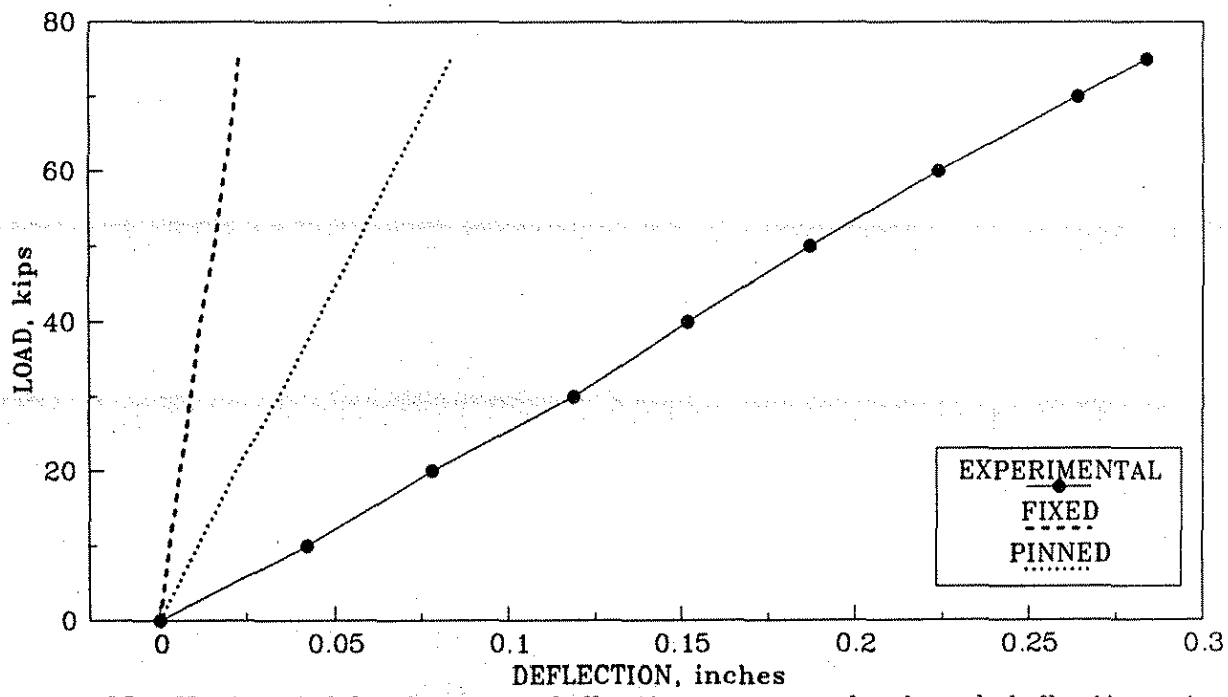

Fig. 4.63. Horizontal load versus deflection curves: load and deflection at point 6, RC.1 diaphragms.

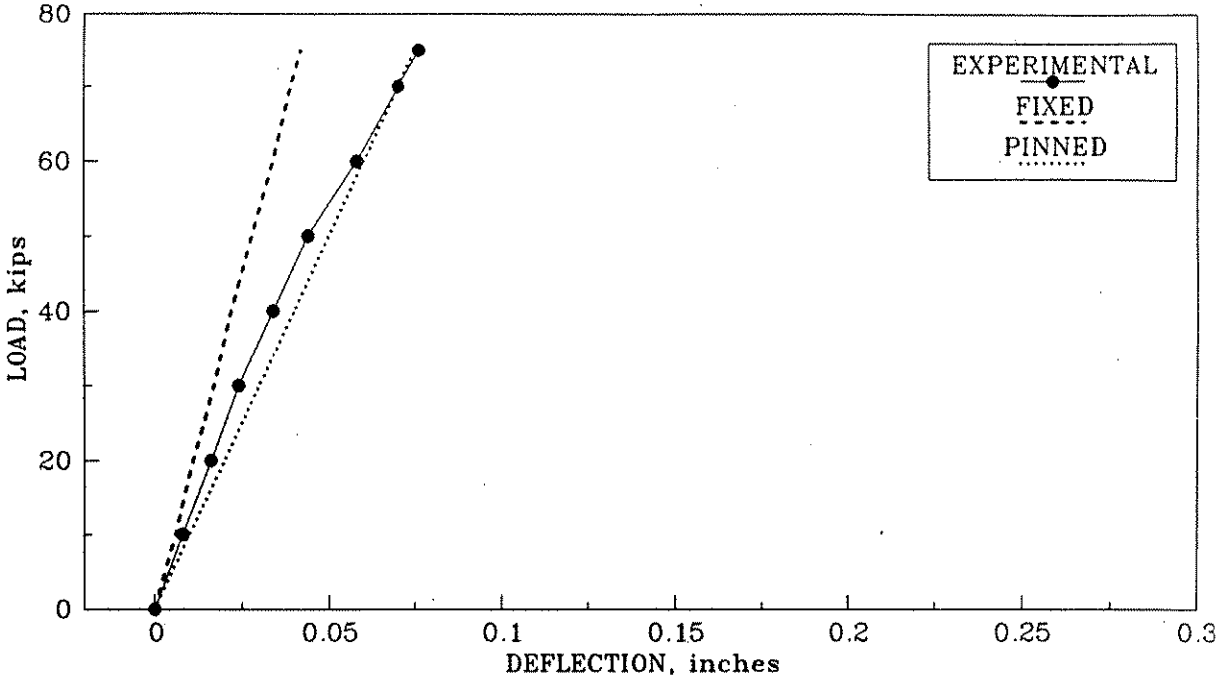

Fig. 4.64. Horizontal load versus deflection curves: load and deflection at point 5, X1.1 diaphragms.

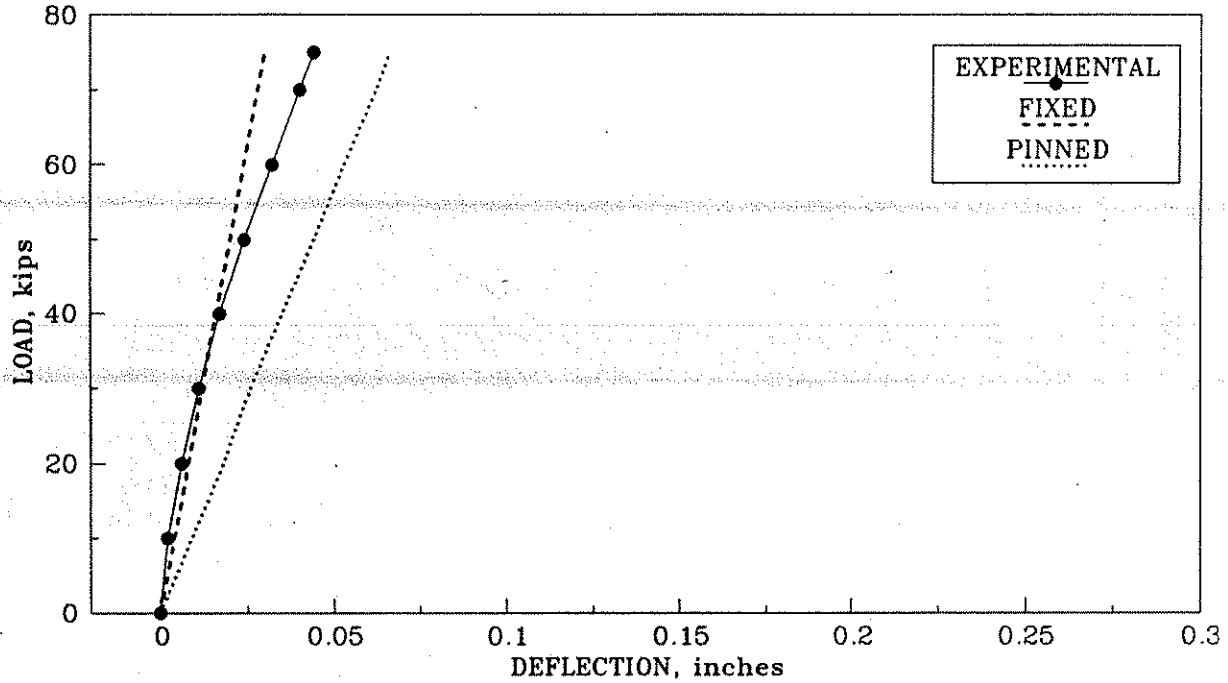

Fig. 4.65. Horizontal load versus deflection curves: load at point 5, deflection at point 6, X1.1 diaphragms.

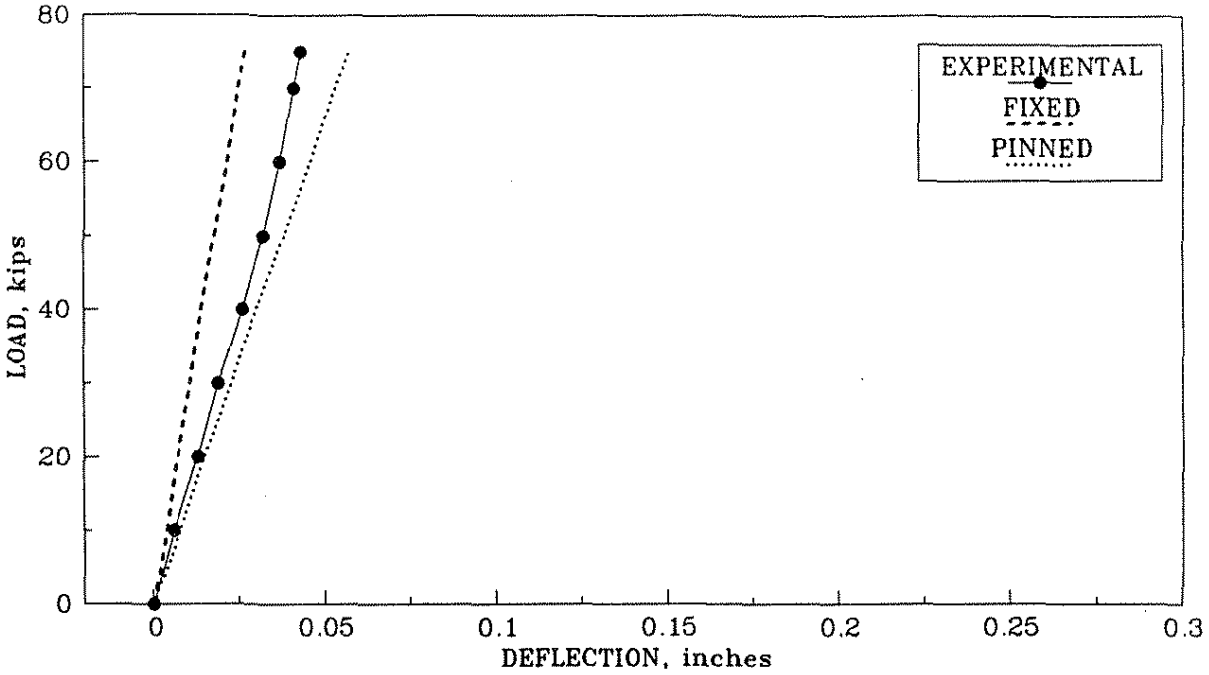

Fig. 4.66. Horizontal load versus deflection curves: load at point 6, deflection at point 4, X1.1 diaphragms.

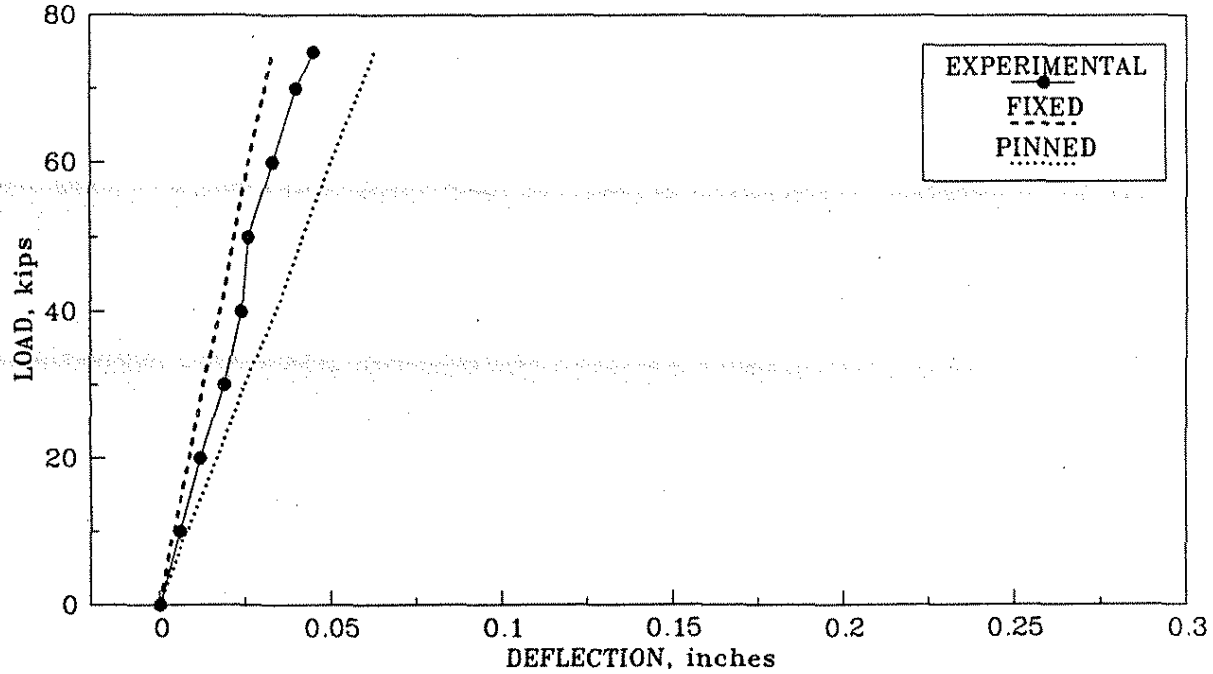

Fig. 4.67. Horizontal load versus deflection curves: load at point 6, deflection at point 5, X1.1 diaphragms.

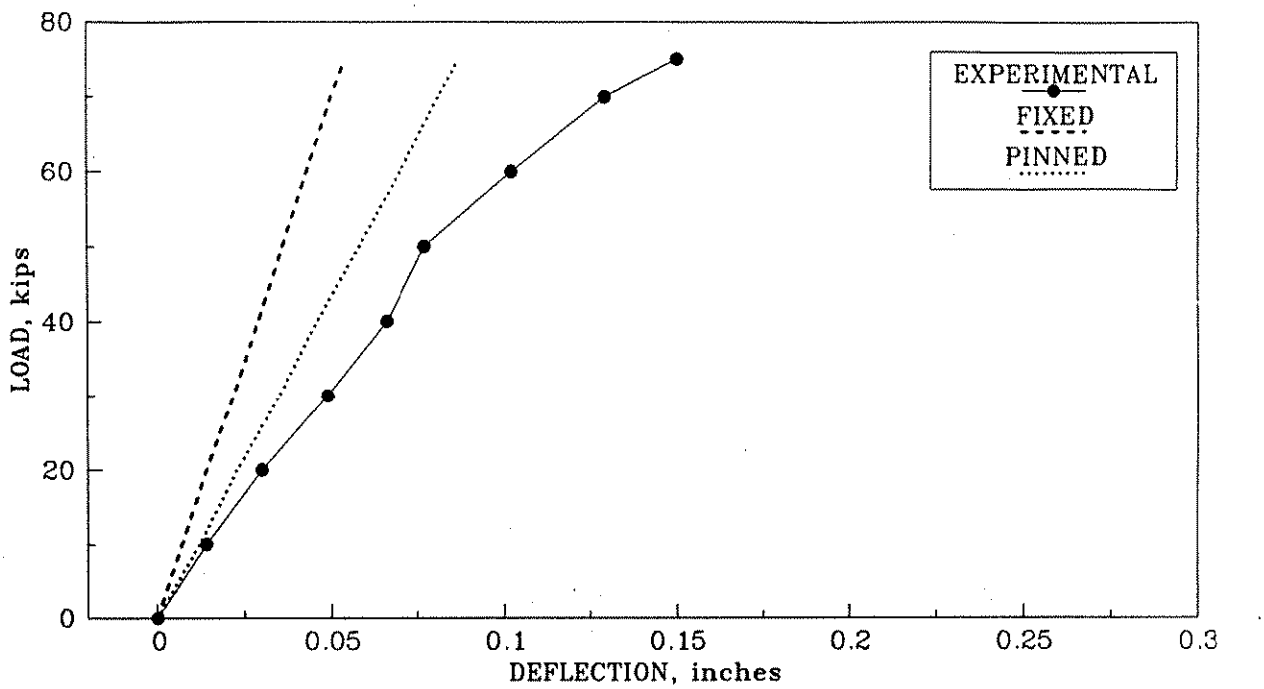

Fig. 4.68. Horizontal load versus deflection curves: load and deflection at point 6, X1.1 diaphragms.

from the analytically predicted responses shown in Fig. 4.68 was attributed to the causes previously discussed. As shown in Figs. 4.65-4.67, the deflection response for the unloaded girders occurred between the limits established by the fixed- and pinned-end analytical models.

Symmetrical deflection behavior, as required by the law of reciprocal displacements, was satisfied for both the analytical and experimental results. Figures 4.65 and 4.67 show that the horizontal deflection at point 6 due to a horizontal load of a given magnitude at point 5 equals the horizontal deflection at point 5 due to a horizontal load of the same magnitude at point 6. Other pairs of figures (not included) revealed similar results for other points.

Figures 4.69-4.73 show the horizontal load versus horizontal deflection relationships for both the interior and north exterior P/C girders (BM2 and BM3 in Fig. 4.8) when the midspan X-brace diaphragms without a strut (X2.1) (see Fig. 2.7c) were installed in the bridge. The behavior for this diaphragm configuration was very similar to the response observed both analytically and experimentally for the X1.1 diaphragm arrangement (see Fig. 2.7a and 2.7b). As expected, the horizontal deflection magnitudes for the loaded P/C girder increased when the horizontal strut was removed from the X1.1 diaphragms to form the X2.1 diaphragms. This effect can be observed by comparing Figs. 4.64 and 4.69 for the interior girder and Figs. 4.68 and 4.73 for the north exterior girder. Conversely, the horizontal deflection magnitudes for the unloaded P/C girders decreased when the horizontal strut was removed, as shown in a comparison of Figs. 4.65 and 4.70, Figs. 4.66 and 4.71, and Figs. 4.67 and 4.72 for BM3, BM1 and BM2, respectively.

4.3.2.3. Third-Point Intermediate Diaphragms

The horizontal load versus horizontal deflection responses at the bottom flange of the three P/C girders, when the third-point, small channel, intermediate diaphragms (C1.3) were installed, are shown in Figs. 4.74-4.76, corresponding to points 4-6, respectively. The horizontal load had been applied on the bottom flange (point 5) at the midspan of the interior girder. These experimentally measured deflection results are consistant with the analytically predicted displacements. The loaded

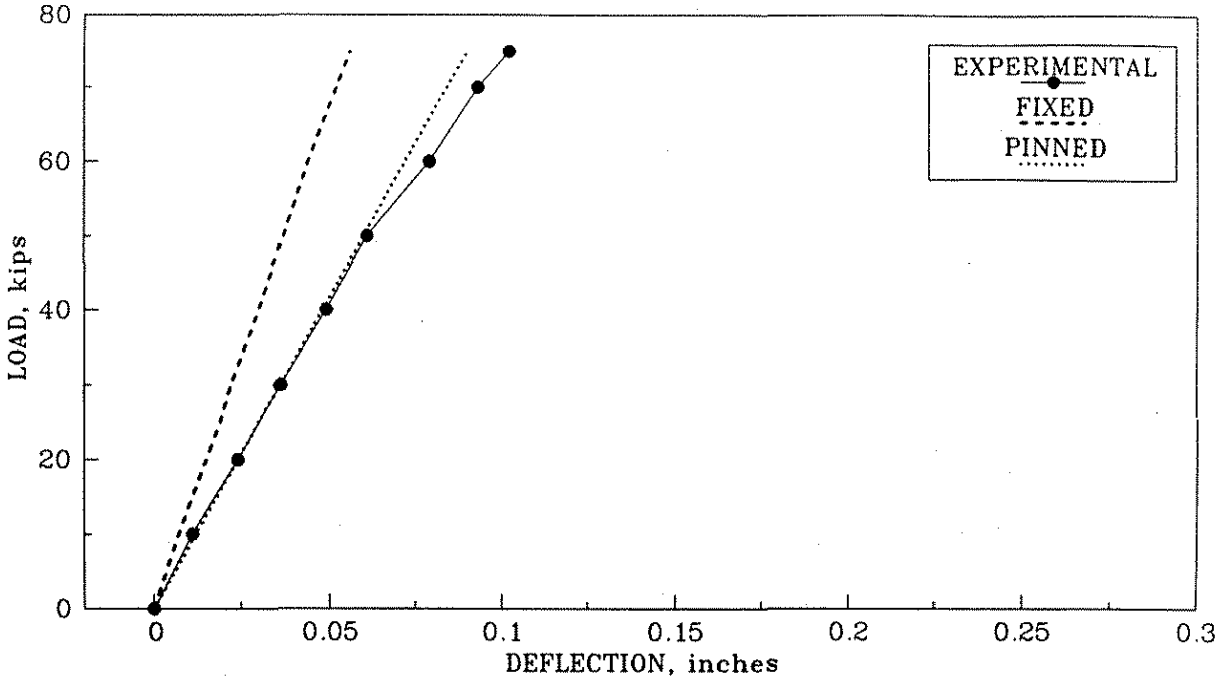

Fig. 4.69. Horizontal load versus deflection curves: load and deflection at point 5, X2.1 diaphragms.

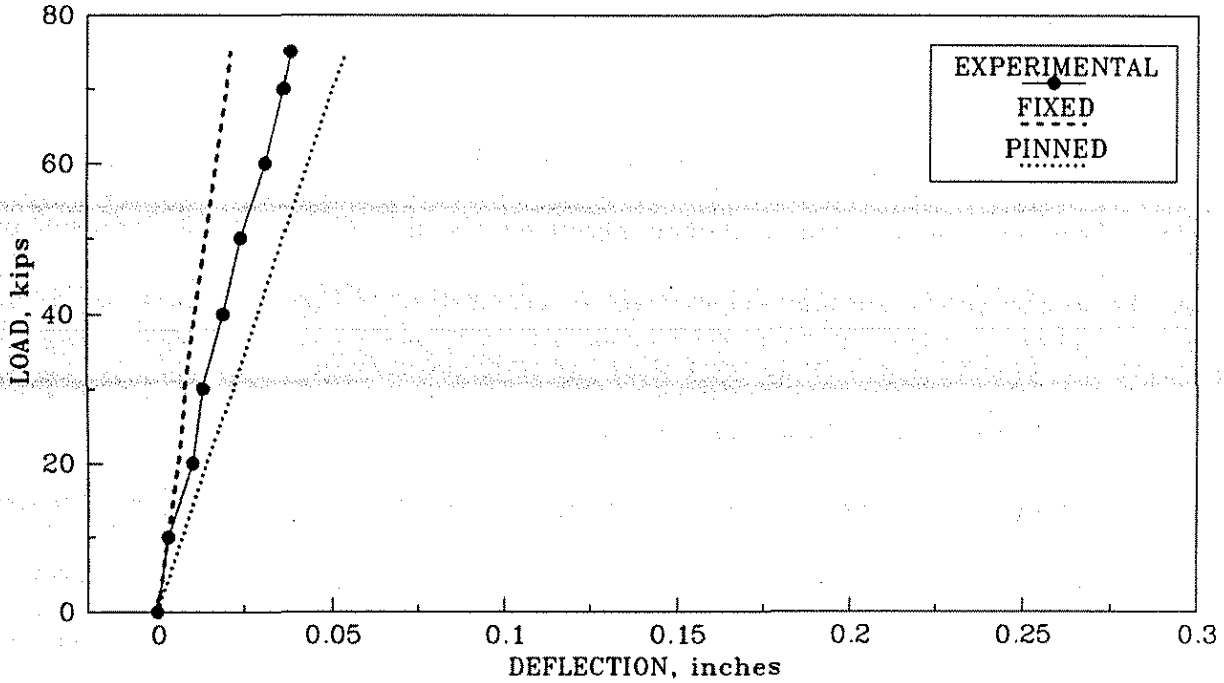

Fig. 4.70. Horizontal load versus deflection curves: load at point 5, deflection at point 6, X2.1 diaphragms.

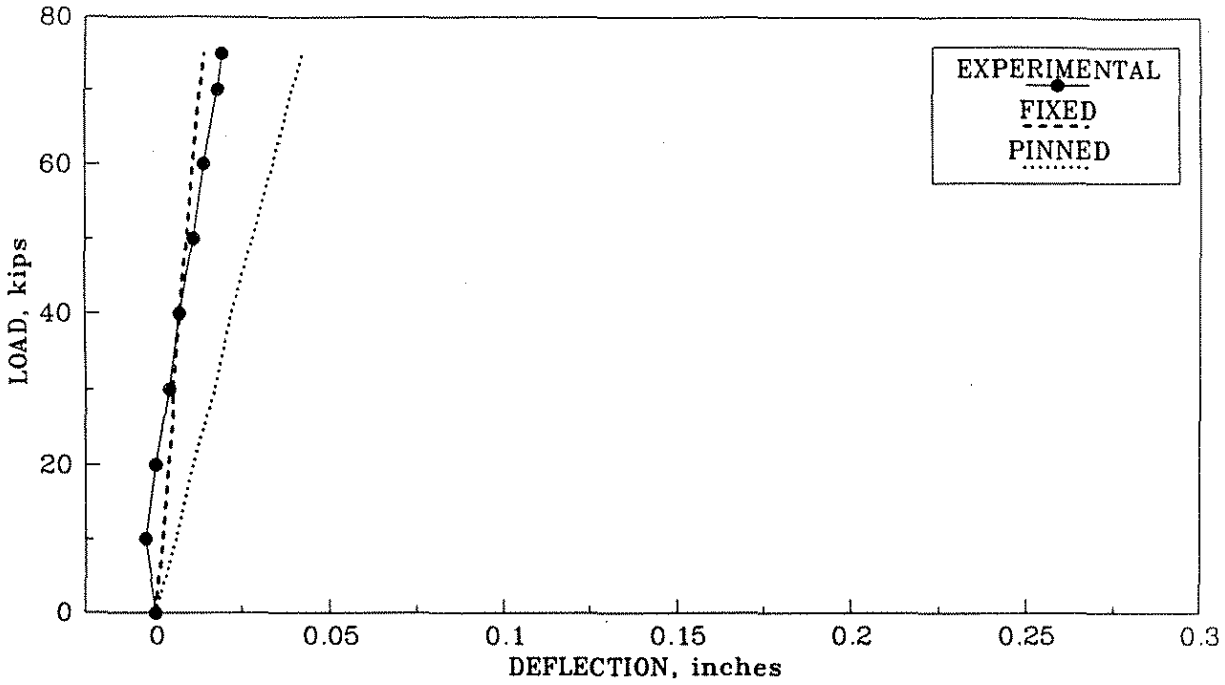

Fig. 4.71. Horizontal load versus deflection curves: load at point 6, deflection at point 4, X2.1 diaphragms.

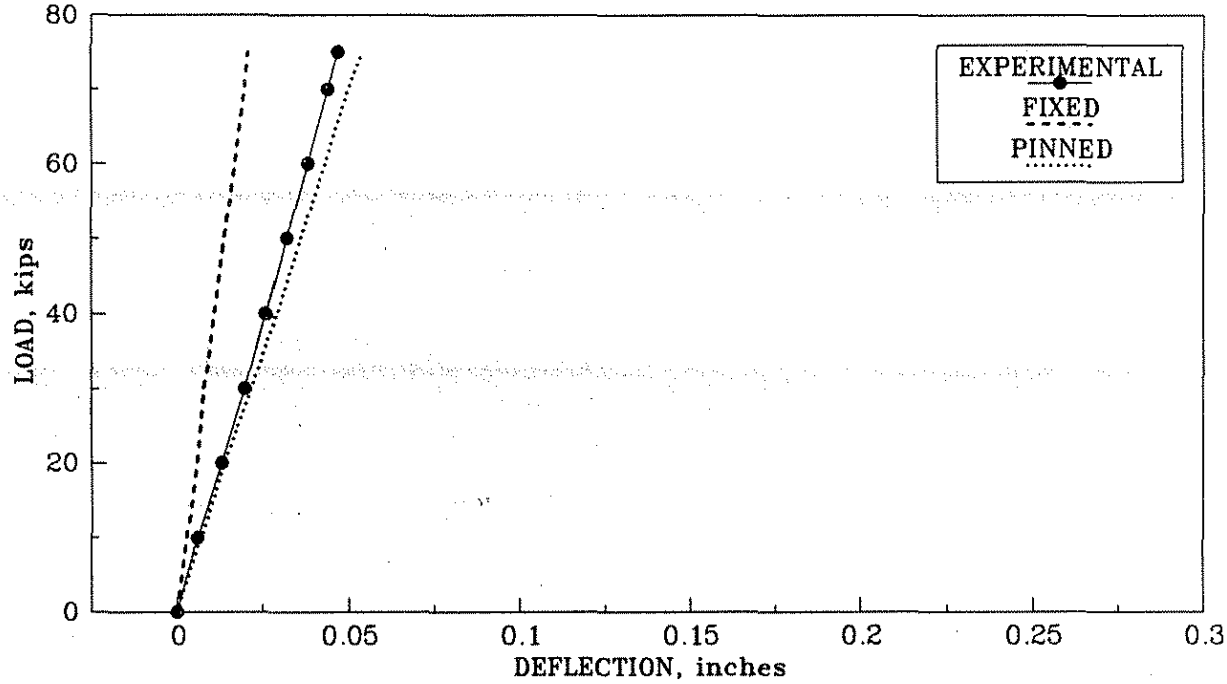

Fig. 4.72. Horizontal load versus deflection curves: load at point 6, deflection at point 5, X2.1 diaphragms.

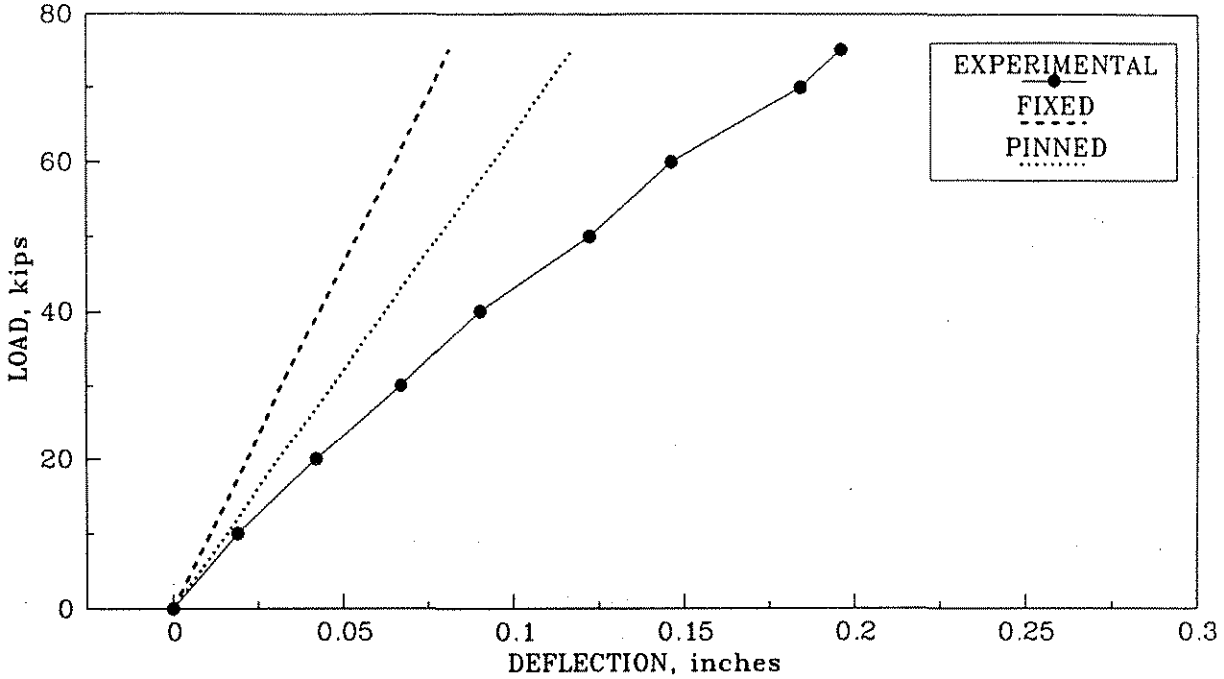

Fig. 4.73. Horizontal load versus deflection curves: load and deflection at point 6, X2.1 diaphragms.

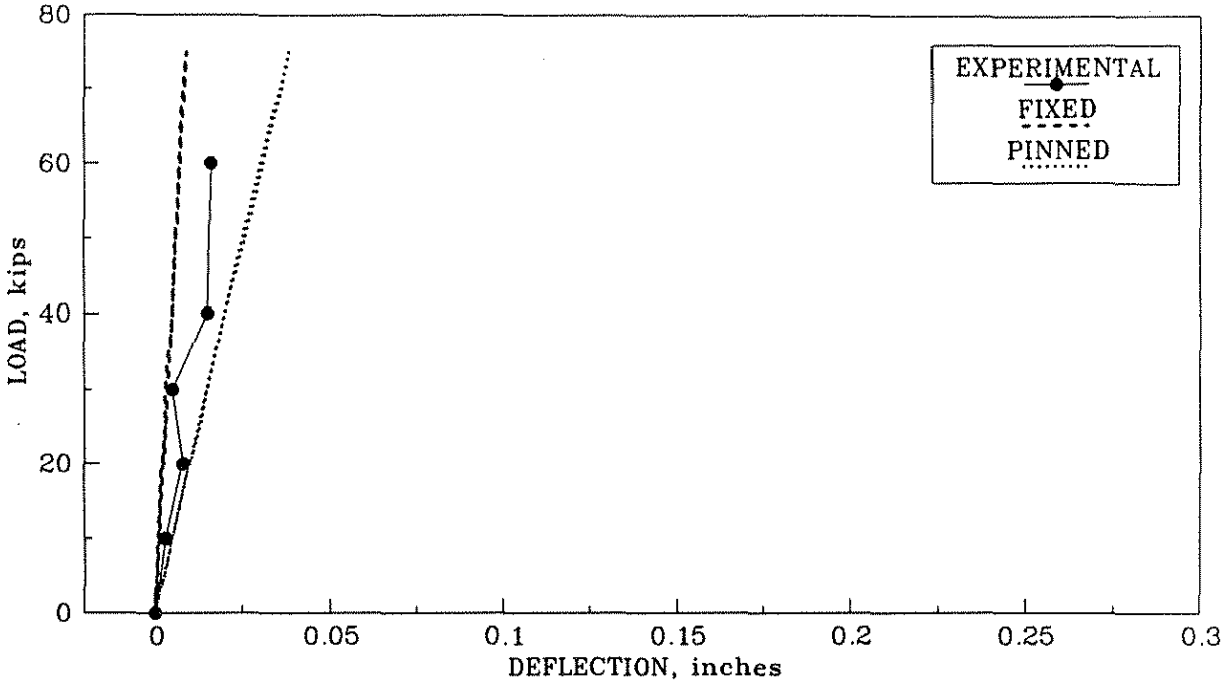

Fig. 4.74. Horizontal load versus deflection curves, load at point 5, deflection at point 4, C1.3 diaphragms.

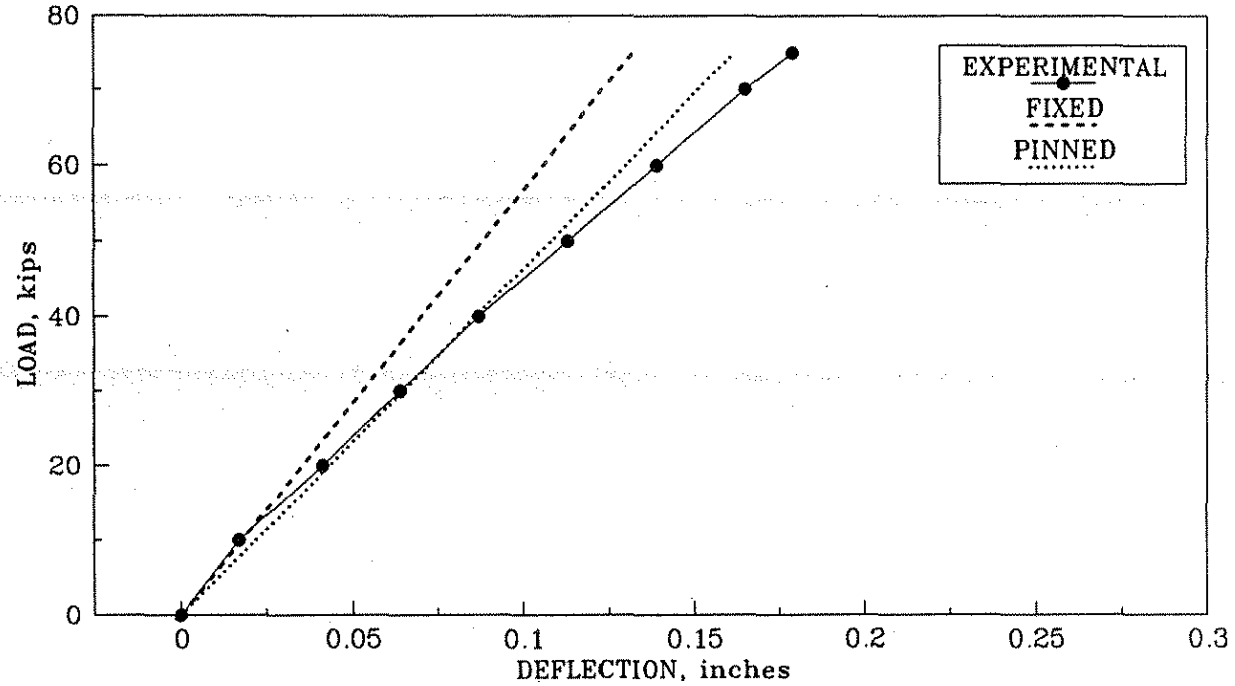

Fig. 4.75. Horizontal load versus deflection curves, load and deflection at point 5, C1.3 diaphragms.

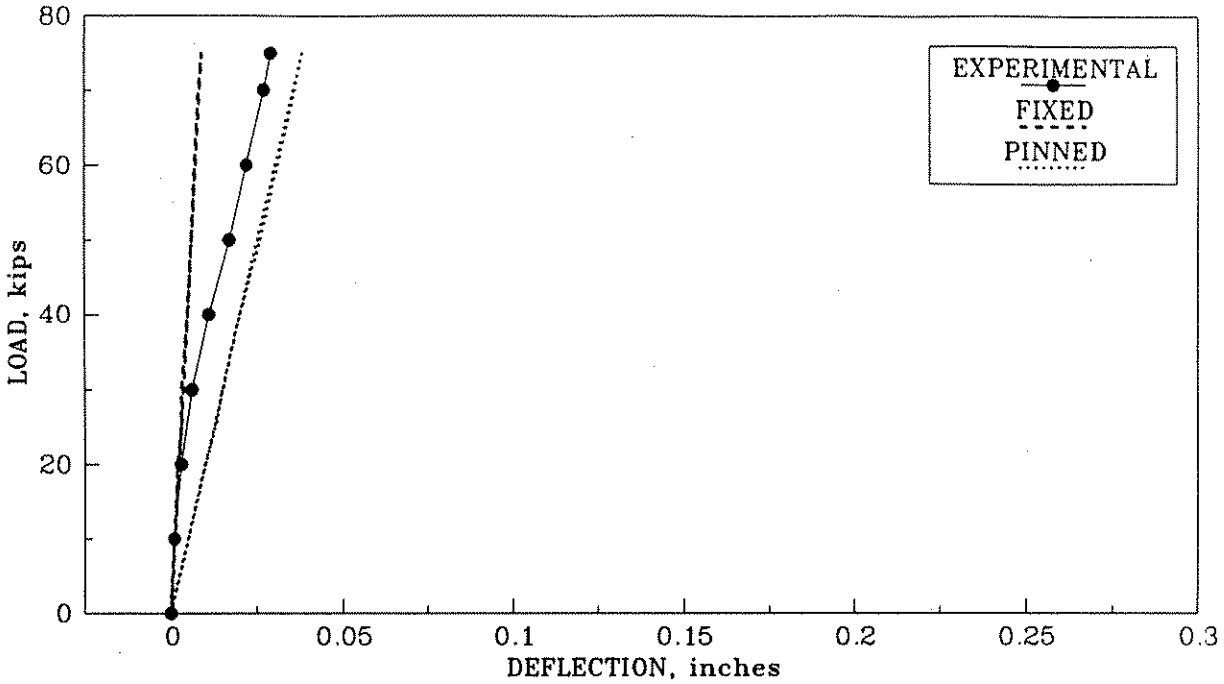

Fig. 4.76. Horizontal load versus deflection curves, load at point 5, deflection at point 6, C1.3 diaphragms.

girder response for the experimental bridge was more flexible than the mathematical model behavior, as shown in Fig. 4.75, for the reasons previously discussed.

Figures 4.77-4.79 show selected horizontal load versus horizontal deflection results for both the experimental and analytical bridge models containing the third-point large channel intermediate diaphragms (C2.3). The horizontal deflections are at points 4-6, respectively, when the horizontal load was applied to the bottom flange of the north P/C girder (point 6). The experimentally obtained horizontal deflections at point 6 (Fig. 4.79) appreciably digressed from the results predicted by the pinned-end finite-element model, while the horizontal deflection responses (Figs. 4.77 and 4.78) of the unloaded girders more closely matched the analytical results. The overall displacement behavior is consistent with the anticipated response considering the differences between the experimental bridge and the analytical bridge model.

The displacement responses for the bridge containing third-point, reinforced concrete, intermediate diaphragms (RC.3) are presented in Figs. 4.80-4.85. The fluxuations shown in the experimental results for the horizontal load versus horizontal deflection for the loaded south exterior P/C girder at point 4 (Fig. 4.80) was attributed to a displacement transducer malfunction and was not an indication of the actual behavior of the bridge. As expected, the analytical models predicted symmetric responses for the bridge, considering reciprocal displacements and geometric symmetry. The construction details for the diaphragms and the longitudinal deck cracks prevented a precise symmetric experimental response. Figure 4.85 shows the greatest divergence of the experimental results from the theoretical solutions. However, this response was the characteristic experimental deflection behavior associated with horizontal loads applied to the bottom flange of the north P/C girder (BM3) when the reinforced concrete intermediate diaphragms (RC.1 or RC.3) were in place.

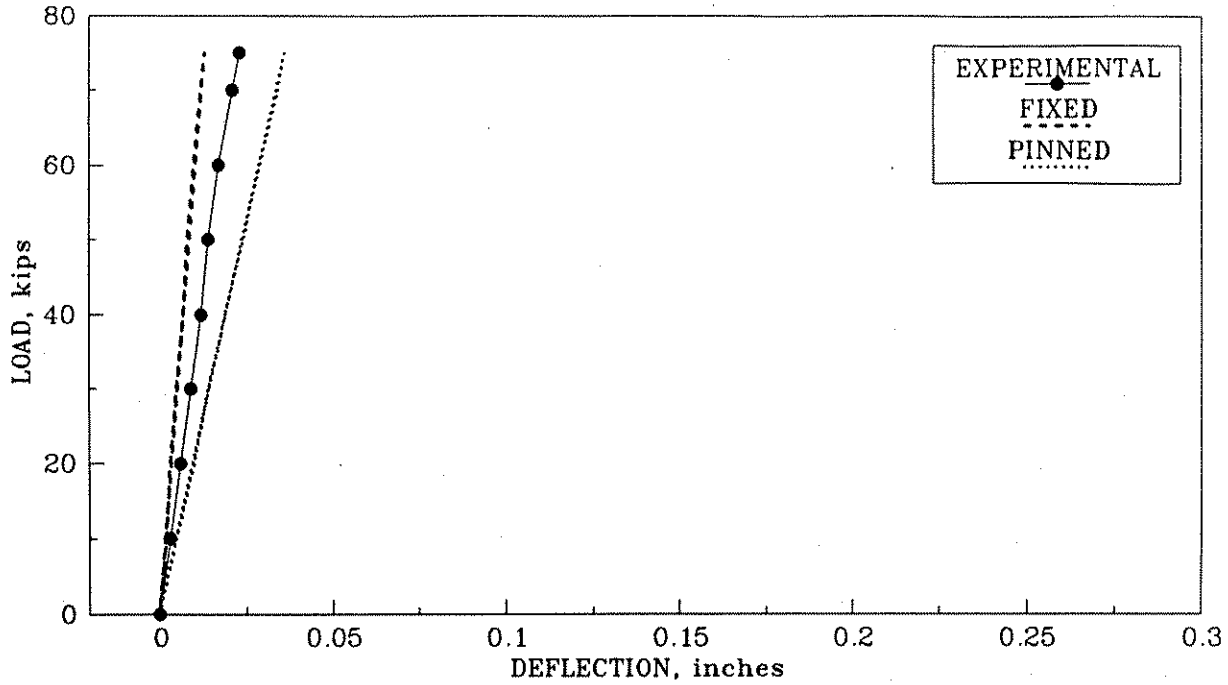

Fig. 4.77. Horizontal load versus deflection curves, load at point 6, deflection at point 4, C2.3 diaphragms.

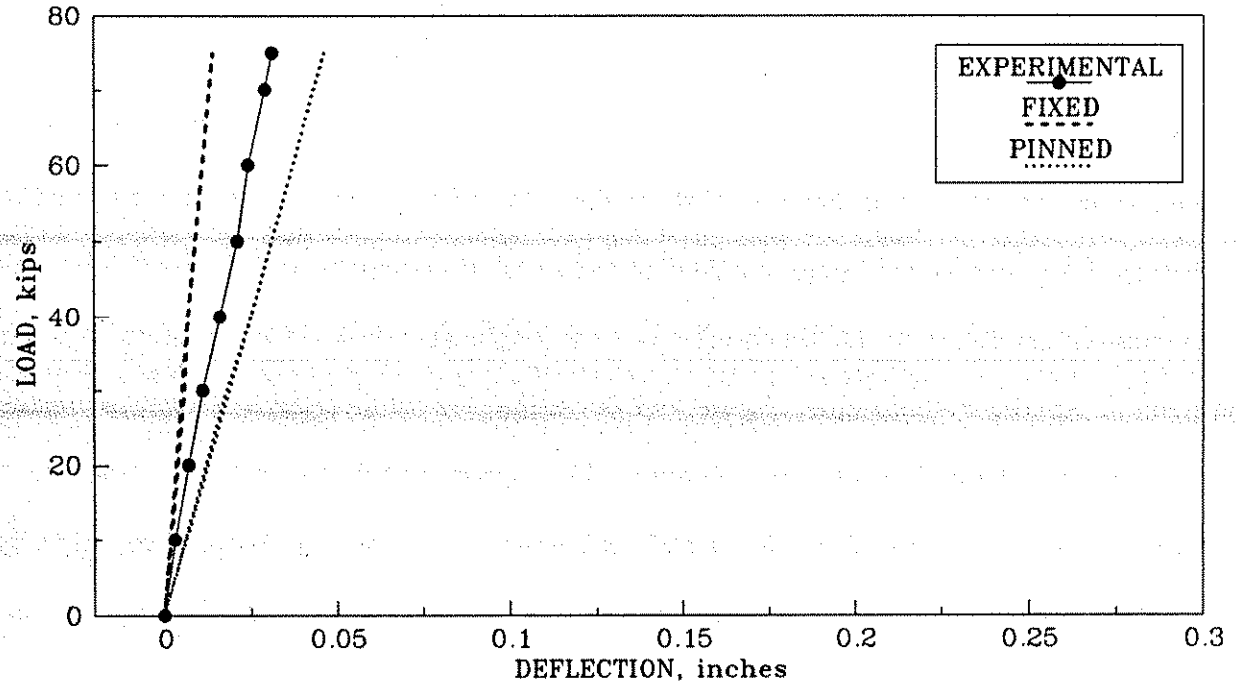

Fig. 4.78. Horizontal load versus deflection curves, load at point 6, deflection at point 5, C2.3 diaphragms.

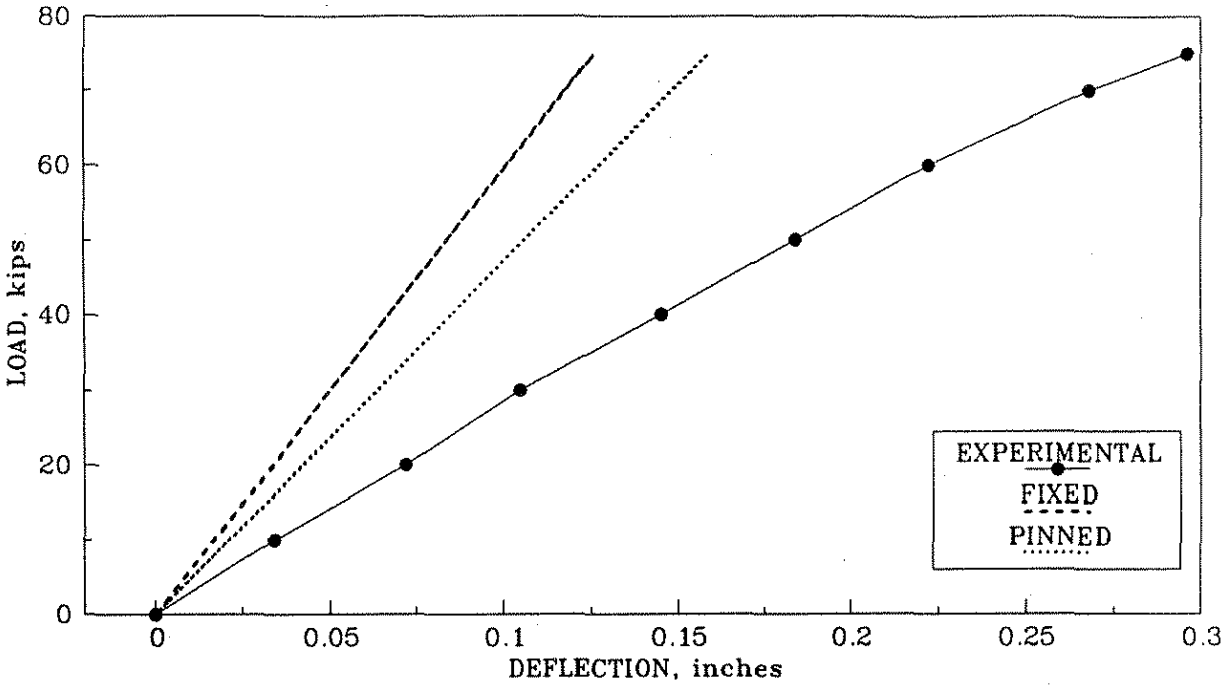

Fig. 4.79. Horizontal load versus deflection curves, load and deflection at point 6, C2.3 diaphragms.

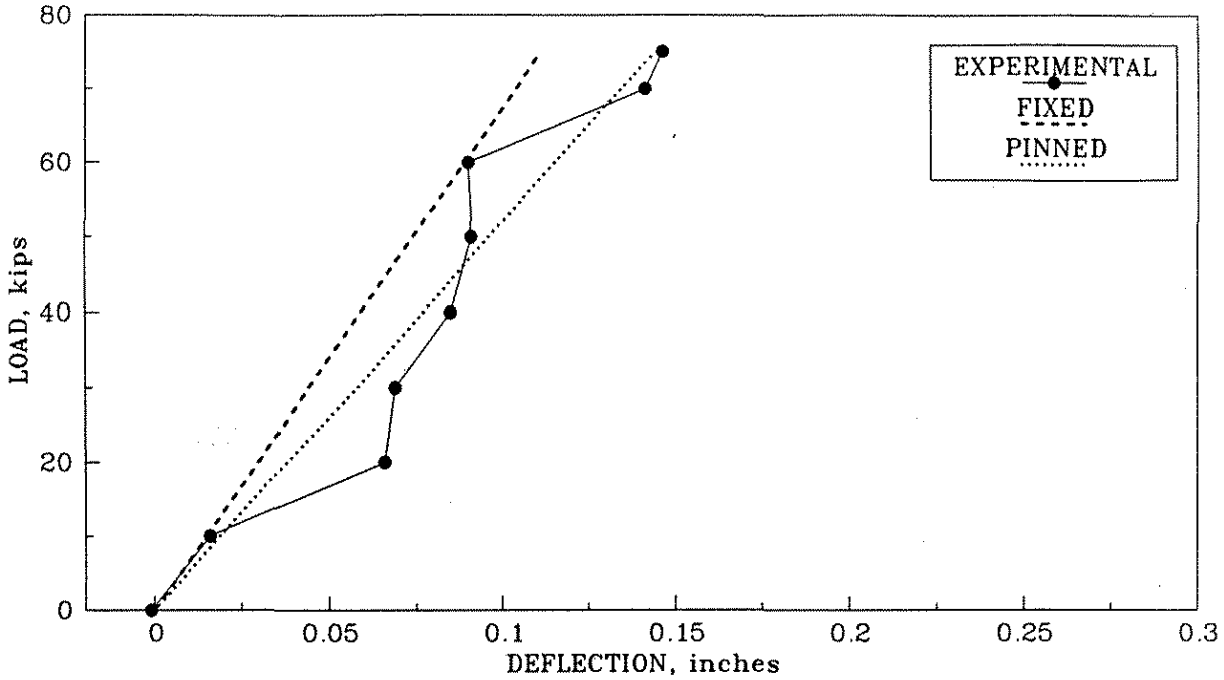

Fig. 4.80. Horizontal load versus deflection curves, load and deflection at point 4, RC.3 diaphragms.

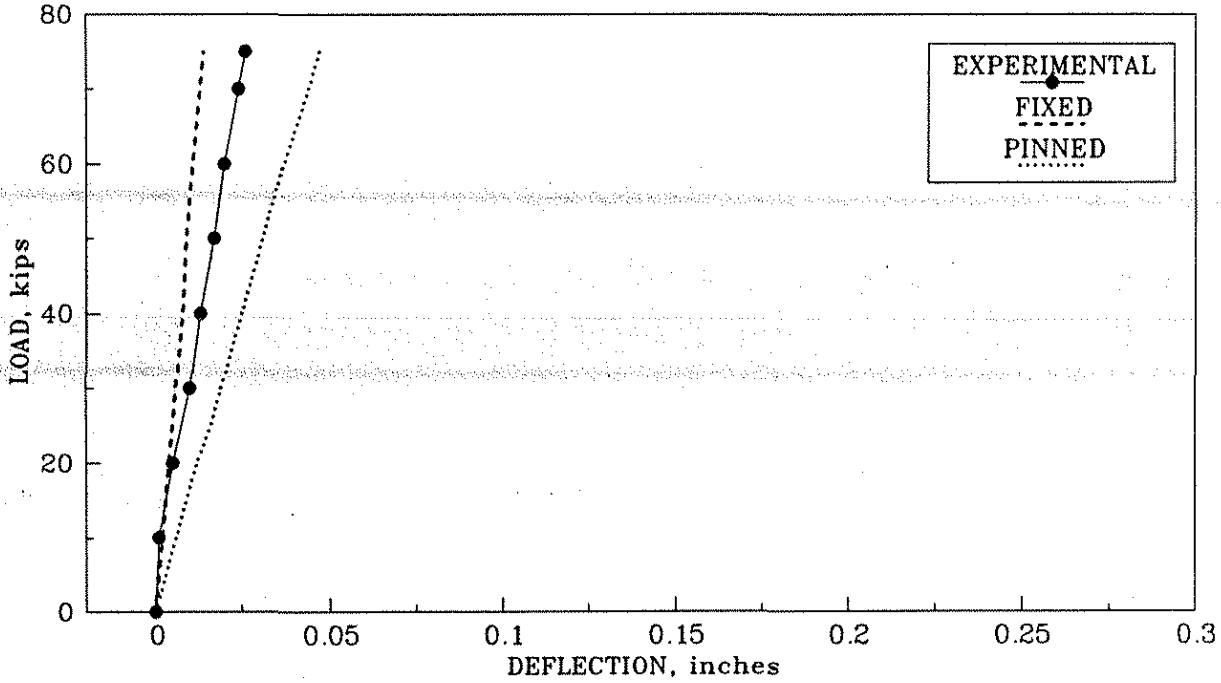

Fig. 4.81. Horizontal load versus deflection curves, load at point 4, deflection at point 5, RC.3 diaphragms.

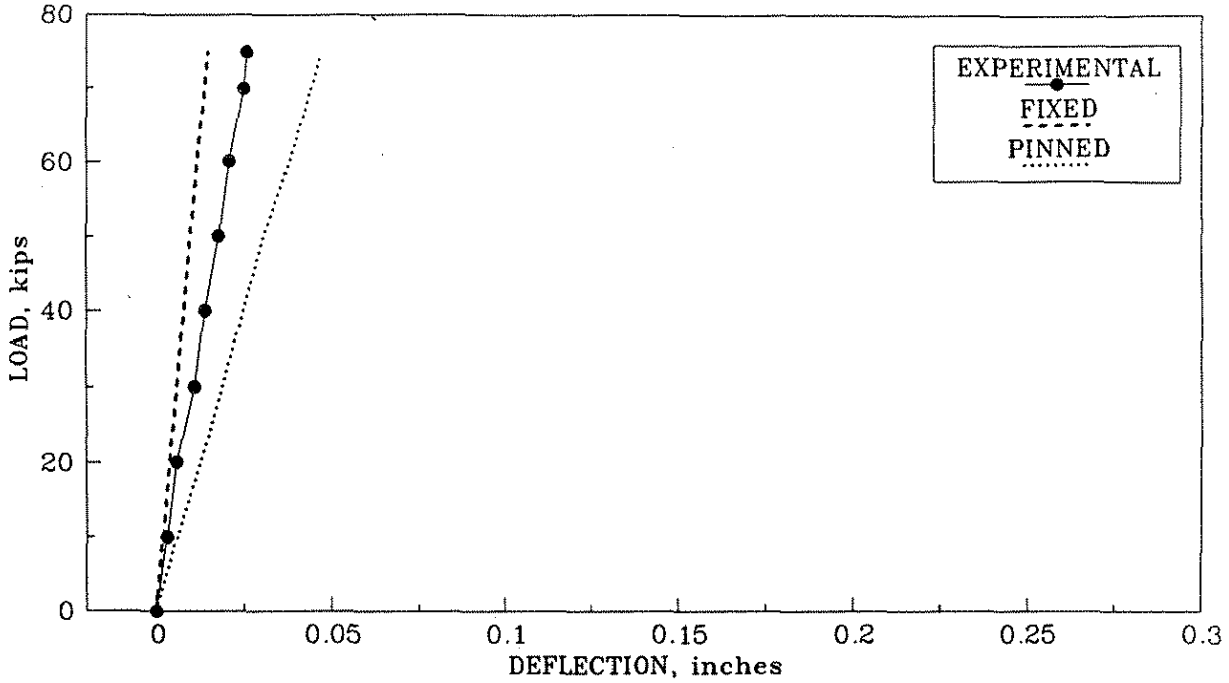

Fig. 4.82. Horizontal load versus deflection curves, load at point 4, deflection at point 6, RC.3 diaphragms.

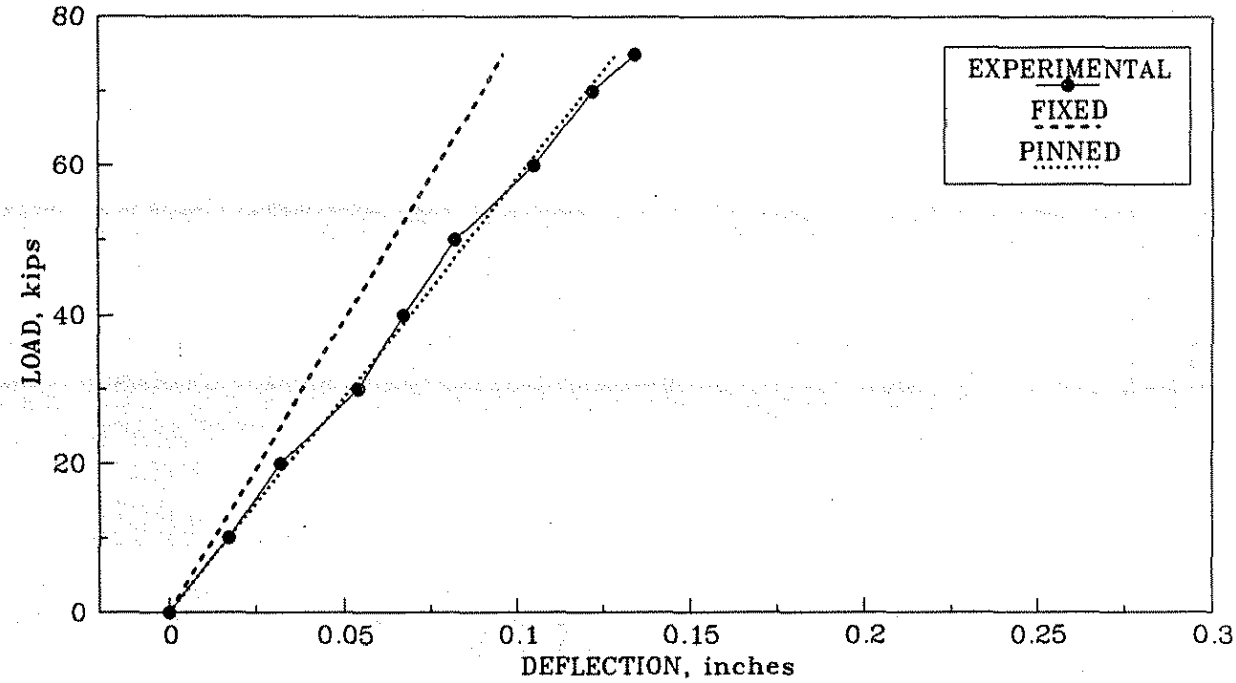

Fig. 4.83. Horizontal load versus deflection curves, load and deflection at point 5, RC.3 diaphragms.

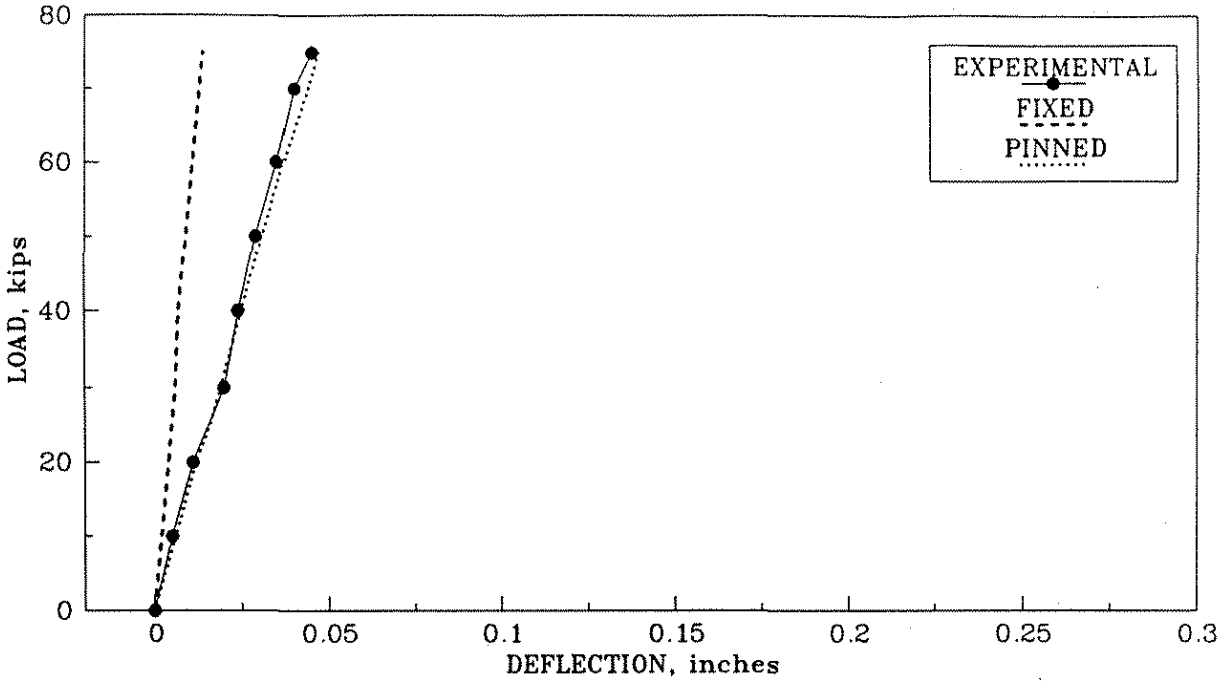

Fig. 4.84. Horizontal load versus deflection curves, load at point 5, deflection at point 6, RC.3 diaphragms.

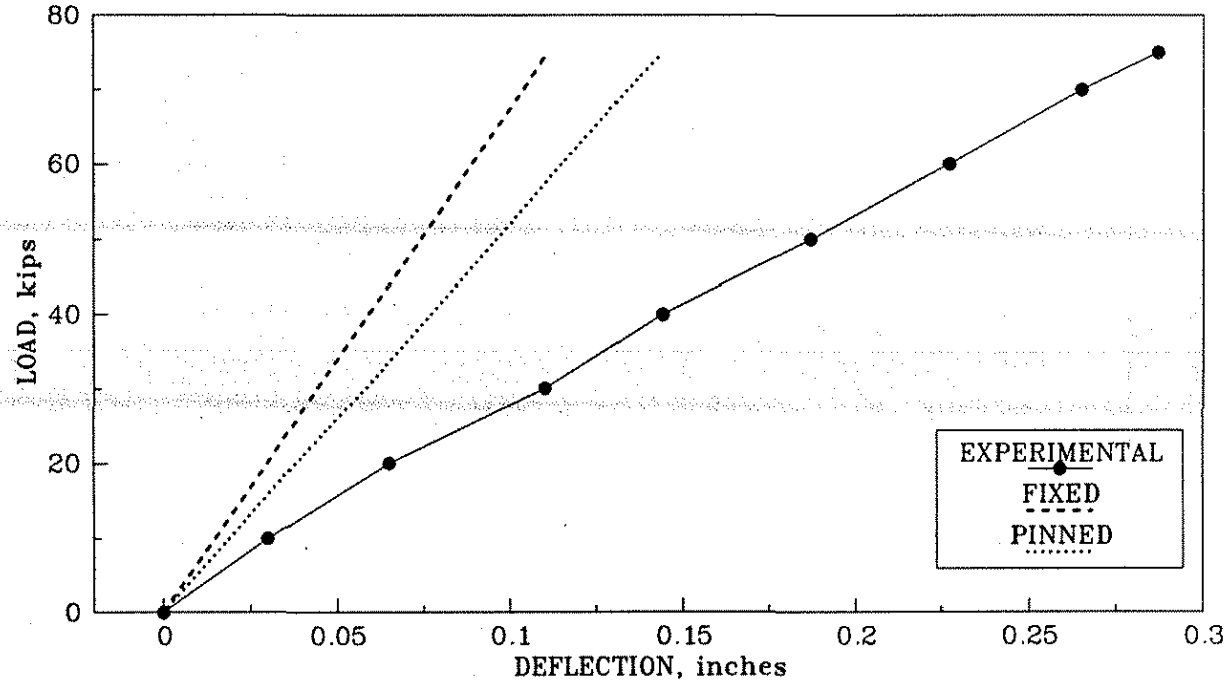

Fig. 4.85. Horizontal load versus deflection curves, load and deflection at point 6, RC.3 diaphragms.

4.3.3. Vertical Load Versus Vertical Deflection Behavior

4.3.3.1. No Intermediate Diaphragms

When the model bridge was subjected to vertical load, in most cases there was excellent agreement between the measured (experimental) and calculated (theoretical) results. The response of the experimental bridge to vertical loads was not appreciably affected by the transverse flexural stiffness of the bridge deck. As discussed in Section 2.1, the thin deck with the transverse reinforcement located near the mid-depth produced small transverse bending strengths for this deck. Therefore, any differences in the bridge behavior, associated with the various diaphragm configurations, could be more easily attributed to the diaphragms. After the deck had experienced the longitudinal cracks shown in Fig. 4.8, the resistance to an upward force on a girder would be provided primarily by the longitudinal bending stiffness of that loaded composite P/C girder when intermediate diaphragms were not present.

Figures 4.86 and 4.87 show both the experimental and analytical deflection results at points 5 and 6, respectively, that were induced by an upward force at point 6 when no intermediate diaphragms were present in the bridge. As these figures show, the experimental results occurred within the region bounded by the analytical solutions for fixed- and pinned-end P/C girders. A comparison of Figs. 4.86 and 4.87 reveals that the vertical deflections for the interior girder were about one-third of those for the exterior girder.

4.3.3.2. Midspan Intermediate Diaphragms

Two representative graphs showing vertical load versus vertical deflection behavior when the small channel midspan intermediate diaphragms (C1.1) were in place are presented in Figs. 4.88 and 4.89. The first figure shows the vertical deflection results at the midspan of the interior P/C girder (point 5) when the north exterior girder (BM3 in Fig. 4.8) is loaded upwards at point 6. The second figure shows the vertical deflection response for that loaded exterior girder. These figures show that the experimental results were bounded by the two analytical solutions.

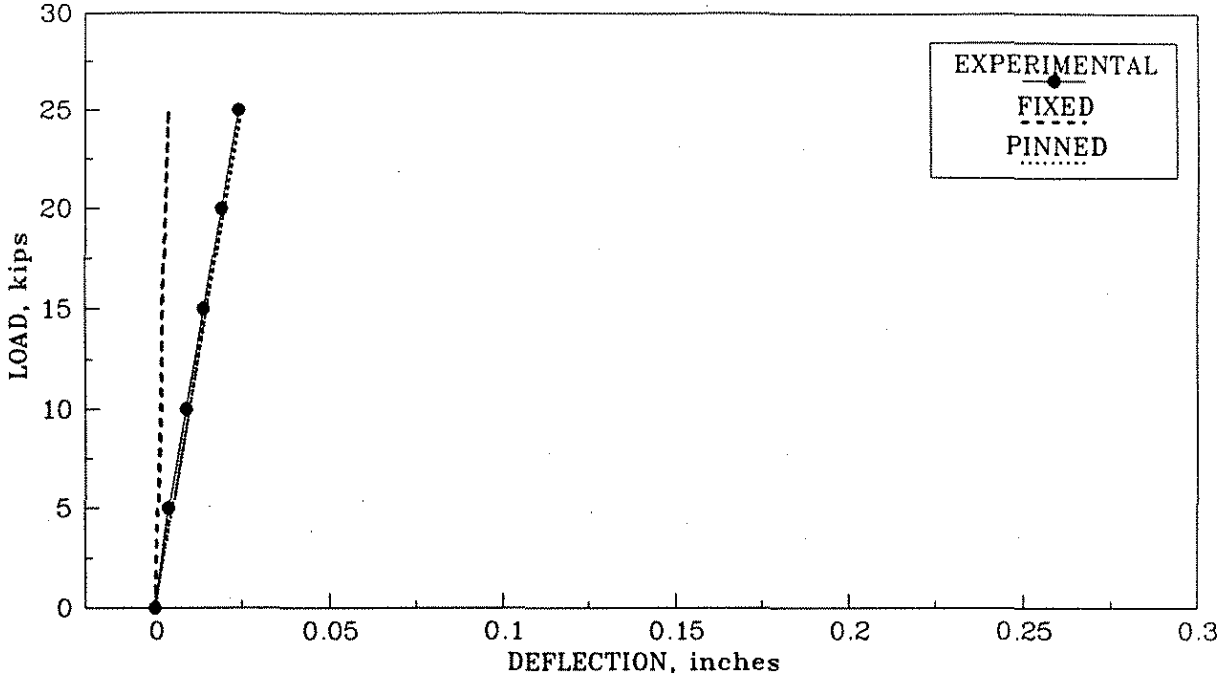

Fig. 4.86. Vertical load versus deflection curves, load at point 6, deflection at point 5, no intermediate diaphragms.

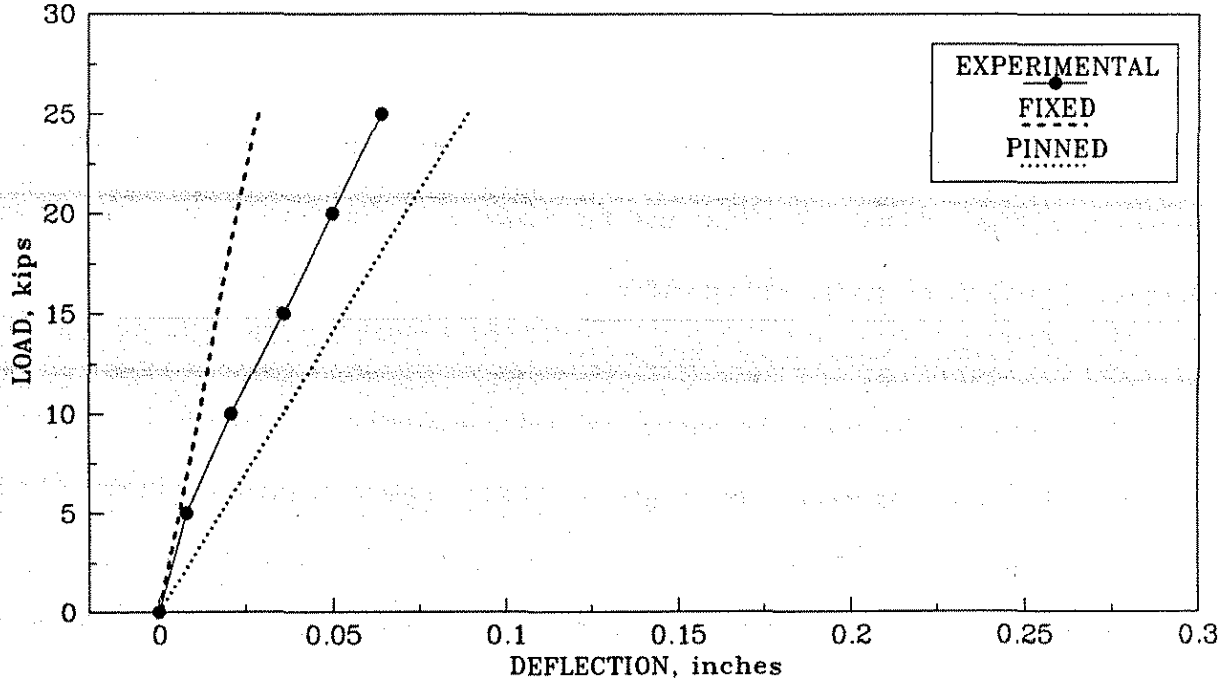

Fig. 4.87. Vertical load versus deflection curves, load and deflection at point 6, no intermediate diaphragms.

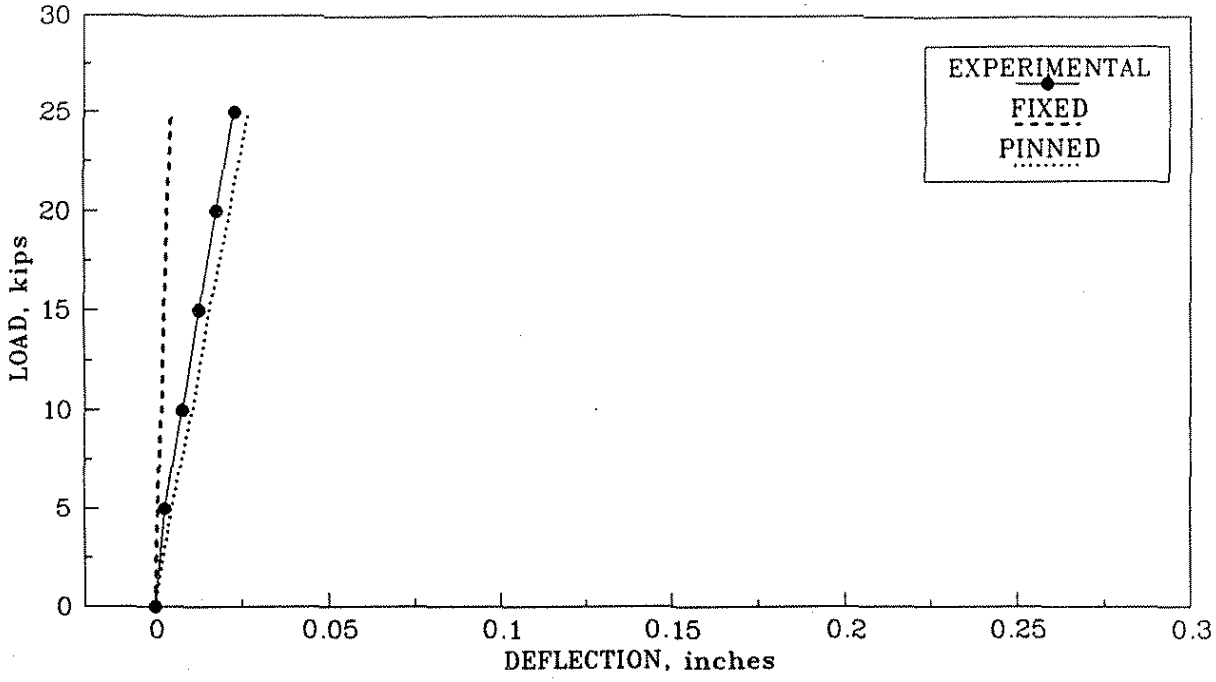

Fig. 4.88. Vertical load versus deflection curves, load at point 6, deflection at point 5, C1.1 diaphragms.

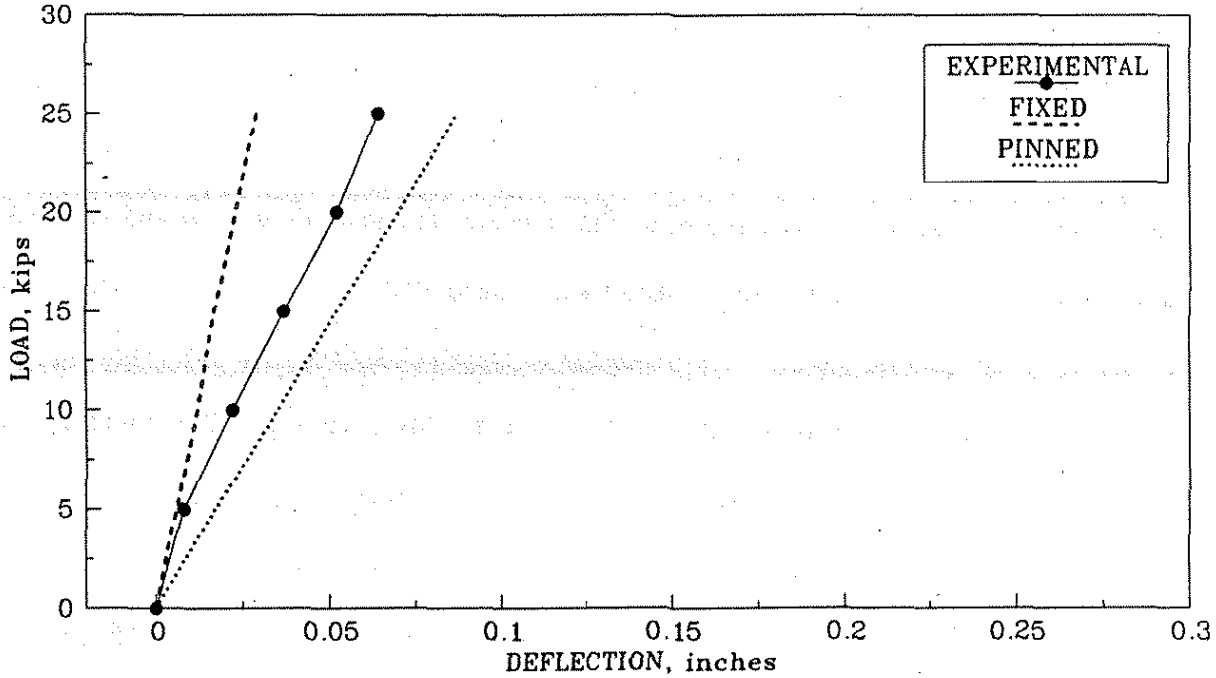

Fig. 4.89. Vertical load versus deflection curves, load and deflection at point 6, C1.1 diaphragms.

The vertical deflection response characteristics of the model bridge with the midspan reinforced concrete diaphragms (RC.1) in place and vertical load at points 4, 5, and 6 are shown in Figs. 4.90, 4.91, and 4.92, respectively. A comparison of the results for the exterior girders shown in Figs. 4.90 and 4.92 reveals analytically predicted symmetrical responses for both the fixed- and pinned-end models and nonsymmetrical, experimentally measured responses. For the exterior girders, the experimental results were within reasonable agreement with the analytical results. For the interior girder (Fig. 4.91), the experimental deflections were significantly larger than the deflections predicted by the analytical models. The deflection differences can be attributed to the presence of the longitudinal cracks in the bridge deck.

An upward force applied to the bottom flange of the interior girder (BM2 in Fig. 4.8) at the midspan of the bridge will cause Cracks 2 and 3a, shown in Fig. 4.8a, to open and Cracks 1 and 3b to close. The presence of Cracks 2 and 3a in the slab span between BM2 and BM3 form a linkage; therefore, the transverse flexural stiffness of this portion of the bridge deck will be significantly smaller than the transverse flexural stiffness of the portion of the bridge deck between BM1 and BM2. As previously noted, the analytical models did not involve deck cracking; thus, the predicted deflection responses were for a structure that was stiffer than the actual experimental bridge. A comparison of the analytical results shown in Figs. 4.90 and 4.91 and in Figs. 4.91 and 4.92 reveals that the interior girder response produced significantly smaller deflections than those associated with the loading of the exterior girders. This response was anticipated, since a vertical force applied to the interior girder will cause a symmetrical uplift on the entire bridge structure. The absence of deck and diaphragm continuity on the one side of an exterior girder will produce a more flexible displacement response for that girder. A comparison of the experimental deflection results shown in Figs. 4.90 and 4.91 and in Figs. 4.91 and 4.92 reveals that the measured vertical deflection magnitudes were not significantly affected by which P/C girder was vertically loaded. This behavior was attributed to the location of the longitudinal bridge deck cracks.

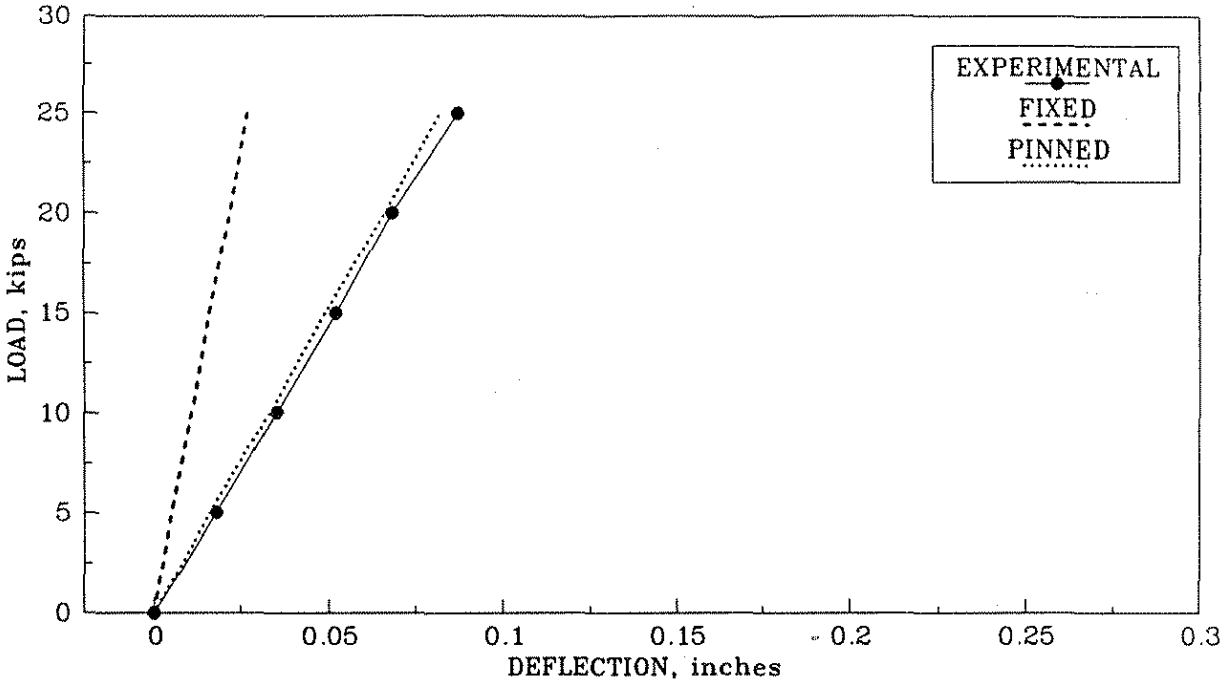

Fig. 4.90. Vertical load versus deflection curves, load and deflection at point 4, RC.1 diaphragms.

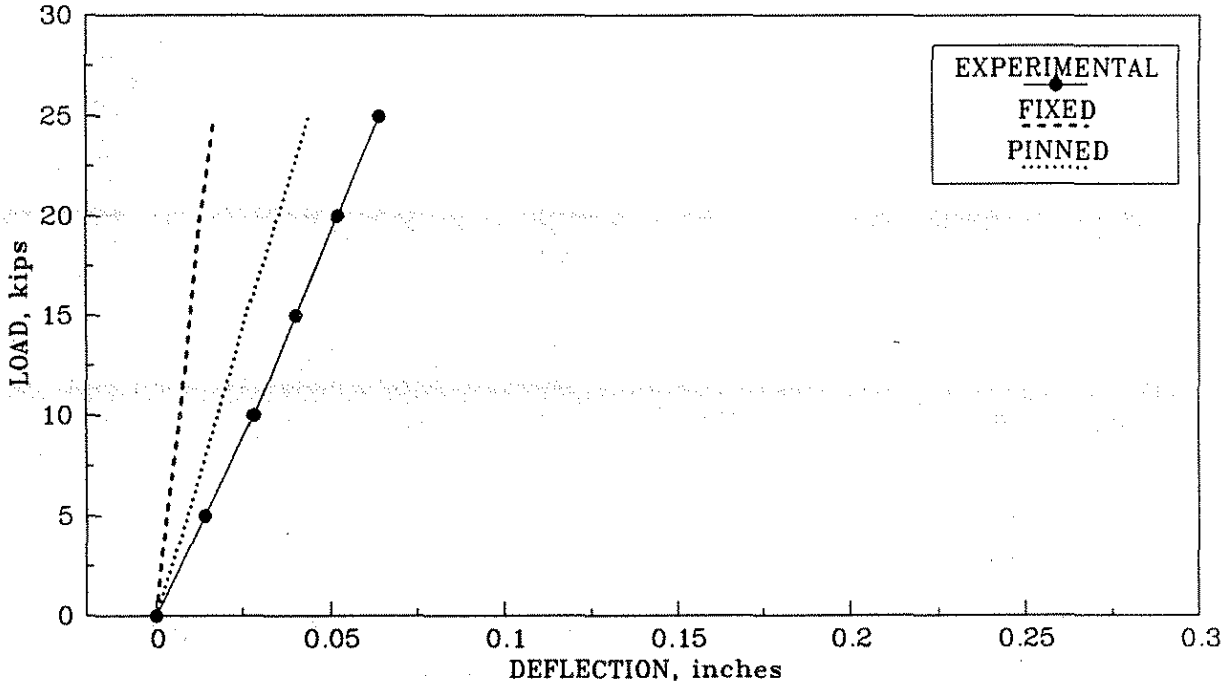

Fig. 4.91. Vertical load versus deflection curves, load and deflection at point 5, RC.1 diaphragms.

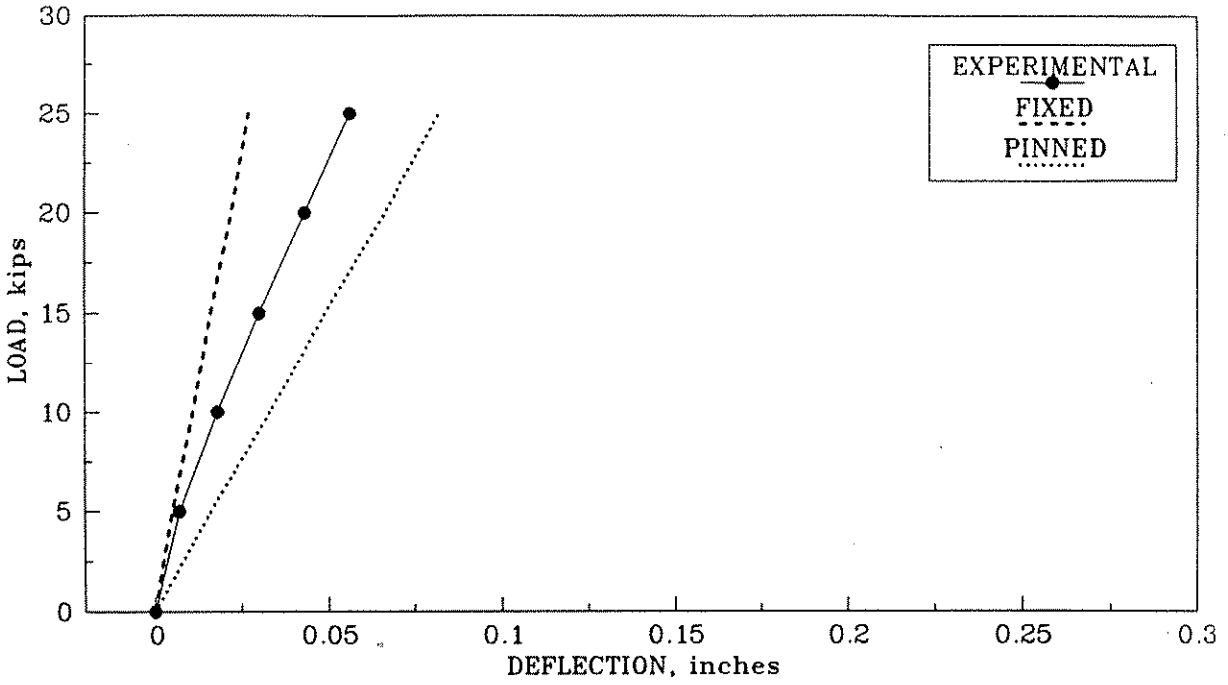

Fig. 4.92. Vertical load versus deflection curves, load and deflection at point 6, RC.1 diaphragms.

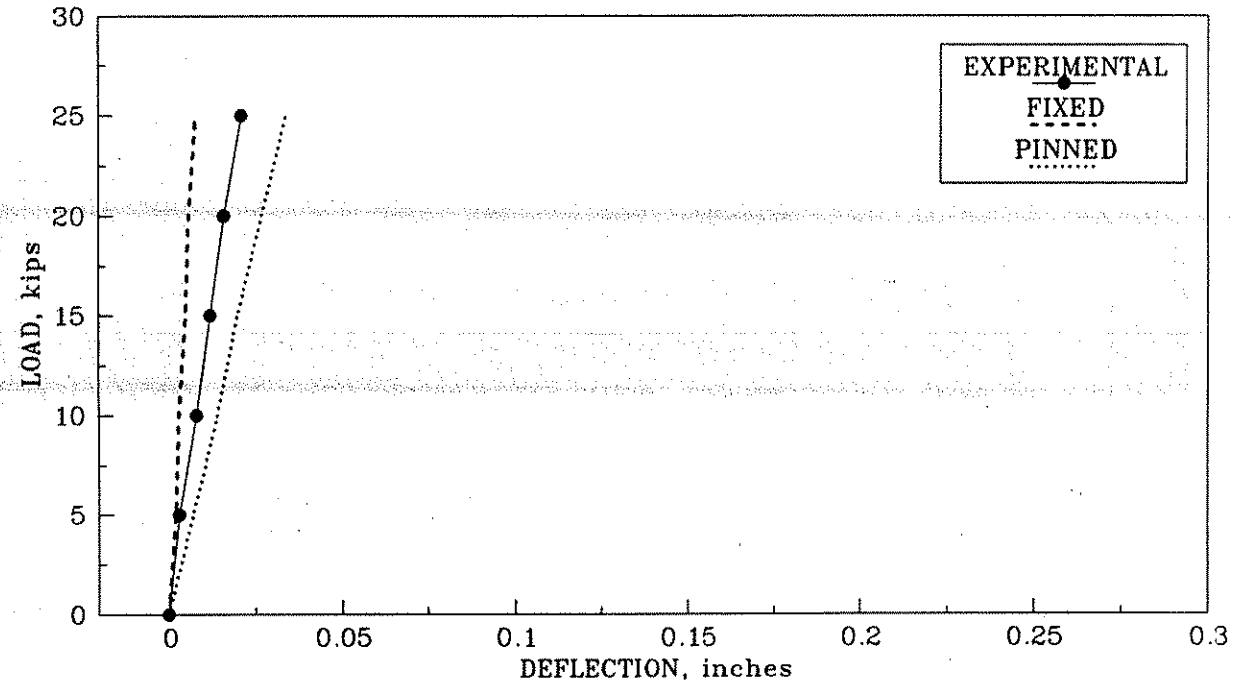

Fig. 4.93. Vertical load versus deflection curves, load at point 6, deflection at point 5, RC.1 diaphragms.

A typical vertical load versus vertical deflection response for an unloaded P/C girder is shown in Fig. 4.93; as may be observed, the experimental results were bounded by the analytical results.

4.3.3.3. Third-Point Intermediate Diaphragms

When diaphragms were located at the third points of the bridge span, the response characteristics for vertical load versus vertical deflection were similar to those obtained when the diaphragms were at the midspan. Therefore, only two figures have been presented to illustrate the vertical deflection behavior for diaphragms at the third points in the bridge. Figures 4.94 and 4.95 present the analytical and experimental deflection results for an unloaded interior girder and loaded exterior girder, respectively, when the third-point, reinforced concrete diaphragms (RC.3) were in place. A comparison of Figs. 4.94 and 4.93 and Figs. 4.95 and 4.92 reveals almost identical vertical load versus vertical deflection behaviors. Therefore, the response of the bridge for reinforced concrete diaphragms at either the third points or at the midspan of the bridge was essentially the same. Similar results occurred for the other types of intermediate diaphragms.

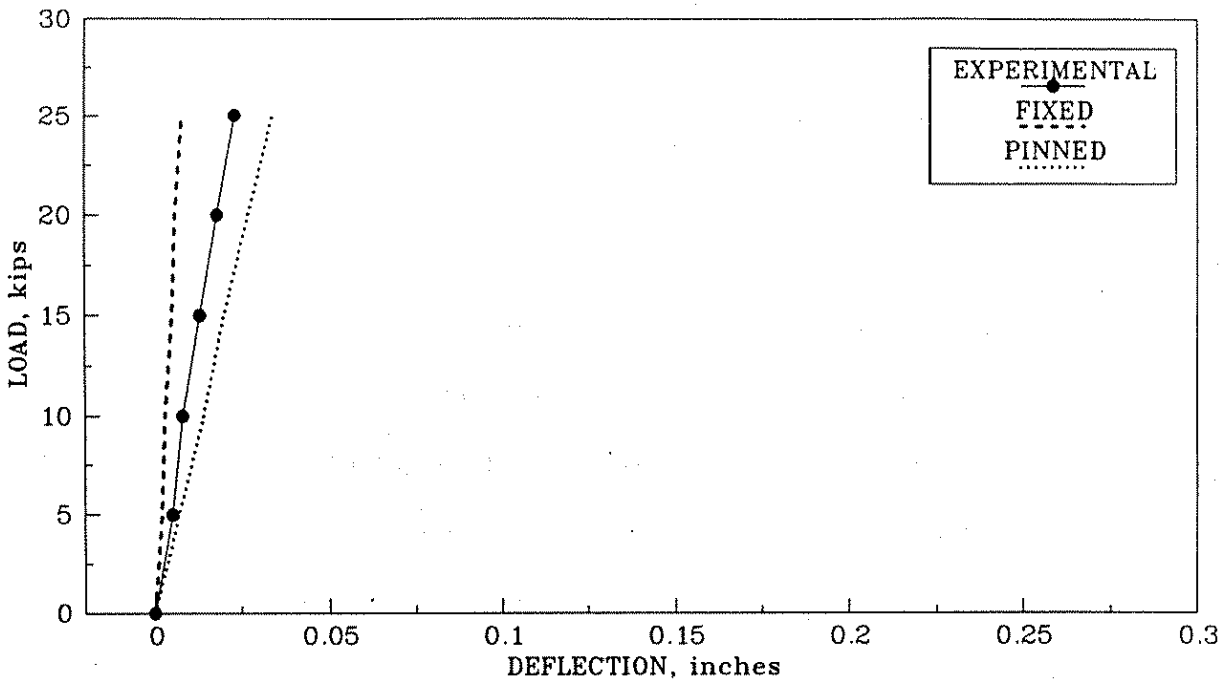

Fig. 4.94. Vertical load versus deflection curves, load at point 6, deflection at point 5, RC.3 diaphragms.

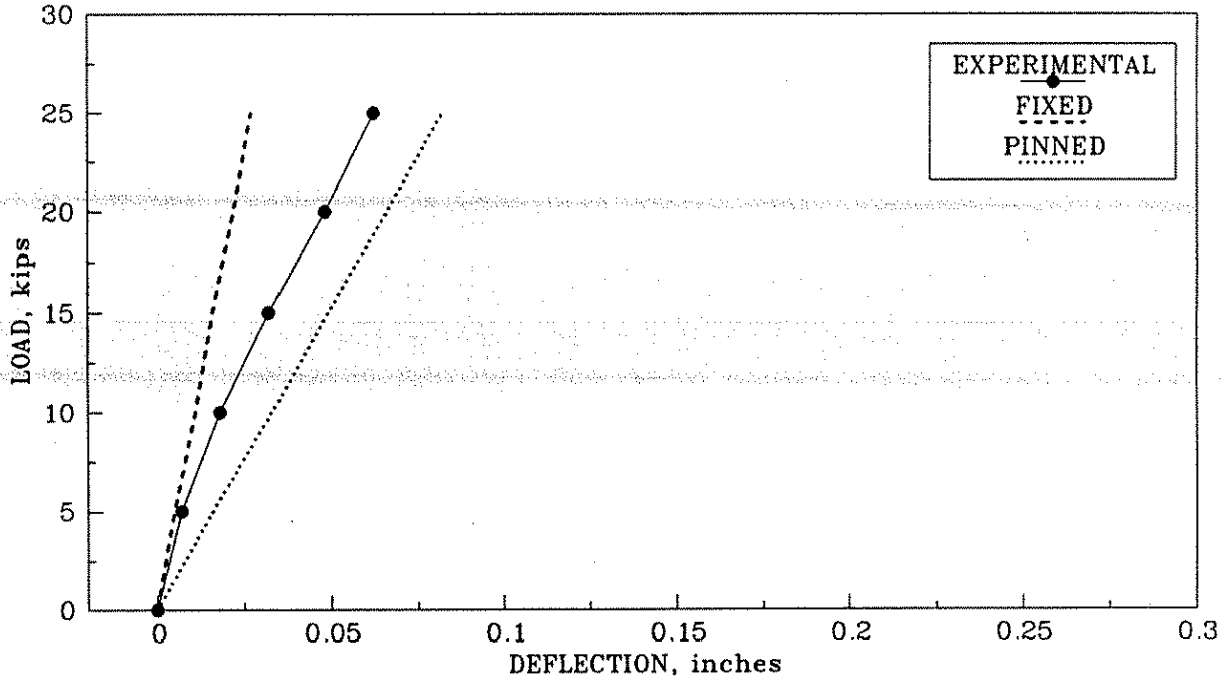

Fig. 4.95. Vertical load versus deflection curves, load and deflection at point 6, RC.3 diaphragms.

5. SUMMARY AND CONCLUSIONS

5.1. Summary

This report summarizes the research that was conducted for the purpose of determining whether steel intermediate diaphragms of some conventional configuration are structurally equivalent to the reinforced concrete intermediate diaphragms that are currently being used by the Iowa DOT. The research included a review of previous investigations related to the performance of P/C girder bridges subjected to lateral forces, a survey of design agencies to obtain information on intermediate diaphragms and lateral impacts, three-dimensional, finite-element analysis of the model P/C girder bridge, and extensive experimental testing of a full-scale P/C girder bridge without intermediate diaphragms and with four types of intermediate diaphragms positioned at either the one-third points along the span or at the midspan.

A review of the literature revealed that although there have been numerous investigations on the performance of intermediate diaphragms when a bridge is subjected to vertical loadings, very little research has been conducted on the performance of intermediate diaphragms when the bridge is subjected to lateral loadings, for example, when vehicles with loads too high to pass under the superstructure strike the bottom flange(s) of the P/C girder(s).

An in-depth questionnaire was sent to 63 design agencies in the United States and Canada; responses were obtained from 86% of those questioned. The survey contained 33 multiple choice questions which addressed topics such as the type of diaphragm used, diaphragm location and depth, connection details to the P/C girders and deck, limitations on the use of either steel or R/C intermediate diaphragms, design criteria for lateral impact loads, approximate occurrence of overheight vehicle-bridge collisions, and categorization of the type and extent of bridge damage caused by over-height loads. The respondents were asked to provide plans and specifications of intermediate diaphragms used in their jurisdiction. Ninety-six percent of the respondents use cast-in-place concrete diaphragms when the bridge is located above a highway or navigable waterway; 23%

of these respondents also specify steel channels. Over 90% of those responding stated that the design of their standard diaphragms and connections is by a "rule of thumb" approach.

A finite-element model of the model bridge was developed using ANSYS. The mesh size was selected to provide nodal points at the locations of the intermediate diaphragms. Each type and configuration of intermediate diaphragm tested was modeled by using finite elements. The analytical model was subjected to both horizontal and vertical loads at the midspan of each beam. Any combination of horizontal and vertical loads could be obtained by the superposition of the results of the respective cases of loading. Construction details, that is, ties between the end diaphragm and the abutments, between the P/C girders and the end diaphragms, and between the deck and the end diaphragm, resulted in considerable end restraint. To "bracket" experimental results, both fixed- and pinned-end conditions were modeled and analyzed. The effects of the prestressing forces in the P/C girders and the dead load of the bridge were not considered in the analysis, so that the results of the analytical study could be compared directly with the experimental data.

A full-scale, simple-span, P/C girder bridge model containing three 40-ft long P/C beams on 6-ft centers was constructed and tested to evaluate the performance of intermediate reinforced concrete and steel diaphragms currently being used by the Iowa DOT and other intermediate steel diaphragms developed in this project. A total of eight different intermediate diaphragm configurations (C1.1, C1.3, C2.1, C2.3, RC.1, RC.3, X1.1, and X2.1) were tested in addition to testing the model bridge without intermediate diaphragms. The tests were conducted to determine the effectiveness of intermediate diaphragms in distributing lateral forces. A secondary study involved an analysis of vertical load distribution. Thus, the model was subjected to both horizontal and vertical loads applied to the bottom flange of each of the girders. The loads were applied at the one-third points along the bridge span and at the midspan. Several tests were conducted by using combined vertical and horizontal forces to verify that the results of the individual vertical and horizontal load tests could be superimposed to obtain the combined effects. The deck, girders, and

diaphragms were instrumented with strain gages to measure strains. Deflections of the bottom flanges of the girders were monitored with direct current displacement transducers; the deflection of the south deck edge was monitored with dial gages. A computer-controlled data acquisition system was used to measure and record the strains and deflections.

The deflection results were extensively analyzed to establish the response characteristics of the experimental bridge when horizontal or vertical loads were applied. Graphs of load versus deflection have been presented to illustrate the deflection behavior associated with the various types and locations of intermediate diaphragms. The experimentally measured deflections were compared to the analytically predicted deflections obtained from a fixed- or pinned-end finite-element model. In most instances, the analytical results bounded the experimental results, as would be expected, since the rotational restraint at the ends of the P/C girders would be between the two types of idealized end conditions. However, in some instances, the experimental deflections were outside of the limits established by the analytical predictions; this behavior was due to the differences between the analytical model and the experimental model bridge. The characteristics in the experimental bridge that could not be modeled analytically included the longitudinal deck cracks; connection slippage and prying that occurred between the steel channel diaphragms and P/C girder webs, and the elongation of the tendons, which tied the R/C intermediate diaphragms and P/C girders together. Also, the connection between the P/C girders and the R/C deck was approximated by connecting all common nodes between the top of the girders and the bottom of the deck.

5.2. Conclusions

The conclusions presented in this section were formulated from the responses to the questionnaire, and from the results obtained from both the analytical and experimental bridge models. Recall that the bridge model contained three, Type A, P/C girders (32 in. total depth) spaced 6-ft on centers and a 4-in.-thick R/C deck. Therefore, the large channel C2, the X-brace plus strut X1, and the X-brace without strut X2, intermediate diaphragms support a large portion of the

P/C girder depth. This obviously is not the case for the larger P/C girders. Tests involving the small channel diaphragm C1 were conducted to address some of the issues related to diaphragm depth versus girder depth. Also, the depth of the Type A P/C girder resulted in small angles of inclination in the diagonal members of steel diaphragms which contained X-bracing. When the bridge model was subjected to horizontal loading, the diagonal members of the X-brace were primarily subjected to axial loading. In the case of larger P/C girders in addition to the axial load, the diagonal members would be subjected to increased bending.

The following conclusions were developed as a result of this investigation:

1. The X-brace plus strut intermediate diaphragms (X1) were determined to be essentially structurally equivalent to the R/C intermediate diaphragms.
2. Vertical load and horizontal load distributions are affected by end restraint; however, vertical load distribution is essentially independent of the type and location of intermediate diaphragms, while the horizontal load distribution is a function of diaphragm type and location.
3. The vast majority of the state departments of transportation require that R/C intermediate diaphragms be used when traffic can pass beneath a P/C girder bridge. However, about one quarter of the design agencies indicated that steel channel diaphragms may also be used in these bridges.
4. Construction details at the girder supports (which were essentially the same as those used in practice) resulted in significant rotational end restraint for vertical and horizontal loading.
5. The channel-shaped steel diaphragms experienced slippage in the connections to the P/C girder webs because of the presence of the horizontally slotted holes. Even though the high-strength bolts were tightened by the turn-of-the-nut method, the frictional resistance offered by the clamping force in the connection was exceeded by the applied horizontal

force. As expected, the small channel diaphragms (C1) connected with 2 bolts at each end experienced connection slippage at magnitudes of horizontal load that were smaller than those that cause slippage for the large channel diaphragms (C2) connected with 4 bolts at each end.

6. The finite-element model with fixed- or pinned-ends for the P/C beams generally bounded the experimental results. In some instances, the analytical model predicted smaller deflections than were measured; these differences were due to the mathematical model being stiffer than the test bridge. Construction details between the P/C girders and the bridge deck and between the P/C girders and the intermediate diaphragms can not be accurately modeled. Also the deck cracks, which could not be included in the finite-element model, reduced the bridge stiffness.
7. When the intermediate diaphragms were located at the midspan of the bridge and when horizontal loads were applied to the outside face of the bottom flange of the exterior girder at its midspan, the measured horizontal deflection at the load point increased as the diaphragm configuration was changed from RC.1 to X1.1, X1.1 to X2.1, X2.1 to C2.1, and C2.1 to C1.1. As expected, the greatest horizontal deflection of the loaded exterior girder occurred when no interior diaphragms were present.
8. The midspan horizontal deflection of a horizontally loaded P/C girder increased, while the horizontal deflection of the unloaded P/C girders decreased, when the horizontal strut was removed from the X1.1 diaphragms to form the X2.1 diaphragms.
9. For the load levels applied during most of the experimental tests of the model bridge, essentially linear load versus deflection behavior was observed.
10. A large percentage of the horizontal deflection of a horizontally loaded girder in the experimental bridge was caused by the rotation of the girder about its longitudinal axis, rather than by the deflection of the bridge as a whole, when an exterior girder was

loaded and any type of intermediate diaphragms were present. The same was true when the interior girder was loaded and either the shallow or deep channel diaphragms were in place.

11. Symmetric load versus deflection behavior was confirmed experimentally, except in those instances where the connection details and deck cracks directly affected the bridge's response.

6. RECOMMENDED CONTINUED STUDIES

1. With the exception of K-shaped diaphragms, essentially all practical configurations of steel diaphragms have been tested. With the existing model P/C girder bridge, data could be obtained on the K-shaped diaphragms (or other configurations) with minimal difficulty.
2. With steel diaphragms, there is less contact area between the diaphragm connection bracket and the webs of the P/C girders than there is in the case of R/C diaphragms. Data is needed on the two-way shear strength of the P/C girder webs to prevent "punching" shear failures of these elements. The P/C beams of the model bridge and the horizontal loading system, (with appropriate modifications) could be used to obtain some of the needed two-way shear data.

7. REFERENCES

1. American Association of State Highway and Transportation Officials. *Standard Specifications for Highway Bridges*, 14th Edition. Washington: American Association of State Highway and Transportation Officials, 1989.

2. American Association of State Highway and Transportation Officials. *Interim Specifications--Bridge--1991.* Washington: American Association of State Highway and Transportation Officials, 1991.

3. Bakht, B., and F. Moses, "Lateral Distribution Factors for Highway Bridges" *ASCE, Journal of Structural Engineering*, Vol. 114, No. 8 (August 1988), pp. 1785-1803.

4. Cheung, M. S., R. Jategaonkar, and L. G. Jaeger, "Effects of Intermediate Diaphragms in Distributing Live Loads in Beam-and-Slab Bridges," *Canadian Journal of Civil Engineering*, Vol. 13, No. 13 (June 1986), pp. 278-292.

5. De Salvo, G. J., and J. A. Swanson, *ANSYS Engineering Analysis System User's Manual*, Vols. I and II, Houston, Penn.: Swanson Analysis System, Inc., 1985.

6. Kostem, C. N., and E. S. deCastro, "Effects of Diaphragms on Lateral Load Distribution in Beam-Slab Bridges," *Transportation Research Record 903*, Transportation Research Board, 1977, pp. 6-9.

7. Kulicki, J. M., D. R. Mertz, I. M. Friedland, and NCHRP 12-33 project team. "Proposed LRFD Bridge Design Code," Modjeski and Masters, Harrisburg, Penn., 1991.

8. McCathy, W., K. R. White, and J. Minor, "Interior Diaphragms omitted on the Gallup East Interchange Bridge--Interstate 40," *Journal of Civil Engineering Design*, Vol. 1, No. 1, (1979), pp. 95-112.

9. Shafer, M. W. "Lateral Load Resistance of Diaphragms in Prestressed Concrete Girder Bridges." Master's thesis (in preparation), Iowa State University, Ames, 1991.

10. Shanafelt, G. O., and Horn, W. B., "Damage Evaluation and Repair Methods for Prestressed Concrete Bridge Members," *NCHRP Report 226*, Nov. 1980, pp. 66.

11. Sengupta, S., and J. E. Breen, "The Effect of Diaphragms in Prestressed Concrete Girder and Slab Bridges," *Research Report 158-1F, Project 3-5-71-158*, Center for Highway Research, The University of Texas at Austin, October 1973.

12. Sithichaikasem, S., and W. L. Gamble, "Effects of Diaphragms in Bridges with Prestressed Concrete I-Section Girders," *Civil Engineering Studies No. 383*, University of Illinois, Urbana, 1972.

13. Wassef, W. G., "Analytical and Experimental Investigations of Shell Structures Utilized as Bridges", Ph.D. diss., Iowa State University, Ames, 1991, pp. 162.

14. Wong, A. Y. C., and W. L. Gamble, "Effects of Diaphragms in Continuous Slab and Girder Highway Bridges," *Civil Engineering Studies, Structural Research Series No. 391*, University of Illinois, Urbana, 1973.

8. ACKNOWLEDGMENTS

The study presented in this final report was conducted by the Engineering Research Institute of Iowa State University and was sponsored by the Iowa Department of Transportation, Highway Division, through the Highway Research Advisory Board.

The authors wish to thank William Lundquist and John Harkin from the Iowa Department of Transportation for their support of the research work on diaphragm effectiveness in distributing lateral loads. Also, an expression of appreciation is extended to two corporate representatives for their support of the research conducted. Donald Henrich, general manager of Iowa Prestressed Concrete, Inc. (Iowa Falls, IA) provided the three A38 and the D P/C Beams, which were an integral part of the experimental model bridge. Economy Forms Corporation (Des Moines, IA), provided the metal forms for casting the abutments, end diaphragms, and the bridge deck. For their contributions, the authors express their appreciation.

The authors acknowledge the assistance of Douglas Wood, Structural Laboratory Supervisor, for his valuable contributions with the experimental program. Many students worked on the construction of the model bridge. Those students who devoted a significant amount of time to the project were Timothy Craven, Bret Farmer, Tony Jacobsen, Chris Maskrey, Amy Rechenmacher, and Stephanie Young. Bret, Chris and Tony also assisted during the extensive testing of the bridge. The authors greatly appreciated their help.

A significant contribution to the analytical investigations was provided by Wagdy Wassef who developed the finite-element models and performed the analyses. For his important contributions to the research work, the authors extend their sincere appreciation. Theresa Connor is to be thanked for her efforts in presenting both the analytical and experimental results in a graphical format. The authors wish to thank Denise Wood, Structures Secretary, for typing this report.

Appendix A

DESIGN AGENCY QUESTIONNAIRE RESULTS

DESIGN AGENCY QUESTIONNAIRE RESULTS

The number in the parentheses ( ) represents the number of design agencies having that particular answer. The notes in the brackets [ ] are paraphrased comments from the respondents. An individual respondent's remarks are separated by a colon.

Part I. General Prestressed Concrete Girder Bridge Geometry and Conditions

1. Has your state or agency ever specified intermediate diaphragms?

   (51) Yes (Please complete the entire questionnaire)

   (1) No (Please stop here. Do not complete questionnaire: however, please return the survey.)

2. Has your state or agency ever discontinued the use of intermediate diaphragms?

   (10) Yes: When? Why?

   [Unnecessary, ____ does not use AASHTO criteria: Not found beneficial in the load distribution or to the construction of concrete girder bridges: Nov. 1982, Except for overheads subject to high load impacts. Tests by others indicated diaphragms had little effect on live load distribution: 1975, Not needed when girders are under 50 ft. long: 1970, Their use was questionable: Early 70's, Due to research conducted by the University of Illinois indicating an adverse load redistribution between interior and exterior beams at location of intermediate diaphragms: Span Lengths less than 40 ft., not required by AASHTO: Feb. 1979, Research had indicated that they contribute very little to the overall performance of structures: 1980's, Research results indicated that diaphragms have little effect after composite slab was placed on beams.]

   (40) No

   Note: If you answered yes to this question, please answer the remaining questions with respect to the last time intermediate diaphragms were used.

3. Is your state or agency currently using intermediate diaphragms?

   (47) Yes

   (9) No

4. Roadway classification for which intermediate diaphragms are used:

   (2) Primary roads only
   (2) Secondary roads only
   (41) Both primary and secondary roads

(9) Other (please specify) [P/C bridges span wetlands only: Overhead structures over any railroad or roadway: Spans over 80 ft. are box beams, I-beams for any roads: Spans over 120 ft. to stabilize girders during erection: All roads: Interstate and off system (county): All Highways.]

5. What types of intermediate diaphragm material is permitted by your state or agency when the bridge is above a highway? (please check all that apply)

(50) Cast-in-place concrete
(4) Precast concrete
(12) Steel channel
(2) Steel I-shape
(4) Steel truss
(7) Steel cross-bracing
(2) Other (please specify) [Bent plate: No other configuration has been requested by contractors.]

6. What types of intermediate diaphragm material is permitted by your state or agency when the bridge is above a navigable waterway? (please check all that apply)

(44) Cast-in-place concrete
(4) Precast concrete
(9) Steel channel
(1) Steel I-shape
(3) Steel truss
(5) Steel cross-bracing
(4) Other (please specify) [Bent plate: No other configuration has been requested: No navigable waterways of any consequence: Generally not applicable in _____.]

7. What types of intermediate diaphragm material is permitted by your state or agency when the bridge is above a railroad right of way? (please check all that apply)

(46) Cast-in-place concrete
(4) Precast concrete
(11) Steel channel
(1) Steel I-shape
(3) Steel truss
(6) Steel cross-bracing
(4) Other (please specify) [Bent plate: No other configuration has been requested: In general, local railroads will not permit concrete superstructures.]

8. What types of intermediate diaphragm material is permitted by your state or agency when the bridge spans a grade separation and has no traffic (highway, water, or rail) of any type below the girders. (please check all that apply)

(48) Cast-in-place concrete
(4) Precast concrete
(13) Steel channel
(2) Steel I-shape
(4) Steel truss

(7) Steel cross-bracing
(2) Other (please specify) [Bent plate]

9. At what location(s) are intermediate diaphragms specified? (please check all that apply)

(27) AASHTO spacing requirements
(22) Girder midspan for girder spans of ____ ft. or more [25:40:50:51:65:80:≥80:40 to 90 ft.: All spans]
(14) Girder 1/3 points for girder spans of ____ ft. or more [50:60:80:>80:100 ft.]
(5) Girder 1/4 points for girder spans of ____ ft. or more [75:90:100 ft.]
(1) Centerline of traffic below
(7) Other (please specify) [25 ft. maximum: None required when spans are less than 40 ft: We had used all three <categories> in the past: Minimum of one at the midspan or 30 ft. maximum spacing: Centerline of spans of 40 ft. or more: Diaphragms are placed at midspan, 1/3 points or 1/4 points with a maximum spacing of 40 ft.: Midspan for spans over 50 ft.: Temporary diaphragms at 1/4 and 3/4 points of exterior girders only.]

PART II. General Diaphragm Geometry and Conditions

1. What nominal depth cast-in-place concrete intermediate diaphragm does your state or agency specify?

(1) Cast-in-place intermediate diaphragms are not used
(0) Full depth of girder
(9) Over the girder web depth (between flanges) only
(31) From the underside of the slab to the top of the girder bottom flange (or top of flared portion of the bottom flange)
(2) From the bottom of the girder to the bottom of the top flange (or bottom of the flared portion of the top flange)
(12) Other (please specify) [Midspan, 1/3 points, or 1/4 points with a maximum spacing of of 40 ft.: From the underside of the slab to the bottom of the flared portion of the bottom flange: From the underside of the slab to the mid-depth of the web: Start the diaphragm 6 in. below the slab, and stop the diaphragm 9 in. from the bottom of the girder: Between the flared portions of the flanges: Done on an individual basis for each design: Bottom of the top flange to the top of bottom flange: 2 ft.-0 in. for AASHTO Type III and IV; 2 ft. - 6 in. for Types V and VI (mesured from top of beam).]

2. What nominal depth precast concrete intermediate diaphragm does your state or agency specify?

(40) Precast concrete intermediate diaphragms are not used
(0) Full depth of girder
(3) Over the girder web depth (between flanges) only
(1) From underside of the slab to the top of the girder bottom flange (or top of the flared portion of the bottom flange)
(0) From the bottom of the girder to the bottom of the top flange (or bottom of the flared portion of the top flange)
(4) Other (please specify) [Between the flared portions of the flanges.]

3. What steel channel shape(s) is (are) used for an intermediate diaphragm? (please check all that apply)

   (32) Steel channel intermediate diaphragms are not used
   (9) Please specify the most commonly used shape (ie: C12x20.7, MC12x31)
   [C12x20.7: C12x20.7, MC18x42.9: C12x15.3, MC18x42.7: C10x15.3, C12x20.7, C15x33.9]
   (1) Welded channel from plate stock. Size ____. [Varies depending on the girder depth.]
   (6) Other (please specify) [C15x33.9: 3/8 in. bent plate with 3 1/2 in. flange and a web height equal to the girder web depth: Sized at time of design to suite individual situation: Varies with girder depth.]

4. What steel I-Shape(s) is (are) used for an intermediate diaphragm? (please check all that apply)

   (42) Steel I-shape intermediate diaphragms are not used.
   (1) Please specify the most commonly used I-shape (ie: W12x22, M14x18, S12x31.8)
   [Bottom of top flange to top of bottom flange: W12x26]
   (0) Welded I-shape from plate stock. Size
   (4) Other (please specify) [Sited at the time of the design to suite the individual situation.]

5. What steel shapes are used for an intermediate truss diaphragm?

   (37) Steel truss diaphragms are not used
   (5) Please specify the shape of the most commonly used truss chord member(s) (ie: L6x4x1/2, WT6x11) [WT6x15: WT12x26: L5x3x1/2]
   (4) Please specify the shape of the most commonly used diagonal member(s) (ie: L6x4x1/2, WT6x11) [L3x3x5/16: L3 1/2x3 1/2 x 1/2]

6. What steel shapes are used for a diagonal brace or cross-brace intermediate diaphragm?

   (35) Steel diagonal brace or cross brace diaphragms are not used
   (8) Please specify the shape of the most commonly used member(s) (ie: L6x4x1/2, WT6x11)
   [L5x3x1/2: L4x4x3/8: L3x3x5/16: WT6x15, L3 1/2x3 1/2 x 1/2]

7. Are intermediate diaphragms used for temporary support of girders during bridge construction?

   (22) Yes

   (27) No

8. Are intermediate diaphragms used to minimize damage to bridge girders caused by impact forces from overheight traffic beneath the bridge?

   (10) Yes

   (40) No

PART III. Connection Details

1. How are intermediate cast-in-place concrete diaphragms, that are in contact with the bottom of the slab, connected to the slab?

(1) Cast-in-place concrete diaphragms are not used
(14) Diaphragms not in contact with the slab
(2) Not connected to the slab
(14) Cast monolithically with the slab with dowels through the interface between the members
(1) Cast monolithically with the slab without dowels through the interface between the members
(22) Steel reinforcing bars pass through a construction joint at the underside of the slab
(4) Other (please specify) [Slab cast into keyway along the top of the diaphragm: Cast monolithically with slab with U-shaped stirrups around steel x-bracing extending into the slab.]

2. How are intermediate precast concrete diaphragms, that are in contact with the bottom of the slab, connected to the slab?

(40) Precast concrete diaphragms are not used
(2) Diaphragms not in contact with the slab
(1) Not connected to the slab
(2) Steel dowels or reinforcement extended above the top of the precast concrete diaphragm to be cast into the slab
(0) Threaded inserts cast in the diaphragm and slab for receiving a steel piece to join members
(0) Anchored weld plates cast in the diaphragm and slab for receiving a steel piece to join the members
(0) Combination of threaded inserts and anchored weld plates for receiving a steel piece to connect the members.
(1) Other (please specify)

3. How are intermediate steel diaphragms that are in contact with the bottom of the slab, connected to the slab?

(31) Steel diaphragms are not used
(12) Diaphragm not in contact with the slab
(4) Not connected to the slab
(0) Weld plates cast in the bottom of the slab to receive a steel piece to connect the members
(0) Steel studs welded to the top of the steel diaphragm which are cast into the slab
(0) Expansion bolts drilled into the bottom of the slab to be used to fasten a steel piece which connects to the members
(0) Other (please specify)

4. How are intermediate cast-in-place concrete diaphragms connected to the girders?

(3) Cast-in-place concrete diaphragms are not used
(0) Not connected to the girders and girder face(s) is (are) not roughened
(0) Not connected to the girders, however, the girder face(s) is (are) roughened
(23) Coil ties placed through sleeves in the girders and extended into the diaphragm

(1) The girder face(s) has (have) a flush mounted weld plate to which steel studs or rods are welded and then cast into the diaphragm
(31) Other (please specify) [Void formed in girder web, reinforcing dowel threaded thru web: Bar thru diaphragm tightened to 180 ft.-lb.: Threaded inserts in girder: Bolt thru hole in web: Reinforcing steel passes thru holes in interior girder webs: Steel reinforcing bars are placed thru girders to engage diaphragm reinforcement: Threaded rods installed into anchors cast in girders: Threaded inserts or sleeves to receive steel rebar: Threaded inserts cast into beam. Reinforcement from diaphragm screwed into inserts: Sleeves cast into webs of interior girders to run continuous: 1 in. diameter rods thru webs and diaphragm: Coil ties in girder. Coil bolts and rods: Threaded inserts in exterior girder and sleeve with rebar through interior girders: Two 8 in. bars thru girder web, grouted in: Holes thru web for No. 6 rebar.]

5. How are intermediate precast concrete diaphragms connected to the girders?

(43) Precast concrete diaphragms are not used
(0) Not connected to the girders
(0) Girder faces and diaphragm faces have flush mounted weld plates to attach a steel piece to connect the members
(5) Other (please specify) [Precast shells are used, Voided portion filled with Class E concrete, coil inserts: No. 5 reinforcement passed thru preformed holes in girder web: Monolithic pour: 1 in. diameter rods thru girders and thru centerline of the diaphragms.]

6. How are intermediate steel (channel, I-shape, truss,, diagonal or cross-brace) diaphragms connected to the girders?

(30) Steel diaphragms are not used
(1) Not connected to the girders
(15) Bolts through the girder web attach a steel bracket or angle(s) to which the diaphragm is fastened
(1) The girder face(s) has (have) a flush mounted weld plate to which a steel bracket or angle(s) is attached to receive the diaphragm
(2) Other (please specify) [Inserts for exterior girders.]

PART IV. Design Criteria

1. Are specific design criterion applied to establish the design of an intermediate diaphragm and/or connections between the diaphragm and the slab or girders?

(1) Yes
(49) No (Standard diaphragm and connections establish by a "rule of thumb" approach or past experience)

If you answered no to the previous question (Question 1 in Part IV), do not answer the remaining questions in Part IV Design Criteria. Skip to Part V, Occurrence and Extent of Damage to Prestressed Concrete Girder.

2. Does your agency or state use lateral impact loads as a basis for diaphragm design, excluding diaphragm location?

   (1) Yes

   (6) No

3. Does your agency or state use lateral impact loads as a basis for diaphragm location?

   (0) Yes

   (6) No

4. What design criterion are applied to establish the diaphragm size?

   (7) No specific design criteria
   (0) Design criteria (please specify)

5. What design criterion are applied to establish the connection between the diaphragm and the slab?

   (1) No mechanical connection
   (5) No specific design criteria
   (1) Design criteria (please specify) [Develop shear.]

6. What design criterion are applied to establish the connection between the diaphragm and the girders?

   (0) No mechanical connection
   (6) No specific design criteria
   (1) Design criteria (please specify) [Steel.]

PART V. Occurrence and Extent of Damage to Prestressed Concrete Girders

1. Number of prestressed concrete girder bridges in your state or agency highway system over:

   Primary highways [38: 1500: 0: 0: 25: 176: 89: 91: 350: 1: 632: 100: 134: 30: 0: 200: 5: 17: 20: 185: 13: 102: 27: 195: 50: 2668: 6: 179: 299: 67: 332: 71]

   Secondary highways [13: 500: 4: 0: 17: 126: 34: 86: 250: 0: 854: 130: 48: 331: 20: 12: 0: 2: 39: 20: 211: 6: 25: 24: 142: 50: 773: 0: 241: 383: 71: 13: 110]

   Interstate highways [10: 2000: 1: 31: 60: 158: 42: 500: 85: 1323: 165: 74: 154: 40: 0: 129: 6: 316: 6: 101: 231: 539: 50: 1660: 20: 102: 116: 46: 182: 126]

2. When an overheight vehicle impacts a bridge superstructure, more than one girder may be damaged. Based on your past experiences (all years), indicate in the table below the occurrence of any type of damage to the girder(s) caused by lateral impacts.

	1 Girder	2 Girders	3 Girders	4 Girders	5 or More Girders
Always	(29)	(0)	(0)	(0)	(0)
Usually	(10)	(16)	(5)	(0)	(0)
Sometimes	(1)	(15)	(19)	(14)	(12)
Never	(1)	(4)	(8)	(12)	(14)

3. For each of the prestressed concrete girder damage categories listed in Table A.1, give the occurrence of impacts from overheight loads in 1988 and 1989 [If possible, provide data for both years.]

4. Based on the total number of repairs, due to any cause, to prestressed concrete girder bridges, approximately what percentage are related to overheight vehicles impacting and damaging the girders?

(10) 0-5%
(0) 5-10%
(1) 10-25%
(0) 25-50%
(5) 50-75%
(26) 75-100%

PART VI. Questionnaire Evaluation

Please indicate those questions that you had difficulty in answering by listing the questionnaire part and question numbers below, (i.e., V3 for Part V, Question 3)

PART VII. Diaphragm Details and Specification

Please send us a copy of your standardized details and specifications for all types of intermediate diaphragms that are used by your state or agency in prestressed girder bridges.

PART VIII. Summary

If you would like a copy of the complete survey, please check here.

(43) Yes, please send me a summary of the collected diaphragm data

(5) No

Table A.1. Impact occurrence and resulting damage.

Damage Description[h]	Occurence Per Year[a]					
	Primary Highways		Secondary Highways		Bridge over Interstate Highways	
	1988	1989	1988	1989	1988	1989
No damage	(50)	(50)	(40)	(40)	(75)	(75)
Minor damage requiring no repairs[b]	(34)	(34)	(20)	(21)	(38)	(37)
Minor damage requiring minor repairs[c]	(12)	(12)	(12)	(11)	(16)	(14)
Moderate damage requiring moderate repair[d]	(7)	(7)	(6)	(6)	(11)	(12)
Moderate damage requiring significant repair but not girder replacement[e]	(10)	(9)	(2)	(2)	(15)	(15)
Severe damage requiring substantial repair but not girder replacement(s)[f]	(15)	(14)	(2)	(2)	(9)	(8)
Major damage requiring girder replacement(s)[g]	(13)	(17)	(0)	(1)	(13)	(14)
Total number of impacts	(122)	(122)	(80)	(81)	(148)	(147)

[a]The tabulated results shown represents totals given by a limited number of design agencies.
[b]15 per year, all highways
[c]12-15 per year, all highways
[d]2 per year, all highways
[e]1 every 2 years, all highways
[f]1 every 5 years, all highways
[g]1 every 10 years, all highways
[h]Comments [Difficult to assess when damage occurred. Many structures get minor damage and nothing is done. To our knowledge, no more than 2 prestressed beams required replacement during the past 20 years: We have had very few cases of damage caused by overheight vehicles: No damage in 1988 and 1989: No data available, but have had occurrences in all categories in both years.]

Appendix B

BRIDGE DETAILS

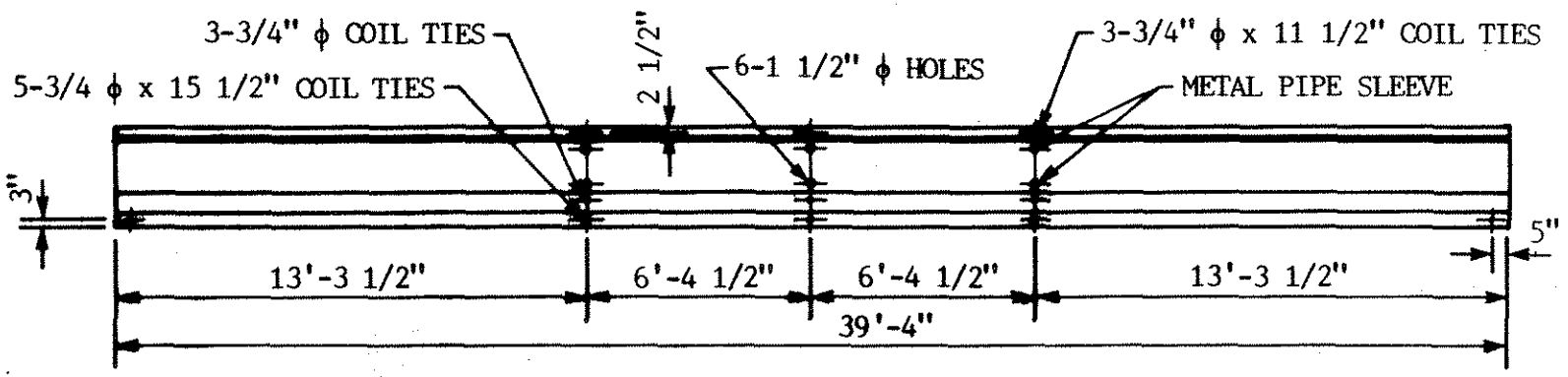

a. Elevation

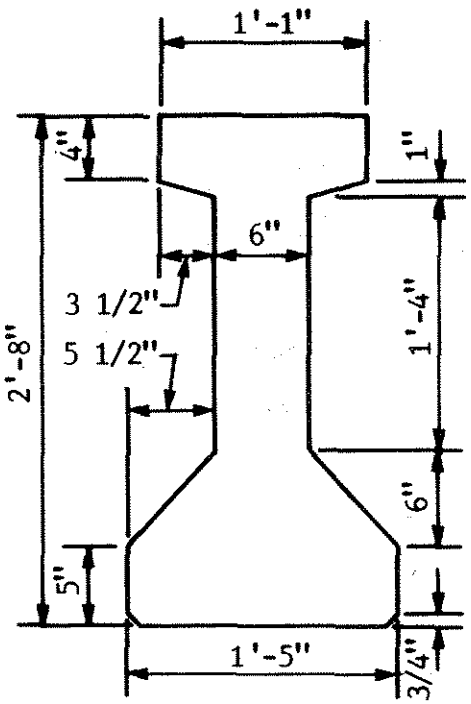

b. Cross section

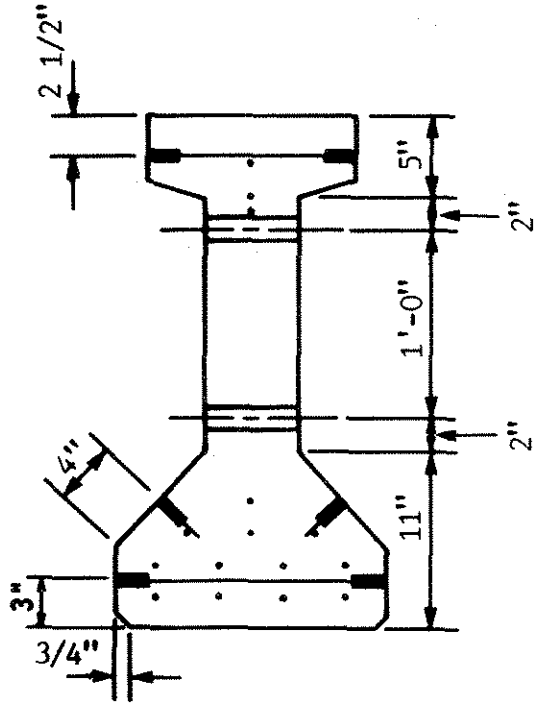

c. Insert location

Fig. B.1. P/C girder inserts.

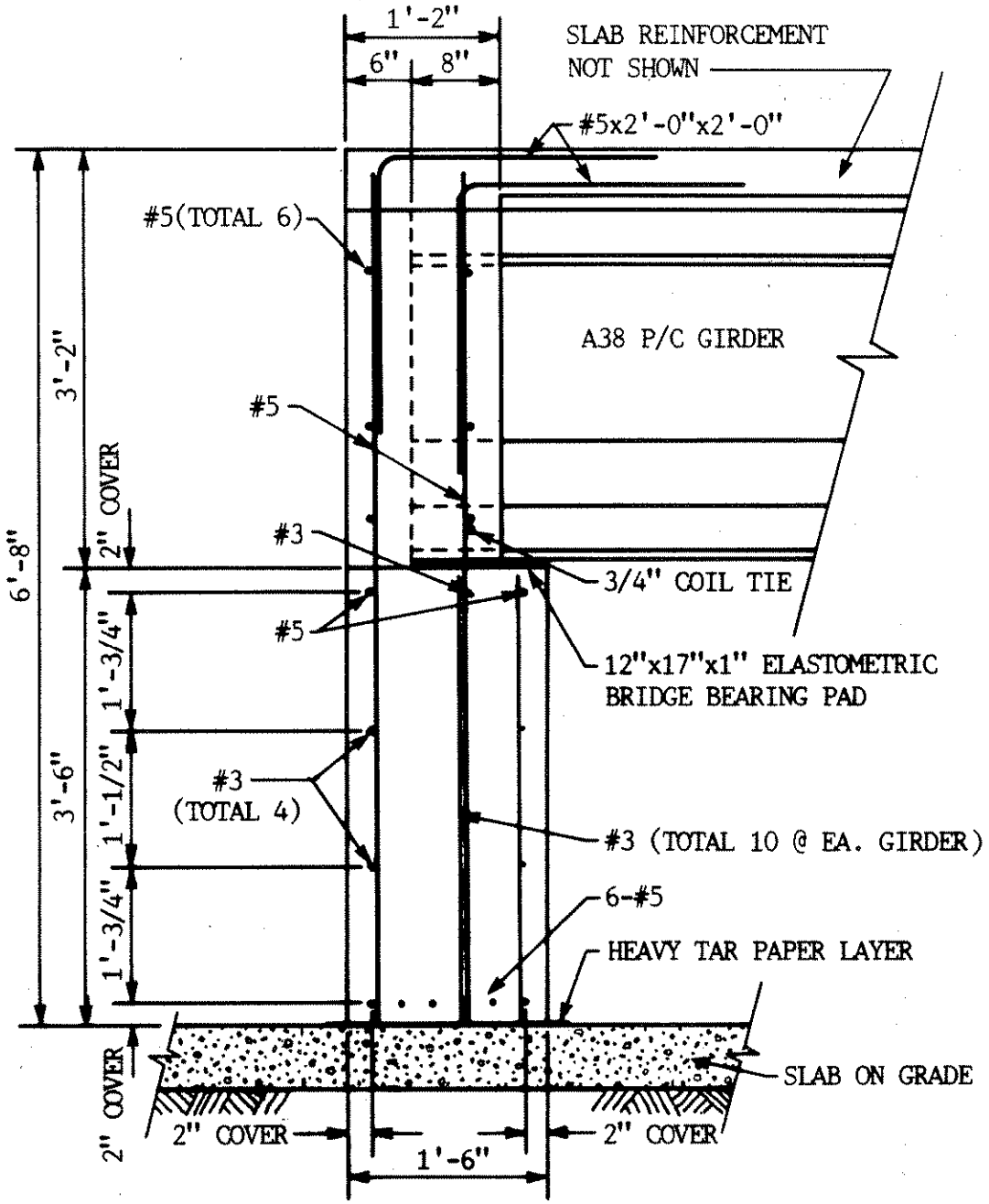

Fig. B.2. P/C girder support details.

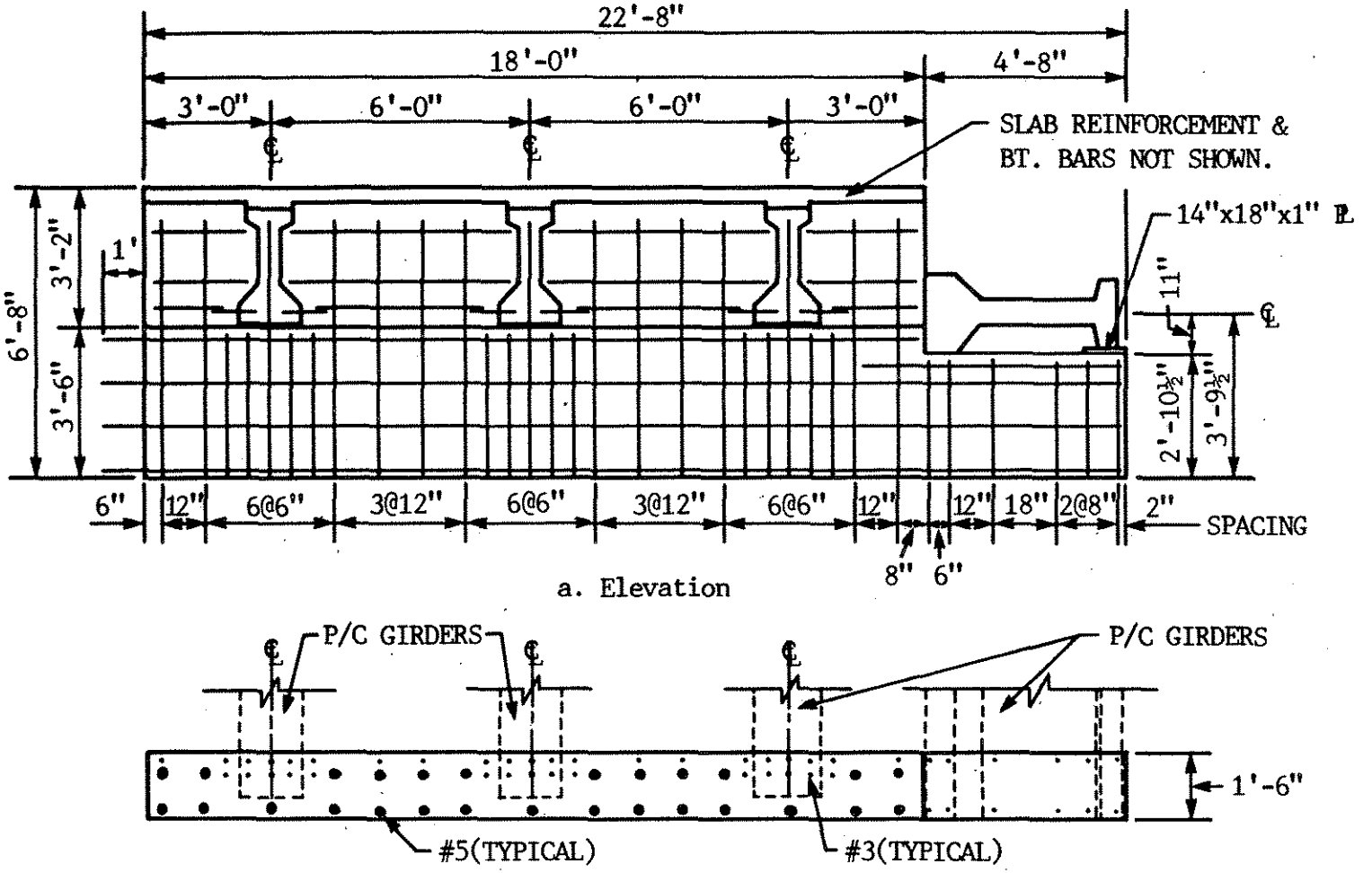

b. Plan section through abutment.

Fig. B.3. Abutment and end diaphragm reinforcement.

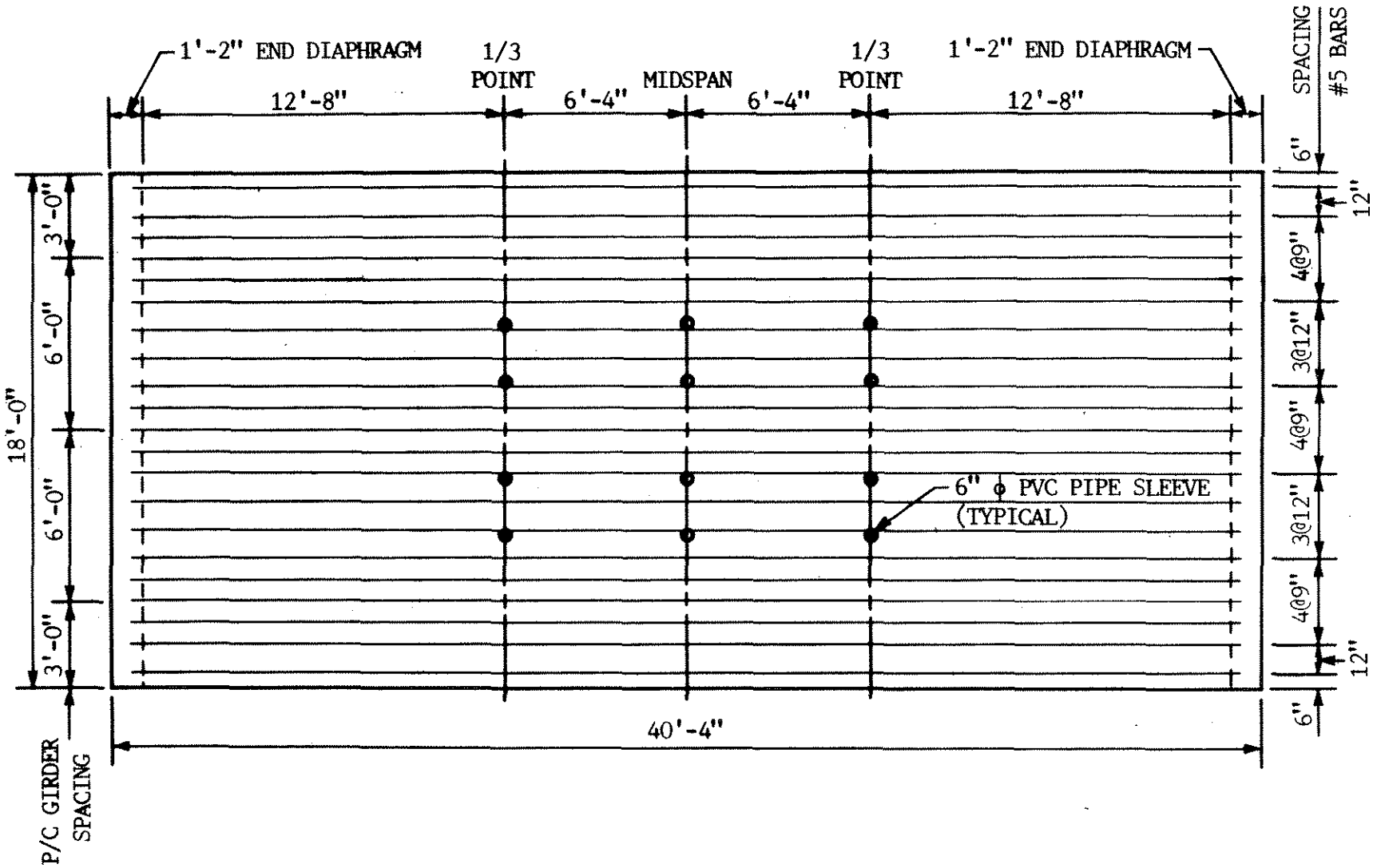

Fig. B.4. Longitudinal reinforcement in top of deck.

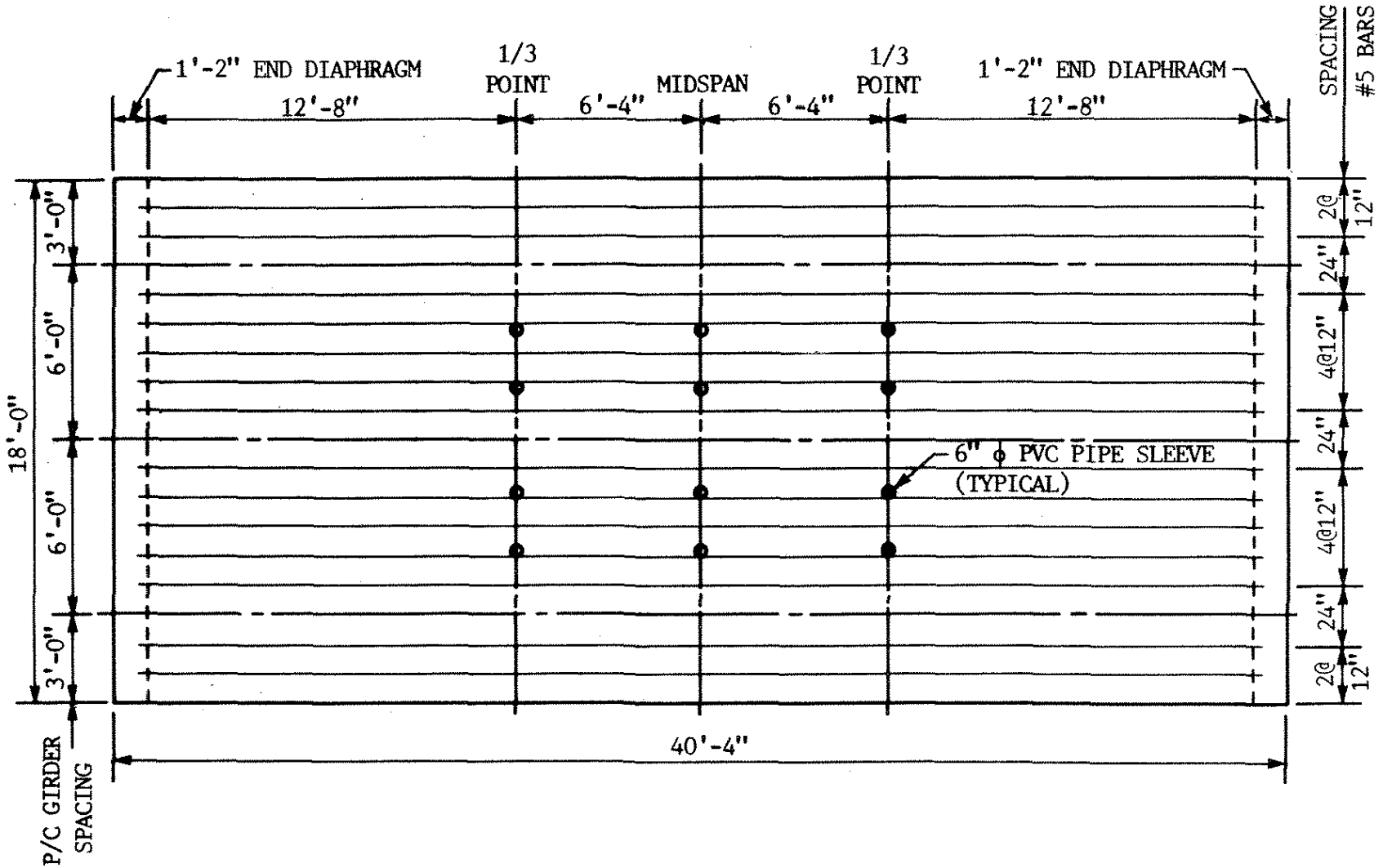

Fig. B.5. Longitudinal reinforcement in bottom of deck.

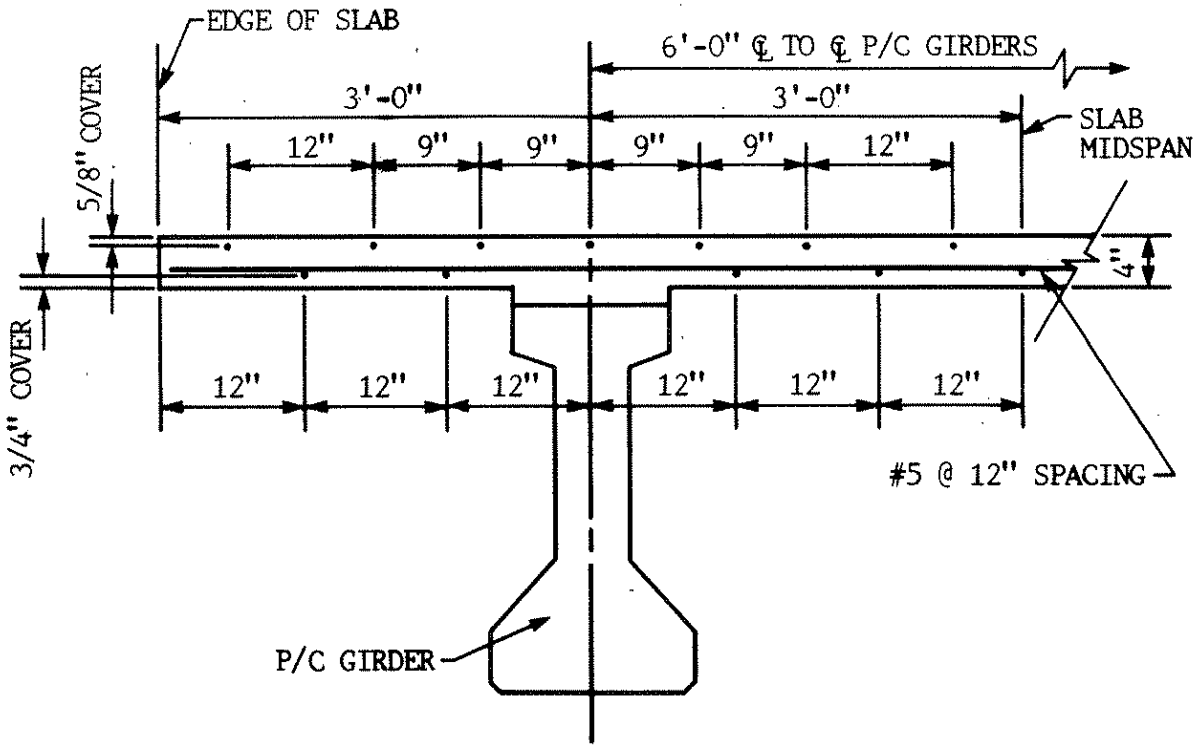

Fig. B.6. Transverse deck reinforcement.